

[REDACTED]

DECLASSIFIED

CLASSIFICATION CHANGED TO:

BY AUTHORITY OF:

BY:

TID-1219

3/29/60

M. Tallent

ORNL-1424  
Progress  
10a

(8/4)

Rev. 57

MARTIN MARIETTA ENERGY SYSTEMS LIBRARIES



3 4456 0360622 0

HOMOGENEOUS REACTOR PROJECT

EDT  
57

QUARTERLY PROGRESS REPORT

FOR PERIOD ENDING OCTOBER 1, 1952



CENTRAL RESEARCH LIBRARY  
DOCUMENT COLLECTION

**LIBRARY LOAN COPY**

DO NOT TRANSFER TO ANOTHER PERSON

If you wish someone else to see this document,  
send in name with document and the library will  
arrange a loan.

OAK RIDGE NATIONAL LABORATORY  
OPERATED BY  
CARBIDE AND CARBON CHEMICALS COMPANY  
A DIVISION OF UNION CARBIDE AND CARBON CORPORATION

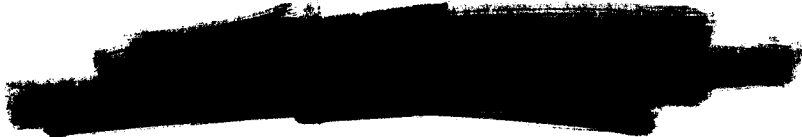


POST OFFICE BOX P  
OAK RIDGE, TENNESSEE

RESTRICTED DATA

This document contains Restricted Data as defined in the Atomic Energy Act of 1946. Its transmittal or the disclosure of its contents in any manner to an unauthorized person is prohibited.

SECRET INFORMATION



ORNL-1424

This document consists of 154 pages.  
Copy 10 of 193 copies. Series A

Contract No. W-7405-eng-26

**HOMOGENEOUS REACTOR PROJECT**  
**QUARTERLY PROGRESS REPORT**  
**for Period Ending October 1, 1952**

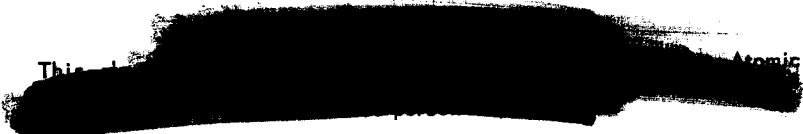
J. A. Swartout - Acting Project Director  
C. H. Secoy - Project Chemist  
C. E. Winters - Project Engineer

Compiled by W. E. Thompson

DATE ISSUED

DEC 19 1952

**OAK RIDGE NATIONAL LABORATORY**  
Operated by  
**CARBIDE AND CARBON CHEMICALS COMPANY**  
A Division of Union Carbide and Carbon Corporation  
Post Office Box P  
Oak Ridge, Tennessee

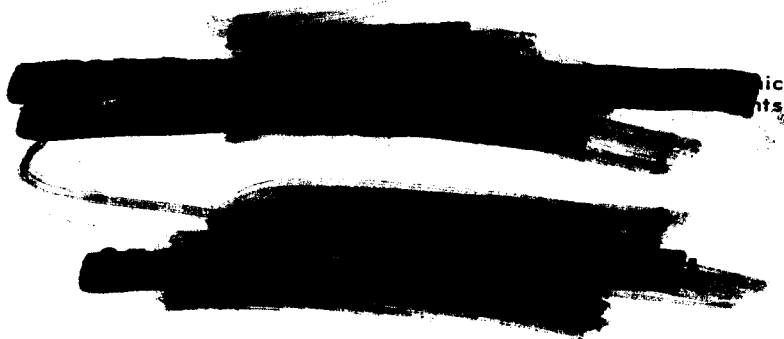


3 4456 0360622 0



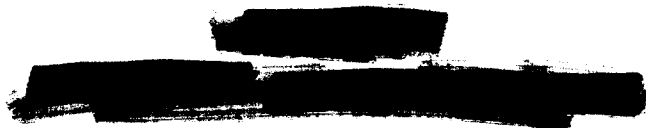
INTERNAL DISTRIBUTION

- |  |  |
|--|--|
| 1. G. T. Felbeck (C&CCC)                         | 50. G. R. Jenkins (C&CCC,<br>South Charleston) |
| 2-3. Chemistry Library                           | 51. C. P. Keim                                 |
| 4. Physics Library                               | 52. M. T. Kelley                               |
| 5. Health Physics Library                        | 53. E. M. King                                 |
| 6. Metallurgy Library                            | 54. A. S. Kitzes                               |
| 7-8. Reactor Experimental<br>Engineering Library | 55. C. E. Larson                               |
| 9-10. Central Research Library                   | 56. L. B. Emlet (Y-12)                         |
| 11-20. Central Files                             | 57. S. C. Lind                                 |
| 21. R. E. Aven                                   | 58. R. S. Livingston                           |
| 22. S. E. Beall                                  | 59. R. N. Lyon                                 |
| 23. E. P. Blizard                                | 60. W. L. Marshall                             |
| 24. E. G. Bohlmann                               | 61. H. F. McDuffie                             |
| 25. G. E. Boyd                                   | 62. J. R. McWherter                            |
| 26. W. M. Breazeale                              | 63. E. C. Miller                               |
| 27. R. C. Briant                                 | 64. K. Z. Morgan                               |
| 28. R. B. Briggs                                 | 65. E. J. Murphy                               |
| 29. F. R. Bruce                                  | 66. P. M. Reyling                              |
| 30. J. H. Buck                                   | 67. H. C. Savage                               |
| 31. A. D. Callihan                               | 68. H. Secoy                                   |
| 32. D. W. Cardwell                               | 69. C. L. Segaser                              |
| 33. C. E. Center                                 | 70. E. L. Shipley                              |
| 34. G. H. Clewett                                | 71. A. H. Snell                                |
| 35. D. D. Cowen                                  | 72. F. L. Steahly                              |
| 36. J. L. English                                | 73. C. D. Susano                               |
| 37. D. E. Ferguson                               | 74. J. A. Swartout                             |
| 38. W. R. Gall                                   | 75. E. H. Taylor                               |
| 39. J. P. Gill                                   | 76. W. E. Thompson                             |
| 40. R. J. Goldstein                              | 77. M. Tobias                                  |
| 41. C. B. Graham                                 | 78. S. Visser                                  |
| 42. J. C. Griess                                 | 79. A. M. Weinberg                             |
| 43. J. H. Goss                                   | 80. T. A. Walton                               |
| 44. C. S. Harrill                                | 81. E. P. Wiener (consultant)                  |
| 45. P. N. Haubenrich                             | 82. C. E. Winters                              |
| 46. C. G. Heisig                                 | 83. F. C. Von der Lage                         |
| 47. A. Hollaender                                | 84. F. C. Zapp                                 |
| 48. A. S. Householder                            | 85. P. C. Zmola                                |
| 49. W. B. Humes (K-25)                           |  |



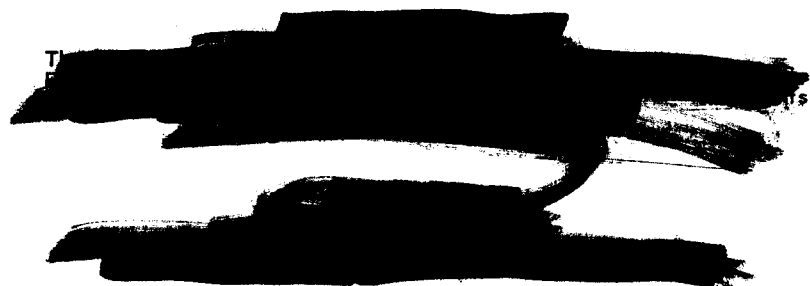
ic  
nts





Reports previously issued in this series are as follows:

- ORNL-527      Date Issued, December 28, 1949
- ORNL-630      Period Ending February 28, 1950
- ORNL-730      Feasibility Report - Date Issued, July 6, 1950
- ORNL-826      Period Ending August 31, 1950
- ORNL-925      Period Ending November,30, 1950
- ORNL-990      Period Ending February 28, 1951
- ORNL-1057     Period Ending May 15, 1951
- ORNL-1121     Period Ending August 15, 1951
- ORNL-1221     Period Ending November 15, 1951
- ORNL-1280     Period Ending March 15, 1952
- ORNL-1318     Period Ending July 1, 1952





## SUMMARY

### PART I HOMOGENEOUS REACTOR EXPERIMENT

#### Status of the HRE

The program of HRE critical experiments, completed early in July, showed that the reactor performed at low power according to expectations, although the amount of reactivity in the control rods and the reflector was somewhat less than calculated.

Critical experiments were carried out to determine the temperature coefficients of reactivity at high temperatures. Extrapolation of experimental data from the highest temperature reached in the experiments, 217°C, indicates a temperature coefficient at 250°C of  $-1.6 \times 10^{-3} k_{eff}/^{\circ}\text{C}$ , as compared with the coefficient of  $-0.38 \times 10^{-3} k_{eff}/^{\circ}\text{C}$  at 30°C. With the core temperature held constant at 200°C, the reflector temperature was varied from 150 to 200°C, and a temperature coefficient for the reflector that was equal to one-fortieth the value for the core was obtained.

Additional inhour data, defined as the excess reactivity as a function of reactor period, were obtained at 100 and 200°C. These data show that at low power the removal of the precursors of delayed-neutron emitters is not affected by temperature. The values obtained fall somewhat below theoretical values calculated on assumptions of uniform activation and uniform importance of neutrons in the core.

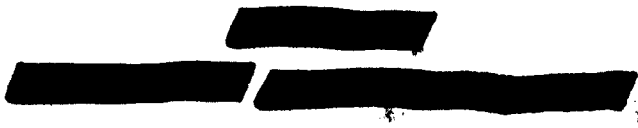
After modifications to the system in preparation for operation at higher power levels, the reactor operation was resumed at a power level of a few watts in mid-July. A leak developed in a threaded connection in the oxygen addition line, and enriched fuel escaped into the cell inside the shield. A complete material balance showed that the loss amounted to 780 grams. Thorough clean-up and recovery efforts over a period of about six weeks resulted in reclaiming at least 560 g of the amount lost.

The reactor system was designed to detect a leak of this type by monitoring the radioactivity in the ventilation air. Unfortunately, this leak occurred while the power level was too low to provide sufficient radioactivity in the fuel to set off the activity monitor. In the future it is planned to raise the reactor power to the kilowatt level for at least a short time at the start of operation to give a readily detectable amount of radioactivity in the fuel. New sampling devices have been installed in the air ducts, and the leak-detection system for monitoring the piping flanges has been improved.

Design of the HRE and its auxiliary equipment has been completed and the *HRE Design Manual* will be issued early in the next quarter.

#### Engineering Studies of Components

Consideration is being given to the design of fuel-injection pumps to



serve as alternates for the pulsafeeder pumps now being used in the HRE. Two types of pumps have been selected for further study: a multistage centrifugal pump and a modified positive-displacement pump of the triplex or Milton Roy type.

**Controls and Instrumentation**

No important changes in HRE instrumentation have been made. Erosion of plugs and seats of certain valves in the HRE system has been troublesome. Therefore several combinations of titanium alloys have been tested for use in these valves, but, to date, no completely satisfactory combination has been found.

Tests of the Densitrol concentration-monitoring instrument indicate that it is very reliable; readings are reproducible within 1%. The sensitivity ranged from 0.29%, equivalent to 0.07 g of uranium per liter of  $UO_2SO_4$  solution when the concentration is 25.98 g of uranium per liter, to 0.18%, which is also equivalent to 0.07 g of uranium per liter of  $UO_2SO_4$  solution when the concentration is 40.93 g of uranium per liter.

**PART II**

**BOILING REACTOR AND SLURRY STUDIES**

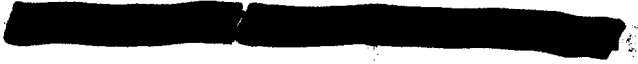
**Boiling Reactor Research**

Experimental data from the UCLA boiling studies indicate that a boiling reactor may be unstable; however, these data are not supported by actual boiling reactor experience or by nuclear calculations. Critical experiments are being planned for

determining the nuclear power-vapor formation relationship governing the power level stability of boiling reactors.

Studies of the mechanisms by which heat might be removed from a boiling reactor indicate that surface evaporation is probably a negligible factor, except in very small reactors operating at low power. For boiling reactors up to 3 or 4 ft in height, the predominant mechanism for power removal is natural bubble rise and growth. Another conclusion is that for boiling reactors having a free surface and using forced circulation, vapor entrainment in the circulating fluid apparently will limit the power removal. Calculations of the uranium enrichment required for criticality at various fuel densities have been made.

Design and study of a hypothetical, full-scale, boiling reactor have been undertaken in an effort to discover and evaluate the problems involved in such a reactor. Boiling reactor experiments are being planned, and to house these experiments a building similar to the HRE building is being designed. It is planned that the shielded reactor and equipment compartments will be located below ground level to reduce the amount of poured concrete shielding required and to conserve space within the building. The building and the cells are being designed to permit a series of reactor experiments to be carried out in the same facilities. It is now planned that the first experiment will be the so-called "Teapot" experiment in which the core will be an 18-in.-dia cylinder. In the second experiment, a 6-ft-dia cylinder will probably be used.



[REDACTED]

To determine the requirements of the off-gas system for these experiments, calculations have been made of the production and heat generation of fission gases. Means for handling the gases are being considered.

The nuclear instrumentation for the boiling reactor experiment has been purchased, and process instrumentation can be selected as soon as the design of the reactor system is frozen.

### Slurry Fuel Studies

In nine short runs (all less than 200 hr) the 100-gpm slurry pumping loop has encountered a variety of difficulties. It has not been possible to maintain the initial slurry concentration during operation at 250°C because of settling of the slurry in various portions of the system and the formation of a slurry coating on the pipe walls. Observation of the pump bearings during the runs indicates that Graphitar may be unsuitable for long operation in the front bearing of a pump if slurry is permitted to enter the bearing.

A glass loop, similar to the 100-gpm loop, has been assembled to allow observation of flow patterns and to aid in developing sampling techniques. Consideration is being given to the design of an additional high-temperature slurry pumping loop to give more flexibility in the testing program.

Studies of the growth and recrystallization of  $\text{UO}_3 \cdot \text{H}_2\text{O}$  slurry particles under various conditions show the marked effect of nitrate and uranyl ion impurities.

Equipment for use in performing slurry critical experiments is being tested and plans for the experiments are being made.

A study of the pumping of thorium oxide slurries has been started. During the first runs it appeared that the slurry coated the pipe walls. Difficulty with the pump caused the loop to be shut down until a new pump of improved design can be provided. Parts for the new pump are on hand.

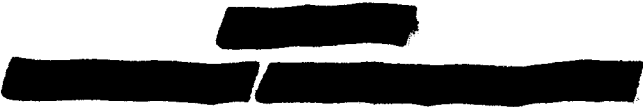
Previous studies indicated that even trace quantities of  $\text{UO}_2^{++}$  and  $\text{NO}_3^-$  ions markedly influence the characteristics of  $\text{UO}_3$  slurries; therefore procedures have been developed for producing  $\text{UO}_3 \cdot \text{H}_2\text{O}$  slurries in either rod or platelet crystal form with a minimum of ionic impurities.

The effect of the  $\text{NO}_3^-$  ion on slurry stability under radiation has been studied and found to be negligible.

Several methods of determining slurry particle sizes have been investigated and found to give values that agree reasonably well.

Further tests with slurries in stainless steel bombs, both in and out of the reactor, indicate that the caking previously observed in in-pile experiments is not solely the result of radiation, since it was also observed in out-of-pile tests.

Further studies on the boiling of slurries gave no evidence of foaming, although some data indicate that corrosion may have taken place. Equipment failure caused the termination of the experiment, and inconsistencies in the data have not yet been resolved.



**PART III  
GENERAL HOMOGENEOUS REACTOR STUDIES**

**Intermediate-Scale Homogeneous  
Reactor Design**

The general features of an intermediate-scale homogeneous reactor (ISHR), developed earlier, have been examined in more detail, especially the design of equipment items, the construction of reactor and equipment cells, and some of the nuclear calculations. With regard to the reactor and equipment cells, it appears advisable to have the cells gas-tight to an internal pressure of 50 psi; to meet this requirement major changes have been made in the originally proposed layout.

An economic study of the ISHR steam power cycle has led to the proposal that, for the initial installation only, a steam-killer condenser be used, with provisions for future addition of a building and equipment for power generation, if this proves desirable. Studies indicate that a forced-convection type of heat exchanger may be attractive, and further studies are planned.

Nuclear calculations have been made to determine the effect of poisons on criticality, the induced activity in external piping, and the build-up of heavy isotopes.

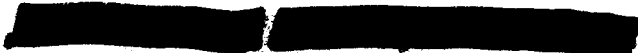
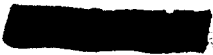
As an alternate to the 6-ft-core reactor, a two-region reactor is being considered that will have a 4-ft core and an 8-ft pressure vessel. A reactor of this type is attractive because it appears that it can be operated under conditions that have been shown in dynamic loop tests to be acceptable

from the corrosion standpoint. Design studies and nuclear calculations for the two-region reactor have been started.

**Engineering Studies of Components**

*Core Development Studies.* An investigation has recently been completed of the velocity distribution and pressure drop in 12-in.-dia, spherical, reactor core models utilizing rotational flow. The studies show that the total pressure loss, including that in the outlet pipe, is about 30% greater than the static pressure drop across the sphere. It has also been found that roughness of the sphere wall has a major effect on the pressure drop - the smoother the wall, the higher the rotational velocity obtained in the sphere, and therefore the higher the pressure drop. In general these studies have led to the prediction that rotational flow probably will not be advantageous for intermediate- or large-scale homogeneous reactors because of the high pressure drop. This prediction will be checked when the 8-ft sphere and circulating system now being constructed are completed.

Several models utilizing different arrangements for achieving straight-through flow have been studied; the most promising of the models has six radial inlets and two polar outlets. The flow in this sphere has a small amount of rotation and gives excellent mixing. The model seemed to work well with as few as three balanced inlets, and it was found that two outlets are necessary to prevent stagnation.



[REDACTED]

Further work on straight-through flow models is planned.

*Main Circulating Pumps.* The Allis-Chalmers Manufacturing Company has completed the preliminary design and engineering studies of the 20,000-gpm, totally enclosed, centrifugal pump. Work on the final design of the pump is nearing completion. The Worthington Corporation has completed the preliminary design and engineering studies of a 20,000-gpm centrifugal pump, which differs from the Allis-Chalmers pump in that instead of having a canned rotor it uses a labyrinth shaft seal with a standard electric motor.

*Large Heat Exchangers.* A preliminary design of a large heat exchanger has been received from the Lummus Company of New York, and, after some revisions of the design at ORNL, the preliminary design data were established. Design studies are being carried out to determine optimum arrangements of tubes in the heat exchanger.

*New Projects.* Work has been started on the design of an in-pile circulating loop for studying the effects of radiation upon various reactor systems under conditions approaching as closely as possible the actual operation conditions in a reactor. Consideration is also being given to the changes required to convert the HRE mockup from operation with fuel in solution to operation with slurry fuel.

### Corrosion

*Dynamic Corrosion Studies.* The stainless steel diaphragms fabricated as replacements for Inconel diaphragms

in Westinghouse model 100A pumps appear to be quite satisfactory, judging from the two tests in which the pumps have operated for over 1000 hr each. The Stellite 98M2 journal bushings and Graphitar No. 14 bearings are giving excellent service, even when very highly concentrated uranium solutions are being pumped. Currently, nine 100-gpm circulating loops are in operation and two more are being constructed.

In runs of over 2500 hr, it has been observed that  $UO_2SO_4$  solutions containing 100 and 300 g of uranium per liter give low corrosion rates, about 0.1 and 0.5 mpy, respectively, at 100°C. There appears to be no localized attack of the type encountered at higher temperatures, but there is evidence that crevice corrosion may be a problem.

Other long-term tests at 250°C show that dilute  $UO_2SO_4$  solutions containing 5 g of uranium per liter cause corrosion at a rate of less than 0.5 mpy. Again, there is no evidence of localized attack.

Under conditions of high temperature and moderate to high uranium concentrations, titanium is the only material tested that shows adequate corrosion resistance. An all-titanium loop is being fabricated to allow a more thorough examination of all aspects of the corrosion of titanium.

*Static Corrosion Studies.* There was no significant effect of dissolved oxygen concentration in the range of 360 to 3100 ppm on short- (48 hr) and long- (5232 hr) term corrosion of type 347 stainless steel in  $UO_2SO_4$  solutions containing approximately 200 and 300 g of uranium per liter at

[REDACTED]

250°C. On a solution-change basis, the corrosiveness of  $UO_2SO_4$  solutions containing 300 g of uranium per liter was two to three times greater than that of the solutions containing 200 g of uranium per liter for similar exposure conditions. Initial corrosion rates, determined by dissolved nickel content after 48 hr, were between 6.7 and 9.9 mpy in the solutions containing 200 g of uranium per liter, as compared with initial rates of 22.5 to 32.6 mpy in the solutions containing 300 g of uranium per liter. Final corrosion rates for 5232 hr were 0.2 to 0.4 mpy in the solutions containing 200 g of uranium per liter and 0.4 and 0.6 mpy in the solutions containing 300 g of uranium per liter.

Solution stability was not maintained in tests operating with  $UO_2SO_4$  solutions containing 300 g of uranium per liter and oxygen partial pressures of 75 psia at 250°C. Increasing the time of continuous exposure at 250°C had no effect on the solution stability. The longest period of continuous exposure was five weeks; no reduction of the uranyl ion was observed in these tests.

Long-term exposure at 250°C, for 5232 hr, showed the susceptibility of type 347 stainless steel to localized corrosion attack. The intensity of the attack was pronounced in the solutions containing 300 g of uranium per liter and appeared to be related to the dissolved oxygen concentration; that is, the magnitude and frequency of pitting attack were more severe with increased dissolved oxygen content. Localized corrosion attack on specimens in  $UO_2SO_4$  solutions containing 200 g of uranium per liter was

not observed after similar exposure times.

In static tests over a period of 29 weeks, the corrosion of titanium in  $UO_2SO_4$  solutions containing 40 and 300 g of uranium per liter at 250°C has been observed. Corrosion attack in the solution containing 300 g of uranium per liter was three times as great as in the more dilute solution; but in both cases the attack was very mild, less than 0.5 mpy.

### Radiation Chemistry

An oxygen-pressurized, type 347 stainless steel bomb containing  $UO_2SO_4$  solution with 40 g of uranium per liter at 250°C was exposed to a neutron flux of  $3.5 \times 10^{12}$  neutrons/cm<sup>2</sup>·sec in the LITR. Based on the consumption of oxygen and the dissolution of nickel, the estimated corrosion over a 14-week period was 0.35 mil. The correlation between the decrease in excess oxygen and the increase in dissolved nickel was good. Since bombs treated in the same way, but not irradiated, showed 0.025-mil penetration, or less, there is indication that reactor radiation significantly increases the static corrosion of type 347 stainless steel by uranyl sulfate. Similar experiments carried out with titanium bombs indicated no detectable corrosion (based on dissolved titanium concentration) during the period of the test either with or without radiation.

Measurements of the gas production rate in the stainless steel in-pile bomb indicated that by the end of the 14 weeks only 30% of the original uranium was still in solution. This was subsequently confirmed analytically. Laboratory tests support the

[REDACTED]

[REDACTED]

[REDACTED]



[REDACTED]

of the poppet was unchanged. The valve will be returned to the loop for further testing.

Impact specimens prepared from commercial titanium, Ti-78A, have been tested under various conditions, and data on the impact strength are given.

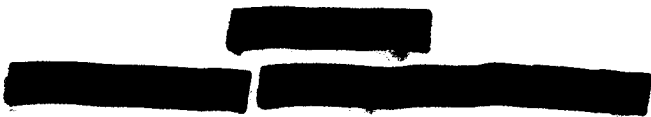
#### Chemical Processing

The emphasis in chemical processing development has shifted from complete processing by Purex to removing plutonium from the reactor continuously. This shift follows the establishment of the feasibility of Purex for processing the uranyl sulfate solution used in a plutonium-producing reactor. By continuously removing plutonium from the reactor, large savings in inventory charges can be effected, and, at the same time, plutonium with a very low  $\text{Pu}^{240}$  content can be produced.

At present, filtering or settling insoluble  $\text{PuO}_2$  from the reactor fuel solution is the most attractive method

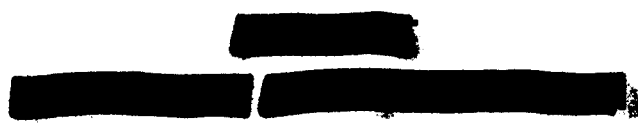
for continuous plutonium removal (precipitation of plutonium will occur in the reactor system unless strong oxidizing conditions are maintained). The precipitation could be performed on a portion of the reactor fuel solution in a tank adjacent to the reactor and the fuel solution returned directly to the reactor system.

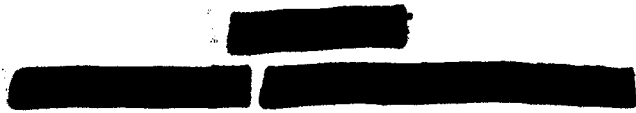
The processing developmental effort this past quarter has been directed toward establishing the chemical behavior of plutonium in the reactor, developing a more economical method than Purex for decontaminating plutonium, improving the tributyl phosphate extraction process, and determining the susceptibility of tributyl phosphate solutions to radiation damage. In addition, the chemical processing group at the Vitro Corporation has carried out developmental work on heavy water recovery, reactor fuel preparation, and removal of fission-product poisons from reactor fuel solutions by adsorption.



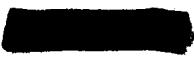
# CONTENTS

	PAGE
SUMMARY . . . . .	v
PART I. HOMOGENEOUS REACTOR EXPERIMENT . . . . .	
STATUS OF THE HRE . . . . .	1
Reactor Operation . . . . .	3
Results of Experimental Program . . . . .	3
Temperature coefficient of reactivity for core . . . . .	4
Temperature coefficient of reactivity for reflector . . . . .	4
Inhour curves . . . . .	5
Future Program . . . . .	5
HRE Design . . . . .	6
ENGINEERING STUDIES OF COMPONENTS . . . . .	7
Development of a Positive-Displacement Pump . . . . .	7
CONTROLS AND INSTRUMENTATION . . . . .	9
Valves . . . . .	9
Concentration Measurement . . . . .	9
PART II. BOILING REACTOR AND SLURRY STUDIES . . . . .	
BOILING REACTOR RESEARCH . . . . .	11
Nuclear Stability of a Boiling Reactor . . . . .	13
Power Removal from a Boiling Reactor . . . . .	13
Surface evaporation . . . . .	14
Natural bubble rise . . . . .	15
Internal circulation . . . . .	15
Power removal by natural internal circulation . . . . .	16
General comments on power removal from boiling reactors . . . . .	17
Criticality calculations . . . . .	19
Study of Large-Scale Boiling Reactor Systems . . . . .	19
Boiling Reactor Experiments . . . . .	20
Boiling Reactor Experiment Design . . . . .	20
Shield design . . . . .	20
Disposal of core tanks . . . . .	24
Teapot design . . . . .	24
Treatment of waste gases . . . . .	24
Instruments . . . . .	24
SLURRY FUEL STUDIES . . . . .	27
Chemical Studies . . . . .	27
Uranium trioxide chemistry . . . . .	28
Preparation of pure uranium trioxide . . . . .	28

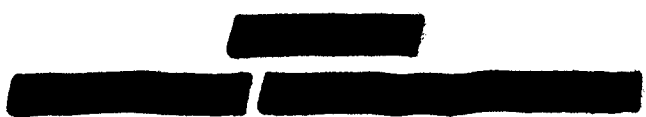




Effect of nitrate on uranium trioxide stability . . . . .	29
Particle size and surface area measurement . . . . .	29
Density of $UO_3 \cdot H_2O$ platelets . . . . .	32
Crystal structure of $UO_3 \cdot H_2O$ bipyramids . . . . .	32
Radiation chemistry . . . . .	32
Slurry irradiations . . . . .	32
Gas recombination studies . . . . .	32
Corrosion studies . . . . .	33
Evaluation of pretreatment procedures . . . . .	33
Effect of impurities on type 347 stainless steel corrosion by slurries . . . . .	33
Slurry boiling studies . . . . .	34
Pumping Studies . . . . .	35
High-pressure slurry circulating system . . . . .	35
Glass loop . . . . .	38
Second high-temperature loop . . . . .	38
Viscosity measurements . . . . .	38
Crystal growth . . . . .	39
Criticality experiments . . . . .	39
Thorium loop test at 150°C . . . . .	40
PART III. GENERAL HOMOGENEOUS REACTOR STUDIES . . . . .	41
ISHR DESIGN . . . . .	43
Equipment Layouts . . . . .	43
Steam System . . . . .	44
Heat Exchanger . . . . .	44
Effect of Poisons on the Criticality of the ISHR at 250 and 100°C . . . . .	48
Induced Activity . . . . .	50
Heavy-Isotope Build-up . . . . .	50
Criticality Calculations . . . . .	53
Core Designs for Two-Region Reactors . . . . .	53
Stress Analysis of 4-ft-dia Core Vessel . . . . .	57
Nuclear Calculations for Two-Region Lithium and Thorium Converters . . . . .	57
ENGINEERING STUDIES OF COMPONENTS . . . . .	59
Core Development Studies . . . . .	59
Small-scale rotating-flow model . . . . .	59
Intermediate-scale rotating-flow model . . . . .	60
Small-scale straight-through model . . . . .	60
Gas separators . . . . .	64
Test Loop for 4000-gpm Pump . . . . .	64
Main Circulating Pumps . . . . .	65
Allis-Chalmers pump development . . . . .	65
Worthington Corporation pump development . . . . .	65
Byron Jackson Company shaft seal development . . . . .	65



Fuel Feed Pump Development . . . . .	66
Isolation Valves . . . . .	66
Small (5 gpm) Centrifugal Pump Development . . . . .	66
Large Heat Exchangers . . . . .	67
New Projects . . . . .	69
CORROSION . . . . .	70
Dynamic Corrosion Studies . . . . .	70
Construction and maintenance of pump loops . . . . .	70
Pump loop test results . . . . .	71
Small-scale dynamic tests . . . . .	73
Static Corrosion Studies . . . . .	73
Effect of dissolved oxygen content on corrosion . . . . .	74
Effect of $\text{CuSO}_4$ additions on corrosion . . . . .	77
Effect of long-term exposure on corrosion . . . . .	82
Corrosion of Titanium in Uranyl Sulfate Solutions . . . . .	92
RADIATION CHEMISTRY . . . . .	94
Long-Term Irradiations at High Temperature and High Flux . . . . .	94
Corrosion results . . . . .	95
Stability of solution . . . . .	96
Catalysis in the Decomposition of Hydrogen Peroxide . . . . .	96
Titanium Bomb Experiments . . . . .	98
In-Reactor Loops . . . . .	100
Catalytic Recombination of Hydrogen and Oxygen . . . . .	100
Dissolved catalysts . . . . .	100
Suspended heterogeneous catalysts . . . . .	101
SOLUTION CHEMISTRY . . . . .	104
Conductivity Measurements of Aqueous Solutions of Uranyl Sulfate and Uranyl Fluoride . . . . .	104
Vapor Pressures of Aqueous Uranyl Sulfate Solutions . . . . .	104
Solubility of $\text{UO}_3$ in Aqueous $\text{UO}_2\text{SO}_4$ and $\text{UO}_2\text{F}_2$ at 175 and 250°C . . . . .	105
Extension of the Study of the Two-Liquid-Phase Region of the $\text{UO}_2\text{SO}_4$ - $\text{H}_2\text{SO}_4$ - $\text{H}_2\text{O}$ . . . . .	108
Alternate Fuel Media and Possible Corrosion Inhibitors . . . . .	113
Static corrosion tests . . . . .	113
Dynamic corrosion tests . . . . .	116
Conductometric and acidimetric titrations . . . . .	116
Solubility and phase behavior in the $\text{M}_x\text{O}$ - $\text{UO}_3$ - $\text{HF}$ - $\text{H}_2\text{O}$ system . . . . .	117
Kinetic behavior of $\text{UO}_4$ formation on addition of $\text{H}_2\text{O}_2$ . . . . .	119
Neutron Capture Cross Section of Protactinium-233 . . . . .	120
METALLURGY . . . . .	120
Titanium Pump Impeller Fabrication . . . . .	120
Titanium for Valve Trim . . . . .	121
Properties of Titanium . . . . .	122



CHEMICAL PROCESSING . . . . .	125
Comparison of Chemical Processing Methods . . . . .	125
Plutonium Chemistry . . . . .	127
Effect of plutonium concentration on the behavior of plutonium in 1 M $UO_2SO_4$ solution . . . . .	127
Solubility of tetravalent plutonium at 100°C . . . . .	128
Effect of oxygen pressure on the rate of oxidation of Pu(IV) at 100°C . . . . .	128
Effect of oxygen pressure on the reduction of Pu(VI) at 100°C . . . . .	128
Effect of a stoichiometric hydrogen-oxygen mixture on the be- havior of plutonium in 1 M $UO_2SO_4$ solution . . . . .	129
Decontamination of Plutonium by TTA Extraction . . . . .	130
Homogeneous TTA chelation . . . . .	130
Effect of iron and sulfate on plutonium extraction . . . . .	131
Dissolution of $PuO_2$ by TTA chelation . . . . .	131
Solvent Extraction . . . . .	131
Neptunium behavior in tributyl phosphate extraction process . . . . .	132
Radiation damage . . . . .	132
Homogeneous Reactor Chemical Processing Development at Vitro Corporation . . . . .	137



**Part I**

**HOMOGENEOUS REACTOR EXPERIMENT**



# HRP QUARTERLY PROGRESS REPORT

## STATUS OF THE HRE

	S. E. Beall, Section Chief		
M. A. Bell	J. J. Harriston	V. K. Pare'	S. Visner
W. S. Brown	J. W. Hill	J. A. Ransohoff	P. M. Wood
J. S. Culver	S. I. Kaplan	M. Richardson	
D. M. Eissenberg	C. W. Keller	T. H. Thomas	

### REACTOR OPERATION

At the beginning of the quarter, the HRE was being operated at a power level of approximately 50 mw for the purpose of completing the nuclear experiments reported below. A scheduled shutdown was made on July 1 in preparation for operation at higher power levels. The reactor was restarted at a power level of a few watts on July 17 and operated until July 20, at which time a leak developed in the oxygen-addition line at the threaded connection of a high-pressure check valve. Several hundred grams of enriched fuel was spilled into the cell compartment within the shield; however, the magnitude of the loss was not realized until the results of a complete material balance were available on July 24.

Upon discovery of the leak, all operations were discontinued until the cells could be decontaminated and washed. Analyses of the material in the waste recovery system indicate that at least 560 of the 780 g of enriched fuel that was spilled has been recovered from the cells thus far. The entire system was examined for other escape routes, and each possibility was investigated thoroughly over a six-week period. One possibility (in fact, it is probable) is that a portion of the fuel solution was dried while being sprayed at 1000 psi from the leak into the hot, dry air being drawn through the cell and that the dried particles were dispersed from the off-gas stack.

Samples taken from various points in the cell ventilation ducts and stack indicated the presence of perhaps 2 or 3 g of enriched uranium on the walls of the ventilation system. The dispersion of fine particles by the stack is so effective that it is exceedingly unlikely that sufficient quantities would collect in one place to give an indication of residual activity on a survey meter. Evidence of alpha contamination was not found on the ground or building near the stack or on the landscape in the direction of the 3- to 4-mph wind prevailing at the time of the leak.

The reactor system was designed to detect such leaks by monitoring of the radioactivity in the ventilation air. Unfortunately, this leak occurred while operation was at too low a power level to provide sufficient radioactivity in the fuel to actuate the activity monitor.

Measures have been taken to prevent the repetition of such a loss when the reactor is operated in the future. First, the activity of the fuel solution will be increased to a readily detectable level by raising the reactor power to kilowatt levels for a short time in order to make use of the activity monitors designed into the system to warn of leakage. Also, a precipitron type of sampling device has been installed to detect the presence of alpha activity in the stack gases. The hydrostatic leak detector attached to the piping flanges has been overhauled completely; however, it would not have detected

# HRP QUARTERLY PROGRESS REPORT

the leak at the threaded connection of the check valve. The reactor instruments that indicate the total inventory have been recalibrated.

## RESULTS OF EXPERIMENTAL PROGRAM

During the early part of the quarter, information was obtained on the temperature coefficient of reactivity for the reactor core at temperatures up to 217°C, the temperature coefficient of reactivity for the reflector, the shim rod calibration at 200°C, and the inhour data at 100 and 200°C.

**Temperature Coefficient of Reactivity for Core.** The experimental measurements of the temperature coefficient were extended from 100 to 217°C, with the entire reactor system operating. The fuel concentration was changed by means of the concentration control system, and oxygen was bled into the high-pressure system, which was pressurized chiefly with steam. The experimentally determined critical concentration is plotted against the temperature in Fig. 1, and the theoretical curve is shown for comparison. At room temperature, the

agreement between experiment and theory is within 0.3 g of  $U^{235}$  per kilogram of  $H_2O$ , whereas at 217°C, the calculated value is higher by 1.6 g of  $U^{235}$  per kilogram of  $H_2O$ . The temperature coefficient,  $\partial k_{eff}/\partial T$ , is obtained by determining the slope of the experimental curve at various temperatures and multiplying the slope by the corresponding conversion factor between concentration and  $k_{eff}$ . The coefficients are plotted in Fig. 2 along with the curve calculated by differentiating, with respect to temperature, the two-group criticality equation for the equivalent bare sphere. The agreement between the observed coefficients and the calculation is within about 10%. The value of the temperature coefficient at 30°C is  $-0.38 \times 10^{-3} k_{eff}/^{\circ}C$ , at which temperature the contribution from the variation of nuclear cross section with temperature is approximately equal to the contribution from the density variation. At 250°C, the

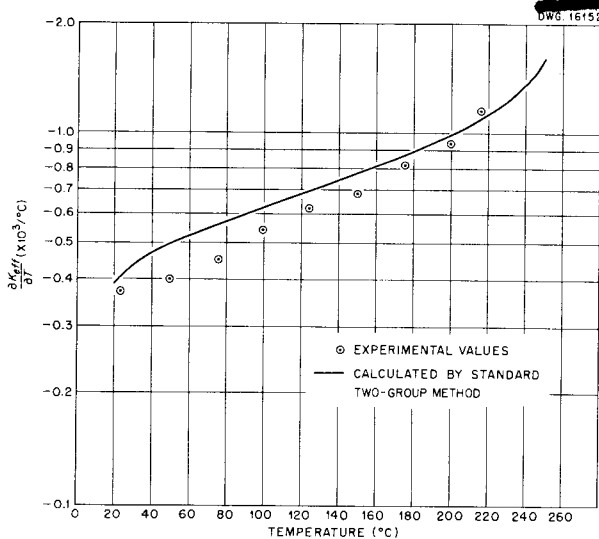


Fig. 1. Temperature Coefficient of Reactivity for the HRE.

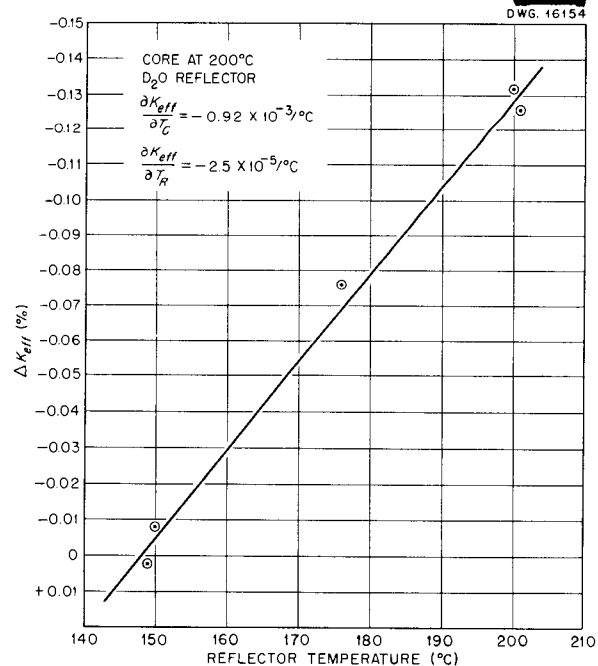


Fig. 2. Effect of Reflector Temperature on Reactivity.

predicted temperature coefficient is  $-1.6 \times 10^{-3}$ , of which only  $0.2 \times 10^{-3}$  is the nuclear effect.

**Temperature Coefficient of Reactivity for Reflector.** With the core temperature held in the vicinity of  $200^\circ\text{C}$ , the change in reactivity was determined for the range of reflector temperatures between  $150$  and  $200^\circ\text{C}$ . The change in reactivity is  $0.13\%$  in  $k_{eff}$  for the  $50$ -deg range, Fig. 3, which yields a temperature coefficient for the reflector of  $0.026 \times 10^{-3}$ , or one-fortieth the value for the core. The value calculated is five times

larger than that measured. If the assumption is made that the reflector temperature coefficient is overestimated by a factor of 5 over the temperature range from  $20$  to  $217^\circ\text{C}$ , the discrepancy of  $1.6$  g of  $\text{U}^{235}$  per kilogram of  $\text{H}_2\text{O}$  between calculations and theory, as shown in Fig. 1, can be explained. The basis for the discrepancy may be that the ratio of the value of the fast diffusion constant for the reflector to its value in the core is not completely corrected at different temperatures by density effect alone.

**Inhour Curves.** Additional inhour data, which give the excess reactivity as a function of the reactor period, were obtained at  $100$  and  $200^\circ\text{C}$ . The data (Fig. 4) at the different temperatures agree, which indicates that at low power the removal of the precursors of the delayed-neutron emitters is not affected by temperature. However, the data do fall somewhat below the theoretical values calculated on the assumptions of uniform activation and uniform importance of neutrons in the core.

#### FUTURE PROGRAM

The experimental program for the next quarter is outlined in the following:

1. Increase power stepwise from  $10^{-3}$  to  $10^5$  w at fuel and reflector temperatures of  $100$  to  $150^\circ\text{C}$  and pressures of  $500$  psi.
2. At a power of approximately  $10^5$  w,
  - a. determine shield effectiveness and off-gas activity,
  - b. determine minimum operating pressure,
  - c. obtain information for determining power (gas) coefficient of reactivity,
  - d. obtain information for power-demand control,

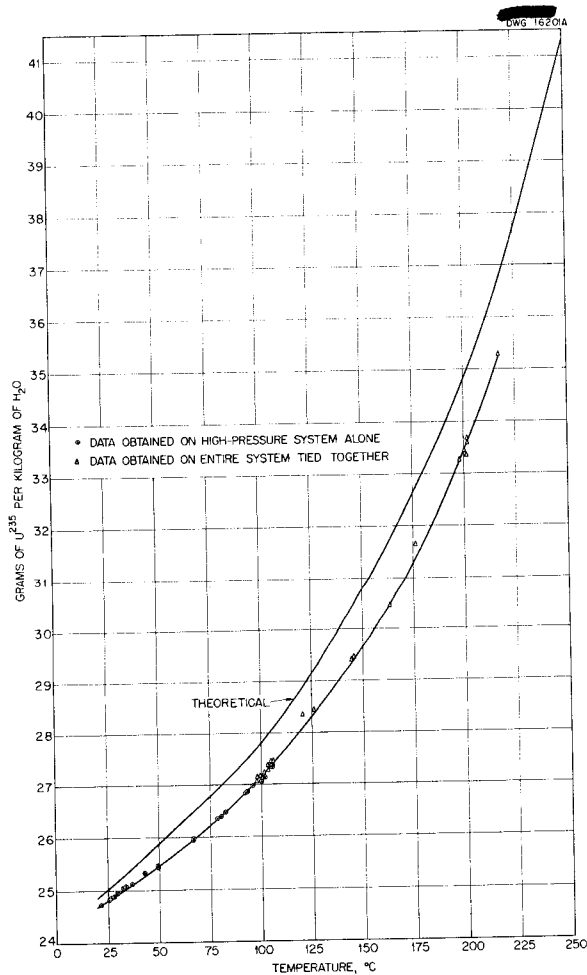


Fig. 3. Dependence of Critical Concentration on Temperature in HRE.

# HRP QUARTERLY PROGRESS REPORT

DWG. 15213A

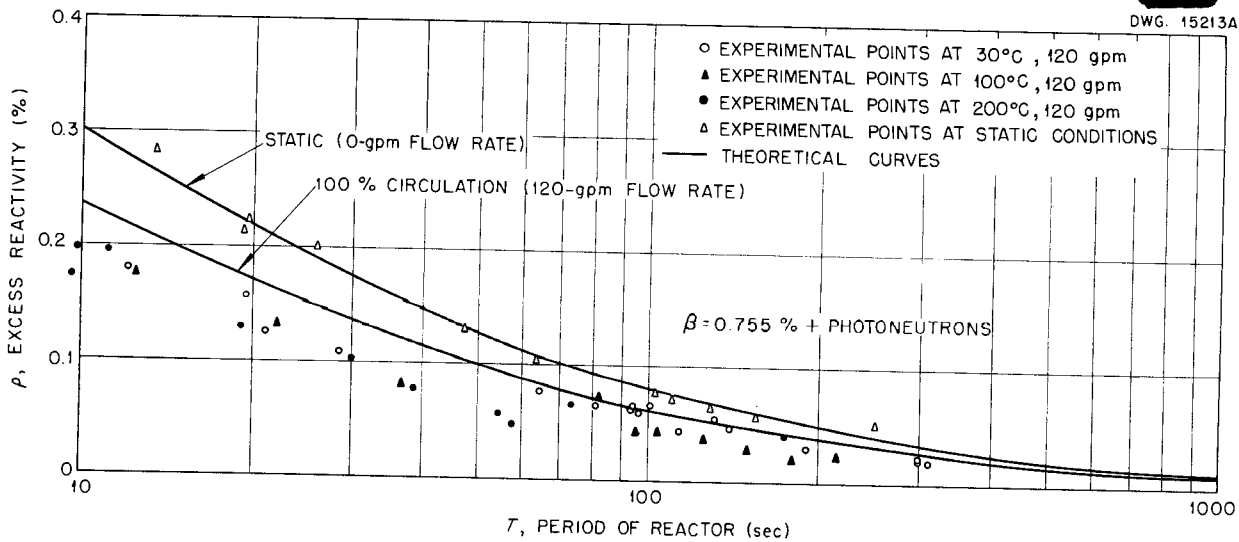


Fig. 4. Inhour Curves for the HRE.

- e. determine response to reactivity changes,
  - f. determine power by heat balance.
3. At increased power and temperature, determine
    - a. maximum power at 150, 200, and 250°C,
    - b. power coefficient of reactivity,
    - c. stability.
  4. At 250°C, 1000 psi, and approximately 1000 kw,
    - a. determine heat balance,
    - b. evaluate the adequacy of the shield and the off-gas system,
    - c. obtain information of decomposition, that is, the G value for H<sub>2</sub> and O<sub>2</sub> formation in the core, the fuel let-down system

- d. obtain information for power-demand control.

5. Make system-activation estimates and perform other experiments as required.

## HRE DESIGN

R. B. Briggs, Section Chief  
 C. L. Segaser                      F. C. Zapp

Design of the HRE and its auxiliary equipment has been completed. A final design report<sup>(1)</sup> has been prepared and will be issued soon.

(1) C. L. Segaser and F. C. Zapp, *HRE Design Manual*, ORNL CF-52-6-160 (in press).

ENGINEERING STUDIES OF COMPONENTS

C. B. Graham, Section Chief  
L. F. Goode

DEVELOPMENT OF A POSITIVE-  
DISPLACEMENT PUMP

High-head, low-capacity pumps will be needed for injection of fuel in future reactors, as well as for HRE operation. It appears that the pulsafeeder pump will operate satisfactorily for the HRE; however, the possibility of additional trouble remains. Therefore the development of a reliable high-head pump is necessary for future reactors and to provide an alternate to replace the pulsafeeder pump.

Two types of pumps have been selected for further study: a multistage centrifugal pump (cf., "Fuel Feed Pump Development") and a modified positive-displacement pump of the triplex or Milton Roy type. The principal problem to overcome with a plunger type of positive-displacement pump is to eliminate leakage without the use of grease and without frequent adjustment of the seals.

Test work has been started on a Milton Roy pump and a Union Triplex pump in an effort to find a suitable packing scheme that will minimize pumped-fluid leakage along the plungers and the leakage return to the pump suction. The basic scheme being considered is shown in Fig. 5. The

Union Triplex pump is now being set up to test this design. Components of the design have been tested separately with carbon-fluorethene Chevron packing rings. The Garlock Packing Company has proposed a special, pure-nylon, Chevron packing that holds promise of a reasonable operating life from the standpoint of radiation and corrosion resistance and adjustment-free operation. The necessary packing has been ordered and delivery is expected in the near future.

Both the Garlock Packing Company and the Union Steam Pump Company have aided considerably in working out the problems inherent in this type of stuffing-box design. It is to be noted that one of the basic objections to the packing scheme shown in Fig. 5 is that of having a constant, small, water leakage into the fuel system. This water leakage is necessary to assure that no fuel will leak past the packing and out of the system.

If the preliminary test results are favorable, the Union Steam Pump Company can fabricate a modified pump head of Stellite, stainless steel, and chrome-plated steel that will incorporate the necessary design changes and will operate on the existing pulsafeeder pump frame and drive mechanism of the HRE.

UNCLASSIFIED  
DWG. 17088

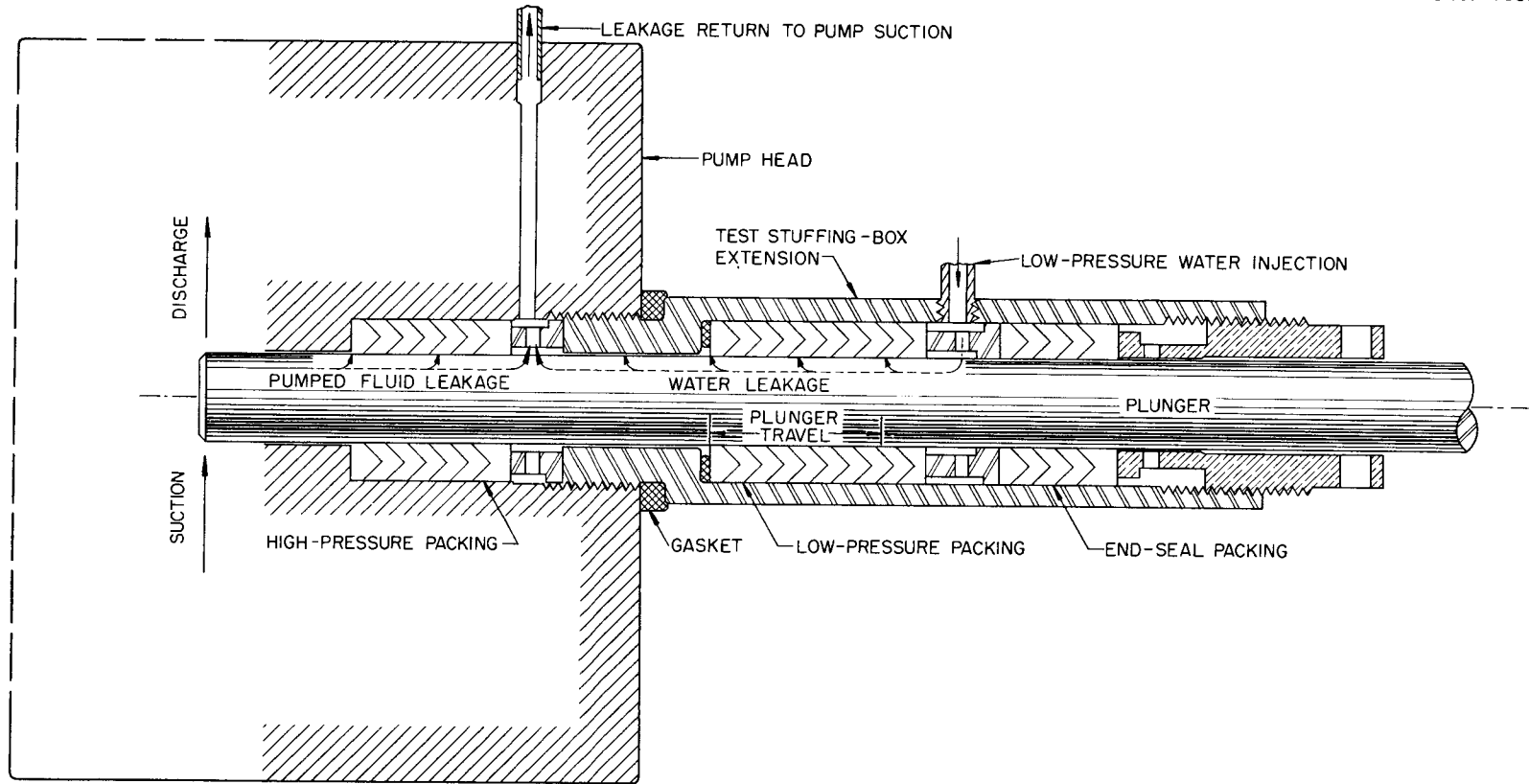


Fig. 5. Adapter for Testing Chevron Packing and Leakage Control Methods.

CONTROLS AND INSTRUMENTATION

W. M. Breazeale, Section Chief

A. M. Billings	L. P. Inglis	R. H. Powell
D. G. Davis	C. A. Mossman	D. S. Toomb
C. G. Heisig	J. E. Owens	W. P. Walker

An appreciable amount of work was required this quarter by the HRE, principally in the calibration of instruments and in making minor repairs. No important changes in instrumentation were made.

Design of the control and instrumentation system for the boiling reactor experiments is proceeding, and a description of the present design will be found in Part II.

VALVES

Life-testing of the Fulton-Sylphon type of bellows seal valve has continued. Thus far, one valve has been pressurized to 3800 psi to check rupture strength, cycled for 100,000 cycles with 1000 to 1500 psi applied to the bellows, and rechecked for rupture strength at 3800 psi. Inspection of the bellows at the completion of the test showed that the convolutions had been flattened slightly, but there was no sign of material damage. Testing will be continued on several more bellows in order to obtain more representative data.

Erosion of plugs and seats of certain valves has given trouble, and no completely satisfactory solution has been obtained to date. Several combinations of titanium alloys have been tested. The first consisted of a plug of Ti-150A and seat insert of Ti-75A. It was hoped that the small difference in hardness would minimize galling. However, after a few operations, it was found that galling was sufficiently serious to render the Ti-75A seat useless. A new seat was then fabricated, the plug and seat

were refinished, and both were hardened by nitriding. With the new seat, appreciable chipping of the valve occurred under test. Possibly the chipping was due to either an increased diffusion rate of nitrogen along the edge of the seat chamfer or cracking of the case because of strains in the soft base (Ti-75A). Next, a hardened plug and an unhardened seat, both Ti-150A, were tested. After about 50 cycles of opening and closing, the seat was found to be cracked in several separate areas. Some Ti-100A has been ordered for fabrication into plugs and seats, and further tests will be carried on.

CONCENTRATION MEASUREMENT

In the last quarterly report, results of rough preliminary checks on the radiation stability of synthetic gems were given. Work during the past quarter has covered the design of specimen holders that will permit testing of these synthetic gems in the ORNL graphite reactor with and without exposure to light. A facility for handling the hot samples and holders is being designed.

A plastic model of the spectrophotometer cell has been received from the shop and is being tested to determine the optimum design of the inlet and outlet ports. The light source, which will be an argon discharge tube, and an interference filter are being designed. The photocell amplifier has been ordered.

The Densitrol<sup>(1)</sup> has been mounted on the system mockup at Y-12 and

<sup>(1)</sup>HRP Quar. Prog. Rep. July 1, 1952, ORNL-1318, p. 20.

several tests have been completed. This unit contained an insulated, copper-wire-wound, bakelite microformer whose response has been measured and found to be linear. Two glass plummet and a stainless steel plummet were installed, in turn, and tested.

Results of the tests indicate that the system is very reliable and that chart indications are reproducible to within 1%. A sensitivity of 0.29%, equivalent to 0.07 g of uranium per liter when the concentration is 25.98 g of uranium per liter, was observed. With solution containing 40.93 g of uranium per liter, the sensitivity was 0.18%, which is also equivalent to 0.07 g of uranium per liter. The specific gravities of these solutions are 1.0330 and 1.0530.

The Densitrol was placed in a bypass in series with a cooler and operated at 1000 psi at a temperature of 42 to 52°C. (The instrument is temperature compensated over this

range.) It was found that the reproducibility of the Densitrol readings is somewhat better than the analytical results. However, analytical determinations are necessary for absolute calibration. No trouble is experienced from gassing of the solution. The high pressure under which the Densitrol operates is advantageous in this respect.

It is planned to install two titanium plummets, which will be internally pressurized, and to perform the same tests on them.

It was interesting to note that the Densitrol indicated a change in concentration, which was due to a small leak and the dilution accompanying makeup with pure water, some time before the leak was discovered. In other words, under these conditions, the Densitrol gives a good indication of the system condition.

A report giving a detailed description of the Densitrol installation and test results is now being prepared.

**Part II**

**BOILING REACTOR AND SLURRY STUDIES**



## BOILING REACTOR RESEARCH

R. N. Lyon, Section Chief

The current boiling reactor research program is designed to provide the necessary information for a broad evaluation of boiling homogeneous reactors in comparison with other types of reactors. The required information falls into three categories: (1) information regarding the controllability of this type of reactor, (2) information regarding the possible operating levels of this type of reactor, and (3) information on the mechanics of actually designing, building, and operating a boiling reactor for a practical application.

### NUCLEAR STABILITY OF A BOILING REACTOR

P. R. Kasten

In a boiling reactor, in order that power surges resulting from an imposed reactivity increase be limited effectively, it is important that the vapor bubbles form and grow in a manner closely related to the nuclear power level. The functional relationship between nuclear power and vapor formation is not known, but some experiments are being carried out and others are planned to give this information. At present, data obtained from UCLA experiments indicate that boiling reactors are unstable, but actual boiling reactor experience indicates that such data are not directly applicable.

The influence of changes in power level on the density of the reactor fluid can be described as:

$$\rho - \rho_0 = \left( \frac{\partial \rho}{\partial H_t} \right)_{fv} \left\{ (H_t - H_{t_0}) + \zeta \int_0^\infty G(s) [H_t(t-s) - H_{t_0}] \right\} ds \quad (1)$$

where

$\rho$  = average fluid density of core region,

$\rho_0$  = fluid density required for reactor criticality,

$$\xi = \frac{\left[ \left( \frac{\partial \rho}{\partial H_t} \right)_T - \left( \frac{\partial \rho}{\partial H_t} \right)_{fv} \right]}{\left( \frac{\partial \rho}{\partial H_t} \right)_{fv}}$$

$G$  = normalized vapor-delay function,

$\left( \frac{\partial \rho}{\partial H_t} \right)_{fv}$  = change in core fluid density per unit energy injected as liquid superheat,

$\left( \frac{\partial \rho}{\partial H_t} \right)_T$  = change in core fluid density per unit energy injected as vapor,

$H_t$  = total energy content of the reactor core,

$H_{t_0} = H_t$  evaluated under steady-state conditions.

The restrictions necessary to ensure stability of the linearized equations of motion<sup>(1)</sup> are dependent upon the form of  $G(s)$ . If the rate of vapor formation is directly proportional to the bulk-liquid superheat,

$$G(s) = \nu e^{-\nu s} \quad (2)$$

where  $\nu$  is the rate at which superheat energy is dissipated into vapor energy per degree superheat. Under this condition, stability of boiling reactors appears assured. This corresponds to the situation in which decomposition gas bubbles are generated internally in direct correspondence with the nuclear power, for these gas bubbles are then vapor-bubble nuclei with

<sup>(1)</sup> P. R. Kasten, *Reactor Physics of Teapot. Part IV. Linearized Kinetics*, ORNL CF-52-8-128 (Aug. 15, 1952).

## HRP QUARTERLY PROGRESS REPORT

superheat as the driving force for bubble growth. In regard to the formation of decomposition gases within water, L. D. P. King (of Los Alamos) believes that in the Los Alamos Water Boiler the gases form as such within the liquid, inasmuch as bubbles rising to the surface at temperatures below the boiling point have appeared to be so small that if they were formed on the wall or tubing they would not detach themselves from the metal. Also, in the November 1951 radiation burst of the Hanford homogeneous reactor, the killing of the reaction could only be attributed to the expansion of the liquid caused by the decomposition gases forming within the core.

Simulated volume boiling experiments at UCLA, however, have revealed vapor-delay functions that can be approximated by

$$G(s) = \frac{\nu (\nu s)^n e^{-\nu s}}{n!} \quad (3)$$

where  $n$  is a measure of the time for a given nuclear power surge to be transmitted into vapor energy for a given value of  $\nu$ . For the above situation, restrictions are necessary on  $\nu$  to ensure system stability, and these will increase with  $n$  and decrease with power density.

In experimentally determining the stability of a boiling reactor, it is desirable that the results be applicable to homogeneous boiling reactors in general. The investigations, to include all aspects of these reactors, should cover the effects of reactor size, geometry, fuel concentration, fuel enrichment, fuel type, and operating conditions as represented by operating pressure and vapor fraction within the core. It is obviously difficult and prohibitively expensive to cover all of this in one reactor experiment. The stability analyses indicate that large pressure and vapor-fraction ranges affect the

degree of stability to a much greater degree than the other variables, and on this basis a small reactor capable of operating over large pressure ranges is a reasonable one to build for a first experiment. Critical experiments that will best determine the nuclear power-vapor formation relationship are presently being considered, and calculations are in progress to indicate the effect of reactor size, fuel concentration, fuel enrichment, and operating conditions on stability.

The power fluctuations that occur in a boiling reactor operating in a quasi-steady state are probably due to large vapor bubbles escaping from the reactor surface. If the assumption is made that bubble size increases with increased power level, these fluctuations will increase with the power density at any given pressure. However, if at a given power level the number of bubbles is constant, the fluctuations will decrease with increasing pressure.

### POWER REMOVAL FROM A BOILING REACTOR

R. V. Bailey      H. A. MacColl  
E. N. Lawson      P. C. Zmola

The power removal analysis has been reviewed and extended in the direction of greater generality in an effort to determine how much each of the various heat removal mechanisms contributes to the total heat removal under given operating conditions. The ultimate utility of a boiling reactor depends on the removal of appreciable quantities of energy from the unit, without decreasing the mean density to the extent of requiring excessive size or excessive fuel enrichment. The problem of relating the power density in the core to the mean fluid density as a function of the system pressure was considered in terms of the three available mechanisms for energy removal. These mechanisms are: (1) surface evaporation, (2) bubble growth

and rise in a fluid with negligible internal circulation, and (3) bubble growth and rise in a fluid with internal circulation velocities that are large compared with the relative bubble velocity.

In considering these mechanisms, the nomenclature given in Table 1, p. 21, is used.

**Surface Evaporation.** For a cylindrical reactor core, with a height equal to the diameter, in which heat is carried to a point near the surface of the liquid by convection within the liquid, the contribution of surface evaporation to the power density,  $P_{se}$ , is given by

$$P_{se} = \frac{(h\Delta)_s}{96,500Y} \quad (4)$$

Qualitative experimental data, presented below, indicate that for volume boiling with high power densities,  $(h\Delta)_s$  is of the order of 70,000 Btu hr<sup>-1</sup> ft<sup>-2</sup>. Therefore the contribution of surface evaporation from a boiling reactor core appears negligible for high-power-density operation.

**Natural Bubble Rise.** The following postulations were made:

1. The maximum bubble rise rate is

$$U_b = \left( \frac{4g}{3} \left| \frac{\rho_l - \rho_v}{\rho_l} \right| \left| \frac{D_b}{f_D} \right| \right)^{1/2} \quad (5)$$

2. Bubble nucleation occurs uniformly in the reactor core.
3. The heat flux to a bubble is independent of position in the reactor core (uniform power-density distribution).
4. The reactor core is a vertical, right-circular cylinder.

On the basis of the above postulations, the following equation was developed for the power density owing to natural rise and growth rates:

$$P = 0.01 \left( 1 - \frac{\rho_{av}}{\rho_l} \right) \left( \frac{1}{Y} \right)^{2/3} \left( \frac{H_{fg}}{v_{fg}} \right)^{2/3} \left( \frac{h_b \Delta}{f_D} \right)^{1/3} \quad (6)$$

Plots of this expression are shown in Fig. 6.

A limited amount of rough experimental information on volume boiling of water by electrical-resistance heating has been obtained and is presented in Fig. 7. The data represent boiling liquid heights from 0.1 to 1.5 ft and power densities from 0.8 to 12 kw per liter of boiling water. The pressure was 1 atmosphere. The solid line in Fig. 7 is a plot of Eq. 6, in which the rather optimistic value,  $h_b \Delta / f_D = 150,000$ , was used. It can be seen that the trend of the data appears to confirm the theoretical considerations. If the contribution to power removal by bubble rise and growth is taken as  $h_b \Delta / f_D = 7500$  (value based on data presented by Jakob<sup>(2)</sup>), the dashed line represents Eq. 6. In this case, the remainder of the power removal is due to surface evaporation

(2) M. Jakob, *Heat Transfer*, Vol. I. Chap. 29, p. 620-635, Wiley, New York, 1949.

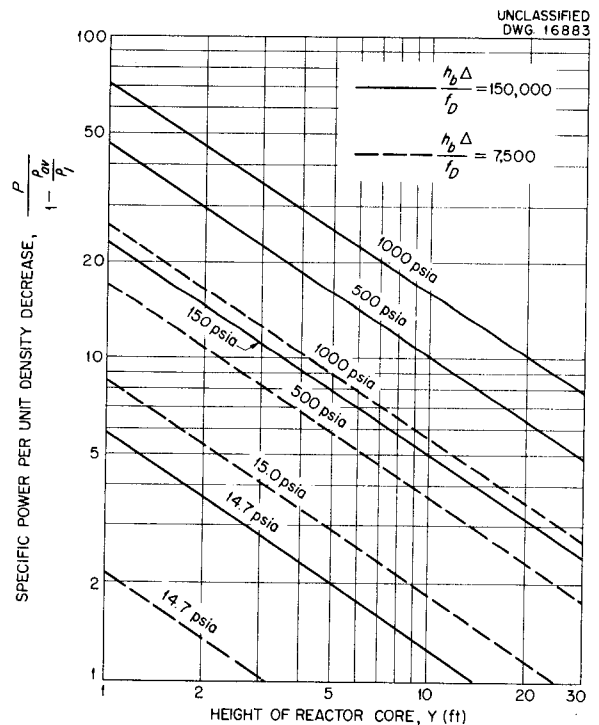
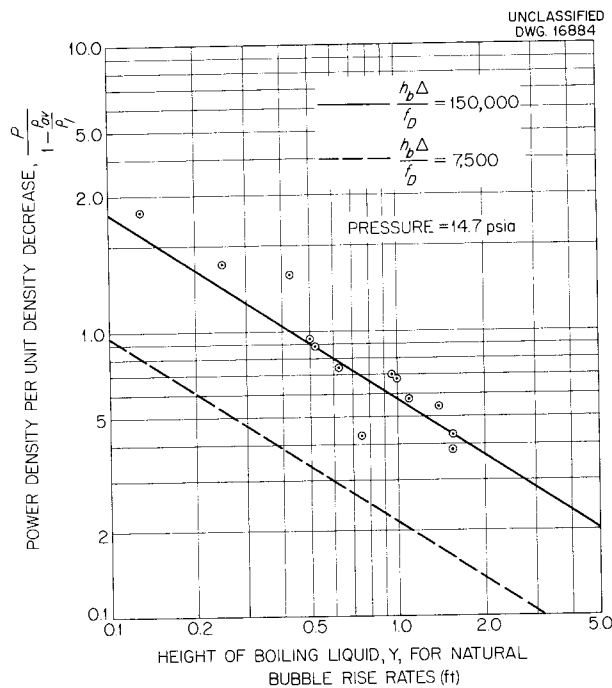


Fig. 6. Power Density from Natural Bubble Rise Rates.

# HRP QUARTERLY PROGRESS REPORT



**Fig. 7. Comparison of Theory with Experiment in Volume Boiling.**

and amounts to approximately  $70,000 \text{ Btu hr}^{-1} \text{ ft}^{-2}$  for this range of experimental work. These results can hardly be considered conclusive, since an independent check on the value of  $h_b \Delta / f_D$  should be obtained (from high-speed photographs of the bubble rise and growth in a volume boiling system, for example).

**Internal Circulation.** For an internal circulation velocity in the vertical plane that is appreciably greater than the relative bubble velocity, the average power density in a boiling reactor core is given by

$$P = \frac{U_1}{26.8} \left( \frac{A_1}{AY} \right) \left( \frac{h_{fg}}{v_{fg}} \right) \left( \frac{\rho_1}{\rho_2} - 1 \right), \quad (7)$$

where subscript 1 refers to the inlet condition and subscript 2 refers to the terminal condition. A schematic design of two possible systems is shown in Fig. 8.

In order to relate the average power density (Eq. 8) to the mean

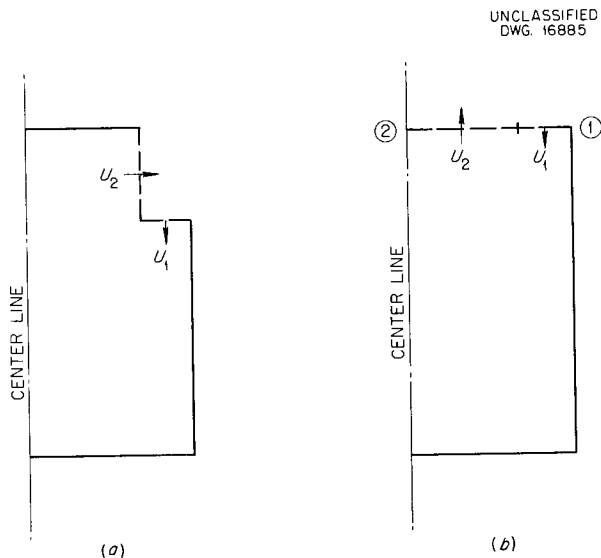


**Fig. 8. Schematic Diagram of Two Idealizations of a Cylindrical Reactor Core in Which Internal Circulation Exists.** The center lines are axes of symmetry.

density of the reactor core, it is necessary to consider the circulation pattern and the manner of vapor formation in the core. Postulating that the circulation velocity can be derived from a potential function, the equation for vapor generation and conservation of mass become, respectively,

$$\frac{\partial^2 \psi}{\partial y^2} + \frac{4}{r} \frac{\partial}{\partial r} \left( r \frac{\partial \psi}{\partial r} \right) + w''' = 0 \quad (8)$$

and

$$\frac{\partial}{\partial y} \left( \rho \frac{\partial \psi}{\partial y} \right) + \frac{4}{r} \frac{\partial}{\partial r} \left( r \rho \frac{\partial \psi}{\partial r} \right) = 0, \quad (9)$$

where  $r$  and  $y$  are normalized to the core radius and height.

The average density is

$$\rho_{av} = \frac{\iint r \rho \, dr \, dy}{\iint r \, dr \, dy}. \quad (10)$$

If the volume generation function,  $w'''$ , is taken proportional to the product of the macroscopic fission cross section and the thermal-neutron flux, it appears that an iterative process

can be applied to determine  $w'''$  and hence  $\rho$  and  $\rho_{av}$  by utilizing the standard two-group equations and taking advantage of the thermal-neutron flux being relatively insensitive to density changes.

As a start,  $w'''$  has been taken proportional to the thermal-neutron flux for the uniform density case [ $J_0 (2.405 r) \sin(\pi y)$ ]. With this assumption, Eqs. 8, 9, and 10 will provide a first approximation to the relationship between the core mean density and the initial and terminal densities,  $\rho_1$  and  $\rho_2$ . This calculation is being carried out by the Mathematics Panel.

Since the initial and terminal densities are unknown quantities, it is necessary to provide an additional relationship between them and the mean density in terms of a quantity that might be subject to estimation. The equation relating these densities in terms of the fraction of vapor recirculation is

$$\frac{\rho_{av}}{\rho_1} = \frac{\rho_{av}}{\rho_1} \left( \frac{1 - \eta \frac{\rho_1}{\rho_2}}{1 - \eta} \right), \quad (11)$$

where  $\eta$  is the fraction of the vapor that is recirculated.

In order to obtain a qualitative indication of the fraction of vapor recycled by the circulating fluid, a very simple flow pattern at the top (free surface) of the reactor core was postulated, and the following relation was obtained:

$$1 - \eta = 8 \left( \frac{1}{\frac{U_1}{U_b} + 1} \right)^2. \quad (12)$$

Rough calculations employing this equation indicate that internal circulation in a boiling reactor with a free surface may not permit any higher

power density than could be obtained by natural bubble rise rates.

**Power Removal by Natural Internal Circulation.** In order to estimate the power removal owing to natural circulation in the core of a cylindrical reactor, the following equations have been obtained:

$$P = \frac{U_2 A_2}{26.8 AY} \left( \frac{h_{fg}}{v_{fg}} \right) \left( 1 - \frac{\rho_2}{\rho_1} \right) \quad (13)$$

and

$$U_2 = \left[ \frac{2_g Y}{K_1} \left( \frac{\rho_0 - \rho_i}{\rho_{av}} \right) \right]^{1/2} = \left[ \frac{2_g Y}{K_2} \left( 1 - \frac{\rho_i}{\rho_0} \right) \right]^{1/2}. \quad (14)$$

Equation 13 is a rearrangement of the general expression for power density as previously presented in Eq. 7. Equation 14 provides the natural circulation velocity for use in Eq. 13. The densities  $\rho_0$ ,  $\rho_i$ ,  $\rho_2$ , and  $\rho_1$ , can be expressed in terms of the mean density of the reactor core and the fraction of vapor recirculated by using the potential flow solutions and Eq. 11.

Since the results of the potential flow considerations were not expected to be available for some time, some preliminary qualitative estimations of natural-circulation velocities and power removal for natural circulation were made to permit design of experiments. The equations for three postulated systems were developed for this purpose. The geometry considered is a right-circular cylinder with height equal to the diameter. In all cases it was considered that the circulation velocity was sufficiently large compared with the relative velocity of the bubbles that the fluid could be considered homogeneous. Additional postulations and resulting equations for each case are as follows:

*Case I.* For case I it was postulated that the circulation pattern,

## HRP QUARTERLY PROGRESS REPORT

bubble nucleation, and bubble growth are such that

$$U_1 = U_2 ,$$

$$\rho_0 - \rho_i = \frac{\rho_1 - \rho_2}{2} ,$$

$$\rho_{av} = \frac{\rho_1 + \rho_2}{2} ,$$

and the following equations were obtained:

$$\frac{P}{\left(\frac{\rho_i}{\rho_{av}} - 1\right)} = \left(\frac{\sqrt{2g}}{26.8}\right) \left(\frac{h_{fg}}{v_{fg}}\right) \left(\frac{\left(\frac{\rho_1}{\rho_{av}} - 1\right)^{1/2}}{K_1 Y}\right) , \quad (15)$$

along with Eq. 11.

*Case II.* For case II it was postulated that (1) the fluid flows downward in an annular region along the walls of the containing vessel to the bottom of the reactor core, reverses, and flows upward in the center to the top of the reactor core, (2) the cross-sectional area of the riser,  $A_2$ , is equal to that of the downcomer,  $A_1$ , and (3) the rate of vapor formation is uniform throughout the reactor core.

The following equations were then obtained:

$$U_2 = \left(\frac{2gY}{K_2}\right)^{1/2} \left[ 1 - \frac{\ln\left(\frac{2}{1 + \frac{\rho_2}{\rho_1}}\right)^{1/2}}{\ln\left(\frac{1 + \frac{\rho_1}{\rho_2}}{2}\right)} \right] , \quad (16)$$

$$\frac{\rho_{av}}{\rho_1} = \frac{\ln\left(\frac{\rho_1}{\rho_2}\right)}{\left(\frac{\rho_1}{\rho_2} - 1\right)} , \quad (17)$$

along with Eqs. 11 and 13.

*Case III.* For case III it was postulated that (1) the fluid flows downward in an annular region along the walls of the containing vessel to the bottom of the reactor core, reverses, and flows upward in the center to the top of the reactor core, (2) the cross-sectional area of the riser,  $A_2$ , is equal to that of the downcomer,  $A_1$ , and (3) the rate of vapor formation at any point is proportional to  $J_0 (2.405 r) \sin \pi z$ . The following equations were obtained, along with Eqs. 11, 13, and 14:

$$\frac{\rho_{av}}{\rho_1} = \frac{\rho_0 + \rho_i}{2\rho_1} = \frac{1}{2} \left\{ \frac{1}{\left[1 + 0.184 \left(\frac{\rho_1}{\rho_2} - 1\right)\right]^{1/2}} + \frac{\frac{\rho_2}{\rho_1}}{\left[1 - 0.78 \left(1 - \frac{\rho_2}{\rho_1}\right)\right]^{1/2}} \right\} , \quad (18)$$

$$1 - \frac{\rho_i}{\rho_0} = 1 - \frac{\frac{\rho_2}{\rho_1} \left[1 + 0.184 \left(\frac{\rho_1}{\rho_2} - 1\right)\right]^{1/2}}{\left[1 - 0.78 \left(1 - \frac{\rho_2}{\rho_1}\right)\right]^{1/2}} . \quad (19)$$

Cases I, II, and III are being examined and compared over a range of the pertinent variables.

A simple experiment is being planned in which air will be bubbled through a 6-ft-dia tank filled with water. Although no quantitative results applicable to water-steam systems are expected from this experiment, it appears that this study can yield information on the behavior of large-scale two-phase systems. In particular, the density decrease for various air-volume-throughput rates and the influence of circulation on density decrease for a given air throughput will be determined.

**General Comments on Power Removal from Boiling Reactors.** At the present time a number of tentative conclusions can be drawn from the work outlined: (1) surface evaporation is probably a negligible factor in power removal except for very small reactors operating at low power; (2) for boiling reactors up to 3 to 4 ft in height, the predominant mechanism for power removal is natural bubble rise and

growth; (3) for boiling reactors having a free surface and in which circulation exists, it appears that vapor entrainment in the circulating fluid will limit the power removal.

**Criticality Calculations.** In order to get a rough indication of permissible density decrease for power removal considerations, enrichment required for criticality was calculated for a number of  $UO_2SO_4-D_2O$  systems. For each operating condition, the influence of decreasing the density ratio ( $\rho_{av}/\rho_l$ ) was determined. Representative results for 250°C operation are shown in Figs. 9 and 10. Figure 9 displays the influence of the density

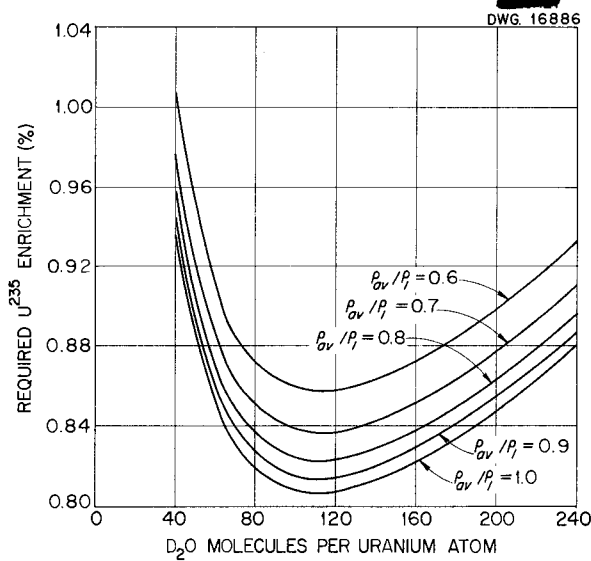


Fig. 9. Influence of Density Decrease on Required Enrichment for a 20.5-ft-dia, Square Cylindrical,  $UO_2SO_4-D_2O$  System at 250°C.

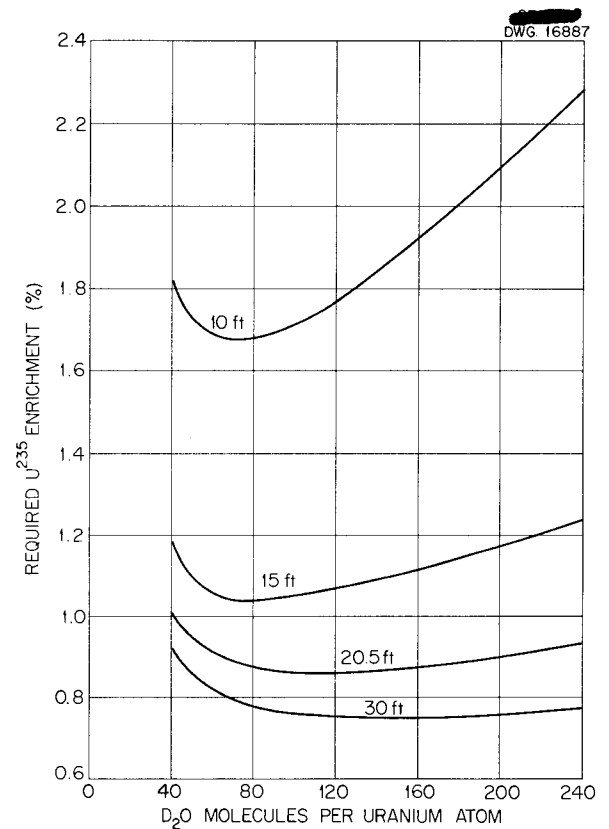


Fig. 10. Influence of Core Size on the Required Enrichment for a Square Cylindrical,  $UO_2SO_4-D_2O$  System for an Operating Temperature of 250°C and a Density Ratio ( $\rho_{av}/\rho_l$ ) of 0.6.

## HRP QUARTERLY PROGRESS REPORT

ratio for a 20.5-ft-dia square cylindrical core. Figure 10 shows the influence of core size for a density ratio of 0.6. Calculations were based on the two-group criticality equation for bare cylinders. Uniform density was postulated.

### STUDY OF LARGE-SCALE BOILING REACTOR SYSTEMS

P. C. Zmola

A study has been initiated of a large-scale homogeneous boiling reactor that will exist only on paper (paper boiling reactor, PBR). The purpose of the study is to help evaluate, clarify, and possibly uncover problems that would arise if an actual boiling reactor were designed for some specific economic objective. During the course of the study the envisioned specific application of the reactor may be changed from time to time so that the maximum understanding of the nature of boiling reactor problems will be obtained. Initially the PBR will be a power and plutonium producer. Because of the limited effort allocated to this program, only a preliminary outline of the problem is available.

### BOILING REACTOR EXPERIMENTS

At least two boiling reactor experiments are planned in the future: (1) the Teapot, a small reactor capable of operating over a wide pressure range, and (2) a 6-ft reactor to operate at 1 atmosphere. A building has been designed to house these experiments, as well as other reactor experiments that may be proposed. The building is to provide maximum flexibility in changing from one reactor system to another.

### BOILING REACTOR EXPERIMENT DESIGN

R. B. Briggs, Section Chief  
J. B. Brown      W. R. Gall  
R. L. Cauble      J. R. McWherter  
                    W. Terry

**Shield Design.** The boiling reactor experiment (BRE) is to be housed in a

building, similar to the HRE Building, located 90 ft to the west of the HRE Building. According to the present thinking, the reactor and associated equipment are to be housed in underground shields or pits, with access from the top. Flooding is considered desirable to facilitate maintenance of equipment. Although the first experiment, the Teapot, is to involve a core only 18 in. in diameter, the shield must be large enough that a 6-ft-dia reactor can be tested.

One of the more attractive proposals is shown in Fig. 11 with a 6-ft-dia core in place. The shield is divided into several compartments to permit segregation of equipment items containing materials of varying activity levels or having varying accessibility requirements. Induced activity and radiation damage are important considerations in the reactor compartment only. Part of the shielding between the reactor and the other cells will be in the form of permanent concrete walls to permit flooding of individual cells for equipment removal or repairs.

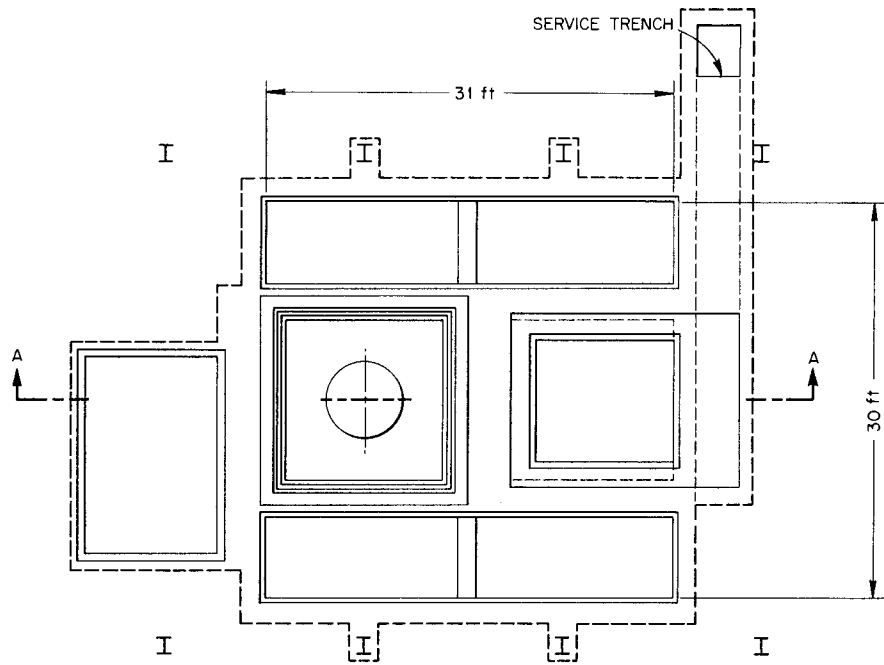
A 12-ft-square compartment is considered to be large enough to accommodate a 6-ft-dia reactor. Additional shielding water or concrete will be provided between the core tank and the cell walls to reduce the induced activity in the permanent walls. A similar cell at a lower level is provided to house the dump tanks to permit a gravity dump from the core. Seven-foot-wide compartments along both sides of the core and dump tank cells will provide housing for other components and instrumentation. With allowance for permanent concrete walls between cells, approximately a 30-ft-square space is required within the outer shield.

The optimum elevation of the reactor shield with respect to the building floor depends on the saving in shielding and building costs vs. the cost of excavation and retaining walls. Calculations indicate that the underground

TABLE 1. NOMENCLATURE

$P_{se}$ = power density due to surface evaporation, kw/liter	$U_2$ = average final fluid velocity in circulating system, ftsec <sup>-1</sup>
$h$ = heat transfer coefficient, Btu hr <sup>-1</sup> ft <sup>-2</sup> °F <sup>-1</sup>	$g$ = gravitational constant, ft sec <sup>-2</sup>
$\Delta$ = temperature difference, °F	$D_b$ = diameter of bubble, ft
$(h\Delta)_s$ = heat flux in surface evaporation, Btu hr <sup>-1</sup> ft <sup>-2</sup>	$f_D$ = drag coefficient of bubble, dimensionless
$h_b$ = heat transfer coefficient to the bubble, Btu hr <sup>-1</sup> ft <sup>-2</sup> °F <sup>-1</sup>	$h_{fg}$ = latent heat, Btu lb <sup>-1</sup>
$Y$ = height of reactor core, ft	$v_{fg}$ = specific volume change in evaporation, ft <sup>3</sup> lb <sup>-1</sup>
$P$ = power density, kw/liter	$A$ = cross-sectional area of cylindrical core, ft
$\rho_l$ = density of liquid, lb ft <sup>-3</sup>	$A_1$ = initial flow area in circulating system, ft <sup>2</sup>
$\rho_v$ = density of vapor, lb ft <sup>-3</sup>	$A_2$ = final flow area in circulating system, ft <sup>2</sup>
$\rho_{av}$ = average density of reactor core, lb ft <sup>-3</sup>	$\psi$ = velocity potential function, dimensionless
$\rho_1$ = average initial core fluid density in circulating system, lb ft <sup>-3</sup>	$r$ = normalized radius, dimensionless
$\rho_2$ = average final core fluid density in circulating system, lb ft <sup>-3</sup>	$y$ = normalized height, dimensionless
$\rho_i$ = average fluid density in outside annular region of a circulating system, lb ft <sup>-3</sup>	$\eta$ = fraction of vapor arising at top of reactor core that is entrained and recirculated, dimensionless
$\rho_0$ = average fluid density in central region of a circulating system, lb ft <sup>-3</sup>	$K_1$ = loss coefficient based on $\rho_{av}$ , dimensionless
$U_b$ = maximum bubble rise velocity, ft sec <sup>-1</sup>	$K_2$ = loss coefficient based on $\rho_0$ , dimensionless
$U_1$ = average initial fluid velocity in circulating system, ft sec <sup>-1</sup>	





PLAN  
TOP PLUGS REMOVED

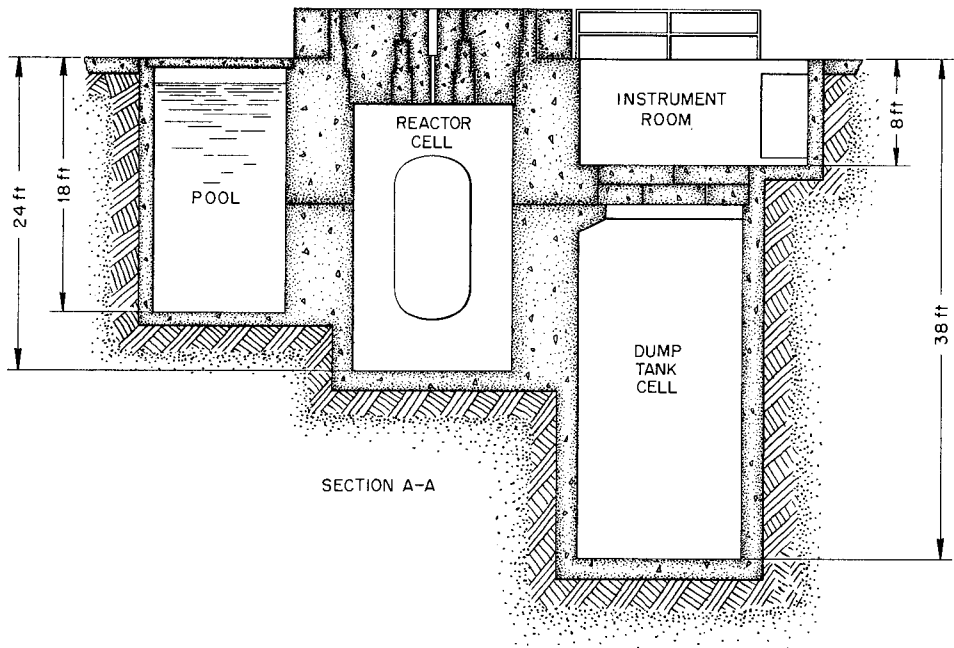


Fig. 11. BRE Shield Layout.

## HRP QUARTERLY PROGRESS REPORT

shield shown in Fig. 11 is much less expensive than one above ground with the same free volume.

**Disposal of Core Tanks.** A study of the induced activity in the 18-in.- and 6-ft-dia core tanks indicates that no serious radiation hazard will be encountered in remotely handling the tanks after shutdown. Equipment can be dismantled with the cells flooded. A temporary shadow shield can be used to protect the crane operator while the core tank is being lifted out of the shield and moved to an underwater storage pit adjacent to the reactor.

The thermal-neutron leakage from the 18-in. core tank during operation will be  $3 \times 10^{12}$  neutrons/cm<sup>2</sup>·sec at 1 megawatt. The thermal leakage from the 6-ft core will be  $1 \times 10^{10}$  neutrons/cm<sup>2</sup>·sec at 2 megawatts. After six months of full-power operation and one day of decay, the difference in radiation doses an operator would receive with or without a 16-in., ordinary-concrete, shadow shield are shown in Table 2.

**Teapot Design.** Efforts have been directed toward detailed design of components and piping layouts of the 18-in.-dia core vessel experiment. A layout has been made of the reactor components mounted on a steel framework so that the experimental equipment can be assembled and tested at one location and then moved as a unit to the site. One of the main disadvantages to this type of setup is the radiation hazard encountered in replacing equipment. Removable shielding can be used to partially protect equipment from excessive

induced activity and radiation damage. It will be possible to flood the cell when maintenance is required, but precautionary measures will have to be taken to prevent damage to electronic equipment.

The Teapot flowsheet is shown in Fig. 12, exclusive of the off-gas system. The possibility of using a single dump tank is being investigated. Addition of fuel by pressurizing the small weigh tank will be tried. If this is unsatisfactory, a diaphragm feed pump will be used.

The 18-in.-dia core tank is being designed for a pressure of 1000 psi with 3/4-in.-thick, type 347 stainless steel walls and ellipsoidal end caps. Designs have been made for the catalytic recombiner and the after-condenser. An assembly drawing of these units is shown in Fig. 13.

The design of a quick or remote method of replacing rupture disks has been started. The development of this method may require considerable effort, but it will be useful in other experiments in which radiation is a problem, as well as in this experiment.

**Treatment of Waste Gases** (C. W. Oxford, C. G. Lawson). The off-gas stream from the boiling reactor will contain xenon, krypton, hydrogen, and oxygen and possibly elemental iodine and bromine or HI and HBr. For a reactor operating at 250 kw for a period of 8 hr, the quantities of gases formed, assuming the fission yields given by Hunter and Ballou<sup>(3)</sup> and the

(3) H. F. Hunter and N. E. Ballou, *Simultaneous Slow Neutron Fission of U<sup>235</sup> Atoms*, ADC-65 (Feb. 24, 1949).

TABLE 2. RADIATION FROM BOILING REACTOR VESSELS

DISTANCE FROM VESSEL CENTER (ft)	BIOLOGICAL DOSE RATE (mr/hr)			
	18-in.-dia Vessel		6-ft-dia Vessel	
	No Shield	Shadow Shield	No Shield	Shadow Shield
25	$9.2 \times 10^3$	183	245	5
50	$2.3 \times 10^3$	46	61	1

DWG. 16662

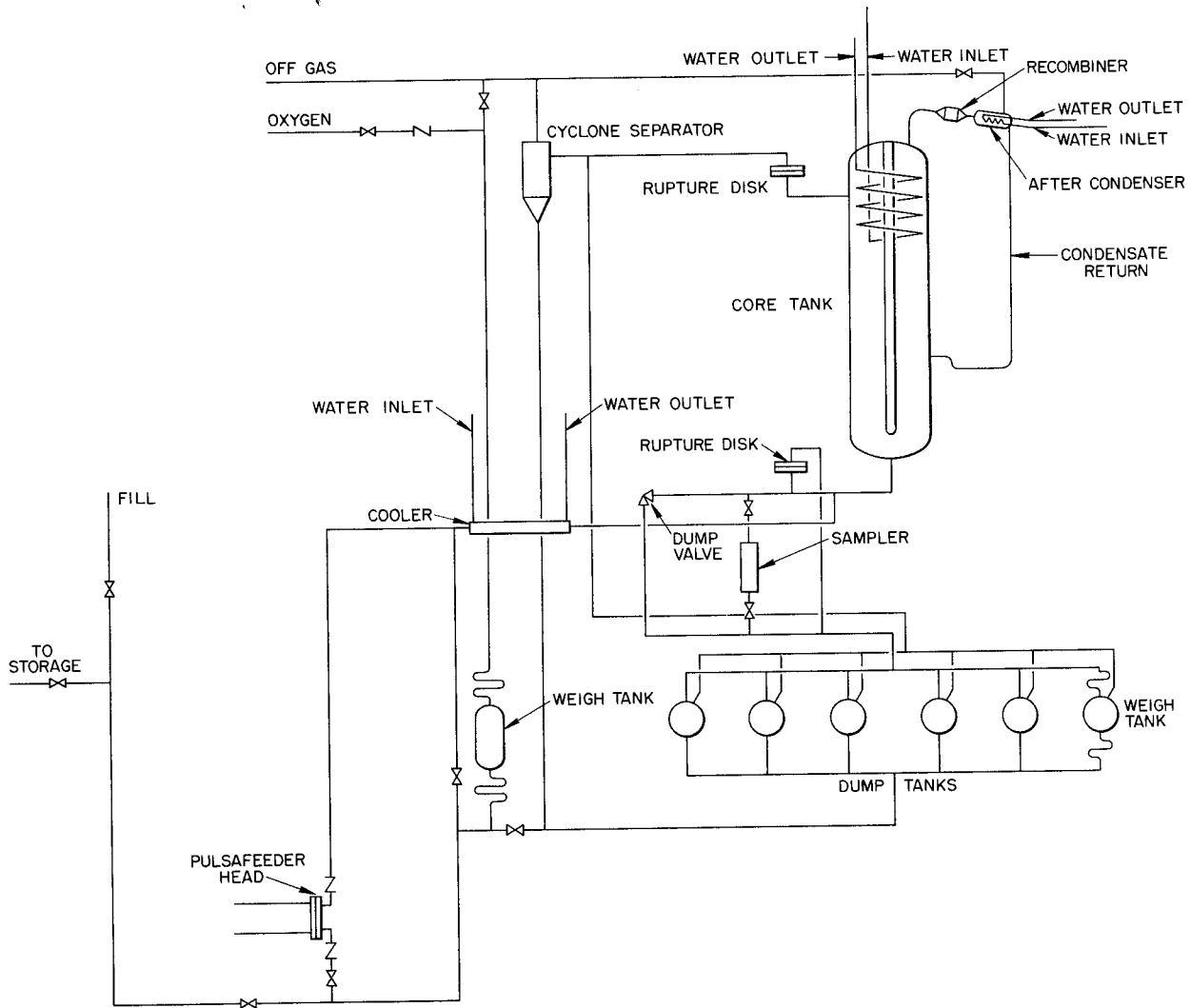


Fig. 12. Teapot Experiment.

decay rates given in the General Electric Company *Chart of the Nuclides*, are: Br,  $7.3 \times 10^{-5}$  g; I,  $6.24 \times 10^{-4}$  g; Kr,  $1.25 \times 10^{-3}$  g; Xe,  $1.39 \times 10^{-2}$  g;  $H_2 + 1/2 O_2$ , 2176 g (assuming a 99% efficient recombiner).

The heat generation during decay of these gases, if all the gamma energy and one-third the beta energy are converted to heat, is given in Table 3. The heat generation by the bromine and krypton are negligible within 15 hr after shutdown. The remaining heat generation is distributed approximately

TABLE 3. HEAT GENERATION DURING DECAY OF WASTE GASES

TIME AFTER 8 hr OF OPERATION (hr)	HEAT GENERATED (Btu/sec)
0	1
1	0.25
15	0.03
24	0.015
48	0.005
120	0.001

# HRP QUARTERLY PROGRESS REPORT

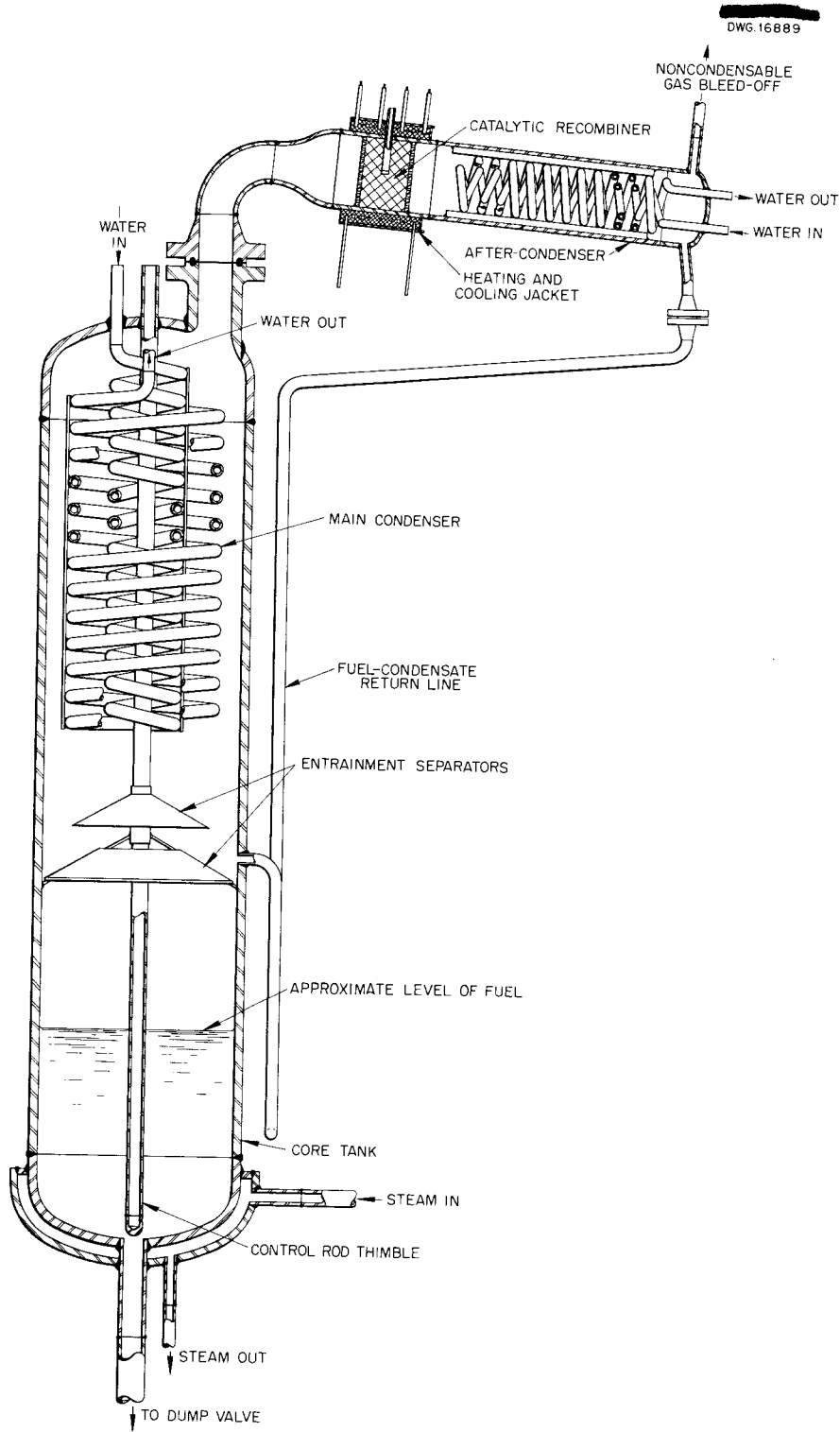


Fig. 13. Recombiners, Condensers, and 18-in.-dia Core Tank for Boiling Reactor Experiment.

evenly between the iodine and xenon. Further details will be given in a memorandum being prepared by C. W. Oxford.

The requirements for the off-gas system are to (1) prevent the build-up of an explosive concentration of  $H_2 + 1/2 O_2$ , (2) prevent active iodine from being discharged to the atmosphere, (3) reduce the quantities of activity discharged to the atmosphere to within tolerance levels. Design studies are being made to determine the optimum system for accomplishing these aims. The catalytic recombination of  $H_2 + 1/2 O_2$  will be accomplished by using either platinized alumina or heated copper. Iodine and bromine will be removed by using a silver nitrate tower or by charcoal adsorption. The xenon and krypton activity levels will be reduced by using a charcoal adsorbent bed or dilution tanks combined with a breather tank operating between the reactor core and the fuel storage vessel.

**Instruments** (W. Walker). The types of instruments necessary to perform the objectives of the boiling reactor experiment are being investigated, and during the investigation the diffi-

culties faced in operation of the HRE are being kept in mind. The nuclear instrumentation will consist of the standard nuclear instruments with the additions necessary to measure flux transients and vertical flux distribution.

Safety requirements will be satisfied by two replaceable rupture disks and a quick-opening dump valve. The dump valve is to be interlocked with nuclear and process instruments.

The process instrumentation will provide for the measurement of pertinent temperatures and pressures. Increased emphasis has been placed on accountability for the solution to at least 2% accuracy. A weight system will be provided to measure the amount of solution in the core vessel to at least 1%. Provision for a device to indicate the average vapor fraction in the core has also been made. A valve test loop is being designed that should yield valuable design data for the selection of valves for the BRE.

Package nuclear instrumentation has already been purchased, and design of the BRE should be frozen sufficiently in the next few weeks to enable selection of the process instruments.

## SLURRY FUEL STUDIES

### CHEMICAL STUDIES

F. R. Bruce, Section Chief  
 J. O. Blomeke      L. E. Morse  
 J. M. Fulmer      J. P. McBride

Work has continued on the development of slurries for use as homogeneous reactor fuels. At the present time the preferred slurry consists of  $UO_3 \cdot H_2O$  platelets, which are prepared by alternately hydrating at 80 to 90°C, autoclaving at 250°C, and calcining at 400°C. When prepared as slurries containing 250 g of uranium per liter, these platelets

exhibit relatively low settling rates, and complete sedimentation occurs in about 60 minutes. They have a pH of 6.5, which indicates that very low corrosion rates in stainless steel are to be expected. The erosion problem in a circulating system should be minimized, since the hardness of these crystals is only about one-third that of steel. The viscosity of this slurry is 50% greater than that of water and it has good flow and heat transfer characteristics.

Preliminary data obtained during the previous quarter indicated considerable corrosion when slurries

## HRP QUARTERLY PROGRESS REPORT

were irradiated at 250°C in type 347 stainless steel bombs. Further, there was evidence that caking was promoted by the irradiation process. In this quarter attention was centered on out-of-pile studies of corrosion and caking. More complete treatment of all the radiation data showed that the corrosion of type 347 stainless steel by slurries at 250°C was less than 1 mpy. This low corrosion rate was confirmed by out-of-pile tests that otherwise duplicated the radiation experiments. These experiments also demonstrated caking, which proved that caking cannot be attributed solely to the radiation process.

It now seems that there are no chemical factors that preclude the use of slurries contained in type 347 stainless steel for power- and plutonium-producing reactors operating at 250°C.

### Uranium Trioxide Chemistry

**Preparation of Pure Uranium Trioxide** (J. O. Blomeke). Previous studies have indicated that impurities, even when present in trace quantities, can influence markedly the characteristics of  $UO_3$  slurries heated at 250°C. The most significant impurities are  $UO_2^{++}$  and  $NO_3^-$  ions originating from the  $UO_2(NO_3)_2$  solutions used as starting material for  $UO_3$  preparation. The  $UO_2(NO_3)_2$  is occluded with the product  $UO_3$  in concentrations as high as 0.01 to 0.1%. Upon fragmentation of the  $UO_3$  crystals, the  $UO_2^{++}$  and  $NO_3^-$  are liberated and play an important role in determining the type and size of crystal that is ultimately formed in water at 250°C. Uranyl nitrate present in solution in concentrations of several hundred parts per million promotes caking, makes the redispersion of settled solids more difficult, and enhances corrosion.

The importance of eliminating the uranyl nitrate impurities from slurries becomes obvious in light of the above, and two methods have been found useful

for removing these impurities. One method was based on the known fact that part of the  $UO_2(NO_3)_2$  impurities may be leached from the  $UO_3$  by first grinding and then washing and digesting the solids at 250°C in water. By repeating this procedure a number of times, the  $UO_2(NO_3)_2$  concentration in the solid may be reduced to a very low value. It was also found that, under some conditions, repeated hydration and dehydration of  $UO_3$  resulted in degradation of particle size and liberation of trapped ions. Two samples of purified  $UO_3 \cdot H_2O$  have been prepared by following these procedures. The starting material for both preparations was  $UO_3 \cdot H_2O$  rods containing more than 500 ppm  $NO_3^-$ .

One sample of rods was micronized, washed, and autoclaved at 250°C three times. The product was in the form of small, irregular platelets of an average particle size of 3 microns. The solids were light yellow in color, had a nitrate concentration of 105 ppm, and a water content of 0.99 moles of  $H_2O$  per mole of  $UO_3$ . These platelets exhibited little tendency to grow to larger sizes at 250°C and, when prepared as a slurry containing 250 g of uranium per liter, did not cake or pack, and they settled to an even lower bulk density than comparable slurries of rods.

The second sample of rods was treated with the calcination-hydration procedure four times. After three calcinations (4 hr at 350°C) and hydrations, the  $NO_3^-$  concentration in the solids had dropped below 50 ppm, the limit of analytical detection. Following the fourth calcination and hydration, the hydrated  $UO_3$  was autoclaved at 250°C. It then formed very small platelets that were similar in size, color, and slurry characteristics to the micronized preparation.

Of these two procedures, the second appears to be the more attractive from the standpoint of purity of product and simplicity of processing. However,

the calcination-hydration technique has not been found to be entirely reproducible on a laboratory scale. At the present time a study is being made of the variables associated with this procedure, and it is hoped that a more dependable process that is suitable for larger scale production will result.

**Effect of Nitrate on Uranium Trioxide Stability** (J. O. Blomeke). Specimens of  $UO_3 \cdot H_2O$  slurries that have been exposed to radiation in the ORNL graphite reactor have repeatedly shown evidence of some reduction to a lower valence state. This is in contradiction to out-of-pile experiments in which  $UO_3$  has exhibited high stability at  $250^\circ C$  under pressures of hydrogen and oxygen mixtures. Since it is known that nitrate under radiation may be reduced to nitrite, which is a good reducing agent, it was suggested that the nitrate impurities present in these slurries might have served in this manner as a catalyst in the reduction of  $UO_2^{++}$  to  $U^{+4}$ . To determine whether nitrate would reduce  $UO_3$  at  $250^\circ C$ , three experiments were performed, as noted in Table 4. In none of these cases was there any tendency for the uranium to be reduced in the presence of nitrite. The oxidation of  $U^{+4}$  observed in these experiments confirms earlier work that indicated high  $UO_3$  stability. It

**TABLE 4. EFFECT OF NITRITE ON  $UO_3$  STABILITY**

Slurry: 100 g of U(as  $UO_3 \cdot H_2O$ ) per liter, with 1 g of  $NO_2^-$ (as  $NaNO_2$ ) added per liter

HEATING TIME AT $250^\circ C$ (hr)	$U^{+4}$ IN SOLID (%)	
	Originally	After Heating
92	0.36	0.29
92	0.097	0.04
112	0.097	0.005

was concluded from these experiments that the reduction observed under radiation was due either to some impurity other than nitrate or was a direct result of the radiation process itself.

**Particle Size and Surface Area Measurement** (L. E. Morse). The problem of determining particle sizes and surface areas of  $UO_3 \cdot H_2O$  powders and their relationships to sedimentation rates in slurries containing 250 g of uranium (as  $UO_3 \cdot H_2O$ ) per liter has been studied.

Several methods have been investigated for the desired measurements and the results are compiled in Table 5. Since the nitrogen adsorption determination is generally accepted as the best method, all other methods should agree reasonably well with it, and deviations should be low and such as might be reasonably expected from the particular measurement. It may be seen from the results presented that all three methods investigated satisfy these conditions.

The surface area per gram and the particle diameter,  $d_{s,v}$ , were related by the following equation:

$$S_v = \frac{6}{\rho d_{s,v}}$$

where

$S_v$  = surface area per gram,

$\rho$  = density,

$d_{s,v}$  = particle diameter =  $\frac{\text{surface area of particles}}{\text{volume of particles}}$ .

The term  $d_{s,v}$  is particularly suited for comparison of various methods, since the surface area can be determined in several different ways. Further, surface area is an important property in determining particulate properties of solids.

The results are not complete at this time, since methods of correlating particle diameters and sedimentation

# HRP QUARTERLY PROGRESS REPORT

**TABLE 5. PARTICLE DIAMETER AND SURFACE AREA OF A  $UO_3 \cdot H_2O$  POWDER OBTAINED BY VARIOUS METHODS**

METHOD	SURFACE AREA ( $\mu^2/g$ )	DIAMETER, $d_{sv}$ ( $\mu$ )
Sample 1		
Nitrogen adsorption isotherm	0.60	1.8
Sedimentation rate (100-g/l uranium suspensions)	0.41	2.6
Microscopic	0.25	4.3
Sample 2		
Nitrogen adsorption isotherm	0.45	2.4
n-Heptoic acid adsorption	0.41	2.6

rates in slurries containing 250 g of uranium (as  $UO_3 \cdot H_2O$ ) per liter have not been evaluated.

*Determination of Particle Size from Sedimentation Rates.* It is well known that sedimentation rates in concentrated suspensions differ from those in dilute suspensions in which Stokes law is applicable. A method of calculating particle sizes from sedimentation rates in concentrated suspensions has been presented by Allison and Murray.<sup>(1)</sup> It is pointed out that the movement of a mass of particles through a stagnant column of fluid and the flow of a fluid through a porous bed of particles are analogous. The equations applicable to the latter case, which are well known, should also apply to the former case. This leads to the following result:

$$\frac{dV_s}{dt} = \frac{60gAe^3d_s}{5\eta S_v^2 (1-e)^2},$$

where

$\frac{dV_s}{dt}$  = change in volume of sediment with time,

(1) E. B. Allison and P. Murray, *Sedimentation from Concentrated Suspensions in Relation to Particle Size*, AERE M/R 829 (Nov. 26, 1951).

$g$  = 980 cm/sec<sup>2</sup>,  
 $A$  = area of cross section of sediment bed,  
 $d_s$  = density of sediment at time  $t$ ,  
 $\eta$  = viscosity of fluid,  
 $S_v$  = surface area of particles per unit volume,  
 $e$  = porosity of sediment =  $V_l/V_s$ ,  
 $V_l$  = volume of liquid in sediment,  
 $V_s$  = volume of sediment.

It follows then that if  $dV_s/dt$  is plotted versus  $e^3d_s/(1-e)^2$  a straight line passing through the origin will be obtained that has a slope equal to

$$\frac{60gA}{5\eta S_v^2},$$

and since all values except  $S_v$  are known, the surface area may be calculated.

The surface area per unit volume,  $S_v$ , is related to  $S_v$  and  $d_{sv}$  by the following expression:

$$\frac{S_v}{\rho} = S_v = \frac{6}{\rho d_{sv}}.$$

It is worthwhile to note that the particle diameter is determined from the surface area.

The results given in Table 5 were obtained by observing the sedimentation rate of slurries containing 100 g of uranium per liter in a Nessler tube.

It was found that when the concentration of uranium was increased to 250 g of uranium per liter, this treatment was not applicable. The explanation for this appears to be that at a uranium concentration of 100 g/liter, flocculation during sedimentation does not occur, whereas at higher concentrations, flocculation does occur. Sedimentation-time curves are given in Fig. 14 for the two slurries at different concentrations. It will be seen that with 100 g of uranium per liter, the settling rate decreases with time, whereas with 250 g of uranium per liter, the sedimentation rate remains constant. This would indicate the formation of larger particles at such a rate that the decrease in sedimentation rate is opposed by the more rapid settling rate of the larger particles. Since the method of treatment is based on the flow of fluids through a porous

bed of unchanging particles, the occurrence of flocculation renders the treatment invalid.

Comparison of the nitrogen adsorption results with sedimentation results shows that lower values of  $S_w$  and  $d_{s,v}$  were obtained by the latter method. This is expected since the formation of a fluid film about the particles will effectively increase the particle diameter.

*Microscopic Method of Surface Area Determination.* Photomicrographs (800X) of  $UO_3 \cdot H_2O$  powders were made and particle diameter and surface area obtained according to methods described by DallaValle.<sup>(2)</sup> The values given in Table 5 were calculated from the following results and equations:

$$d_g = \text{geometric mean particle diameter} = 3.4 \mu,$$

$$\sigma_g = \text{geometric standard deviation} = 2.7 \mu,$$

$$\log d_{s,v} = \log d_g + 5.757 \log^2 \sigma_g,$$

$$S_w = \frac{6}{d_{s,v}}.$$

The  $d_{s,v}$ , defined as above, contains a statistical correction for a spread in particle size distribution.

It is believed that the explanation for the larger values obtained for the particle diameter by microscopic analysis compared with those obtained by nitrogen adsorption lies in a subconscious tendency to bias results in favor of the larger particles, since they are easier to see.

*n-Heptonic Acid Adsorption Method of Surface Area Determination.* The n-heptonic acid adsorption method was developed to have at hand a rapid method for measuring surface areas that would give results comparable with those obtained by nitrogen adsorption. Table 5 shows that this method will yield the desired results.

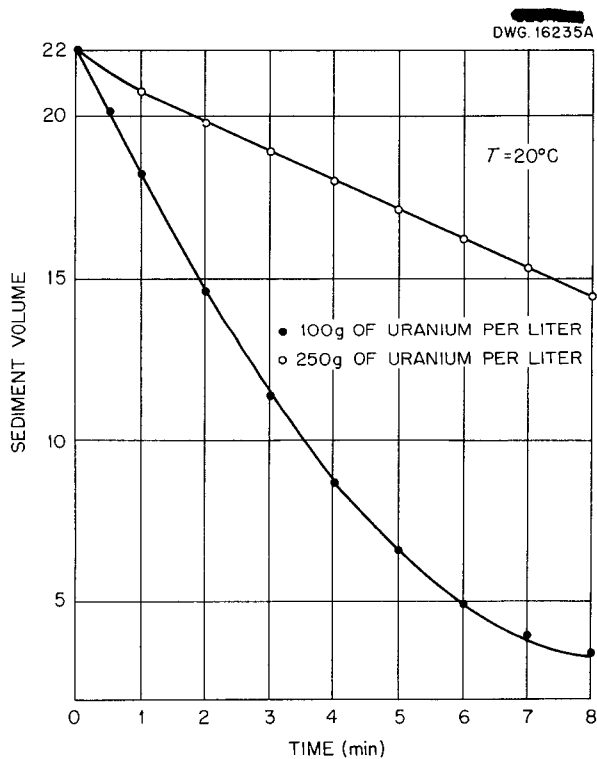


Fig. 14. Sedimentation Curves for  $UO_3 \cdot H_2O$  Slurries.

(2) J. M. DallaValle, *Micromeritics*, 2d ed., Pitman, New York, 1948.

## HRP QUARTERLY PROGRESS REPORT

Briefly, the procedure finally evolved was to shake a weighed sample of  $\text{UO}_3 \cdot \text{H}_2\text{O}$  powder (4 to 5 g) with 50 ml of *n*-heptoic acid-isopropyl alcohol (0.3 mg/ml *n*-heptoic acid/ml) solution for 1 hour. An aliquot of the supernatant was run into an equal volume of 0.01 *N* NaOH and the excess alkali was back-titrated with 0.01 *N* HCl to a phenolphthalein end point. The change in concentration of acid owing to adsorption is related to the surface area of the powder by assuming that the cross-sectional area of the *n*-heptoic acid molecule is  $25 \times 10^{-16}$   $\text{cm}^2$ . This method was adapted from one described by Saunders,<sup>(3)</sup> who used aqueous solutions of *n*-heptoic acid.

**Density of  $\text{UO}_3 \cdot \text{H}_2\text{O}$  Platelets** (J. O. Blomeke). As an adjunct to particle size studies, the density of a very pure sample of  $\text{UO}_3 \cdot \text{H}_2\text{O}$  platelets was measured by using a pycnometer and found to be 5.72 g/ml at 25.4°C. This value lies within the range of 5.5 to 6.0 g/ml that is most frequently quoted for  $\text{UO}_3 \cdot \text{H}_2\text{O}$  in the literature.

**Crystal Structure of  $\text{UO}_3 \cdot \text{H}_2\text{O}$  Bipyramids** (J. O. Blomeke). Single crystal x-ray diffraction studies made with a precession camera by R. D. Ellison have indicated that the cell sizes and intensities of reflections of the bipyramid crystals are those of a  $\beta\text{-UO}_3 \cdot \text{H}_2\text{O}$ , reported by Zachariassen.<sup>(4)</sup> This indicates that the bipyramids, originally reported here as being triclinic, have, instead, an orthorhombic structure.

### Radiation Chemistry

J. P. McBride

**Slurry Irradiations.** In current radiation work, emphasis is still on

(3) L. Saunders, *J. Chem. Soc.*, p. 969-73 (1948).

(4) W. H. Zachariassen, *X-Ray Diffraction Studies of Miscellaneous Uranium Compounds*, MDDC-1152 (June 1946).

the reactor irradiation of both natural and enriched slurries in steel containers. To facilitate this, hole 11 of the ORNL graphite reactor has been modified and instruments have been installed for recording pressure and controlling and recording temperature. These instruments were tested and adjusted in an extended irradiation run. The bombs prepared for use in the experiments have been modified to include an improved magnetic stirring device, and the rounded bottoms have been flattened. It is hoped that these modifications will keep the slurry dispersed during irradiation and make subsequent removal of the slurry from the bomb easier.

The installations at hole 11 were tested in a radiation run in which a natural uranium slurry of  $\text{UO}_3 \cdot \text{H}_2\text{O}$  platelets with 250 g of uranium per liter and about 0.01%  $\text{NO}_3^-$  impurity was used. The slurry was irradiated 21 days at 250°C and full flux. Gas production was insignificant, rising to 150 psi in excess of steam pressure in 4 days and dropping to 10 to 70 psi during the latter part of the run. Analysis of the irradiated slurry is still incomplete.

**Gas Recombination Studies.** The out-of-pile rate of recombination of hydrogen and oxygen in a slurry of  $\text{UO}_3 \cdot \text{H}_2\text{O}$  platelets with 250 g of uranium per liter at 250°C was determined by E. L. Compere and H. H. Stone of the Chemistry Division. The studies were carried out in new stainless steel bombs simultaneously with analogous studies in which  $\text{UO}_2\text{SO}_4$  solutions containing 40 g of uranium per liter were used. The rate of recombination in the slurry system was approximately one half that of the  $\text{UO}_2\text{SO}_4$  solution and gave a first-order solution rate constant of 2  $\text{hr}^{-1}$ .<sup>(5)</sup> The rates observed in the  $\text{UO}_2\text{SO}_4$  solution were about ten times faster

(5) H. F. McDuffie et al., *HRP Quar. Prog. Rep. March 15, 1952*, ORNL-1280, p. 161.

than previously observed by these investigators and were presumably due in part to activation by the interior surfaces of the new bombs. A rate constant approximately ten times less than the above could account for the 1500 to 3000 psi of gas pressure in excess of steam observed in previous irradiation studies in which enriched slurries were used.

### Corrosion Studies

**Evaluation of Pretreatment Procedures** (J. P. McBride). To find the effect of pretreatment on the corrosion rate of type 347 stainless steel and to determine the corrosion to be expected out of the reactor but under conditions analogous to those during the radiation experiments, three corrosion experiments were performed. The bombs used in the studies were pretreated by etching for 1/2 hr at room temperature with 2% HF-20% HNO<sub>3</sub> solution and then one bomb was contacted with 1% HNO<sub>3</sub> at 275°C for 13 to 14 hr, one bomb was treated with tank oxygen at about 180 psi and 260°C for 20 hr, and the third bomb was subjected to saturated steam and a partial pressure of 180 psi of oxygen at 255°C for 16 hours. The surfaces resulting from the 1% HNO<sub>3</sub> pretreatment and the wet-oxygen pretreatment had dull brown discolorations, whereas the surface resulting from the treatment with tank oxygen was not discolored and, if anything, had a more lustrous appearance than originally. An average corrosion rate of about 0.5 mpy was observed in all tests on heating with slurry at 250°C (Table 6). It is significant that caking was observed in all three bombs under conditions duplicating previous radiation runs. Consequently, it is concluded that caking is not solely a result of irradiation.

For the corrosion experiments, each bomb was charged with 15 ml of a slurry of UO<sub>3</sub>·H<sub>2</sub>O rods with 250 g of uranium per liter and a weighed

corrosion sample (1/8 by 1/8 by 1/2 in.). Heating and shaking were accomplished by mounting the bombs in heaters placed on a Cenco-Meinzer seine shaker. Heating and shaking were continued for 15 days, and then the bombs were allowed to stand undisturbed an additional week before opening.

The experiment carried out in the dry-oxygen pretreated bomb went to dryness during the run and yielded an orange-red powder resembling the anhydrous oxide. The slurries from the other experiments were strongly caked and not easily transferred from the bombs. In addition, there was complete transformation to very large platelets and bipyramids. As mentioned above, some difficulty has been experienced in transferring the slurries from the radiation bombs after they have been allowed to stand several days at room temperature before opening. All the variables contributing to this apparent loss of dispersibility have not been studied, but it would appear that the phenomenon as observed in the radiation studies is not necessarily a radiation effect. Factors which may influence the caking are the conversion of rods to platelets, changes in the state of hydration occurring in the settled slurry on being cooled from 250°C to room temperature, and the geometry of the bomb interior.

**Effect of Impurities on Type 347 Stainless Steel Corrosion by Slurries** (J. M. Fulmer). The effect of UO<sub>3</sub> contaminants and hydrogen and oxygen gas on slurry corrosion of type 347 stainless steel was investigated. Pure UO<sub>3</sub>·H<sub>2</sub>O slurries under an atmosphere of hydrogen and oxygen exhibited a corrosion rate of about 0.6 mpy on type 347 stainless steel, whereas distilled water and uranyl sulfate showed corrosion rates of 0.4 and 45 mpy, respectively (Table 7). Dissolved salts, such as NaNO<sub>3</sub> and K<sub>2</sub>SO<sub>4</sub>, accelerated the corrosion rate

# HRP QUARTERLY PROGRESS REPORT

**TABLE 6. STATIC TESTS OF TYPE 347 STAINLESS STEEL CORROSION BY  $UO_3 \cdot H_2O$  SLURRIES**

OBSERVATION	ORIGINAL SLURRY	PRETREATMENT		
		1% $HNO_3$	Dry Oxygen	Oxygen and Steam
Duration of experiments (days)		15	15	15
Average temperature ( $^{\circ}C$ )		237	228	231
Average corrosion rate (mpy)				
From corrosion sample data		0.8	0.8	1.0
From Fe in slurry*		0.3	0.2	0.1
Analysis of solids				
U (%)	77.7	72.2	62.8	74.5
Fe (ppm)	58	262	199	121
Ni (ppm)	10	18	16	<12
Cr (ppm)	10	8	27	16
Analysis of Supernatants				
U (mg/ml)	< 0.020	0.140		0.076
$NO_3^-$ (mg/ml)	0.036?	0.025		0.028
Color of solids	Yellow	Yellow-tan	Orange-red	Yellow-tan
Crystal habit	Rods, < $5\mu$	Platelets, bipyramids, $\sim 80\mu$	Rods, < $5\mu$	Platelets, bipyramids, $\sim 40\mu$
State of slurries		Caked	Anhydrous	Caked

\*Based on the surface area covered by the settled slurry (about 0.9 in.<sup>2</sup>).

slightly, increased the concentration of soluble uranium, and promoted caking.

For this work, test specimens of type 347 stainless steel were held in the rocking autoclaves by type 347 stainless steel wires. The autoclave rocked 30 degrees through the horizontal, 37 cycles a minute, and the temperature was held at 250°C. The 320-ml autoclave contained 200 ml of the slurry. The corrosion film on the specimen was removed by electrolytic stripping in a 5% sulfuric acid bath containing an organic inhibitor, rodine.

## Slurry Boiling Studies

J. O. Blomeke

A description of the slurry boiler designed for investigating the characteristics and behavior of a  $UO_3 \cdot H_2O$  slurry boiling at 250°C was given in the previous quarterly report. It was pointed out that the most notable result of the first experiment with this boiler was the lack of any indication that foaming had occurred during the 4 1/2 hr of the experiment. The second boiler run also used washed, micronized, Mallinckrodt  $UO_3$ , but the run was of longer duration. After 288 hr of boiling the 1000-w

TABLE 7. CORROSION RATES ON TYPE 347 STAINLESS STEEL  
EXPOSED TO  $\text{UO}_3 \cdot \text{H}_2\text{O}$  SLURRIES AT  $250^\circ\text{C}$

Duration of Test: 20 hr  
Uranium concentration: 250 g/l

CORROSIVE MATERIAL	CORROSION RATE (mpy)
Distilled $\text{H}_2\text{O}$ (evacuated)	0.4
Distilled $\text{H}_2\text{O}$ plus 0.25% $\text{K}_2\text{SO}_4$	0.9
$\text{UO}_3 \cdot \text{H}_2\text{O}$ platelets (evacuated)	0.6
$\text{UO}_3 \cdot \text{H}_2\text{O}$ platelets plus air and 10 psi $\text{O}_2$	0.9
$\text{UO}_3 \cdot \text{H}_2\text{O}$ platelets plus air and 0.5% $\text{NaNO}_3$	0.5
$\text{UO}_3 \cdot \text{H}_2\text{O}$ platelets plus air and 0.25% $\text{K}_2\text{SO}_4$	0.7
$\text{UO}_3 \cdot \text{H}_2\text{O}$ platelets plus 60 psi of $\text{O}_2$ and 120 psi of $\text{H}_2$	0.6
$\text{UO}_3 \cdot \text{H}_2\text{O}$ platelets plus air and 0.25% $\text{NaNO}_3$	0.8
Washed, Mallinckrodt $\text{UO}_3 \cdot \text{H}_2\text{O}$ plus air	1.1
$\text{UO}_3 \cdot \text{H}_2\text{O}$ rods used in loop studies	0.3
$\text{UO}_2\text{SO}_4$ (270 mg of uranium per milliliter, pH 1.65)	45

heater failed and the run was terminated. Inspection of the slurry revealed that a large loss in volume had occurred that was attributable to a vapor leak around the gasket. It should be pointed out that, as a result of this leak, a constant power density was not maintained within the boiler.

The results itemized in Table 8 are for the most part self-explanatory. This run was characterized by very large increases in the iron and chromium content of the solids. Although it is difficult to explain these increases except in terms of corrosion, it should be pointed out that such high corrosion rates have never been observed previously for purified slurries. A second inconsistency appears in the very large decrease in nitrate within the solids after boiling. This is not substantiated by a corresponding increase in the soluble uranium that would have

been expected to occur had the nitrate dissolved in the supernatant. This poor material balance might be explained on the basis of the nitrate decomposing to nitrogen oxides; however, this has never been previously observed in slurries heated at  $250^\circ\text{C}$ .

Contrary to observations of the first run, 7.6 g of uranium was found caked on the sides and bottom of the boiler. This material was removed by a dilute nitric acid wash. However, there was no evidence of foaming having occurred during the run.

#### PUMPING STUDIES

R. N. Lyon, Section Chief  
A. S. Kitzes            P. R. Crowley  
R. B. Gallaher        W. Q. Hullings  
C. A. Gifford

**High-Pressure Slurry Circulating System.** The total operating time of the  $250^\circ\text{C}$ , 1000-psi, slurry system has reached just over 1200 hr, of which

# HRP QUARTERLY PROGRESS REPORT

**TABLE 8. RESULTS OF SECOND SLURRY BOILER RUN**

Feed Material: Micronized, Mallinckrodt UO<sub>3</sub>, 250 g of uranium per liter  
 Heating Conditions: 288 hr at 250°C; 3793 w.net heat input; 134 g of H<sub>2</sub>O per minute, boil-up rate  
 Boiler Pretreatment: 1% HNO<sub>3</sub>

OBSERVATION	STARTING MATERIAL	AFTER BOILING
Physical character of slurry		
Volume (ml)	1000	315
Color	Yellow	Dark yellow
Crystal shape	Irregular solids	Very irregular platelets
Crystal size (μ)	1.5 <sup>(a)</sup>	15 <sup>(a)</sup>
Chemical character of slurry		
Solids (ppm)		
Fe	100	5530
Ni	< 50	< 50
Cr	< 50	1325
NO <sub>3</sub>	983	230
Supernatant		
U (ppm)	4	50 <sup>(b)</sup>
pH	5.40 <sup>(c)</sup>	5.87
Foaming <sup>(d)</sup>		None
Uranium in caked solids (g)		7.6

<sup>(a)</sup>Based on microscopic analysis.

<sup>(b)</sup>Corrected to basis of 1000 ml of volume.

<sup>(c)</sup>Not deaerated before measurement.

<sup>(d)</sup>Estimated from height of solids deposited on walls.

1120 hr represent the total time in which slurry was actually being circulated. The remainder of the time consists of short runs with water, nitric acid, and trisodium phosphate solution, which were used in preliminary tests of the equipment and in cleaning between slurry runs. A resume of the operating conditions and results follows:

1. A pretest run of 25 hr was made with demineralized water at 250°C.

2. Test S-1 was run for 3 hr with a slurry containing 78 g of uranium (as UO<sub>3</sub>·H<sub>2</sub>O) per liter. This test was shut down when it was found that a portion of the slurry was circulating through the bearings and up through a condensate line to the pressurizer. The condition was remedied by moving an orifice in the main stream to a point down stream from the pressurizer.

3. A pretest run of 30 hr was made with demineralized water to test the revised purge system.

## FOR PERIOD ENDING OCTOBER 1, 1952

4. Test S-2 was run for 113 hr with a slurry containing 50 g of uranium per liter. During operation, the concentration dropped to 26 g of uranium per liter, apparently because of oxide accumulation in the pressurizer. After the test, the main system was clean and there was no measurable wear of the bearings.

5. Test S-3 was run for 171 hr with a slurry containing 80 g of uranium per liter. During operation, the concentration dropped to 20 g of uranium per liter, and, finally, clear water was obtained in a sample from the main stream. Again, oxide apparently accumulated in the pressurizer.

6. A pretest run of 15 hr was made with demineralized water.

7. Test S-4 was run for 41 hr with a slurry containing 229 g of uranium per liter. During operation, the concentration dropped, in the first 21 hr, to 97 g of uranium per liter, and finally the system was shut down. For this run, a portion of the stream was by-passed to a point above the slurry surface in the pressurizer, and, after the test, dried oxide was observed on the walls of the pressurizer. Again, the oxide accumulation accounts for the drop in main stream concentration. No wear was observed on the bearings.

8. Test S-5 was run for 160 hr with a slurry containing 200 g of uranium per liter. During operation, the concentration dropped to 109 g of uranium per liter. After 2 1/2 hr of this run, the purge of condensate through the back of the motor was stopped. At the end of the run, approximately 0.0005 in. of wear was observed on the front Graphitar motor bearing.

9. Test S-6 was run for 179 hr with a slurry containing 133 g of uranium per liter. During operation, the concentration dropped to 97 g of uranium per liter. For some reason,

the power to the pump increased suddenly from 13.8 to 16.5 kw. The front bearing was found to have approximately 0.002 in. of wear on the diameter. The rear bearing and both front and back journals showed no change.

10. Test S-7 was run for 186 hr with a slurry containing 175 g of uranium per liter. During operation, the concentration dropped to 34 g of uranium per liter. After this test was started it was found that the oxide was impure; for example, it contained 120 ppm of nitrate. The position of the orifice was changed, and the orifice opening was increased to 1 inch. This raised the pump power demand to 15 kw. The total accumulated wear of the front bearing was unchanged after this test; that is, it remained at 0.002 inch. After this test, the equipment was torn down and examined carefully; no evidence of erosion was found. The system was then rebuilt as before, except that a new pressurizer was installed so that the entire process stream entered the pressurizer below the liquid surface and then passed out the bottom. In effect, the lower part of the pressurizer was made part of the main flow system.

11. Test S-8 was run for 95 hr with a slurry containing 177 g of uranium per liter. During operation, the concentration dropped to 110 g of uranium per liter, in 70 hr, and dropped rapidly thereafter. In this test 100 psi of helium was used, with steam, for pressurization. It was found at the end of the test that the pressurizer was clean, but coating was observed in the main stream piping.

12. Test S-9 was run for 162 hr with a slurry containing 215 g of uranium per liter, and the system was subjected to a partial pressure of 100 psi of oxygen at room temperature. During operation, the concentration dropped in 18 hr to 131 g of uranium

## HRP QUARTERLY PROGRESS REPORT

per liter. Twenty-six hours later the system pressure was increased by 100 psi (to 1100 psi) by raising the pressurizer temperature, and 4 hr afterward a sample was taken that showed a concentration increase to 235 g of uranium per liter. The fact that the uranium content was greater than the initial concentration is attributed to the number of samples taken with low concentration, which reduced the water inventory, and possibly to incomplete removal of the oxide coating after the preceding test. The pressure was then reduced to 1000 psi, and a day later the concentration was 180 g of uranium per liter. Ninety-one hours later the concentration dropped to 23 g of uranium per liter, and the system was shut down. Severe coating of the pipes was again observed, and the front pump bearing was found to be worn 0.009 inch. It was decided to replace the bearing with another Graphitar bearing, even though the bearing was not yet causing difficulty.

The principal conclusions to be drawn from these tests are that maintenance of slurry concentration in a circulating system at 250°C has not yet been achieved and that Graphitar may be an unsuitable material for long operation in the front bearing of a pump if slurry is to be permitted to enter the bearing.

The fact that increased pressure caused the concentration to increase is of interest, and an attempt will be made to observe this phenomenon again. In a subsequent test, now in operation, the addition of water to the system also caused a recovery of the concentration. The explanation in the latter case is that the flowing system is not completely full after several samples have been removed and that adding water helps to sweep away the coating that accumulates in the partly filled pipes.

Since the new pressurizer has been installed, all coating has appeared in the pipes rather than in the pressurizer. In most cases the coating is easily reslurried, and this lends support to the theory that the pipes are not completely full. There is no reason to believe that the problem of concentration drop cannot be solved, but at present there are insufficient experimental data to point positively to the solution of the problem.

It is believed that solution of the bearing problem lies either in a continuous purge of the bearings by water (perhaps condensate from the pressurizer as in the first four runs listed above) or in the use of harder bearing materials. A separate bearing test at room temperature has already indicated wear of Graphitar against titanium carbide in a slurry but no measurable wear with Stellite against Stellite under similar conditions.

**Glass Loop.** A 100-gpm glass loop has been built to observe flow patterns and to develop sampling techniques. The minimum velocities required to transport slurries of varying concentrations will also be determined.

**Second High-Temperature Loop.** Consideration is being given to the design of a second high-temperature slurry loop. The loop will be longer to provide a larger capacity for periodic sampling, and provisions will be made for heat transfer and pressure drop studies. A number of flanged sections will be made available for insertion of test sections of other materials for corrosion and erosion studies. Low-carbon steels and other alloy steels are some of the materials being considered for use in a slurry reactor.

**Viscosity Measurements.** As the purity of available oxides has been improved, it has become increasingly difficult to determine the plasticity parameters with the apparatus described in previous quarterly reports. The

settling rates of the pure oxide (low nitrate and uranyl ion content) slurries have increased so markedly (1 to 5 mm/sec) that solids settle out in the body of the cut-off valve and plug the capillary tube. The data do indicate, however, that for concentrations up to 200 g of uranium per liter, the coefficient of rigidity approximates the coefficient of viscosity for water, and the yield stress, if any, is low.

Existing equipment has been modified to eliminate the settling of solids in the cut-off valve body, and other techniques for measuring the apparent viscosity of  $\text{UO}_3 \cdot \text{H}_2\text{O}$  slurries are being studied in an effort to improve the reliability of the results obtained.

**Crystal Growth.** Uranium trioxide monohydrate crystals in the form of rods grew when autoclaved at  $250^\circ\text{C}$  for 24 hr or longer in stainless steel bombs. In 24 hr the rods increased from 1 to  $3 \mu$  in diameter and 5 to  $6 \mu$  in length to  $4 \mu$  in diameter and 15 to  $17 \mu$  in length. No perceptible increase in dimensions was found when the rods were autoclaved at  $250^\circ\text{C}$  for longer periods of time.

The crystal structure of  $\text{UO}_3 \cdot \text{H}_2\text{O}$  rods did not change when autoclaved for less than 48 hr in the presence of nitrate ions ( $\text{KNO}_3$ ). Some platelets were found upon microscopic examination when the rods were autoclaved at  $250^\circ\text{C}$  for at least 48 hr in the presence of 100 ppm of excess nitrate ions. At this nitrate content, the platelets converted from rods grew until some reached 400 to  $500 \mu$  after 168 hr of autoclaving at  $250^\circ\text{C}$ . The conversion of rods to platelets and the rate of crystal growth of the platelets were not augmented by increasing the nitrate ion concentration above 100 ppm. No change was evidenced when the rods were autoclaved at  $250^\circ\text{C}$  in the presence of 40 ppm of excess nitrate ions.

Tests are being continued in which the uranyl ion content is varied to determine the effect of these ions on the crystal structure of both rods and platelets. Information obtained by the Chemical Technology Division indicates that in the presence of excess uranyl ions, both rods and platelets convert to the bipyramid form.

**Criticality Experiments.** Equipment has been built and is being tested for determining the criticality of  $\text{UO}_3 \cdot \text{H}_2\text{O}$  particles settling in a static slurry. The tests will include the determination of settling rates of slurries containing 50 to 250 g of uranium per liter and the reliability of level indication and the dump valve system. The objective of these criticality experiments is two-fold: (1) to determine the critical height of a reactor using a turbulent, unstable,  $\text{UO}_3 \cdot \text{H}_2\text{O}$  slurry of varying concentrations, for a given moderator (normal water) height and (2) to determine the change in reactivity at various concentrations as the turbulence (agitation) is removed and the particles settle.

It is anticipated that the equipment will be checked and ready for installation in the Criticality Building (9213) by October 1, 1952, provided no major alterations to the system are needed. The system consists of a canned-rotor, fluid-bearing pump to supply slurry to the reactor and also to keep the slurry agitated in the storage tanks. An agitator will keep the particles suspended in the reactor, which is baffled to prevent formation of a vortex. A quick-opening dump valve in the bottom of the reactor and the immediate insertion of a safety rod are the means of controlling the reactor if it goes supercritical. Arrangements are being concluded for the preparation of enriched  $\text{UO}_3 \cdot \text{H}_2\text{O}$  rods. The rod form will be used because the process by which rods are

made is well standardized and a consistent product can be obtained, whereas the platelet process has not yet been well standardized. Since only nuclear data are to be obtained in the critical experiment, the results should be the same with either rods or platelets.

A second critical experiment program to study the influence of eddying in pumped solutions and slurries has been terminated to provide for better use of available manpower.

**Thorium Loop Test at 150°C.** A slurry containing 100 g of ThO<sub>2</sub> per liter (80 g of thorium per liter) has been circulated in the 110 to 150°C loop for over 100 hours. <sup>(6)</sup>

<sup>(6)</sup>A. S. Kitzes *et al.*, *HRP Quar. Prog. Rep.* Aug. 15, 1951, ORNL-1121, p. 160.

Heat transfer and abrasion studies were made. Preliminary data from this test showed that the ThO<sub>2</sub> was collecting on the walls of the heat transfer surfaces, as evidenced by a continual decrease in the over-all heat transfer coefficients. Chemical analysis of samples drawn from the loop during operation also indicated abrasion, since an increase in the iron, chromium, and nickel content of the solids was found.

This work has been temporarily halted because the packed stuffing box in the pump caused serious difficulty. Further use of this loop awaits construction of a new pump. A Richardson-Frithsen type, 3-hp pump appears suitable for this work, and parts are available for its construction.

**Part III**

**GENERAL HOMOGENEOUS REACTOR STUDIES**



## ISHR DESIGN

R. B. Briggs, Section Chief  
C. H. Barkeley      W. R. Gall      C. L. Segaser      F. C. Zapp  
R. H. Chapman      P. N. Haubenreich      M. Tobias

The necessity for designing and building an intermediate-scale homogeneous reactor as a second step in the development of aqueous homogeneous reactors for producing power and plutonium was discussed in a previous report.<sup>(1)</sup> The reasons for selecting 48 megawatts as the operating power and a 6-ft-dia spherical core for the reactor were explained. Information was presented concerning the heat production in the reactor vessel, shielding requirements, induced activity in equipment external to the reactor, and explosion hazards resulting from the presence of the explosive mixtures of D<sub>2</sub> and O<sub>2</sub> that form as the moderator is decomposed by radiation.

Discussion of this reactor was continued in the last HRP quarterly report.<sup>(2)</sup> A preliminary flow sheet was included, as were several arrangements of core tank and fuel-circulating system. A design for the reactor vessel was proposed and thermal stress calculations were reported. Some general information was given regarding the pumps, heat exchangers, and gas separators in the fuel-recirculating system and the high-pressure recombiner. Nuclear calculations reported<sup>(2)</sup> included the effect of temperature and concentration upon the critical enrichment, the criticality of dump tanks, and the effects of uranium concentration and pressurizer location upon the magnitude of power and pressure surges.

During the past quarter, effort has been devoted to a more detailed

examination of equipment items, the construction of the reactor and equipment cells, and some of the nuclear calculations. A start has been made in the investigation of a two-region, multipurpose ISHR as an alternate to the single-region reactor described in the previous reports.

### EQUIPMENT LAYOUTS

A requirement that the combined cells must retain all the solution and gases, which can be released in the event of a major break in the reactor vessel or piping, has been imposed on the design of the equipment cells for the ISHR. Estimates have been made of the volume required to contain the liquid and vapor resulting from expansion of the contents of the reactor system. Initial and final conditions for operating the ISHR, based on adiabatic expansion to 14.7 and 50 psia, are given in Table 9.

It is evident from the data in Table 9 that the actual pressure will depend upon the amount of condensation that occurs on cell walls and equipment as the liquid is discharged. The amount of condensation that can be expected is being investigated. In the meantime, it is being assumed, taking into account the air in the cells, that the pressure will not exceed 65 psia or 50 psig in the cells. This assumption appears to be reasonable, since the total free volume of cells within each shield that has been examined is near 50,000 ft<sup>3</sup>.

Previous cell layouts were not well suited for design to contain pressures up to 50 psi; therefore a new study layout, shown in Fig. 15,

<sup>(1)</sup>R. B. Briggs et al., *HRP Quar. Prog. Rep.* March 15, 1952, ORNL-1280, p. 113 ff.

<sup>(2)</sup>R. B. Briggs et al., *HRP Quar. Prog. Rep.* July 1, 1952, ORNL-1318, p. 95 ff.

**TABLE 9. INITIAL AND FINAL CONDITIONS FOR OPERATING THE ISHR**

CONDITIONS	INITIAL VALUE	FINAL VALUE	
Pressure (psia)	1000	14.7	50
Temperature (°F)	482	217	286
Concentration of uranium as UO <sub>2</sub> SO <sub>4</sub> (g/l)	250	420	370
Volume of liquid (ft <sup>3</sup> )	371	245	273
Volume of H <sub>2</sub> , O <sub>2</sub> , and D <sub>2</sub> O vapor (ft <sup>3</sup> )	70		
Volume of H <sub>2</sub> and O <sub>2</sub> vapor (ft <sup>3</sup> )		1,977	624
Volume of D <sub>2</sub> O vapor (ft <sup>3</sup> )		184,800	44,900

has been prepared. The new layout has the following features:

1. The cells are gas tight to an internal pressure of 50 psi. The concrete walls are reinforced, lined with metal or an acceptable substitute, and tied together with cross beams. The narrowness of the cells reduces the upward load and simplifies the problem of anchoring the cell cover.

2. The fuel solution circulates through two external loop systems at 5000 gpm in each. Each heat exchanger removes 50 megawatts of heat so that the reactor may be operated at full rated power on one loop.

3. Either of the two circulating systems may be isolated, drained, and covered with water, for maintenance purposes, without shutting down the reactor.

4. All equipment, except the reactor vessel, is mounted on rollers to allow for thermal expansion away from the reactor core.

#### STEAM SYSTEM

An economic study of a steam power cycle for the ISHR<sup>(3)</sup> indicates that

<sup>(3)</sup>R. C. Robertson, *Preliminary Design and Cost Study of Power Generation Equipment for the Intermediate Scale Homogeneous Reactor*, ORNL CF-52-8-56 (Aug. 8, 1952).

a period of 3.3 years would be required for the power generated to pay off the investment in generating equipment and auxiliaries. The total investment would be approximately \$1,000,000, and the power generated would be worth \$350,000 per year at an 80% load factor. In contrast, a steam "killer" to condense the 200 psia saturated steam generated in the reactor boilers would require an investment of less than \$50,000. Consequently, it has been recommended that initial construction of the reactor include only a steam killer with provision for future addition of a building and equipment for power generation.

#### HEAT EXCHANGER

A survey of the literature has been made to obtain heat transfer data for boiling liquids on the shell side of a shell-and-tube exchanger. Complete results of the survey have been reported.<sup>(4)</sup>

Figure 16 is a plot of the calculated shell-side heat transfer coefficients for nucleate boiling from vertical surfaces and for forced convection of water boiling at 388°F and

<sup>(4)</sup>C. L. Segaser, *Heat Exchanger Design Study for the ISHR*, ORNL CF-52-10-195 (Oct. 22, 1952).

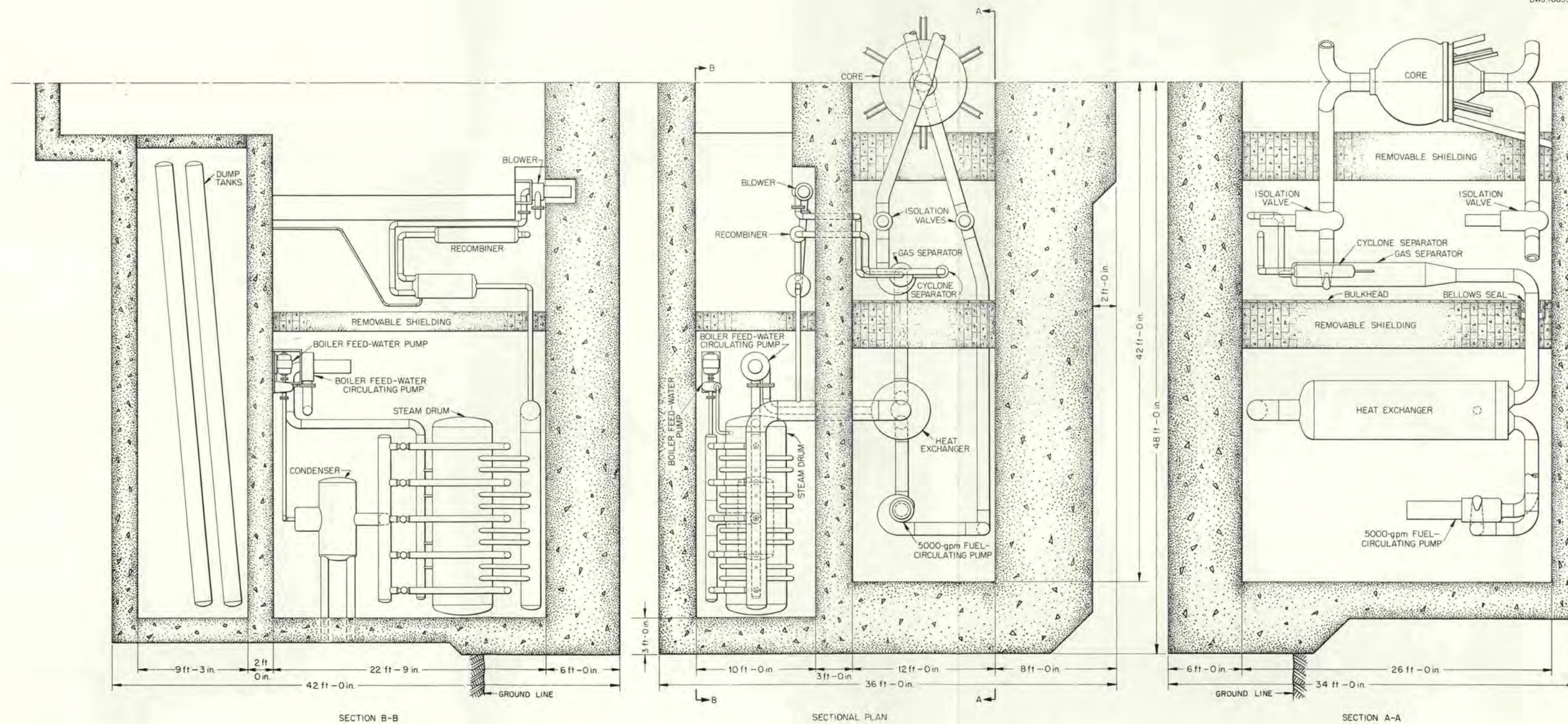
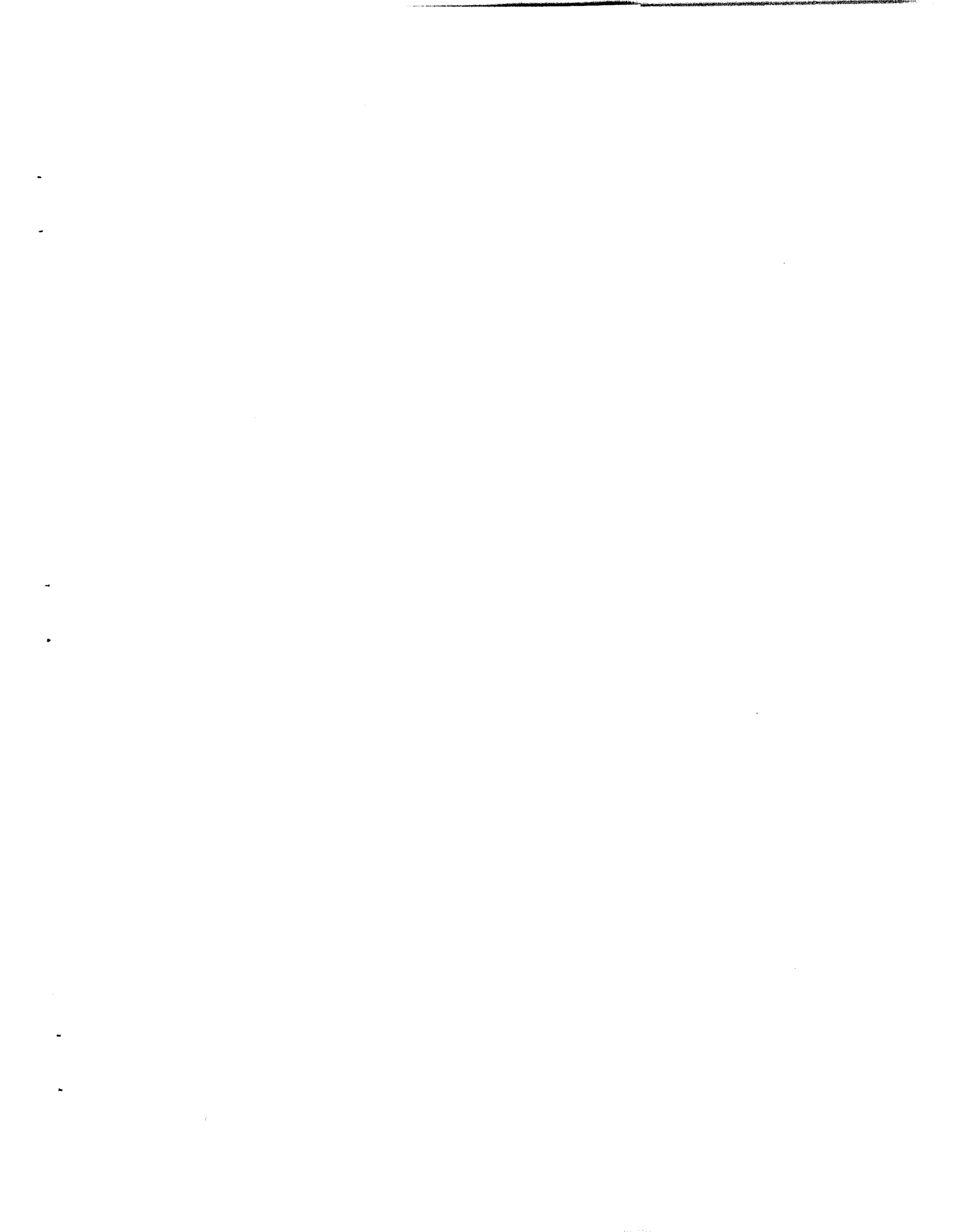


Fig. 15. Proposed ISHR Layout.



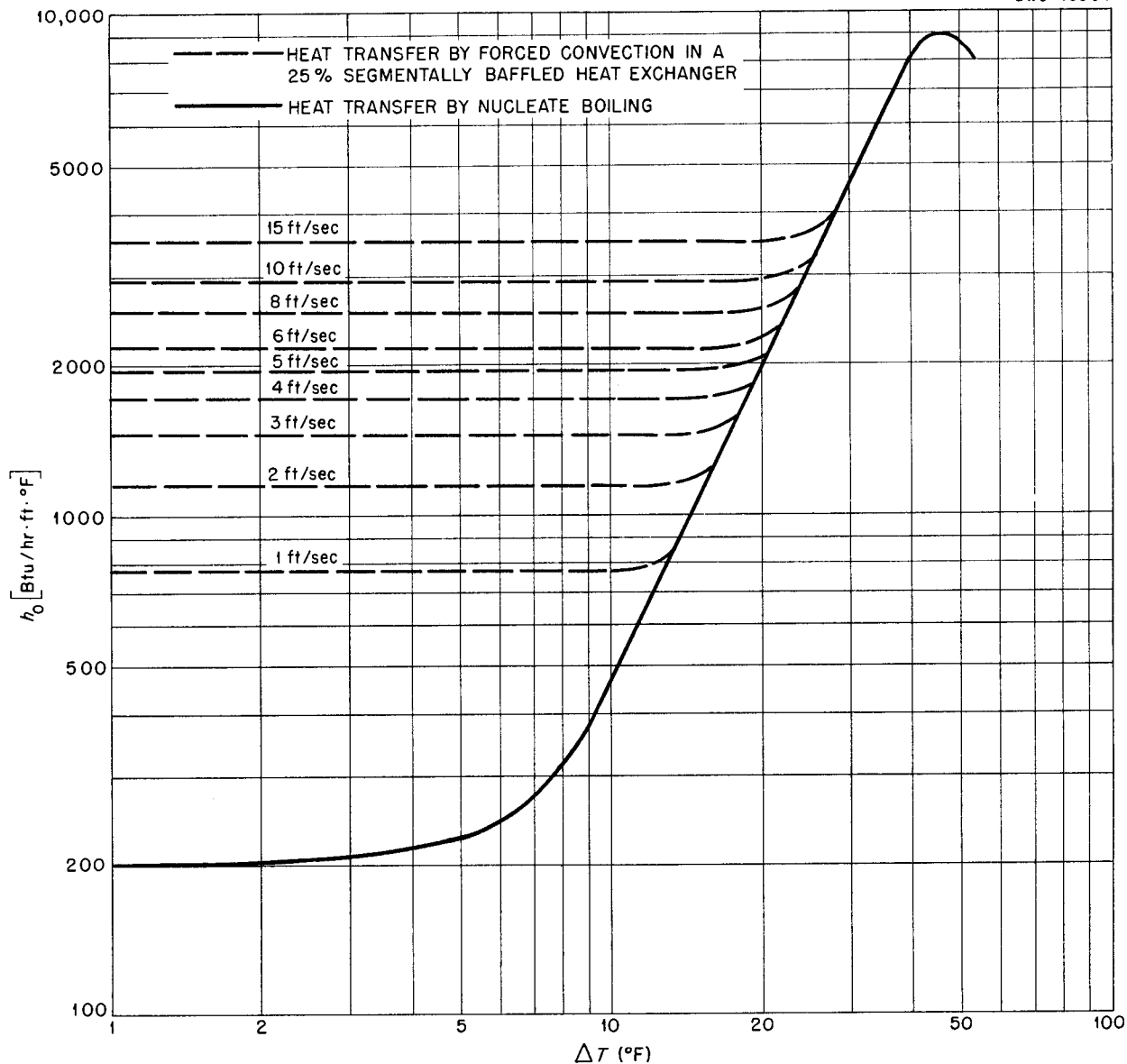


Fig. 16. Shell-Side Heat Transfer Coefficients for Water Boiling at 387.9°F and 215 psia on the Outside Surfaces of 1/2-in.-OD Vertical Tubes.

215 psia on the outside surfaces of 1/2-in.-OD, vertical tubes in a 25% segmentally baffled heat exchanger. The data are presented in terms of the film coefficient,  $h_o$ , as a function of temperature difference,  $\Delta T$ , between the boiling water and metal surface, with the forced-convection velocity

over the tubes as a parameter. The straight section of the nucleate boiling curve can be represented by

$$h_o = 3.80\Delta T^{2.07}$$

The forced-convection curves were calculated by using Colburn's equation

## HRP QUARTERLY PROGRESS REPORT

corrected for the number of tubes and leakage past the baffles:

$$h_0 = 0.198 \left( \frac{k_f}{D_0} \right) \left( \frac{c_p \mu_f}{k_f} \right)^{1/3} \left( \frac{D_0 V \rho_f}{\mu_f} \right)^{0.6}$$

where

$h_0$  = film coefficient for heat transfer, Btu/hr·ft<sup>2</sup>·°F,

$D_0$  = outside diameter of tube, ft,

$k_f$  = thermal conductivity, Btu/hr·ft<sup>2</sup>·°F/ft,

$c_p$  = specific heat, Btu/lb·°F,

$\mu_f$  = absolute viscosity, lb/hr·ft,

$\rho_f$  = density, lb/ft<sup>3</sup>,

$V$  = linear velocity, ft/hr.

Details of the calculations have been reported elsewhere.<sup>(4)</sup>

It was concluded from the study that heat transfer coefficients in forced-convection evaporators should be calculated from the forced-convection relationship for low values of  $\Delta T$ . When  $\Delta T$  exceeds the value at which the forced convection curve for the velocity being considered intersects the nucleate boiling curve, the effect of boiling is to increase the heat transfer coefficient.

The surface required to transfer 50 megawatts of heat from a uranyl sulfate solution flowing through tubes to water on the outside of the tubes in a shell-and-tube exchanger was calculated for the condition of nucleate boiling and for forced convection with boiling. It was assumed that the uranyl sulfate solution contained 250 g of uranium per liter and flowed through the 1/2-in.-OD tubes at a rate of 5000 gpm, entering at a temperature of 482°F and leaving at 418°F. Water was evaporated on the shell side at a temperature of 388°F and a pressure of 215 psia. Surface areas and pressure drops are given in Tables 10 and 11.

The improvement in over-all coefficient with consequent reduction in

fuel solution holdup and exchanger cost makes the forced-convection type of exchanger appear attractive, and the studies are being continued.

### EFFECT OF POISONS ON THE CRITICALITY OF THE ISHR AT 250 AND 100°C

The effect of Xe<sup>135</sup>, Sm<sup>149</sup>, and other poisons was calculated for the one-region, 6-ft-dia reactor in terms of the lowering of temperature that would be necessary to maintain criticality at the fuel enrichments corresponding to 100 and 250°C operation with a concentration of 250 g of uranium per liter of solution and no poison. That is, by knowing that at 250°C the reactor is critical if the fuel enrichment is 2.48%, the fuel concentration is 250 g of uranium per

TABLE 10. REQUIRED SURFACE AREAS TO TRANSFER HEAT BY NUCLEATE BOILING\* AT VARIOUS FLOW VELOCITIES

VELOCITY INSIDE TUBES (ft/sec)	SURFACE AREA (ft <sup>2</sup> )
10	8350
15	7900
20	7820

\*Metal wall resistance and scale resistance = 0.00125 (Btu/ft<sup>2</sup>·hr·°F)<sup>-1</sup>.

TABLE 11. REQUIRED SURFACE AREAS TO TRANSFER HEAT BY FORCED CONVECTION\* AT VARIOUS VELOCITIES

SHELL-SIDE VELOCITY OVER TUBES (ft/sec)	SURFACE AREA (ft <sup>2</sup> )		
	Tube Side Velocity		
	10 ft/sec	15 ft/sec	20 ft/sec
2	7995	7765	7600
4	7145	6920	6813
6	6817	6574	6448
8	6608	6364	6243
10	6467	6238	6098

\*Metal wall resistance and scale resistance = 0.0015 (Btu/ft<sup>2</sup>·hr·°F)<sup>-1</sup>.

liter, and there is no absorption other than by  $D_2O$  and  $UO_2SO_4$ , a calculation could be made to determine the temperature lowering necessary to maintain criticality if normal fission-product poisons are present. The effect of the poisons was estimated by incorporating the absorptions into previously made two-group calculations for a "clean" reactor. The following operating conditions were considered, in turn:

1. no fission-product gas separation,
2. steady-state distribution of xenon between the gas stream that is recycled through the gas separator and recombiner and the reactor fluid (xenon is removed by decay in gas and liquid and by burn-up only),
3. removal of the xenon from the gas stream at a rate of 1% per cycle,
4. complete removal of xenon from the recycle gas stream on each cycle.

These conditions were calculated at  $250^\circ C$  on the assumption that xenon was the only poison. They were then recalculated to include the effect of

other poisons on the assumption that 312 liters of solution was removed daily from the system and all poisons were eliminated from this stream. The procedure employed was that outlined by D. T. Bray,<sup>(5)</sup> and the results of the calculations are given in Table 12.

In both cases it was assumed that the reactor was operating at a power of 48 megawatts. The total volume of the liquid-circulating systems was estimated at 12,000 liters with the core size of 3200 liters. The gas-circulation system volume was estimated to be  $50 \text{ ft}^3$ . An estimate was made of the effect of flux owing to delayed neutrons in the circulating system outside the core, and the effect was found to be negligible. Consideration is being given to means for xenon removal from the gas system. Calculations are presently being made to estimate the activity owing to fission products in the circulating system.

<sup>(5)</sup>D. T. Bray, *Decrease in Pile Reactivity Due to Build-up of Fission Products*, ORNL CF-51-7-132 (July 27, 1951).

TABLE 12. EFFECT OF FISSION-PRODUCT POISONS ON OPERATING TEMPERATURES

OPERATING CONDITIONS	TEMPERATURE LOWERING DUE TO XENON ONLY ( $^\circ C$ )	TEMPERATURE LOWERING DUE TO ALL POISONS ( $^\circ C$ )
Case I: "Clean" reactor; temperature, $250^\circ C$ ; 2.48% enrichment, $U^{235}$		
No fission-gas separation	18	26
Gas circulation, no Xe removal	16	24
Gas circulation, 1% Xe removal	1	9
Gas circulation, 100% Xe removal	0	8
Case II: "Clean" reactor; temperature, $100^\circ C$ ; 1.67% enrichment, $U^{235}$		
No gas circulation	43	48
No gas circulation, no Xe removal	35	40
Gas circulation, 1% Xe removal	1	6
Gas circulation, 100% Xe removal	0	5

# HRP QUARTERLY PROGRESS REPORT

## INDUCED ACTIVITY

Induced activity in external piping may necessitate devices for remote connection of replacement equipment. Preliminary calculations indicate that ordinary type 347 stainless steel becomes so radioactive that the feasibility of making welds directly is not certain. Arrangements have been proposed that may make conventional welding possible. Sections of pipe in which welds would ordinarily be made in replacing equipment could be made from a special melt of type 347 stainless steel containing as little cobalt and tantalum as possible. Such sections of pipe could also be wrapped with Boral or some other strong thermal-neutron absorber to reduce the number of neutrons entering the pipe from the outside. Radiation in the work area could be reduced by shielding all sources of activity except the minimum amount of pipe necessarily exposed for the operation.

Cobalt and tantalum are introduced into the steel with the nickel and niobium, respectively. At present, electrolytic nickel is being produced with a cobalt content of 0.1 to 0.3%, but older nickel scrap may contain up to 0.8% cobalt. Under the present specifications niobium for alloying may have a tantalum content up to 40% of the total of niobium and tantalum. However, special selection of niobium-tantalum ore may yield niobium with only 1 or 2% tantalum.

The results in Table 13 serve to show the relative importance of tantalum and cobalt. The dose rates are those at a point 18 in. from a 2½-in. exposed section of 12-in. pipe in the ISHR circulating system after various irradiation and cooling periods. The absolute values may be high by perhaps as much as a factor of 4 owing to the nature of the calculations. The assumptions tending to cause an overestimate are that all leakage neutrons are absorbed in the pipe walls and that there is no self-shielding. The assumptions having an opposite effect are that there are no fission products on the pipe walls and there is no scattered radiation from the pipe inside the shield.

## HEAVY-ISOTOPE BUILD-UP

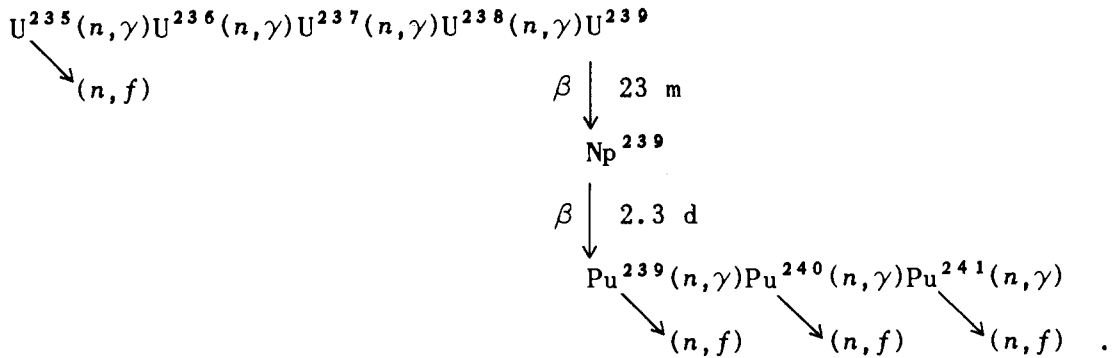
The long-term operation of the ISHR will be affected by the build-up of heavy isotopes. The differential equations describing the build-up are based upon the following assumptions: (1) constant flux, (2) constant temperature, (3) constant processing rate, (4) make-up containing no heavy isotopes other than  $U^{235}$  and  $U^{238}$ , (5) concentration of  $U^{235}$  and  $U^{238}$  held constant, (6) instantaneous decay of  $U^{239}$ , (7) no absorption of neutrons in  $Pu^{239}$ .

The reactions and isotopes of greatest importance are

TABLE 13. RADIATION FROM CONSTITUENTS OF TYPE 347 STAINLESS STEEL

CONSTITUENT	DOSE RATE 18 in. FROM 2½-in. SECTION OF 12-in. PIPE (mr/hr)			
	1 y - 1 d*	1 y - 7 d	2 y - 1 d	2 y - 7 d
Co (0.01% of steel)	179	179	336	336
Ta (0.01% of steel)	123	119	137	132
Fe + Cr + Ni + Mn	710	533	711	534

\*One year of operation and one day of decay.



The equations are

$$\frac{dN_{25}}{dt} = 0, \quad (1)$$

$$\frac{dN_{26}}{dt} = N_{25}\sigma_c(25)\phi - N_{26}\sigma_a(26)\phi - N_{26}R, \quad (2)$$

$$\frac{dN_{28}}{dt} = 0, \quad (3)$$

$$\frac{dN_{39}}{dt} = N_{28}\sigma'_a(28)\phi - N_{39}\lambda_{39} - N_{39}R, \quad (4)$$

$$\frac{dN_{49}}{dt} = N_{39}\lambda_{39} - N_{49}\sigma_a(49)\phi - N_{49}R, \quad (5)$$

$$\frac{dN_{40}}{dt} = N_{49}\sigma_c(49)\phi - N_{40}\sigma_a(40)\phi - N_{40}R, \quad (6)$$

$$\frac{dN_{41}}{dt} = N_{40}\sigma_c(40)\phi - N_{41}\sigma_a(41)\phi - N_{41}R, \quad (7)$$

where

- $\sigma_a$  = total absorption cross section,
- $\sigma_c$  = radiative capture cross section,

$\sigma'_a(28)$  = equivalent thermal-absorption cross section for  $\text{U}^{238}$ , including resonance absorption,

$\lambda_{39}$  = decay constant for  $\text{Pu}^{239}$ ,  
 $R$  = continuous processing rate, reactor volumes per unit time,

$\phi$  = average thermal-neutron flux.

In the case of batch processing without addition of uranium, the  $\text{U}^{235}$  concentration will decrease because of burnup, and Eq. 1 should be replaced by

$$\frac{dN_{25}}{dt} = -N_{25}\sigma_a(25)\phi. \quad (1a)$$

The assumption of constant  $\text{U}^{238}$  concentration is still valid for normal periods of operation since the burnup of  $\text{U}^{238}$  is quite slow. The other equations are the same as for continuous processing, with  $R = 0$ . The solutions of the equations for batch processing are shown in Fig. 17. The initial fuel concentration was assumed to be 250 g of uranium per liter at  $250^\circ\text{C}$  with an enrichment of 2.48%. The cross sections listed in Table 14 were used in evaluating the solutions and were taken from BNL-170.<sup>(6)</sup> Other constants used were  $\nu(\text{U}) = 2.50$ ,  $\nu(\text{Pu}) = 2.96$ , and  $\lambda_{39} = 3.5 \times 10^{-6} \text{ sec}^{-1}$ .

<sup>(6)</sup>D. J. Hughes et al., A Compilation of the AEC Neutron Cross Section Advisory Group, BNL-170 (May 15, 1952).

# HRP QUARTERLY PROGRESS REPORT

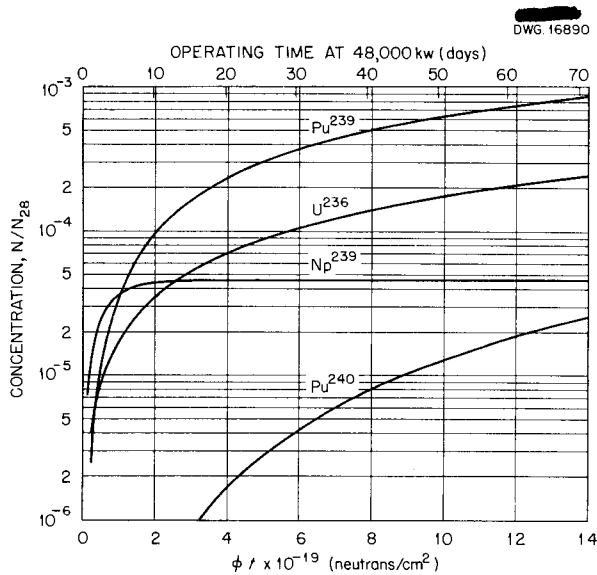


Fig. 17. Heavy Isotope Build-up for Batch Processing.

TABLE 14. THERMAL CROSS SECTIONS AT 250°C

ISOTOPE	$\sigma_a$ (barns)	$\sigma_f$ (barns)	$\sigma_c$ (barns)
U <sup>235</sup>	460	390	70
U <sup>236</sup>	6	0	6
U <sup>238</sup>	2.1	0	2.1
Pu <sup>239</sup>	1120	690	430
Pu <sup>240</sup>	400	25	375
Pu <sup>241</sup>	1000	750	250

Figure 18 shows the ratio of Pu<sup>240</sup> to Pu<sup>239</sup> as a function of operating time without processing. If this ratio is to be no more than 0.02, the reactor solution must be processed after 50 days of full-power operation. At this time the reactor will contain 1900 g of plutonium (including Np<sup>239</sup>) for an average production rate of 0.792 g per megawatt day. If a continuous processing cycle is chosen, the Pu<sup>240</sup> can be held to the desired fraction by adjusting the processing

rate. The rate necessary for  $N_{40}/N_{49} = 0.02$ , at equilibrium, can be found from Eq. 6:

$$dN_{40} = N_{49}\sigma_c(49)\phi - N_{40}\sigma_a(40)\phi - N_{40}R = 0$$

Therefore,

$$R = \frac{\sigma_c(49)\phi}{\frac{N_{40}}{N_{49}}} - \sigma_a(40)\phi = 0.479 \times 10^{-6} \text{ sec}^{-1}$$

This rate is equivalent to 484 liters per day or one reactor volume (11,700 liters) in 24.2 days. With this processing rate the production of plutonium will be 38.8 g per day or 0.809 g per megawatt day.

As the plutonium builds up in the reactor it becomes an added source of fissions, counteracting to some extent the burnup of U<sup>235</sup>. But because of the lower value of  $\eta$  for plutonium and because the conversion ratio is less than one, the infinite multiplication constant must decrease with time unless additional U<sup>235</sup> is added to the reactor. Figure 19 shows only the effects of depletion of U<sup>235</sup> and the build-up of plutonium on  $k_{\infty}$ . It does not take into account the effect of fission-product poisons, which will cause a more rapid decrease.

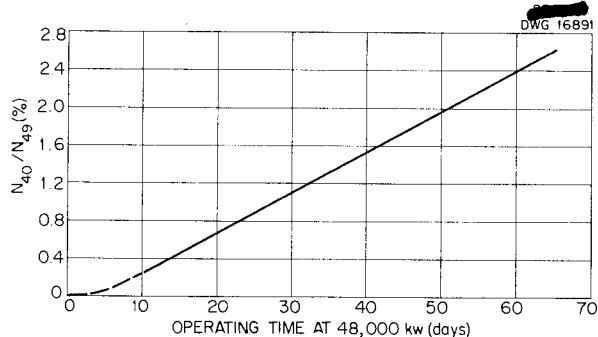


Fig. 18. Build-up of Pu<sup>240</sup> for Batch Processing.

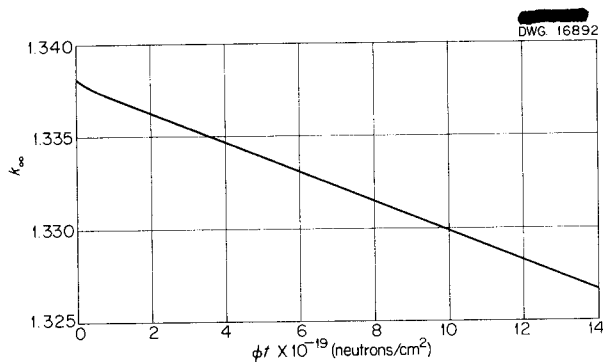


Fig. 19. Effect of Heavy Isotopes on the Infinite Multiplication Constant.

### CRITICALITY CALCULATIONS

The criticality calculations for the 6-ft sphere given in the previous report<sup>(7)</sup> have been checked by the Mathematics Panel with the use of IBM computing machines. In the previous calculations it had been assumed that the fast and slow buckling, as calculated by the method in LA-524,<sup>(8)</sup> were functions primarily of temperature and practically independent of solution composition and uranium enrichment. This assumption, which greatly reduced the amount of work done by hand, was found to be quite good when checked by the IBM machines following the trial-and-error procedure for each point on the curves of enrichment vs. concentration.<sup>(9)</sup> Calculations were extended to include critical concentration as a function of temperature for 93.5% enriched uranium.

### CORE DESIGNS FOR TWO-REGION REACTORS

Results of corrosion tests made during the past several months show that the concentrated uranyl sulfate

solutions (> 100 g of uranium per liter) required for producing plutonium in single-region reactors cannot be contained in stainless steel at temperatures high enough to make power production attractive. Metals such as titanium or zirconium would be required for the entire fuel-circulating system. On the other hand, it appears that dilute uranyl sulfate solutions (~ 5 g of uranium per liter) are only slightly corrosive to stainless steel. A two-region reactor consisting of an enriched core containing a dilute solution of uranium and a blanket of thorium for a breeder, a lithium compound to produce tritium, or uranium to produce plutonium appears attractive, provided a blanket can be obtained that does not corrode stainless steel severely at 250°C. An investigation has been started to assess the possibilities of such a reactor.

Suggested core vessel arrangements for the two-region converters are shown in Figs. 20, 21, and 22. In all designs the core shape approximates a 4-ft-dia sphere, and a control thimble is incorporated to permit start-up and shut-down with a full core containing the operating concentration of fuel.

Figure 20 is a design for straight-through flow of fuel solution. Although core and blanket are intended to operate at the same temperature and pressure, provision is made for differential expansion of the two shells operating at a temperature difference of 300°F and maximum stress of 10,000 psi. The design shown in Fig. 20 accomplishes this by use of concentric right angle bends of pipe for core inlet and blanket outlet. Figure 21 accomplishes the same thing by use of a bellows in the concentric pipes. Figure 22 provides for reverse flow in the core with concentric fuel inlet, fuel outlet, and control element. No differential thermal expansion problem exists in this

(7) R. B. Briggs et al., *HRP Quar. Prog. Rep. July 1, 1952*, ORNL-1318, p. 108.

(8) R. P. Feynman and T. A. Welton, *Calculations of Critical Masses Including the Effect of the Distribution of Neutron Energies*, LA-524 (Jan. 21, 1947).

(9) Figure 50, *HRP Quar. Prog. Rep. July 1, 1952*, ORNL-1318, p. 109.

UNCLASSIFIED  
DWG. 16658

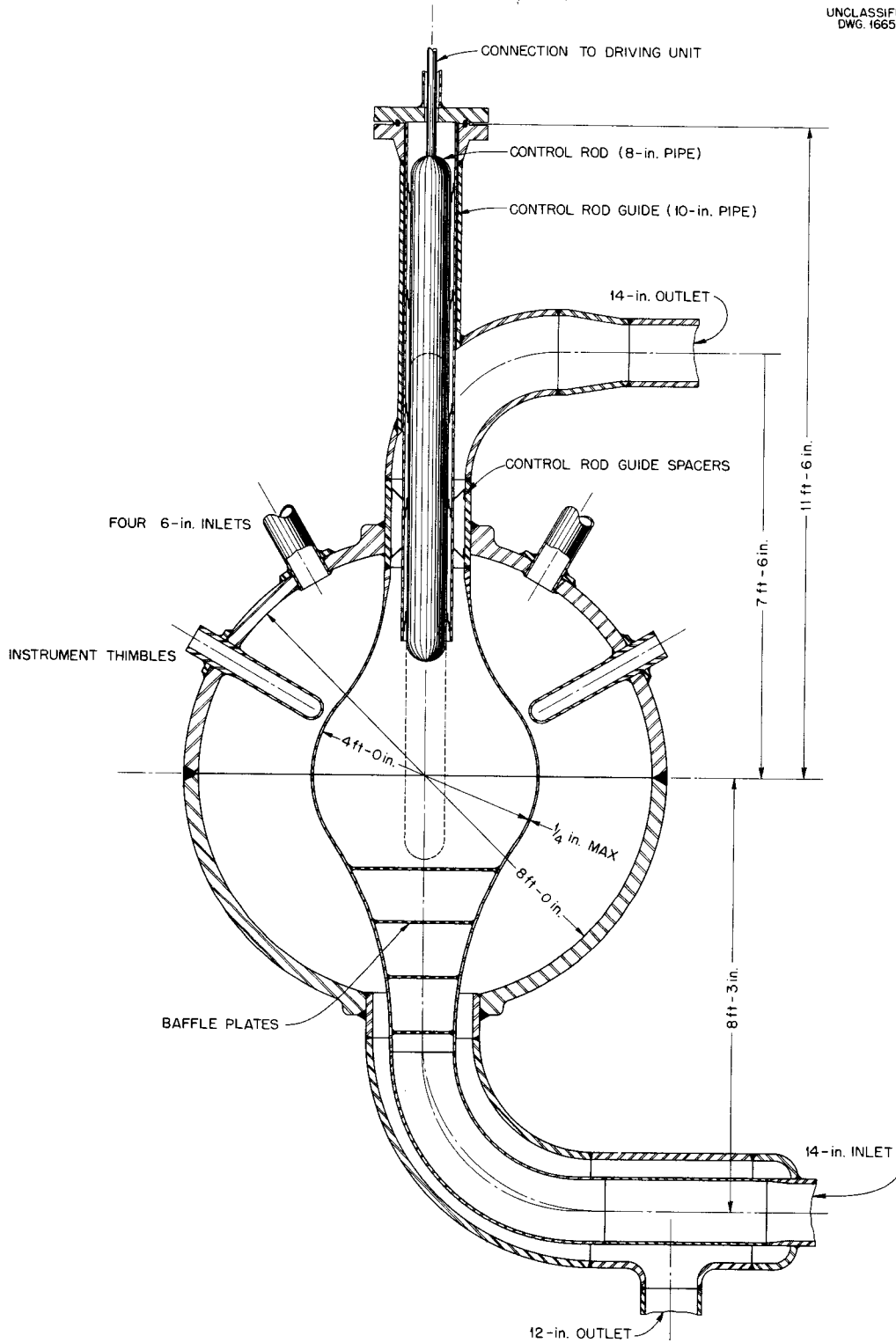
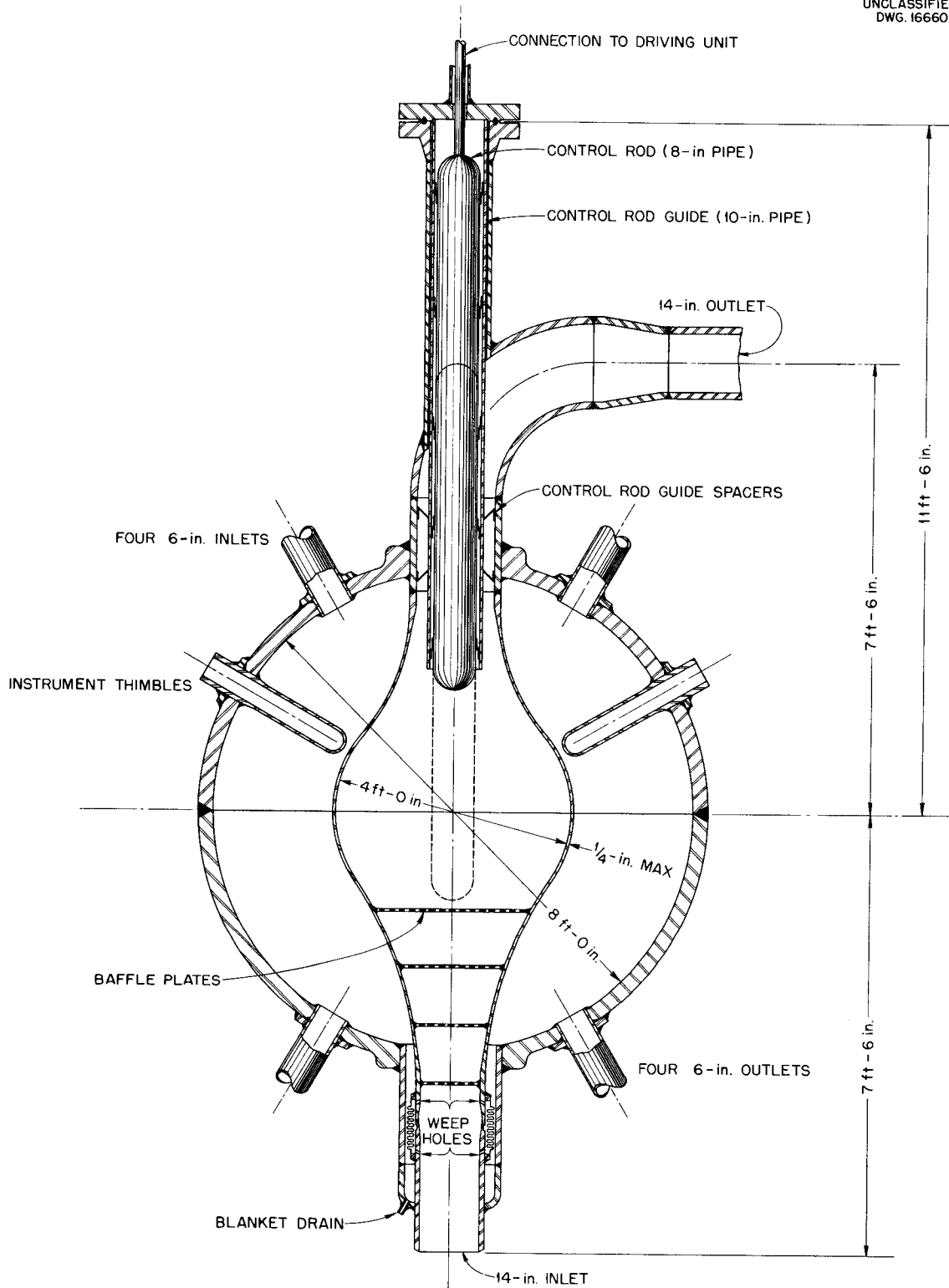


Fig. 20. Core Vessel for Straight-through Flow Without Bellows Expansion Joint.

UNCLASSIFIED  
DWG. 16660



**Fig. 21. Core Vessel for Straight-through Flow with Bellows Expansion Joint.**

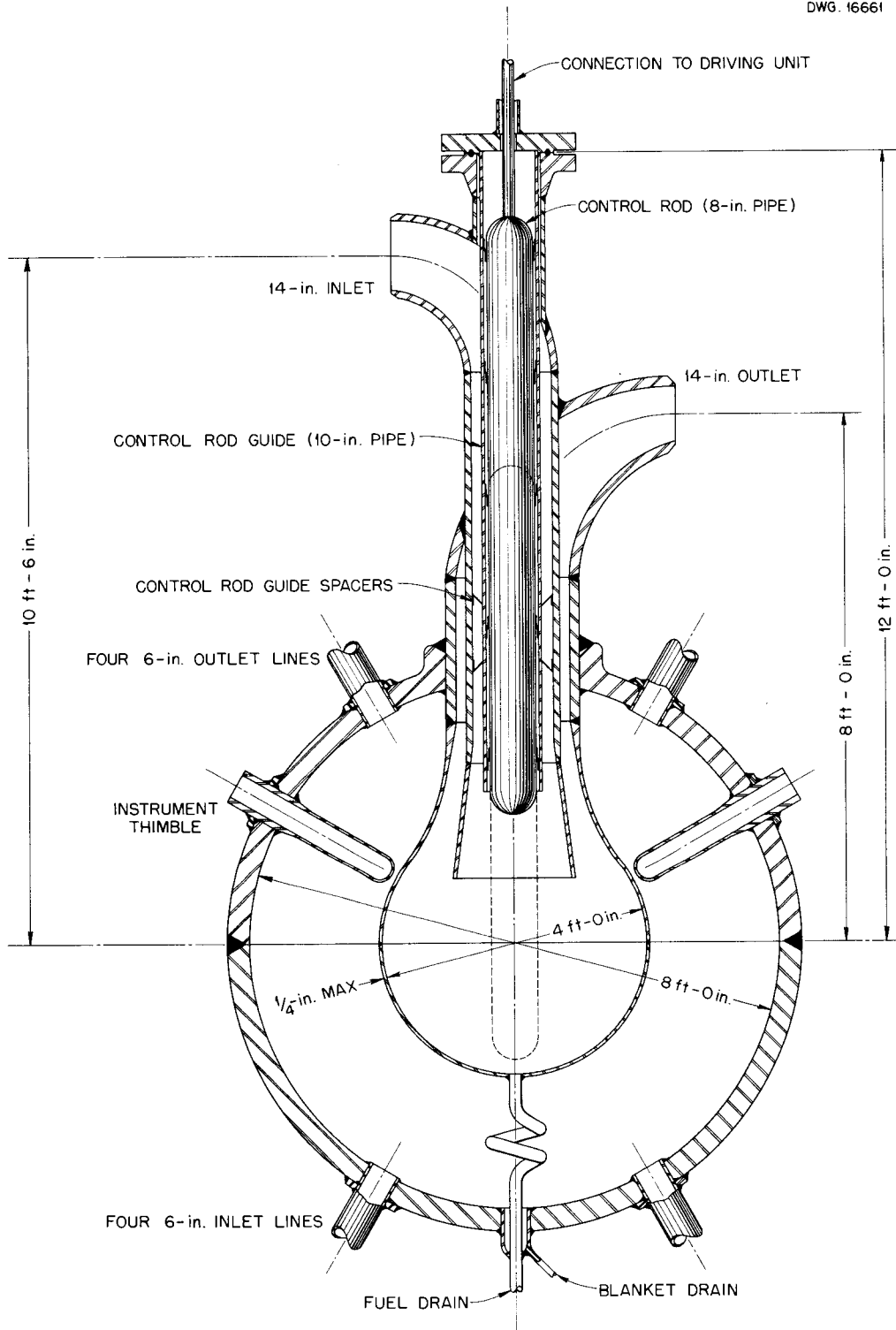


Fig. 22. Core Vessel with Concentric Inlet and Outlet.

design, but residence time of gas bubbles would be greater than for the straight-through flow types.

**STRESS ANALYSIS OF 4-ft-dia CORE VESSEL**

Since the conversion ratio is strongly affected by thickness of the core vessel wall, some time has been spent in studying the structural strength of this vessel against both internal and external pressure. A simple spherical shape is assumed.

The allowable internal pressure in excess of the external pressure is given by

$$P = \frac{4ts}{d}$$

where

- t = wall thickness, in.,
- s = allowable stress, psi,
- d = internal diameter of vessel, inches.

Under normal operating conditions the pressure difference across the core tank and the resulting stresses will be small. The pressure differences that could be sustained before exceeding the yield stress for 4-ft-dia spheres of various thicknesses and materials of construction are given in Table 15.

The collapsing pressure is calculated by the method of Timoshenko<sup>(10)</sup> in which a perfect sphere in simple compression is assumed. By using this method, the collapsing pressure is

$$P = \frac{2Et^2}{r^2 \sqrt{3(1 - \nu^2)}}$$

<sup>(10)</sup>S. Timoshenko, *Theory of Elastic Stability*, Chap. ix, p. 491-497, McGraw-Hill, New York, 1936.

where

- E = modulus of elasticity, psi,
- r = internal radius of vessel, in.,
- t = wall thickness, in.,
- ν = Poisson's ratio = 0.3.

In all cases the theoretical collapsing pressures exceed those required to yield the material; so failure will occur by plastic flow rather than by elastic buckling. Therefore the excess of external pressure over internal pressure should not be greater than the values of yielding pressure given in Table 15. Deformation of a practical vessel may occur at pressures as low as one half those reported in the table owing to departures from a spherical shape.

The basis taken for design is that the core tank should withstand a pressure differential of about 250 psi without deforming. This requires a stainless steel tank 3/16 in. thick, a titanium tank 5/16 in. thick, or a zirconium tank 1/2 in. thick.

**NUCLEAR CALCULATIONS FOR TWO-REGION LITHIUM AND THORIUM CONVERTERS**

Estimates of the conditions for criticality have been made for each of eight separate conversion arrangements for making U<sup>233</sup> or tritium. The design data the arrangements had in common are:

Temperature	250°C
Core solution	UO <sub>2</sub> SO <sub>4</sub> -D <sub>2</sub> O, ~ 5 g of uranium per liter
Core tank	Type 347 stainless steel
Core diameter	4 ft
Blanket thickness	2 ft

**TABLE 15. YIELDING PRESSURES FOR SPHERES**

MATERIAL	YIELD STRESS (lb/in. <sup>2</sup> at 500°F)	ALLOWABLE PRESSURE DIFFERENCE (lb/in. <sup>2</sup> )		
		1/16-in. wall	1/8-in. wall	1/4-in. wall
Type 347 stainless steel	32,000	168	334	668
Titanium	20,000	104	208	416
Zirconium	11,000	58	116	232

## HRP QUARTERLY PROGRESS REPORT

Fuel enrichment            93.5% U<sup>235</sup>  
 Poisons in core            None  
 Poisons in blanket        None

blanket to reduce the losses in the tank wall, with reflectors, with increased blanket thickness and beryllium oxide moderator to reduce the fast-neutron losses in the case of the molten lithium, and with uranium and D<sub>2</sub>O in the blanket to obtain plutonium production rates.

Results of the calculations are presented in Table 16. Additional calculations will be made with higher concentrations of thorium in the

**TABLE 16. CRITICAL CONCENTRATION AND NEUTRON BALANCE FOR TWO-REGION CONVERTERS**

	BLANKET							
	1000 g of Th (as oxide) in D <sub>2</sub> O		Molten Lithium		10% Li-90% Mg Alloy Pellets, 40% of Voids Filled with D <sub>2</sub> O		30% Li-70% Mg Alloy Pellets, 40% of Voids Filled with D <sub>2</sub> O	
Core tank wall thickness (in.)	1/8	1/4	1/8	1/4	1/8	1/4	1/8	1/4
Critical concentration (g of uranium per liter)*	4.47	4.79	5.91	5.91	5.25	5.25	5.40	5.40
Neutron Balance for $\eta = 2.12$ (neutrons absorbed per absorption in U <sup>235</sup> in core)								
Parasitic absorption in the core	0.007	0.007	0.007	0.007	0.007	0.007	0.007	0.007
Blanket absorption	0.903	0.793	0.653	0.588	0.907	0.826	0.909	0.835
Shell absorption	0.194	0.307	0.065	0.130	0.081	0.161	0.075	0.149
Leakage								
Slow neutrons	0.0093	0.0087						
Fast neutrons	0.0074	0.0073	0.395	0.395	0.126	0.126	0.129	0.129

\*Three per cent voids in core, 93.5% U<sup>235</sup>.

## ENGINEERING STUDIES OF COMPONENTS

C. B. Graham, Section Chief

J. M. Baker	L. B. Lesem	P. N. Stevens
J. A. Hafford	W. L. Ross	S. R. West
R. J. Kedl	I. Spiewak	R. H. Wilson
J. I. Lang		C. D. Zerby

## CORE DEVELOPMENT STUDIES

The most favorable geometry for the reactor from both the nuclear and engineering points of view is a sphere that has minimum holdup of fissionable material and minimum weight of structural material. A suitable core must satisfy the requirements of heat removal from all points, gas removal rapid enough from the nuclear standpoint, low pressure drop, and economy in construction.

The core developmental program, which is under way, consists of examining small models of possible reactors as a guide for the design of 8-ft (intermediate scale) models. Information obtained on an intermediate scale can then be employed directly for the ISHR and for industrial-scale cores.

The general types of flow pattern being considered are rotating flow and straight-through flow. The first core has tangential inlets at or near the equator and outlets at the poles, which give the fluid a rotating motion that aids considerably in gas separation. The other core is designed for little or no rotation and a considerably lower pressure drop than the rotating core.

**Small-Scale Rotating-Flow Model.** Results of an investigation of velocity distribution and pressure drop in a 12-in. sphere with four 2-in. tangential inlets and two 2-in. polar outlets have been given in previous quarterly reports.<sup>(1,2)</sup> This work has

(1) C. B. Graham et al., *HRP Quar. Prog. Rep.* March 15, 1952, ORNL-1280, p. 144.

(2) C. B. Graham et al., *HRP Quar. Prog. Rep.* July 1, 1952, ORNL-1318, p. 119.

been completed recently, and a full report will be issued in the next quarter. The latest information on pressure drop, however, is of immediate interest. Inserts were placed in the inlet and outlet pipes to vary their size. The following equation expresses the data obtained in the sphere:

$$\Delta P = 15.44 \left( \frac{A_{in}}{\pi R_s^2} \right) \left( \frac{V_{in}^2}{2g} \right) \left[ \left( \frac{R_s}{R_o} \right)^2 - 1 \right],$$

where

$\Delta P$  = the static pressure drop from inlet to outlet, ft of fluid,

$A_{in}$  = total inlet area, ft<sup>2</sup>,

$V_{in}$  = inlet velocity, ft/sec,

$R_s$  = sphere radius, ft,

$R_o$  = outlet radius, ft,

$g$  = the gravitational conversion factor, 32.2 ft/sec<sup>2</sup>.

The equation correlates values of  $A_{in}/\pi R_s^2$  between 0.0263 and 0.1061. Extrapolations to larger inlet areas should be reasonably good. The outlet diameter should be larger than 1/12 of the sphere diameter.

Two further qualifications must be considered. First, the total pressure loss, including the outlet pipe, will be about 30% greater than the static pressure drop across the sphere. Fluid in the outlet will be spinning rapidly, and the amount of recoverable kinetic energy probably will be small. Outlet behavior is currently being investigated at the University of Tennessee. Second, it has been found that roughness of the sphere wall is an important parameter that affects pressure drop - the smoother the wall, the higher the rotational velocity

## HRP QUARTERLY PROGRESS REPORT

attained in the sphere, and therefore the higher the pressure drop. Tests on the 12-in. sphere were conducted with a rusty steel surface, and a pressure drop increase of 30% was observed after the interior had been sandblasted. Since the sandblasted wall was still rough, an additional increase in pressure drop could be expected with a smooth, machined surface.

The above equation was used to estimate the pressure drop in 15-ft cores utilizing a rotating type of flow. The predictions, presented in Table 17, are optimistic because no correction was made for outlet loss or smooth surfaces. It is noted that the pressure losses are still rather high.

Possible modifications of the tangential entry that would preserve the advantages of a rotating type of core but reduce the pressure drop are being considered. For example, baffles (constructed from light sheet metal) inside the reactor could slow down the inlet stream considerably and thereby reduce the pressure drop. Another possibility is to construct the inlets at an angle rather than tangentially, which would also slow the rotation.

**Intermediate-Scale Rotating-Flow Model.** Construction of an 8-ft sphere that will represent an intermediate-size rotating core is being completed; this system has been described previously.<sup>(3)</sup> If the energy losses

<sup>(3)</sup> *Ibid.*, p. 122.

are excessive in this core, the system will be altered to test one of the straight-through type of cores.

**Small-Scale Straight-through Model.** Flow pattern, gas removal, and pressure drop have been studied in several spherical straight-through models that were scaled to approximate 15-ft reactor cores that would operate at 1000 to 2000 megawatts. Figure 23 shows a glass model with six radial inlets and two polar outlets. The inlets actually constructed made a 2-deg angle with a sphere radius, so that a small amount of rotation is present. It is believed that a small amount of rotation is unavoidable in this geometry, even if great care is exercised in construction. The flow pattern was studied by introducing methylene blue into one or more inlets. Mixing was quite rapid; insertion of dye in one inlet produced a uniform color in the sphere in about one-third the average residence time. Decay of the dye after ceasing to add dye, as determined colorimetrically, was exponential. The rate of decay was quite close to the theoretical value, which indicates excellent mixing. This reactor configuration would result in approximately constant-temperature distribution. The model seemed to work well with as few as three balanced inlets. Two outlets are necessary to prevent stagnation. Gas bubbles had no difficulty escaping from the sphere. There was a small central gas void along the polar axis,

**TABLE 17. ESTIMATED PRESSURE DROP IN 15-ft CORES UTILIZING A ROTATING TYPE OF FLOW**

FLOW RATE (gpm)	NO. OF INLETS	INLET DIAMETER (ft)	INLET VELOCITY (ft/sec)	OUTLET DIAMETER (ft)	OUTLET AXIAL VELOCITY (ft/sec)	PRESSURE DROP (ft of fluid)
100,000	4	2.18	15	4.36	7.5	49.7
100,000	4	1.88	20	3.76	10	90.4
200,000	4	3.08	15	4.36	15	98.5
200,000	4	2.66	20	3.76	20	180.7

UNCLASSIFIED  
DWG.15749

but the amount of gas separation did not appear to be very great. The pressure drop was less than three inlet velocity heads. In terms of a 15-ft reactor with 20 ft/sec inlet and outlet flow, this would amount to about an 18-ft head of fluid.

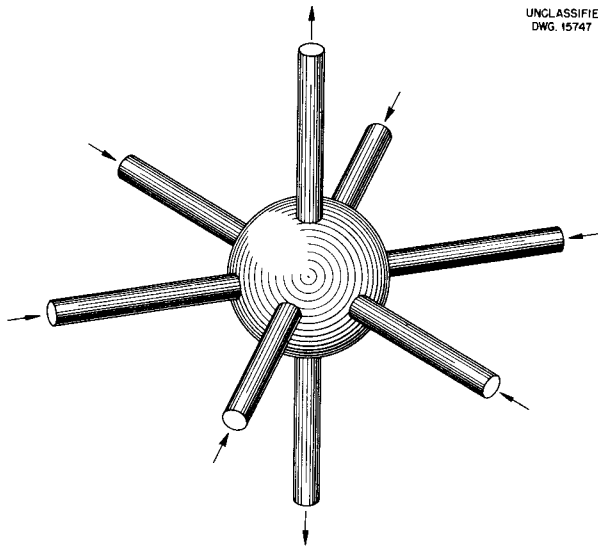
UNCLASSIFIED  
DWG. 15747

Fig. 23. Sphere Model of Core with Six Radial Equatorial Inlets and Two Axial Outlets.

Figure 24 shows a model with a large axial inlet at the north pole and four smaller axial outlets in the northern hemisphere. The dye analysis revealed that there was a small amount of slug flow in addition to the mixing. Color disappeared faster in this model than in the previous one because of the slug component. This type of reactor would also be close to uniform temperature, except for the cooler downdraft at the central axis. There was a definite tendency for gas bubbles to be trapped in eddies, especially in the southern hemisphere. This tendency was not corrected by reversing inlet and outlets. The poor behavior of gas probably limits this geometry to a medium in which gas generation is not a serious problem. The pressure drop was quite low.

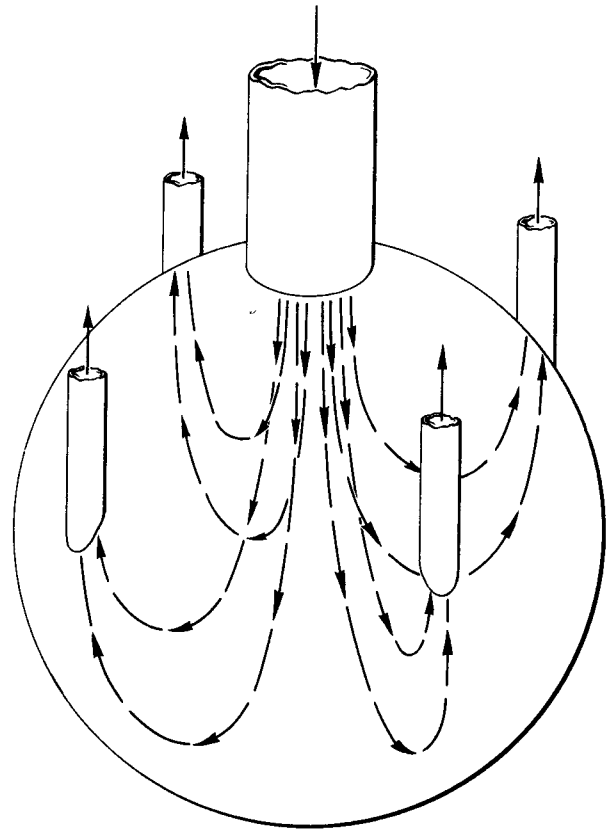


Fig. 24. Sphere Model of Core with One Axial Inlet and Four Axial Outlets.

Figure 25 shows a hybrid of the rotating and the straight-through types of cores. There are two tangential inlets and two radial inlets, all at the equator. The flow pattern through this sphere was similar to the flow through rotating cores in that there was a strong rotational component and also a definite tendency for slug flow. Slug flow and mixing appeared, qualitatively, to be of the same order of magnitude. This type of reactor would tend to be hotter at the center than at the periphery, but there was no trace of a stagnant region that would overheat. Gas was centrifuged in toward the center, but the central gas void was less uniform in shape than the voids found in rotating reactors.

# HRP QUARTERLY PROGRESS REPORT

The gas content of this type of a reactor would be between the rotating type and the straight-through type. Pressure drop in the model was one-sixth of that predicted if all inlets had been tangential.

UNCLASSIFIED  
DWG.15752

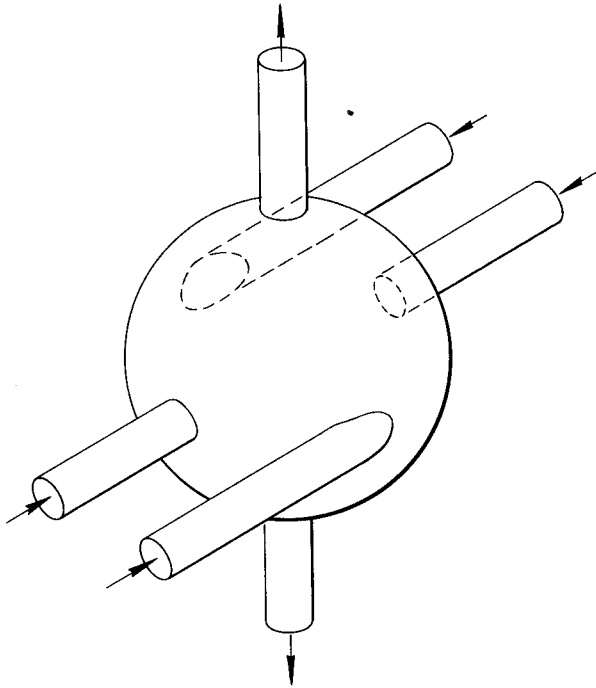


Fig. 25. Sphere Model of Core with Two Tangential Inlets, Two Radial Inlets, and Two Axial Outlets.

Figures 26, 27, and 28 represent 18-in. plastic models with similar inlet configurations. The inlets are 1-in. pipe nipples, with one at the center, six in the next circle, and 12 in the outer circle.

The model of Fig. 26 had an annular outlet surrounding each inlet jet. The arrows indicate the general flow pattern. Inlet jets remain intact and gradually diverge, until they reach the equator or slightly above. There they merge, and about 59% of the fluid turns around and goes back down. The remaining 41% mixes with the eddies shown in the northern hemisphere. There is also a boundary layer at the

UNCLASSIFIED  
DWG.16893

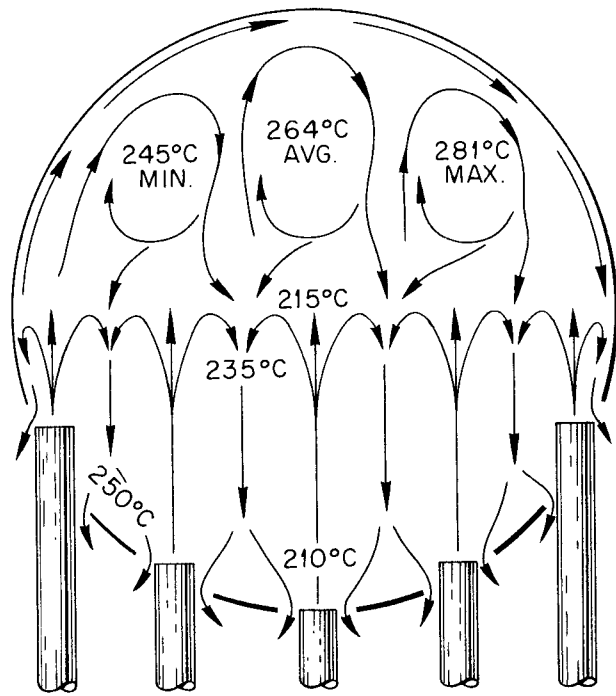


Fig. 26. Multijet Sphere Model of Core with Annular Outlets.

UNCLASSIFIED  
DWG.16894

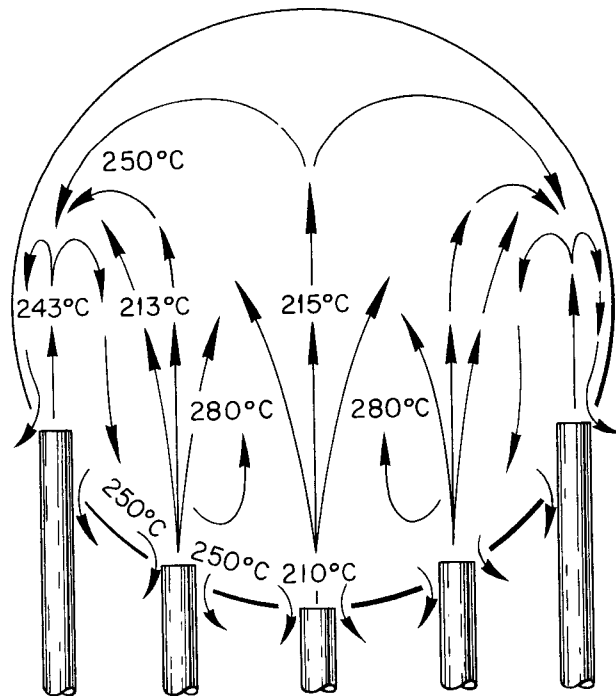


Fig. 27. Multijet Sphere Model of Core with Annular Outlets; One Half of Outer-Ring Jets Closed.

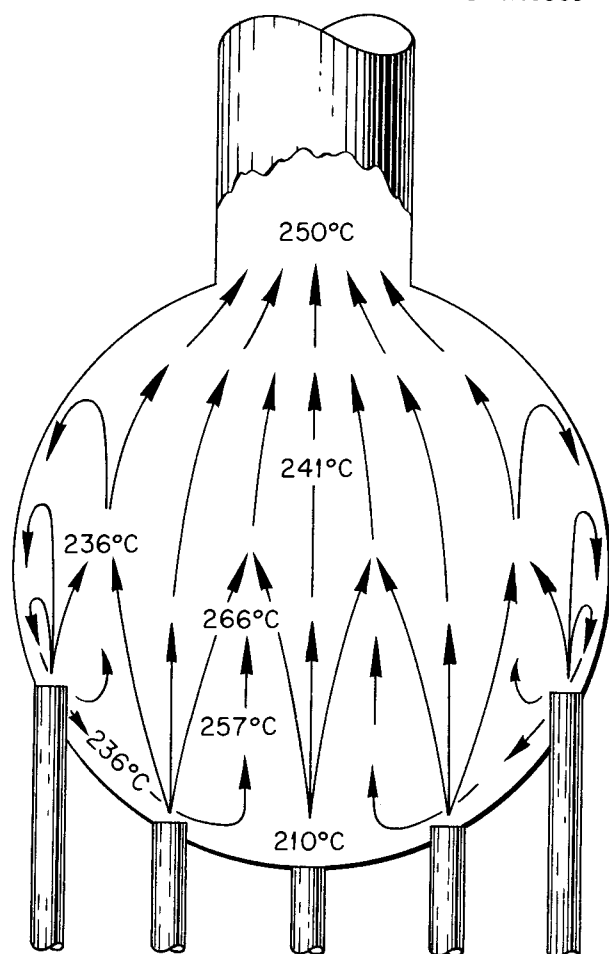
UNCLASSIFIED  
DWG. 16895

Fig. 28. Sphere Model of Core with One Northern Hemisphere Outlet.

northern hemisphere wall that moves from one side of the sphere to the other; perfect hydrodynamic balancing appears impossible in this respect. This eddy is not important from the heat removal standpoint because it would be in a low-flux region. It is possible to predict an approximate temperature distribution from the flow pattern by assuming a temperature change from 210°C at the inlet to 250°C at the outlet. The inlet jets are heated to 215°C at the equator. The temperatures of the northern hemisphere eddies range from 245 to 281°C and average 264°C. The temperatures of the southern hemisphere downcurrents

are 235°C at the equator and 250°C at the outlet. These estimates were made with the aid of dye injection and salt conductivity studies. Gas is removed satisfactorily in this model by including a small vent at the top. The pressure drop was three inlet-velocity heads.

Figure 27 is the same as the model described in the previous paragraph, with six of the outer 12 inlet jets shut off. The fluid travels up the center and down the outside. The inlet jets merge close to the equator and entrain liquid from the southern hemisphere surrounding the jets. At the equator, the jets in a reactor would be at 215°C and the entrained liquid would be at 280°C. After the liquid has made the turn in the northern hemisphere, it mixes with the outer jets at about the equator. The outer jets cool the downdraft from 256 to 243°C. By the time the downdraft has reached the bottom it is at 250°C. It then splits off into the outlet stream at 100 gpm and the recirculating stream at about 60 gpm, where it is subsequently heated to 280°C by the time the remnant reaches the equator.

Figure 28 utilizes the same inlets as Fig. 26, but the outlet is a 6-in. pipe at the north pole. Liquid from the seven inner jets entrains fluid originating in the outer jets; the inner jets make a single pass through the sphere. The liquid in the outer part of the sphere is well mixed and at a reasonably uniform temperature, 236°C. Liquid from outside enters the central region between jets and is heated to an average of 257°C and a maximum of 266°C before it is entrained. At the equator, where the jets merge, the temperature is 241°C. From the equator the flow is smooth to the outlet, where it is at 250°C. The pressure drop is about two inlet-velocity heads. Gas is removed from the sphere by the liquid, without difficulty.

## HRP QUARTERLY PROGRESS REPORT

Of the models tested, that of Fig. 23 appears the most promising. Its pressure drop is about one-tenth that of a corresponding rotating type of reactor. The gas removal and temperature distribution appear to be adequate. The model shown in Fig. 24 is unsatisfactory from the gas-removal standpoint. The model shown in Fig. 25 may be useful as a modified rotating type of core with relatively low pressure loss. The models shown in Figs. 26, 27, and 28 are likely to overheat at some points.

Future work is planned to evaluate the use of screens in inlet expanders. According to information in the literature, screens can be used to produce slug flow in wind tunnels. This type of flow would be very useful in high power-density machines where the relative size of the inlet is large, provided that the metal of the screens does not absorb too many neutrons.

**Gas Separators.** If a rotational flow pattern is used in an intermediate-scale reactor, gas will probably be removed from the core itself. This will be tested in the 8-ft model described previously. If the gas removal is shown to be incomplete or if a straight-through core is used, external gas separation will be required. This can be accomplished in a separator such as shown in Fig. 29. Vanes produce rotation of liquid flow-

ing in the pipe, which centrifuges gas into the center where it is removed.

A 5-in. model separator has been tested at flows up to 600 gpm. Preliminary measurements of gas-separating efficiency show a maximum of 80%. However, this can probably be increased to almost 100% by enlarging the gas outlet.

A thorough investigation of energy losses in the vanes, pipe, and volute is under way. Rotational and axial velocity traverses have been performed, and these indicate that the losses will not be severe. Other vane systems will be tested in the separator. These will be made from sheet metal rather than Lucite to facilitate accurate construction.

### TEST LOOP FOR 4000-gpm PUMP

Approximately 15% of the major components of the test loop and auxiliary equipment have been received. The Byron Jackson, 4000-gpm, canned-rotor pump has been delivered from Westinghouse. All other major items of equipment are on order. Completion of delivery of all material for the loop is anticipated by December 1952.

A description of the loop design was given in a previous quarterly report.<sup>(4)</sup> The design of the loop has been made on the basis of operation with  $\text{UO}_2\text{SO}_4$

<sup>(4)</sup>C. B. Graham et al., *HRP Quar. Prog. Rep.* Nov. 15, 1951, ORNL-1221, p. 18-20.

UNCLASSIFIED  
DWG. 15753

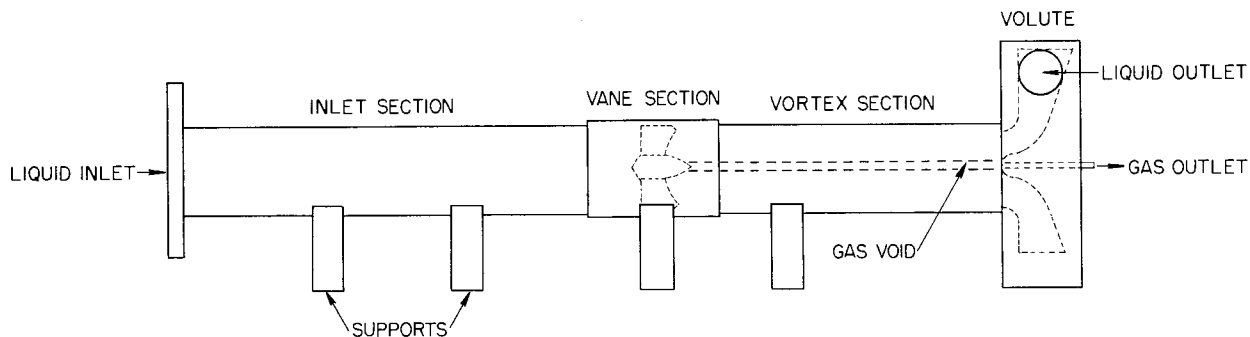


Fig. 29. Test Model of Pipe Gas Separator.

solution at 250°C. If it becomes desirable to operate the loop with a uranium slurry or cold solutions, the Byron Jackson pump will probably perform satisfactorily, with minor design changes.

#### MAIN CIRCULATING PUMPS

**Allis-Chalmers Pump Development.** The Allis-Chalmers Manufacturing Company has completed the preliminary design and engineering studies (phase I) for the 20,000-gpm, totally enclosed, centrifugal pump. Work on the final design (phase II) for the pump is approaching completion. The pump is designed for 1200 synchronous rpm to develop 160 ft of fluid head at a capacity of 20,000 gpm. It is a canned-rotor, totally enclosed type of pump that employs a metallic diaphragm to seal the motor stator from high-pressure fluid. The canned rotor rotates submerged in the high-pressure fluid.

All removable parts of the pump can be assembled or disassembled from the top of the pump, which is about 8 ft from the pumped fluid (radioactive) end of the pump. This will permit all reactor pump maintenance work to be performed some distance from the induced activity of the fuel circuit. A description of the pump design was given in the last quarterly report.<sup>(5)</sup>

Allis-Chalmers has been asked to complete detailed drawings and specifications, to make a cost estimate, and to submit a final report. Construction of the pump will be deferred until a fuel-container system with satisfactorily low corrosion has been obtained and additional funds are available.

If a smaller capacity pump is desired for the ISHR, the 20,000-gpm pump can be scaled down without sacrificing the many advantages in the present design.

An alternate to this plan would be to build the pump as designed and operate it at reduced capacity by using reduced speed or a smaller impeller.

**Worthington Corporation Pump Development.** The Worthington Corporation has completed a preliminary design and engineering studies (phase I) for a 20,000-gpm centrifugal pump. Work on phase II has produced designs of bearing-test equipment.

The Worthington pump design incorporates a conventional, high-suction pressure pump driven by a standard electric motor. The preliminary design and engineering studies produced a bearing-pressure breakdown design that utilizes an injection pump to introduce a small volume of uncontaminated water into an annulus formed by the drive shaft and a sleeve bearing. The layout of the pump unit shows the pump casing containing the impeller followed by the bearing-pressure breakdown around the drive shaft, which is in turn followed by an atmospheric-pressure mechanical shaft seal. External to the shaft seal is a heavy thrust bearing and the standard motor. A more complete description of the pump is given in the previous report.<sup>(2)</sup> Owing to lack of funds, the testing program, final design, and fabrication of the Worthington pump must be postponed.

**Byron Jackson Company Shaft Seal Development.** Proposals have been discussed with the Byron Jackson Company for initiating a program for the development of a satisfactory high-pressure mechanical shaft seal that can be installed on a conventional type of pump. This development is expected to be long range; but, if successful, should make possible the use of a pump that utilizes a conventional motor and conventional bearings and operates at a high efficiency. The lack of funds has made it necessary to suspend negotiations to initiate the development program.

<sup>(5)</sup> C. B. Graham et al., *HRP Quar. Prog. Rep.* July 1, 1952, ORNL-1318, p. 112.

## HRP QUARTERLY PROGRESS REPORT

### FUEL FEED PUMP DEVELOPMENT

The full-scale homogeneous reactor and the ISHR will require fuel feed pumps. The pulsafeeder pumps used in the HRE probably cannot be used because of low capacity and other limitations. A multistage centrifugal pump may be the preferred type. It is anticipated that future homogeneous reactors will operate at a pressure of about 1000 psi. Therefore the centrifugal pump must be a multistage unit to develop the required high heads (slightly higher than 1000 psi) for injecting fuel fluid into a pressurized reactor or a high-pressure dump tank. The head requirement is similar to that for the HRE; hence, if a high-head centrifugal pump could be developed in a reasonably short time it would provide an alternate pump to replace the pulsafeeder pumps in the HRE. Discussions with pump manufacturing companies regarding a feed pump have been conducted, with dual application of the pump as a service requirement.

The Byron Jackson Company and Allis-Chalmers Manufacturing Company have made preliminary proposals to design and fabricate centrifugal pumps to meet the service requirements. However, present funds are insufficient to permit this program to proceed.

### ISOLATION VALVES

Negotiations were initiated with Crane Company to make a predesign study of the feasibility of constructing the 20-in. isolation valves required in the external circulating system of a large homogeneous reactor. The study was to include valves for an aqueous solution and valves for a system containing a slurry. The negotiations have been suspended due to lack of funds.

### SMALL (5 gpm) CENTRIFUGAL PUMP DEVELOPMENT

At the request of ORNL, the Allis-Chalmers Manufacturing Company has

designed and built a canned-rotor pump rated at 5 gpm with a head of approximately 40 feet. It is designed to operate at pressures up to 2000 psi and temperatures up to 500°F. The special stator windings would permit even higher temperatures. All bearings are the fluid-piston type, the radial bearings being on a stationary shaft and the thrust bearing being on the impeller shrouds. All surfaces of the pump that come in contact with the fluid being pumped are constructed of type 347 stainless steel, except the bearings, which have a chrome-plated surface. The pump will possibly operate without the chrome-plate on the bearings, but this has not yet been demonstrated. The pump is sealed by means of a back-up flange; however, for high-pressure work a seal weld is also required.

One of these pumps was obtained, on loan, from Allis-Chalmers and is being tested. At present the pump has operated a total of 400 hr with 282 starts and stops. Allis-Chalmers has run the pump at 1000 psi with a fluid temperature of 400°F for 30 minutes. Experience at ORNL with the pump indicates that a seal weld is necessary for the pump to be leak free at pressures over 100 psi. An attempt was made to run slurry (with about 100 g of uranium per liter) in the pump loop at low temperature. It appeared that most of the slurry was centrifuged out in the rotor chamber of the pump. With the slurry in the rotor chamber, the pump would not start if once stopped. Power input to the pump indicated that the separation occurred within a few minutes after the pump was started.

The pump is designed to be used primarily for laboratory and pilot plant work where high efficiency is not required. Low cost was stressed in the design so that the pump could be scrapped if damaged by corrosion or contaminated by radioactivity. The characteristic curve is flat, and there

is approximately 40 ft of head from zero flow to about 18 gpm. Allis-Chalmers is considering several design changes to (1) provide closure without necessity of seal welding, (2) make circulation of slurry possible, and (3) lower the temperature in the rotor chamber.

### LARGE HEAT EXCHANGERS

Development has continued on large heat exchangers, the tentative specifications of which have been presented previously.<sup>(6)</sup> A preliminary design has been received from the Lummus Company of New York and, after some revision of the design at ORNL, the following preliminary design data were established:

Heat transfer	200,000 kw	
Steam capacity	650,000 lb/hr at 200 psig, saturation	
Conditions on boiling water side		
Operating pressure	200 psig	
Operating temperature	388°F	
Feedwater inlet temperature	180°F	
Conditions on fuel side		
Operating pressure	1000 psig	
Inlet temperature	482°F	
Outlet temperature	409°F	
Flow rate	20,000 gpm	
U tubes		
Outside diameter, in.	3/8	1/2
Heat transfer surface, <sup>(7)</sup> ft <sup>2</sup>	17,600	17,200
Material	347 SS, 18 BWG	347 SS, 18 BWG
Average length, ft	19.4	30
Quantity	9,250	4,400
Average flow velocity, ft/sec	11.5	11.5
Pressure drop, psi	29	30
Holdup, ft <sup>3</sup>	75	116

No conclusions can be drawn from the above data regarding the optimum tube size. The considerable saving in holdup afforded by the use of 3/8-in.-OD tubes may possibly be offset by the

<sup>(6)</sup> C. B. Graham *et al.*, *HRP Quar. Prog. Rep.* March 15, 1952, ORNL-1280, p. 139-140.

<sup>(7)</sup> Based on 75% of "clean" heat transfer coefficient.

additional cost involved in their fabrication, since approximately twice as many 3/8-in. tubes would be required.

One of the major problems encountered in the design of large liquid-to-boiling liquid heat exchangers is the proper removal of steam. In order to keep all tubes wet at all times and thereby keep heat transfer rates high, various tube bundle arrangements have been studied. Three of the possibilities appear promising.

1. The arrangement comprising a horizontal tube bundle and an elevated horizontal steam drum connected by conventional risers and downcomers, shown in Fig. 30a, produces a head on the exchanger that tends to keep the tubes submerged and at the same time provides a moderate natural-circulation head. Steam being removed from the exchanger through the risers will carry up water that will return through the downcomers and be recirculated through the heat exchangers. Feedwater will be injected into the circulation loop at the rate required to replace water evaporated during the cycle. For more positive control at various loads, it may be desirable to install pumps or injectors in the loop and thus eliminate dependence on natural circulation. If forced circulation is used, the amount of heat transfer surface required will be reduced slightly.

The arrangements shown in Figs. 30a and 30c offer the advantage of having comparatively small heat exchanger units that could be replaced individually in the event of failure. Among the disadvantages are the rather complex water-side piping systems, with corresponding expansion problems, and the comparatively large shields required. Shielding requirements have been based on the belief that it will be desirable to have the steam drums shielded to reduce the radiation hazard in the event of fuel leakage from the heat exchanger.

DWG. 16896

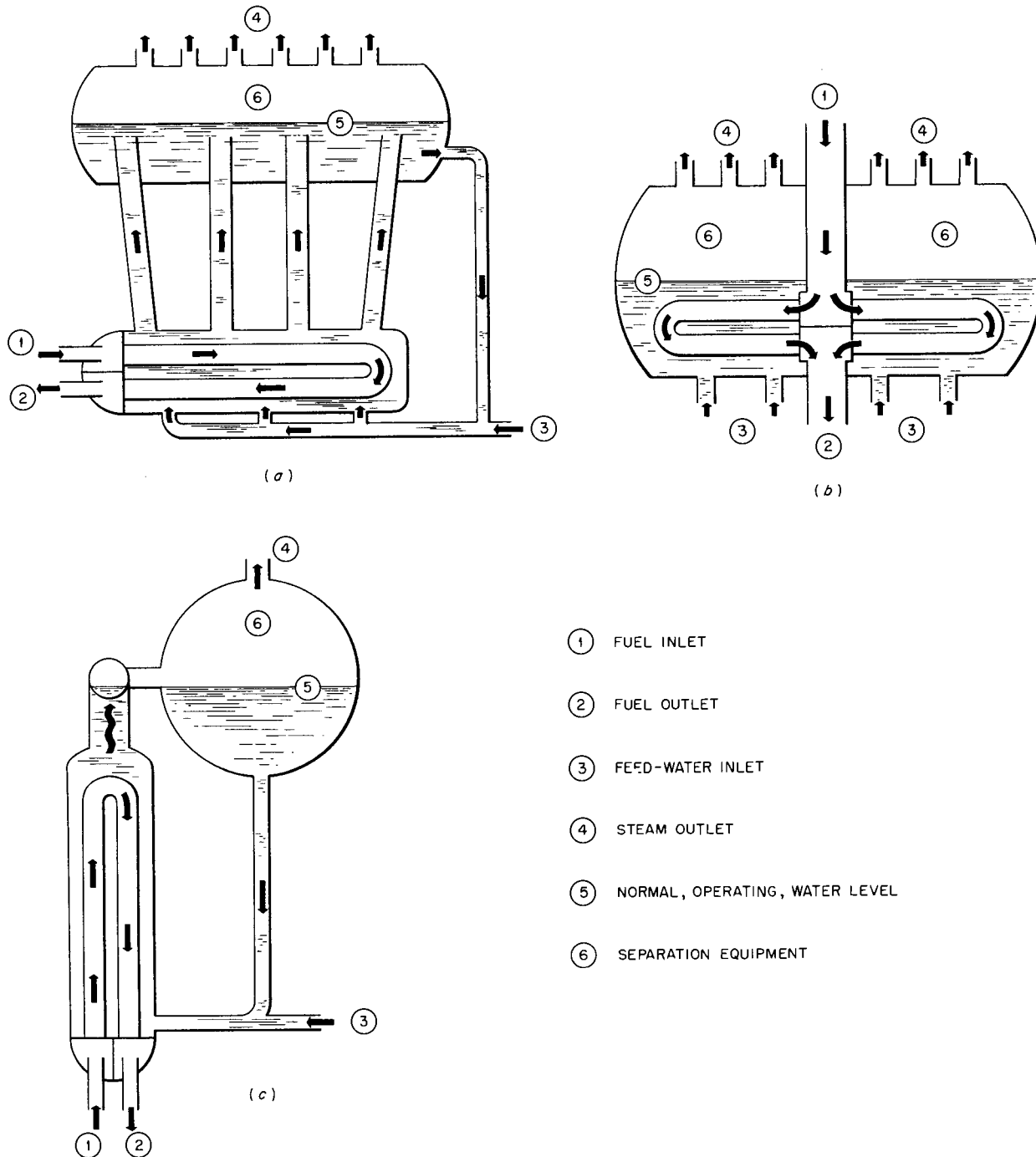


Fig. 30. Three Possible Arrangements for the Main Heat Exchanger.

2. A more compact design can be obtained with a horizontal tube bundle placed within a horizontal drum. A design has been proposed in which fuel enters a common header located centrally in the lower half of the drum and then flows outward toward the drum ends through U-tube bundles (Fig. 30b). The level of the steam-water surface will be maintained near the center of the drum to provide the maximum steam liberation area. The upper portion of the drum provides adequate space for steam separation equipment. This design creates a minimum of expansion problems and provides minimum holdup in the exchanger header and header piping. It is expected that the cost of this unit will be somewhat lower than that of the designs shown in Figs. 30a and 30c. A study is being made to determine the optimum tube system for this type of steam generator. Factors such as the number of tubes, tube size, tube pitch, depth of tube rows, and feedwater distribution are being thoroughly investigated in order to avoid the possibility of steam binding in the tube bundle. Thus far, industrial heat exchanger concerns have been unable to supply this information, and it is possible that an experiment may be required in order to obtain sufficient design data.

3. In another arrangement, vertical exchangers are connected by headers to an elevated horizontal steam drum (Fig. 30c). The vertical arrangement is an alternative to removing steam from horizontal tube bundles. With forced circulation, little difficulty may be expected in steam formation and removal. However, in a vertical U-tube system, there arises the problem of gas binding within the tubes. This will be encountered at start-up and perhaps to a limited extent during steady-state operation. The determination of the degree of seriousness and the most practicable method of dealing with this problem must await

further development of the reactor and methods of operating the reactor.

A memorandum covering the large heat exchanger investigation will be issued in the near future.

#### NEW PROJECTS

In collaboration with G. H. Jenks of the Chemistry Division, an in-pile circulating loop will be designed for experiments in the LITR. This loop, or loops, should be capable of operation with either solution or slurry. It should consist of a pump, core, recombiner, and suitable accessories such as heaters, corrosion samplers, and controls. It should be fabricated largely from stainless steel, but the components that will be subjected to radiation should be designed for reasonably easy fabrication from titanium. The loop should be capable of operating at any temperature between 100 and 250°C.

Allis-Chalmers and ORNL are considering revisions in the design of the 5-gpm pump for this application. Gas removal from water in a preliminary, laboratory model of a small core has been demonstrated by Jenks. Layouts of the loop should be started in the near future.

Conversion of the HRE mockup to one suitable for operation with uranium oxide slurry containing 200 to 300 g of uranium per liter is being studied. In discussion with those who have circulated slurries, a list of components that may be troublesome because of settling or plugging has been prepared. These components are dump tanks, let-down system, pressurizer (and its level control), core, heat exchanger, and pulsafeeder pump. Component tests have not yet been planned, but it is expected that relatively inexpensive experiments will indicate the difficulties that will be encountered. If serious difficulty is encountered, a redesign of the fuel system may be desirable.

# HRP QUARTERLY PROGRESS REPORT

## CORROSION

E. G. Bohlmann, Section Chief

### DYNAMIC CORROSION STUDIES

**Construction and Maintenance of Pump Loops** (J. H. Gross, H. C. Savage). The Westinghouse model 100A pumps used in the circulating test loops continue to give satisfactory service, except for the difficulties noted previously.<sup>(1)</sup> No pump failures occurred during the past quarter. The program to repair the pump stators in the local shops has been very successful. Three pumps have been repaired by removing the Inconel diaphragms, rewinding the stators, and installing new stainless steel diaphragms to replace those of Inconel. Two repaired pumps with type 347 stainless steel diaphragms are now in operation and appear to be quite satisfactory after more than 1000 hr of operation in a uranyl sulfate solution containing 100 g of uranium per liter. In one pump an increase of approximately 2 amp per terminal (54 to 56) was noted in changing from an Inconel diaphragm to a type 347 stainless steel diaphragm. A third pump has now been repaired by rewinding and installing a type 321 stainless steel diaphragm. After the pump has been tested in a loop and seal welded, it will be sent to the HRE site as a spare for the present pump.

The Stellite 98M2 journal bushings and Graphitar No. 14 bearings in the model 100A pumps are giving excellent service. Wear on the radial surfaces of these bearings is negligible in all concentrations of both uranyl sulfate and uranyl fluoride solutions tested. Concentrations of uranyl sulfate up to 800 g of uranium per liter and of uranyl fluoride con-

taining 300 g of uranium per liter have been used. Wear of the radial bearing surfaces has occurred only when the circulating solution became contaminated with large amounts of dirt or other abrasive material or when the bearings were run dry. One pump operating in clean uranyl sulfate solution (300 g of uranium per liter) has shown no measurable bearing wear (<0.001 in.) after more than 3000 hours. All pumps are adjusted so that a hydraulic balance keeps the rotor "floating" free between the front and rear thrust bearing surfaces. Wear on these thrust surfaces will occur only as a result of loss of hydraulic balance. Unless excessive corrosion occurs at the impeller hubs and seal rings or the welded balance pads,<sup>(2)</sup> this hydraulic balance will be maintained indefinitely. Several pumps operating under conditions of low corrosion rates have shown no loss of thrust balance after 2000 to 3000 hr of operation. In this respect, tantalum or titanium impeller seal rings and an impeller of corrosion-resistant material, such as titanium, are essential in maintaining hydraulic thrust balance over a long period under corrosive conditions (concentration,  $\geq 40$  g of uranium per liter of solution; temperature,  $> 100^\circ\text{C}$ ).

Loop A has been rebuilt, with a 1 1/2-in. circulating line, a new pressurizer, and a number of new safety features, for operation with mixtures of hydrogen and oxygen. All valves were installed inside the safety shield with extension handles to the front of the control board so that the operator is protected by the safety shield and the panel board when valves are opened or closed.

<sup>(1)</sup> J. H. Gross and H. C. Savage, *HRP Quar. Prog. Rep.* July 1, 1952, ORNL-1318, p. 40-41.

<sup>(2)</sup> Figure 13, *HRP Quar. Prog. Rep.* March 15, 1952, ORNL-1280, p. 42.

Separate gas addition lines and valves were installed for hydrogen and oxygen; the valves are below the liquid level in the circulating line. The two exposed pressure gages (for low- and high-pressure readings) were moved to a panel beside the main panel board and are now behind a 1-in. thick Lucite shield covered with heavy screen wire. The high-pressure gage is a blow-out-back type.

Because of the evidence of excellent corrosion resistance of titanium to concentrations of uranyl sulfate solution from 5 to 300 g of uranium per liter at temperatures up to 250°C, test inserts of titanium were installed in loop A. One section of the 1 1/2-in., type 347 stainless steel, circulating line was replaced with a 15-in.-long venturi test section of titanium (Fig. 31). Two additional pieces of titanium tubing were inserted in a tee at the pump discharge (Fig. 32). In effect, the titanium inserts serve as a liner. Flats were milled on one half the circumference in order that crevice corrosion between the type 347 stainless steel and the titanium might be minimized in that area.

The Westinghouse pump installed in loop A was rebuilt in the local shop with a type 347 stainless steel diaphragm to replace the Inconel diaphragm. In addition, the standard

stainless steel impeller was replaced by a titanium (type RC-70) impeller that was also fabricated in the local shop. The front shroud of the impeller was attached to the rear shroud vanes by plug welds and titanium rivets, and titanium seal rings were installed around the impeller hubs.

With the modified loop A back in service, nine loops are now available for dynamic corrosion tests, and two additional loops are being constructed. One is a 1-in., type 347 stainless steel loop, identified as I, with various types of welded and forged fittings similar to those of loop C;<sup>(3)</sup> the other one, identified as G, will be an all-titanium loop, except for the pressurizer, which will have to be type 347 stainless steel because suitable large-diameter titanium pipe is not available. Loops C and I will be used to evaluate corrosion rates and effects at points of high turbulence, and loop G will be used to further evaluate the corrosion resistance, effect on solution stability, and metallurgical properties of titanium.

**Pump Loop Test Results.** During the past year the pump loop dynamic corrosion work has emphasized exploratory studies. The corrosion of various metals and alloys by uranyl

<sup>(3)</sup>Gross and Savage, *op. cit.*, p. 36.

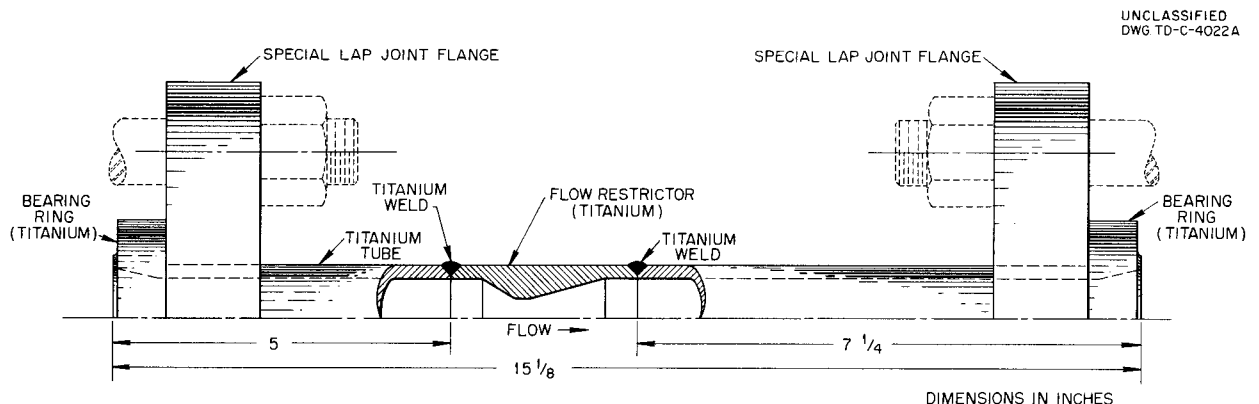


Fig. 31. Titanium Test Assembly.

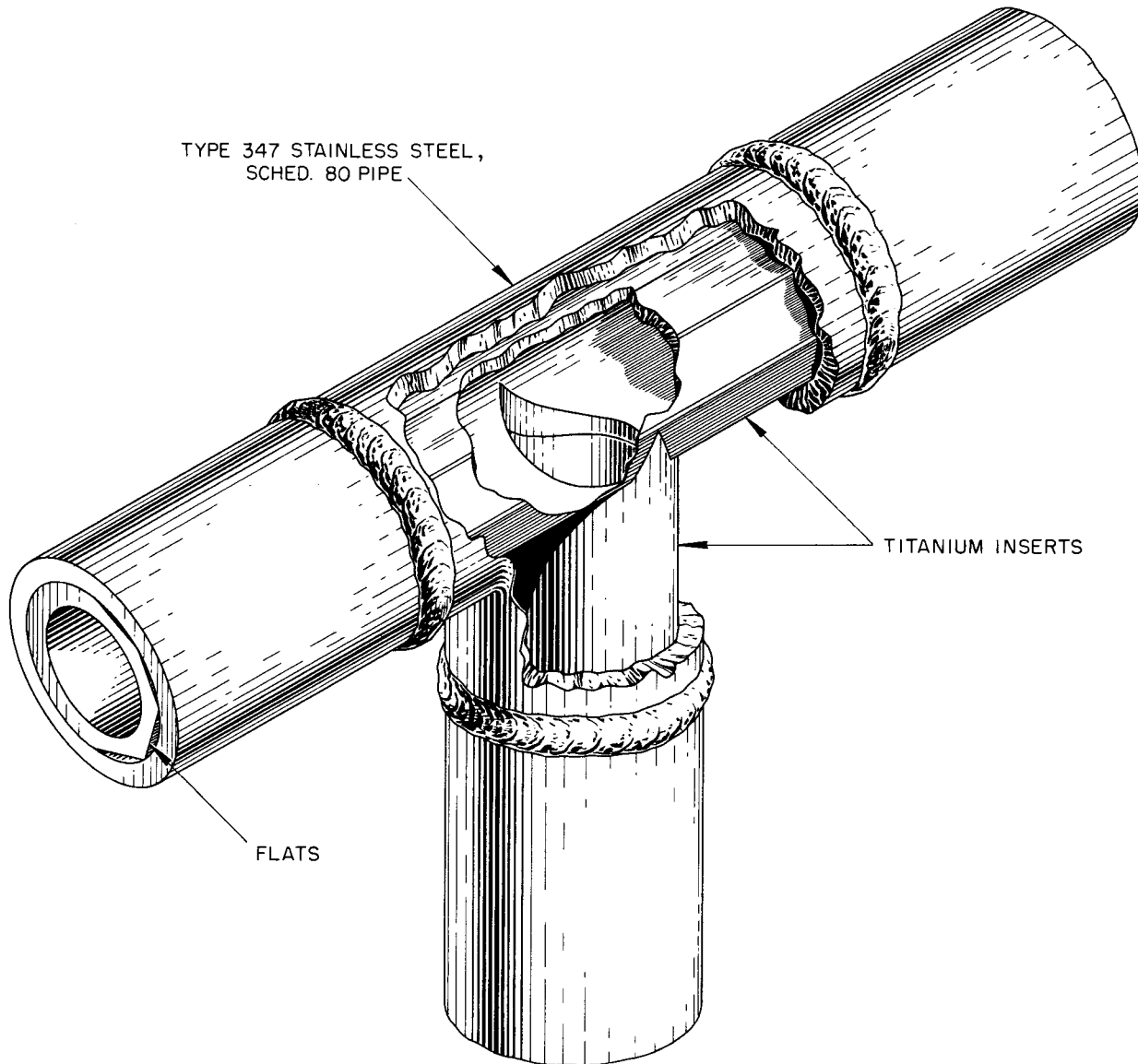


Fig. 32. Titanium T Inserts.

sulfate solutions, and to a lesser extent by uranyl fluoride solutions, has been studied as a function of concentration, temperature, velocity or turbulence, and additives. This phase of the program is now being superseded by a program that will emphasize more thorough examination of those systems that appear promising on the basis of the exploratory tests. The exploratory studies have been

primarily concerned with uranyl sulfate solutions; however, experimental data on uranyl fluoride solutions suggest that in most cases they do not differ substantially from uranyl sulfate solutions in their corrosion behavior. The apparently promising systems are discussed below:

1. Twenty-five hundred hours of operation of a type 347 stainless steel system at about 100°C have been

accumulated with a uranyl sulfate solution containing 100 g of uranium per liter. The general corrosion rate shown by the rate of increase of nickel concentration in solution is approximately 0.1 mpy.

2. Twenty-eight hundred hours of operation of a type 347 stainless steel system at about 100°C have been accumulated with a uranyl sulfate solution containing 300 g of uranium per liter. The general corrosion rate in this equipment has been consistently less than 0.5 mpy.

Examination of the loop and specimens in both experiments revealed no visible evidence of localized attack such as was described in previous reports. A rather severe crevice type of attack that requires further investigation has been encountered, however.

3. One thousand hours of operation of a type 347 stainless steel system at about 100°C have been accumulated with a uranyl fluoride solution containing 100 g of uranium per liter. The indicated corrosion rate based on specimen weight changes was approximately 0.5 mpy.

4. Thirty-two hundred hours of operation of a type 347 stainless steel at about 250°C have been accumulated with uranyl sulfate solution containing 5 g of uranium per liter. The general corrosion rate has been consistently less than 0.5 mpy, and there is no visible evidence of localized attack.

5. A titanium system will be operated at 150 to 250°C, with uranyl sulfate solution containing 40 g or more of uranium per liter. Under conditions of high temperature and moderate and higher uranium concentration, titanium is the only metal or alloy that has shown adequate corrosion resistance. An expanded program of investigation of this system is getting under way. Loop A, containing several titanium components, is described in the preceding section

of this report and a substantially all-titanium loop should be in operation in the next quarter.

Although some exploratory work will continue, present plans are to emphasize a thorough examination of all aspects of these promising systems. Many of the available loops are being converted for such tests at the present time.

It is hoped that a summary report on the exploratory studies completed to date can be assembled and issued in the next few months.

**Small-Scale Dynamic Tests** (G. E. Moore, D. Schwartz). Preliminary tests have been carried out on two mechanisms that, it is hoped, will provide an inexpensive method for studying dynamic corrosion in the HRE corrosion program. The first makes use of a bellows to provide a flexible pressure seal through which motion can be transmitted into the conventional autoclaves currently used in the static corrosion program. The second is a toroid loop, such as has been described by NACA.<sup>(4)</sup>

#### STATIC CORROSION STUDIES

J. L. English      S. H. Wheeler

Examination of the uranyl sulfate-type 347 stainless steel system at 250°C was continued during the past quarter with emphasis on the following phases:

1. the effect of dissolved oxygen concentration at 250°C on the corrosion behavior of type 347 stainless steel in uranyl sulfate solutions containing 40 g of uranium per liter, including further appraisal of the analysis of dissolved nickel in solution as a criterion for measurement of corrosion damage,

(4) L. G. Desmon and D. R. Mosher, *Dynamic Corrosion of a Stainless Steel Specimen by Water at 500°F Using a Toroid Circulating Apparatus*, NACA Research Memorandum RME52F03 (July 16, 1952).

## HRP QUARTERLY PROGRESS REPORT

2. the use of copper sulfate additions in oxygenated uranyl sulfate solutions containing 40 g of uranium per liter at 250°C for possible inhibition of corrosion attack on type 347 stainless steel,
3. the effect of long-term exposure on the corrosion behavior of type 347 stainless steel at 250°C in oxygenated uranyl sulfate solutions containing approximately 200 and 300 g of uranium per liter.

The results of these studies are discussed in the following sections of this report.

**Effect of Dissolved Oxygen Content on Corrosion.** The effect of dissolved oxygen concentration on the corrosion of type 347 stainless steel at 250°C in uranyl sulfate solutions containing 40, 100, and 300 g of uranium per liter has been reported previously.<sup>(5,6)</sup> It was observed, generally, that the final corrosion rates after 10 to 11 weeks of exposure in these solutions were independent of dissolved oxygen content in the range of 100 to 3700 ppm at 250°C. The present investigation is concerned with the effect of dissolved oxygen content from 135 to 6275 ppm at 250°C on the short-term corrosion behavior of type 347 stainless steel in uranyl sulfate solutions containing 40 g of uranium per liter.

In order to eliminate the possibility that the surface condition of the type 347 stainless steel test autoclave would influence the final corrosion evaluation and also to confine the entire corrosion process to test specimens that could be handled easily, the uranyl sulfate-type 347 stainless steel test system was isolated in a conventional, 225-ml total capacity, stainless steel autoclave lined with 20-mil platinum

(5) J. L. English and S. H. Wheeler, *HRP Quar. Prog. Rep. March 15, 1952*, ORNL-1280, p. 62-68.

(6) J. L. English et al., *HRP Quar. Prog. Rep. July 1, 1952*, ORNL-1318, p. 42-49.

sheet. The autoclave and liner were sealed with a flat, type 347 stainless steel ring gasket between a lip on the platinum liner and a type 347 stainless steel pressure plug in the vapor phase. A quartz rod, replaced every run, was used to support the corrosion specimen in the uranyl sulfate solution in order to eliminate galvanic corrosion effects between the platinum and the type 347 stainless steel specimen.

The corrosion specimens were machined from 3.175-cm-dia, hot-rolled, type 347 stainless steel bar. The size of the specimens was such that the area for exposure varied between 19 and 20 cm<sup>2</sup>. A 0.5-cm-dia hole was drilled in the center of each specimen to allow for support by the quartz hanger. The average hardness of the stainless alloy was measured as 75 R<sub>B</sub> on a Rockwell tester. No conditioning of the machined specimens was made prior to test other than the usual degreasing in acetone and alcohol, drying, and weighing. The actual chemical composition of the test material and nominal ranges for the various components of type 347 stainless steel are given in Table 18.

The chemical and physical properties of the uranyl sulfate solution used for all corrosion tests are given in Table 19.

**TABLE 18. CHEMICAL COMPOSITION OF TYPE 347 STAINLESS STEEL CORROSION TEST SPECIMENS**

COMPONENTS	ACTUAL wt %	NOMINAL wt %
C	0.07	0.10 max
Mn	1.22	2.00 max
Cr	18.00	17.0 to 19.0
Ni	10.70	9.0 to 12.0
Si	0.44	0.75 max
Nb	0.91	8 × C* min

\*Eight times as much as the carbon content.

TABLE 19. CHEMICAL AND PHYSICAL PROPERTIES OF THE URANYL SULFATE TEST SOLUTION

Total U, g/l	39.50
SO <sub>4</sub> , g/l	15.77
SO <sub>4</sub> :U ratio	0.99
U(IV), g/l	< 0.10
NO <sub>3</sub> , g/l	0.12
NH <sub>4</sub> , g/l	< 0.10
Free acid content	negligible
Nickel, μg/ml	0.4
Density at 25°C, g/cm <sup>3</sup>	1.055
pH (0.1 M solution)	2.65
pH (solution as used)	2.38

The oxygen partial pressures investigated in the corrosion study were produced by the thermal decomposition of 30% H<sub>2</sub>O<sub>2</sub> at 250°C. The H<sub>2</sub>O<sub>2</sub> was added to the UO<sub>2</sub>SO<sub>4</sub> solution at room temperature in amounts calculated to produce the desired oxygen partial pressure at 250°C. The total initial volume of UO<sub>2</sub>SO<sub>4</sub> and H<sub>2</sub>O<sub>2</sub> addition was kept at 150 ± 1 ml so that the solution and vapor phase volumes at 250°C were the same for each test. A dilution effect on the original UO<sub>2</sub>SO<sub>4</sub> solution containing 40 g of uranium per liter resulted from the addition of increasingly larger quantities of H<sub>2</sub>O<sub>2</sub> to produce the higher oxygen partial pressures. The estimated oxygen solubilities, based on the solubility of oxygen in water, are included in Table 20.

The test procedure consisted of placing a single corrosion specimen supported by a quartz hanger in the platinum-lined autoclave containing the UO<sub>2</sub>SO<sub>4</sub> solution and the necessary volume of 30% H<sub>2</sub>O<sub>2</sub> to produce the desired oxygen partial pressure at 250°C. The tests were run for one week at each partial pressure of oxygen in an electrically heated and controlled oven. At the end of each

TABLE 20. ESTIMATED DISSOLVED OXYGEN CONTENT IN URANYL SULFATE SOLUTION CONTAINING 40 g OF URANIUM PER LITER AT 250°C

OXYGEN PARTIAL PRESSURE (psia)	DISSOLVED OXYGEN (ppm)
25	135
50	270
75	405
100	545
150	815
250	1425
500	2850
750	4275
1100	6275

run, the test specimen was removed, scrubbed with a surgical brush in distilled water, degreased, dried, and weighed. After microscopic examination at 30X, the specimens were cleaned cathodically in 5% H<sub>2</sub>SO<sub>4</sub>, containing an organic inhibitor, for 3 min at 75°C by using a cathodic current density of 20 amp/dm<sup>2</sup>. The specimens were then re-examined microscopically for evidences of localized corrosion attack.

Solution samples from the test solutions were submitted for uranium, nickel, manganese, chromium, and iron determinations. The solution pH was measured on a Beckman pH meter.

The results from the chemical analyses and the final pH values are reported in Table 21. These results were corrected for dilution resulting from the peroxide additions; the nickel contents were corrected for the amount of dissolved nickel present initially in the uranyl sulfate solution.

The final uranium analyses were within ±4% of the initial values, with the exception of the results in the 1100-psia oxygen test, in which there was a 7% decrease in total uranium concentration during the

## HRP QUARTERLY PROGRESS REPORT

week of exposure. The dissolved nickel content, although somewhat erratic in agreement, showed no positive trends with increased oxygen concentration. The average dissolved nickel content for the nine tests was 11.4  $\mu\text{g/ml}$ . No unusual corrosion effects were apparent from the dissolved chromium, manganese, and iron contents.

The test specimens were examined microscopically at 30X after removal from the solutions. In all cases, the surfaces were covered with quite uniform, blue-gray colored, oxide films that were semiglossy in ap-

pearance. No signs of localized corrosion attack were observed. After electrolytic defilming, the specimens were re-examined microscopically at 30 and 150X. The defilmed surfaces were dull and silver-white in color. With the exception of lightly etched appearance, there was no evidence of pitting corrosion attack on any surfaces. The defilmed weight losses, corrected for metal loss by attack of the defilming solution on unexposed specimens, are reported in Table 22 with the calculated corrosion rates.

**TABLE 21. ANALYTICAL RESULTS ON FINAL URANYL SULFATE CORROSION TEST SOLUTIONS**

OXYGEN PARTIAL PRESSURE (psia)	DISSOLVED OXYGEN (ppm)	INITIAL URANIUM (g/l)	FINAL URANIUM (g/l)	FINAL pH	DISSOLVED IONS ( $\mu\text{g/ml}$ )			
					Ni	Mn	Cr	Fe
25	135	39.4	38.8	2.39	9.6	1	9	2
50	270	39.3	37.8	2.23	14.6	3	13	< 1
75	405	39.2	38.6	2.36	9.6	1	13	4
100	545	39.1	38.7	2.38	10.6	< 1	19	1
150	815	38.8	38.0	2.38	13.6	< 1	13	< 1
250	1425	38.3	36.8	2.47	9.7	1	13	3
500	2850	37.1	37.2	2.37	12.6	3	14	3
750	4275	35.8	34.8	2.40	10.6	2	12	< 1
1100	6275	34.2	31.8	2.45	11.7	< 1	11	2

**TABLE 22. DEFILMED-WEIGHT-LOSS CORROSION RATES AFTER ONE WEEK AT 250°C ON TYPE 347 STAINLESS STEEL EXPOSED IN OXYGENATED  $\text{UO}_2\text{SO}_4$  SOLUTION CONTAINING 40 g OF URANIUM PER LITER**

OXYGEN PARTIAL PRESSURE (psia)	DISSOLVED OXYGEN (ppm)	DEFILMED WEIGHT LOSS ( $\text{mg/cm}^2$ )	CORROSION RATE	
			$\text{mg/dm}^2/\text{day}$	mpy
25	135	0.57	8.2	1.5
50	270	0.78	11.2	2.0
75	405	0.62	8.9	1.6
100	545	0.60	8.5	1.5
150	815	0.96	13.7	2.5
250	1425	0.78	11.2	2.0
500	2850	0.77	11.0	2.0
750	4275	0.63	9.0	1.6
1100	6275	0.59	8.4	1.5

FOR PERIOD ENDING OCTOBER 1, 1952

A rough approximation of the film weight on the specimens before the defilming operation was obtained by subtracting the as-removed weight loss from the final defilmed weight loss. Film weights ranged from 0.3 to 0.7 mg/cm<sup>2</sup> after one week of exposure. There was no particular orientation of the weights with regard to the dissolved oxygen content in the test solutions.

Since the increase in nickel content of the test solutions resulted from corrosion attack on the type 347 stainless steel specimen only, it was possible to determine rather accurately the extent of corrosion damage on the stainless alloy from the dissolved nickel values. This method is limited by the analytical accuracy of the nickel analytical method and by the fact that corrosion attack on the test specimen is assumed to be uniform. Corrosion rates calculated from the dissolved nickel in solution were based on the nickel content of 10.7% in the original alloy and are compared with the defilmed weight loss corrosion rates in Table 23.

Corrosion rates determined by the dissolved nickel method were slightly

higher than the rates calculated from the defilmed weight losses. The average corrosion rate for the nine tests by defilmed weight losses was 1.8 mpy as compared with an average value of 2.1 mpy obtained by the dissolved nickel method. These results were considered to be indicative of good agreement between the two methods.

The corrosion behavior of the platinum liner was observed closely during the sequence of exposures. The only change noted in appearance was a slight darkening of the surfaces in contact with the uranyl sulfate solutions at 250°C. The surfaces in the vapor phase were unchanged from their original appearance.

It was concluded from the results of this investigation that the corrosion rate for type 347 stainless steel in uranyl sulfate solutions containing 40 g of uranium per liter at 250°C was independent of the dissolved oxygen concentration between 135 and 6275 ppm after one week of exposure.

**Effect of CuSO<sub>4</sub> Additions on Corrosion.** The use of cupric sulfate additions in uranyl sulfate systems at 250°C as a possible corrosion inhibitor of type 347 stainless steel was investigated on the basis of the

**TABLE 23. COMPARISON OF CORROSION RATES ON TYPE 347 STAINLESS STEEL BY DEFILMED WEIGHT LOSSES AND DISSOLVED NICKEL CONTENT AFTER ONE WEEK AT 250°C IN OXYGENATED UO<sub>2</sub>SO<sub>4</sub> SOLUTIONS CONTAINING 40 g OF URANIUM PER LITER**

OXYGEN PARTIAL PRESSURE (psia)	DISSOLVED OXYGEN (ppm)	CORROSION RATE (mpy)	
		Weight Loss	Dissolved Nickel
25	135	1.5	1.7
50	270	2.0	2.6
75	405	1.6	1.7
100	545	1.5	1.9
150	815	2.5	2.7
250	1425	2.0	1.8
500	2850	2.0	2.3
750	4275	1.6	1.9
1100	6275	1.5	2.1

## HRP QUARTERLY PROGRESS REPORT

successful application of the inhibitor in many industrial processes handling sulfuric acid solutions at lower temperatures. It has been reported that the presence of 0.25 to 1.0%  $\text{CuSO}_4$  in 30%  $\text{H}_2\text{SO}_4$  solutions at 95°C reduced corrosion attack to negligible values on types 304 and 316 stainless steels as compared with corrosion rates of 3.5 and 2.4 in./mo on these materials in uninhibited acid at similar concentration and temperature.<sup>(7)</sup> A second and very important reason for acquiring information on the effect of cupric ions on the corrosion of type 347 stainless steel in  $\text{UO}_2\text{SO}_4$  solutions at 250°C was the marked success reported by the Chemistry Division with the use of  $\text{CuSO}_4$  as a homogeneous recombiner for hydrogen and oxygen.<sup>(8)</sup> Dynamic tests of the effect of  $\text{CuSO}_4$  additions on corrosion by  $\text{UO}_2\text{SO}_4$  solutions at 250°C have been reported previously.<sup>(9)</sup> Results from this work indicated that the presence of 1.5 or 6.4 g/l of Cu(II) as  $\text{CuSO}_4$  in  $\text{UO}_2\text{SO}_4$  solution containing 40 g of uranium per liter at 250°C caused an acceleration of the generalized corrosion attack.

Concentrations of  $\text{CuSO}_4$  studied in the present investigation included 260, 790, 1360, and 2910  $\mu\text{g}/\text{ml}$ . These concentrations as  $\text{CuSO}_4$  were in  $\text{UO}_2\text{SO}_4$  solution containing 40.1 g of uranium per liter; the complete analysis for the  $\text{UO}_2\text{SO}_4$  solution used appears in Table 24. The analyzed Cu(II) contents in the four test solutions were 105, 315, 540, and 1160  $\mu\text{g}/\text{ml}$ , respectively.

Type 347 stainless steel corrosion test wafers were machined from 3.175-cm-dia hot-rolled bar. The average specimen area was 20  $\text{cm}^2$ . No prepa-

TABLE 24. CHEMICAL AND PHYSICAL PROPERTIES OF URANYL SULFATE TEST SOLUTION

Total U, g/l	40.1
$\text{SO}_4$ , g/l	15.9
$\text{SO}_4$ :U ratio	0.983
U(IV), g/l	< 0.1
$\text{NO}_3$ , g/l	< 0.1
$\text{NH}_4$ , g/l	< 0.05
Free acid content	negligible
Nickel, $\mu\text{g}/\text{ml}$	1.0
Density at 25°C, $\text{g}/\text{cm}^3$	1.054
pH (0.1 M solution)	2.70
pH (solution as used)	2.38

ration was given the specimens other than the usual degreasing procedure prior to the tests. Duplicate tests were run with each concentration of  $\text{CuSO}_4$  and with a single specimen in each autoclave. A set of specimens was also run for comparison in copper-free uranyl sulfate solutions.

The tests were operated at 250°C with an oxygen partial pressure of approximately 150 psia; the dissolved oxygen content at this partial pressure was estimated as 815 ppm. Calculated amounts of 30%  $\text{H}_2\text{O}_2$  were added to the test solutions at room temperature in order to produce the desired oxygen partial pressure at 250°C by thermal decomposition.

Type 347 stainless steel autoclaves with 225-ml capacity were used to contain the solutions and corrosion specimens. Prior to use, the autoclaves were pickled in 10%  $\text{HNO}_3$ -4% HF at 60°C for 20 to 30 minutes. A volume of 150 ml of test solution, consisting of the  $\text{UO}_2\text{SO}_4$  solution and the necessary amount of 30%  $\text{H}_2\text{O}_2$ , was placed in each autoclave with the corrosion specimen, which was suspended in the test medium by means of a type 347 stainless steel hanger. The original  $\text{UO}_2\text{SO}_4$  solutions were used

(7) "Sulfuric Acid vs. Construction Materials," Corrosion Forum in *Chem. Engr.* 55, July-December, 1948.

(8) H. F. McDuffie et al., *HRP Quar. Prog. Rep.* Nov. 15, 1951, ORNL-1221, p. 36-38.

(9) Gross and Savage, *op. cit.*, p. 37.

for the entire eight weeks of exposure, with the exception that at the end of each weekly period, 15 ml was withdrawn from each test for chemical analysis and replaced with 15 ml of new solution containing similar  $\text{CuSO}_4$  content as present initially in the test. Additions of the 30%  $\text{H}_2\text{O}_2$  were made on a weekly basis also.

The tests were run for weekly intervals in an electrically heated and controlled oven at  $250^\circ\text{C}$ . At the end of each week, the autoclaves were dismantled for examination of the specimens, measurement of solution pH, and solution sampling. The solution samples were analyzed for uranium, copper, and nickel contents. The cumulative test time was eight weeks.

In general, little significance has been attached to the as-removed-and-scrubbed weight changes on type 347 stainless steel corrosion specimens after exposure in  $\text{UO}_2\text{SO}_4$  solutions at  $250^\circ\text{C}$ . An accurate evaluation of corrosion damage is not possible from this type of data, since the presence of bulk oxide films on the metal surfaces obscures the true weight loss of the metal. Usually, in static corrosion studies, little agreement between as-removed weight changes for duplicate sets of specimens can be expected even when the specimens are exposed in the same test autoclave. The as-removed weight loss data for the  $\text{CuSO}_4$  tests were unusual in this respect, however, in that excellent agreement was obtained from the duplicate experiments. The agreement was within  $\pm 0.2 \text{ mg/cm}^2$  for duplicate specimens. There was a definite trend established by the behavior of the specimens: with increased  $\text{CuSO}_4$  concentration, the magnitude of as-removed weight losses decreased. This behavior is shown in Fig. 33. Visually, there was no distinct change in appearance of the specimens as affected by the  $\text{CuSO}_4$

concentration. All surfaces, including those of the blank specimens, were coated with uniform oxide films that ranged in color from dark blue-gray to gray-black. An attempt to electrolytically defilm the specimens at the completion of the tests was unsuccessful because the films were too tenacious.

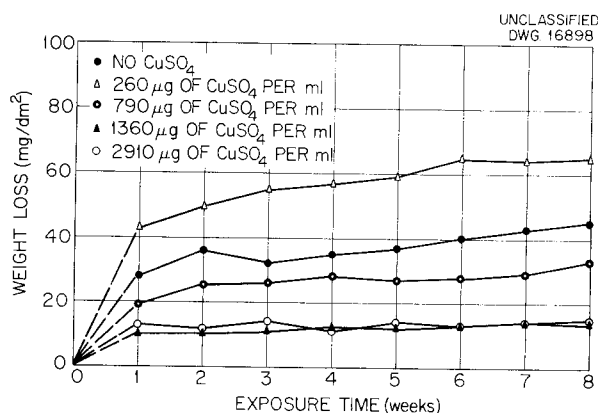


Fig. 33. Average, Cumulative, As-Removed Weight Losses on Type 347 Stainless Steel in  $\text{UO}_2\text{SO}_4$  Solutions Containing 40 g of Uranium per Liter and Various Amounts of  $\text{CuSO}_4$ , Pressurized with 1250 psia of Oxygen at  $250^\circ\text{C}$ .

The cumulative dissolved nickel contents in the solutions, corrected for weekly solution adjustments and  $\text{H}_2\text{O}_2$  dilution effects, are included in Table 25; a graph of these values is shown in Fig. 34. The agreement between nickel contents for duplicate tests was unusually good; variations did not exceed  $\pm 5 \mu\text{g/ml}$ . At the end of the first week, the nickel content in the  $\text{CuSO}_4$  solutions was greater than in the copper-free tests. After eight weeks, however, the copper-free solution contained  $42 \mu\text{g/ml}$  of nickel as compared with the 20 to  $34 \mu\text{g/ml}$  in the  $\text{CuSO}_4$  solutions. The lowest final dissolved nickel content for all  $\text{CuSO}_4$  solutions,  $21 \mu\text{g/ml}$ , was found in the solution that contained  $2910 \mu\text{g/ml}$  of  $\text{CuSO}_4$  initially.

# HRP QUARTERLY PROGRESS REPORT

**TABLE 25. AVERAGE CUMULATIVE DISSOLVED NICKEL CONTENTS IN OXYGENATED  $UO_2SO_4$  SOLUTIONS CONTAINING 40 g OF URANIUM PER LITER AT 250°C WITH AND WITHOUT  $CuSO_4$  ADDITIONS**

EXPOSURE TIME (weeks)	DISSOLVED NICKEL CONTENT ( $\mu\text{g/ml}$ )				
	$CuSO_4$ Concentration ( $\mu\text{g/ml}$ )				
	Copper Free	260	790	1360	2910
1	15	24	26	21	22
2	21	18	19	18	13
3	25	24	25	21	16
4	33	26	29	23	17
5	36	28	31	24	18
6	41	31	31	25	19
7	42	33	36	26	19
8	42	32	35	27	21

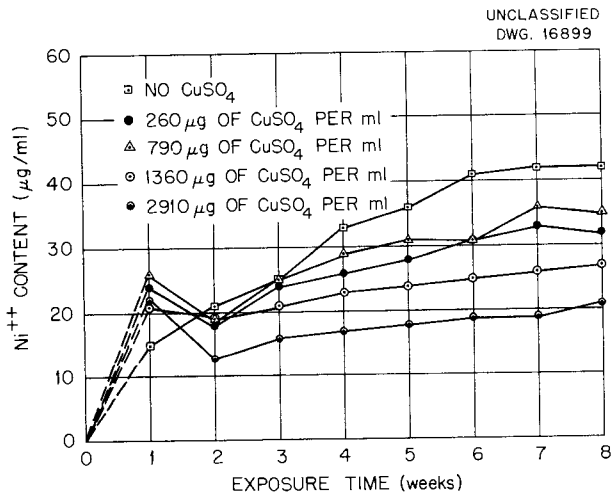


**Fig. 34. Average, Cumulative, Dissolved-Nickel Content from Type 347 Stainless Steel Exposed to  $UO_2SO_4$  Solutions Containing 40 g of Uranium per Liter and Various Amounts of  $CuSO_4$ , Pressurized with 150 psia of Oxygen at 250°C.**

The analytical results for  $CuSO_4$  content, corrected for weekly solution adjustment and dilution effect from  $H_2O_2$  additions, are reported in Table 26. The results for the first week were quite erratic; all solutions showed large increases over initial

concentrations of  $CuSO_4$ , except the solution with 260  $\mu\text{g}$  of  $CuSO_4$  per milliliter, which showed a 9% depletion of  $CuSO_4$  content after the first week. As the exposure time was increased, all solutions except the one containing 1360  $\mu\text{g}$  of  $CuSO_4$  per milliliter exhibited signs of  $CuSO_4$  depletion ranging from 3 to 24% of the initial concentrations. The largest decrease, 24%, was observed in the solution that initially contained 790  $\mu\text{g}$  of  $CuSO_4$  per milliliter. Analyses of the solution with 1360  $\mu\text{g}$  of  $CuSO_4$  per milliliter showed  $CuSO_4$  contents slightly higher than the original concentration during the eight weeks of test.

Weekly analyses for total uranium concentration indicated no reduction of the uranyl ion during the exposure; the analytical results, after correction, were within  $\pm 1.5$  g of uranium per liter of the estimated uranium content at the start of each weekly run. There were no significant changes in the pH of the final test solutions from the starting pH values.

Corrosion evaluation for the complete test system, including all

FOR PERIOD ENDING OCTOBER 1, 1952

surfaces contacted by  $UO_2SO_4$  solutions at 250°C, was made from the increased nickel content of the solutions. Since the actual nickel content of the type 347 stainless steel autoclaves was unknown, an average nickel value of 10.5% was assumed for this evaluation. Corrosion rates after one and eight weeks of exposure are included in Table 27.

The data in Table 27 indicate that the presence of 258 to 2865  $\mu g/ml$

of  $CuSO_4$  in oxygenated  $UO_2SO_4$  solutions containing 40 g of uranium per liter at 250°C has no significant effect on inhibition of corrosion attack on type 347 stainless steel surfaces. Actually, the data showed a slight acceleration of corrosion attack in solutions containing  $CuSO_4$  after one week of exposure. The final corrosion rates after eight weeks were grouped too closely together in magnitude to permit any firm conclusion on the effectiveness

TABLE 26. AVERAGE CUMULATIVE DISSOLVED  $CuSO_4$  CONTENTS IN OXYGENATED  $UO_2SO_4$  SOLUTIONS CONTAINING 40 g OF URANIUM PER LITER AT 250°C

EXPOSURE TIME (weeks)	CUMULATIVE DISSOLVED $CuSO_4$ CONTENT ( $\mu g/ml$ )			
	CuSO <sub>4</sub> Added ( $\mu g/ml$ )			
	260	790	1360	2910
0	258*	780*	1340*	2865*
1	234	848	1694	3067
2	231	596	1378	2807
3	231	576	1375	2794
4	231	575	1388	2790
5	231	582	1396	2798
6	233	590	1401	2784
7	230	601	1407	2795
8	238	623	1409	2780

\*Initial concentrations of  $CuSO_4$  corrected for dilution effect by the addition of 30%  $H_2O_2$  to produce the desired oxygen partial pressure.

TABLE 27. INITIAL AND FINAL AVERAGE CORROSION RATES BY DISSOLVED NICKEL CONTENTS FOR TYPE 347 STAINLESS STEEL IN OXYGENATED  $UO_2SO_4$  SOLUTIONS CONTAINING 40 g OF URANIUM PER LITER AND  $CuSO_4$  ADDITIONS AT 250°C

INITIAL $CuSO_4$ CONCENTRATION ( $\mu g/ml$ )	CORROSION RATE (mpy)	
	Exposed One Week	Exposed Eight Weeks
None	0.22	0.08
258	0.36	0.06
780	0.39	0.07
1340	0.31	0.05
2865	0.33	0.04

## HRP QUARTERLY PROGRESS REPORT

of  $\text{CuSO}_4$  as a corrosion inhibitor for type 347 stainless steel after extended periods of high-temperature exposure.

The effect of the initial surface condition on the corrosion of type 347 stainless steel in  $\text{UO}_2\text{SO}_4$  solutions at  $250^\circ\text{C}$  was well illustrated by comparison of the data from the  $\text{CuSO}_4$  studies with the corrosion data presented in the preceding section of this report. With newly machined surfaces, the corrosion rate for type 347 stainless steel after one week in  $\text{UO}_2\text{SO}_4$  solutions containing 40 g of uranium per liter and pressurized with 150 psia of oxygen at  $250^\circ\text{C}$  was 2.7 mpy, as determined from the increase in dissolved nickel content of the solutions. In the present studies, the surfaces of the type 347 stainless steel autoclaves, which had been used previously for other corrosion studies with  $\text{UO}_2\text{SO}_4$  at  $250^\circ\text{C}$ , were pickled vigorously in  $\text{HNO}_3$ -HF solution before the start of the  $\text{CuSO}_4$  tests; the test specimens were not pickled, however. With a preponderance of pickled surfaces in the test system, the corrosion rate determined from the dissolved nickel in solution was 0.2 mpy after one week of operation at  $250^\circ\text{C}$  in  $\text{UO}_2\text{SO}_4$  solution containing 40 g of uranium per liter pressurized with 150 psia of oxygen. This rate may be slightly high because of the contribution of nickel to the solution by corrosion attack on the machined specimen surfaces. The difference in behavior between the machined and pickled surfaces may be attributed to the presence of semiprotective films formed during the previous corrosion studies in the autoclaves, which were not removed completely by the pickling operation. The action of such films for retarding the progress of corrosion attack would be analogous to the behavior of protective films formed on newly machined stainless steel surfaces after the initial

period of contact. In the latter cases, the steady-state corrosion rate is generally considerably smaller than the initial corrosion rate for the first few hours of contact by  $\text{UO}_2\text{SO}_4$  solutions at  $250^\circ\text{C}$ .

**Effect of Long-Term Exposure on Corrosion.** Thus far, the bulk of the static corrosion data has been based on corrosion tests that usually did not exceed 3000 hr in duration. Actually, most of the data are representative of 1000- to 2000-hr exposure, but a few random studies were extended to as long as 3000 hours. In the present work, the effect of exposure periods up to 5200 hr on the corrosion of type 347 stainless steel in  $\text{UO}_2\text{SO}_4$  solution at  $250^\circ\text{C}$  was studied. Also included in this investigation were studies of the effect of increasingly longer periods of continuous operation at  $250^\circ\text{C}$ , the effect of frequent replacement of the test solution, and the effect of uranium concentration (200 and 300 g of uranium per liter) on corrosion of type 347 stainless steel.

The chemical and physical properties of the two  $\text{UO}_2\text{SO}_4$  solutions used in the study are summarized in Table 28. The solutions were identified in the laboratory as batch 50 and 52.

The corrosion test specimens were machined from 3.175-cm-dia, hot-rolled, type 347 stainless steel bar. The specimens were 3.0 to 3.1 cm in diameter by 0.5 cm thick for an average total surface area of  $20\text{ cm}^2$ . A 0.5-cm-dia hole was drilled in the center of each for means of support in the test media. The specimens were tested in a machined condition after degreasing, drying, and weighing. The chemical composition of the test material in weight per cent was as follows: C, 0.07; Mn, 1.22; Si, 0.44; Cr, 18.0; Ni, 10.7; and Nb, 0.91. Single specimens were exposed in individual autoclaves by means of type 347 stainless steel hangers.

**TABLE 28. CHEMICAL AND PHYSICAL PROPERTIES OF  $UO_2SO_4$  TEST SOLUTIONS**

	BATCH 50	BATCH 52
Total U, g/l	193.1	300.5
$SO_4$ , g/l	78.3	120.6
$SO_4:U$ ratio	1.005	0.993
U(IV), g/l	0.1	0.1
$NO_3$ , g/l	0.03	0.1
$NH_4$ , g/l	0.02	0.02
Ni, $\mu g/ml$	1.0	2.0
Density at 25°C, $g/cm^3$	1.252	1.405
pH (0.1 M solution)	2.52	2.49
pH (solution as used)	1.35	1.10

The oxygen partial pressures investigated included 75, 150, 275, and 650 psia at 250°C. These pressures were obtained by the addition of calculated amounts of 30%  $H_2O_2$  to the solutions at room temperature and subsequent thermal decomposition of the  $H_2O_2$  at 250°C. The estimated oxygen solubilities, based on the solubility of oxygen in water, are given in Table 29.

Conventional type 347 stainless steel autoclaves with a total capacity of 225 ml were used for the tests.

**TABLE 29. ESTIMATED DISSOLVED OXYGEN CONTENT OF  $UO_2SO_4$  TEST SOLUTIONS**

OXYGEN PARTIAL PRESSURE AT 250°C (psia)	DISSOLVED OXYGEN (ppm)	
	Uranium Concentration (g/l)	
	193.1	300.5
75	360	320
150	720	640
275	1310	1170
650	3100	2765

Prior to their use, the autoclaves were machined to remove old corrosion films formed in previous studies.

A total volume of 150 ml of  $UO_2SO_4$  solution and the necessary 30%  $H_2O_2$  addition to produce the desired oxygen partial pressure at 250°C were placed in each autoclave with the test specimen. The addition of the various amounts of  $H_2O_2$  resulted in a dilution effect of the original uranium content in the  $UO_2SO_4$  solutions. The initial uranium content, corrected for the  $H_2O_2$  addition, is shown in Table 30.

**TABLE 30. CORRECTED INITIAL URANIUM CONTENT OF  $UO_2SO_4$  SOLUTIONS AFTER  $H_2O_2$  ADDITIONS**

OXYGEN PARTIAL PRESSURE AT 250°C (psia)	CORRECTED URANIUM CONTENT (g/l)	
	Batch 50	Batch 52
75	191.8	298.7
150	190.5	296.5
275	188.0	292.5
650	181.5	282.5

The sequence of exposure periods at 250°C was as follows: one for 48 hr, two for 240 hr, two for 336 hr, two for 504 hr, two for 672 hr, and two for 840 hours. The total time of exposure, with a few minor exceptions, was 5232 hours for each set of test conditions. The test solutions were replaced at the start of each period. At the end of each period, the specimens were examined and weighed, the solution pH was measured, and solution samples were removed for determination of total uranium, nickel, and manganese. Analyses for manganese were made only in the solutions containing 200 g of uranium per liter. At the completion of the tests, the corrosion specimens were defilmed electrolytically in inhibited 5%  $H_2SO_4$  for 3 min at 75°C for determination of actual metal losses.

## HRP QUARTERLY PROGRESS REPORT

With one exception, all tests were satisfactory as far as solution stability was concerned. The exception was the test in which  $\text{UO}_2\text{SO}_4$  solution containing 300 g of uranium per liter, pressurized with 75 psia of oxygen at 250°C, was used. Completely unstable systems resulted from two attempts to operate with this combination. A reduction of 15 to 20% in uranium concentration was found after 48 hr, and severe corrosion attack occurred as evidenced by dissolved nickel contents on the order of 1500  $\mu\text{g}/\text{ml}$ . The corrosion rate on the type 347 stainless steel after 48 hr was 78 mpy, as determined from the increase of dissolved nickel in solution. Experiences with solution

instability of  $\text{UO}_2\text{SO}_4$  solution containing 300 g of uranium per liter and pressurized with 25 psia of oxygen at 250°C in newly machined type 347 stainless steel autoclaves have been reported previously.<sup>(10)</sup> Included also in the previous report<sup>(10)</sup> were results of tests that operated successfully under the same conditions that resulted in failure in the present investigation.

The corrected cumulative dissolved nickel contents for the seven tests that operated successfully appear in Table 31. In each case, the reported values were corrected for the amount

<sup>(10)</sup>J. L. English *et al.*, *HRP Quar. Prog. Rep.* July 1, 1952, ORNL-1318, p. 43-44.

**TABLE 31. CORRECTED CUMULATIVE DISSOLVED NICKEL CONTENT IN  $\text{UO}_2\text{SO}_4$  SOLUTIONS PRESSURIZED WITH VARIOUS OXYGEN PARTIAL PRESSURES AT 250°C**

ORIGINAL URANIUM CONCENTRATION (g/l)	CUMULATIVE EXPOSURE (hr)	DISSOLVED NICKEL ( $\mu\text{g}/\text{ml}$ )			
		Oxygen Partial Pressure at 250°C (psia)			
		75	150	275	650
193.1	48	143	131	187	127
	288	175	145	258	167
	528	197	159	329	206
	864	235	211	439	237
	1200	264	235	472	265
	1704	314	265	550	294
	2208	352	284	598	323
	2880	382	303	642	344
	3552	409	317	689	358
	4392	434	331	733	373
5232	452	366	751	406	
300.5	48		628	445	448
	288		676	528	549
	528		742	605	564
	864		821	631	590
	1200		880	653	626
	1704		969	677	683
	2208		1041	750	714
	2880		1088	779	750
	3552		1122	801	770
	4392		1153	836	800
5232		1170		809	

of nickel contained initially in the test solutions. Plots of the dissolved nickel content vs. exposure time are shown in Figs. 35 and 36. The results of dissolved manganese analyses on the tests with  $UO_2SO_4$  solutions containing 200 g of uranium per liter are reported in Table 32.

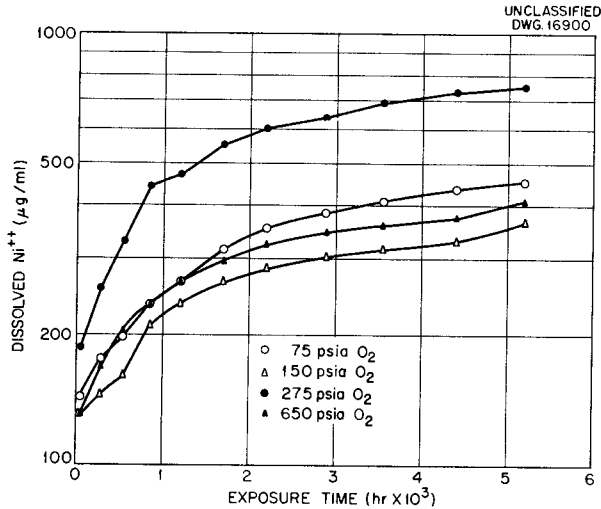


Fig. 35. Cumulative Dissolved-Nickel Content in Oxygenated  $UO_2SO_4$  Solutions Containing 193 g of Uranium per Liter at 250°C.

Analytical results for final total uranium concentration at the end of each exposure period showed no apparent reduction of the uranyl ion during test. The uranium values in the tests with solutions containing

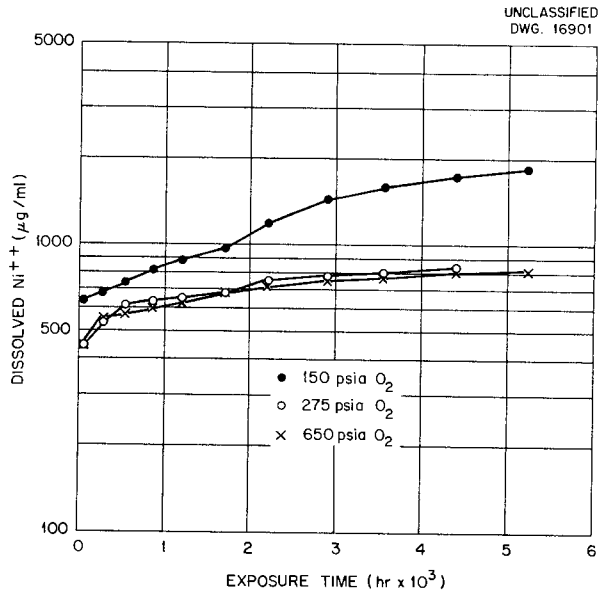


Fig. 36. Cumulative Dissolved-Nickel Content in Oxygenated  $UO_2SO_4$  Solutions Containing 300 g of Uranium per Liter at 250°C.

TABLE 32. CORRECTED CUMULATIVE DISSOLVED MANGANESE CONTENT IN  $UO_2SO_4$  SOLUTIONS CONTAINING 193 g OF URANIUM PER LITER PRESSURIZED WITH OXYGEN AT 250°C

CUMULATIVE EXPOSURE (hr)	DISSOLVED MANGANESE ( $\mu\text{g/ml}$ )			
	Oxygen Partial Pressure at 250°C (psia)			
	75	150	275	650
48	12	14	23	19
288	16	16	30	26
528	18	17	35	29
864	20	19	38	32
1200	21	20	39	33
1704	27	24	48	37
2208	31	26	53	41
2880	35	28	59	44
3552	38	29	65	46
4392	41	31	71	47
5232	43	36	72	51

## HRP QUARTERLY PROGRESS REPORT

193 g of uranium per liter were generally 2 to 3% higher than the corrected starting concentrations for each exposure; the uranium analyses in the tests with solutions containing 300 g of uranium per liter were within  $\pm 2\%$  of the corrected starting values.

Final pH measurements on the corrosion solutions did not show any unusual behavior. The final values ranged from 0.1 to 0.4 unit higher than the starting pH values.

Cumulative as-removed weight changes on the test specimens established no definite trends related to oxygen partial pressure or other variables. After 5232 hr in the tests with solutions containing 193 g of uranium per liter, the cumulative weight changes for oxygen partial pressures of 75, 150, 275, and 650 psia were -0.5, -0.1, +1.0, and -0.1 mg/cm<sup>2</sup>, respectively. The cumulative weight losses on the specimens in solutions containing 300 g of uranium per liter after similar exposure time were -0.4, -7.8 (4392 hr), and -6.1 mg/cm<sup>2</sup> for oxygen partial pressures of 150, 275, and 650 psia, respectively. All specimens were very similar in physical appearance at the end of the tests; surfaces were coated with relatively nonuniform oxide films that were dull and dark gray-black in color. Microscopic examination (at 30X) of the specimens immediately after removal from the solutions disclosed no signs of localized corrosion attack. This was not the case, however, after the corrosion films were stripped electrolytically from the specimen surfaces, as will be discussed later.

Evaluation of corrosion damage on the type 347 stainless steel surfaces in contact with the UO<sub>2</sub>SO<sub>4</sub> solutions at 250°C was made from the increase in dissolved nickel content in solution. The total area of exposed autoclave wall and specimen surfaces was 245 cm<sup>2</sup>. The actual nickel content of the type 347 stain-

less steel autoclaves was unknown, so it was again necessary to assume an average value of 10.5% for the corrosion-rate calculations.

A comparison of the initial and final corrosion rates determined by dissolved nickel content is shown in Table 33 for type 347 stainless steel in oxygenated UO<sub>2</sub>SO<sub>4</sub> solutions containing 193 and 300 g of uranium per liter at 250°C. The data indicated no significant effect of dissolved oxygen concentration in the range of 360 to 3100 ppm on the corrosion of type 347 stainless steel at 250°C in UO<sub>2</sub>SO<sub>4</sub> solutions containing approximately 200 g of uranium per liter. This lack of effect was observed for both short- and long-term exposures. Initial corrosion rates for a 48-hr period were 6.7 to 9.9 mpy; final rates after 5232 hr (218 days) were 0.2 to 0.4 mpy. Corrosion data from the tests with solutions containing 300 g of uranium per liter also showed an independence of dissolved oxygen within the range of 320 to 2765 ppm at 250°C. The 48-hr rate for 640 ppm of dissolved oxygen was 10 mpy higher than initial rates obtained in the solutions with higher dissolved oxygen content, but this effect could just as well be a function of test and/or material variations as an effect of the dissolved oxygen concentration. The final corrosion rates after 5232 hr were 0.4 to 0.6 mpy, and again indicated an independence of dissolved oxygen content on corrosion for long-term exposure of type 347 stainless steel.

As shown by the graphs of cumulative dissolved nickel content vs. exposure time, Figs. 35 and 36, the slopes of the curves after the initial 48-hr period of exposure were nearly identical in all tests, indicating a constant rate of corrosion-with-time relationship. A comparison of the mean incremental increase in dissolved nickel for the two test series is included in Table 34. The corrosion

FOR PERIOD ENDING OCTOBER 1, 1952

vs. time curve is separated into an initial attack and a steady-state attack. The initial period is confined to 48 hr; the steady-state period included the balance of the testing time, 5184 hours.

Some information on the chemical behavior of the manganese in type 347

stainless steel was obtained by determining the ratio of dissolved nickel to dissolved manganese found in the  $UO_2SO_4$  solutions containing 193 g of uranium per liter. An average ratio of 10.5 for nickel-to-manganese content in type 347 stainless steel was assumed. Typical

TABLE 33. INITIAL AND FINAL CORROSION RATES DETERMINED BY DISSOLVED NICKEL CONTENT ON TYPE 347 STAINLESS STEEL IN OXYGENATED  $UO_2SO_4$  SOLUTIONS AT 250°C

OXYGEN PARTIAL PRESSURE AT 250°C (psia)	TOTAL EXPOSURE TIME (hr)	CORROSION RATE (mpy)	
		Original Uranium Content (g/l)	
		193	300
75	48	7.6	
	5232	0.2	
150	48	6.9	32.6
	5232	0.2	0.6
275	48	9.9	22.5
	5232	0.4	0.5*
650	48	6.7	23.2
	5232	0.2	0.4

\*This rate was based on a total exposure time of 4392 hours.

TABLE 34. MEAN INCREMENTAL INCREASE IN DISSOLVED NICKEL CONTENT IN OXYGENATED  $UO_2SO_4$  SOLUTIONS AT 250°C

ORIGINAL URANIUM CONCENTRATION (g/l)	OXYGEN PARTIAL PRESSURE AT 250°C (psia)	DISSOLVED OXYGEN (ppm)	NICKEL CONTENT ( $\mu\text{g/ml/day}$ )	
			Initial	Steady-State
193.1	75	360	72	1.4
	150	720	66	1.1
	275	1310	94	2.6
	650	3100	64	1.3
300.5	75	320		
	150	640	314	2.5
	275	1170	223	2.1
	650	2765	224	1.8

## HRP QUARTERLY PROGRESS REPORT

chemical analyses of type 347 stainless steel corrosion test materials have shown that the nickel-to-manganese ratio varies between 9 and 10, dependent, of course, on the actual nickel and manganese content of the alloy. The assumed average value of 10.5 for the ratio, therefore, was not far from the values indicated by typical type 347 stainless steel analyses.

The ratio of nickel to manganese was calculated from the cumulative dissolved nickel and manganese contents reported in Tables 31 and 32, respectively, for the  $\text{UO}_2\text{SO}_4$  solutions containing 193 g of uranium per liter. The mean values of the ratio for oxygen partial pressures of 75, 150, 275, and 650 psia at 250°C were 11.3, 10.5, 10.4, 7.6, respectively. The over-all mean value of the nickel-to-manganese ratio in the tests was 10.0, which is in excellent agreement with the assumed value of 10.5. Thus it would appear from these data that the manganese involved in the corrosion of stainless steel by  $\text{UO}_2\text{SO}_4$  solutions at 250°C remains in solution in a manner similar to nickel. This suggests that the increase in manganese concentration in the solution might be a measure of corrosion rate similar to the increase in nickel concentration.

At the completion of the corrosion tests, the specimens were cleaned cathodically in inhibited 5 wt %  $\text{H}_2\text{SO}_4$  at 75°C for 3 minutes. Final corrosion rates were calculated from the corrected (for metal loss on unexposed specimens) defilmed weight losses and compared with corrosion rates determined from dissolved nickel in solution after similar exposure periods. These data are included in Table 35.

The agreement between corrosion rates obtained by the two methods was fair in the tests with solutions containing 193 g of uranium per liter but was not good in the tests with solutions containing 300 g of uranium per liter. The rates determined by dissolved nickel content that are higher than those determined by defilmed weight loss may be explained by localized corrosion attack at some unobserved point in the test system; however, the reason for the rates determined by defilmed weight loss being higher than those determined by dissolved nickel content is unknown at the present time.

The effect of frequent changes of the corrosion test solutions on the corrosion of type 347 stainless steel at 250°C in  $\text{UO}_2\text{SO}_4$  solutions

**TABLE 35. COMPARISON OF CORROSION RATES ON TYPE 347 STAINLESS STEEL BY DEFILMED WEIGHT LOSS AND DISSOLVED NICKEL CONTENT IN OXYGENATED  $\text{UO}_2\text{SO}_4$  SOLUTIONS AT 250°C**

ORIGINAL URANIUM CONCENTRATION (g/l)	OXYGEN PARTIAL PRESSURE AT 250°C (psia)	DISSOLVED OXYGEN (ppm)	CORROSION RATE (mpy)	
			Weight Loss	Dissolved Nickel
193.1	75	360	0.18	0.23
	150	720	0.13	0.18
	275	1310	0.07	0.38
	650	3100	0.12	0.20
300.5	75	320		0.58
	150	640	0.27	0.50
	275	1170	1.19	0.40
	650	2765	0.91	

containing 300 g of uranium per liter is shown in Fig. 37 by a comparison of dissolved nickel content in solutions that were and were not replaced at regular intervals. The data for the tests not involving solution replacement, reported in a previous report,<sup>(11)</sup> were obtained under test conditions similar to those described in the present investigation. The previously reported tests operated for a total period of 1848 hr, and the dissolved nickel values obtained at weekly intervals during this exposure time are compared with nickel values from the present test series in which the solutions were replaced five times during a similar exposure period. Comparisons are made in Table 36 for  $UO_2SO_4$  solutions containing 300 g of uranium per liter pressurized with 150 psia of oxygen at 250°C.

The initial corrosion behavior for the two tests was quite different

(11) *Ibid.*, p. 46.

considering that exposure was made in each case with similar conditions. The incremental nickel increase for a 48-hr period in the solution-changed test was 314  $\mu\text{g/ml/day}$  as compared to an extrapolated value of 30  $\mu\text{g/ml/day}$  increase over 168 hr in the no-solution-change test. Nonhomogeneities in metal surfaces or differences in chemical composition of the test

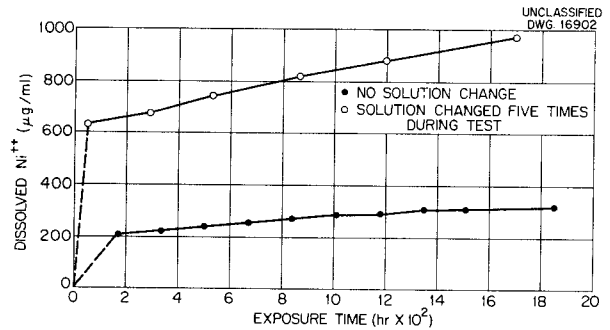


Fig. 37. Effect of Changing Solution on Dissolved-Nickel Content in  $UO_2SO_4$  Solutions Containing 300 g of Uranium per Liter, Pressurized with 150 psia of Oxygen Partial Pressure at 250°C.

TABLE 36. EFFECT OF SOLUTION REPLACEMENT ON THE INCREASE OF DISSOLVED NICKEL CONTENT IN  $UO_2SO_4$  SOLUTIONS CONTAINING 300 g OF URANIUM PER LITER AT 250°C WITH 150 psia OF OXYGEN PARTIAL PRESSURE

NO SOLUTION CHANGE		SOLUTION CHANGED	
Cumulative Period of Test (hr)	Dissolved Nickel Content ( $\mu\text{g/ml}$ )*	Cumulative Period of Test (hr)	Dissolved Nickel Content ( $\mu\text{g/ml}$ )*
168	208	48	628
336	222	288	676
504	241	528	742
672	253		
840	271	864	821
1008	287		
1176	287	1200	880
1344	307		
1512	309		
1848	320	1704	969

\*Values reported are the average for two identical tests.

## HRP QUARTERLY PROGRESS REPORT

autoclaves may account for this lack of agreement. The steady-state portion of the nickel increase vs. time curves indicates that frequent changes of the test environment resulted in a somewhat more corrosive situation. The mean incremental increase of dissolved nickel in the solution-changed test for a period of 1656 hr, exclusive of the initial 48-hr period, was 4.9  $\mu\text{g}/\text{ml}/\text{day}$ . The incremental nickel increase value for the no-solution-change test during 1680 hr, exclusive of the initial 168-hr period, was 1.6  $\mu\text{g}/\text{ml}/\text{day}$ .

The corrosion test specimens, after electrolytic defilming, were examined microscopically at 30X. The specimens exposed in the  $\text{UO}_2\text{SO}_4$  solutions containing 193 g of uranium per liter were dull, silver-white in color and exhibited slightly etched surfaces. No definite signs of pitting corrosion were observed. The defilmed specimens exposed in the  $\text{UO}_2\text{SO}_4$  solutions containing 300 g of uranium per liter exhibited very definite signs of surface corrosion attack, the intensity of which appeared to increase with increased dissolved oxygen concentration. Photographs (at 10X) of the three defilmed test specimens that were exposed in solution-stable systems appear in Fig. 38. The surfaces were deeply etched, as shown, with the most severe attack present on the specimen exposed in  $\text{UO}_2\text{SO}_4$  solution pressurized with 650 psia of oxygen at 250°C. The frequency of pits was much greater on the specimens exposed in solutions pressurized with 275 and 650 psia of oxygen than on the specimen exposed in solutions pressurized with 150 psia of oxygen. Pit depths on the latter specimen did not exceed 1.0 mil, as measured microscopically at 150X; pit depths on the other two specimens ranged between 1.0 and 2.0 mils.

In terms of the original objectives of this investigation, the results may be summarized as follows:

1. There was no significant effect of dissolved oxygen concentration in the range of 360 to 3100 ppm on short-term (48 hr) and long-term (5232 hr) corrosion of type 347 stainless steel in  $\text{UO}_2\text{SO}_4$  solutions containing approximately 200 and 300 g of uranium per liter at 250°C.

2. On a solution-change basis, the corrosiveness of  $\text{UO}_2\text{SO}_4$  solutions containing 300 g of uranium per liter was two to three times greater than that of the solutions containing 200 g of uranium per liter for similar exposure conditions. Initial corrosion rates, determined by dissolved nickel content, were between 6.7 and 9.9 mpy in solutions containing 200 g of uranium per liter as compared with initial rates of 22.5 to 32.6 mpy after 48 hr in solutions containing 300 g of uranium per liter. Final corrosion rates for 5232 hr were 0.2 to 0.4 mpy in solutions containing 200 g of uranium per liter and 0.4 to 0.6 mpy in solutions containing 300 g of uranium per liter.

3. Solution stability was not maintained in tests operating with solutions containing 300 g of uranium per liter and oxygen partial pressures of 75 psia at 250°C.

4. There was no effect of increasing the time of continuous exposure at 250°C on solution stability of the  $\text{UO}_2\text{SO}_4$  solutions. The longest period of continuous exposure was five weeks; no reduction of the uranyl ion was observed in these tests.

5. Long-term exposure at 250°C for 5232 hr resulted in a susceptibility of type 347 stainless steel to localized corrosion attack. The intensity of this attack was pronounced in the solutions containing 300 g of uranium per liter and appeared to be related to the dissolved oxygen concentration; that is, the magnitude and frequency of pitting attack increased with

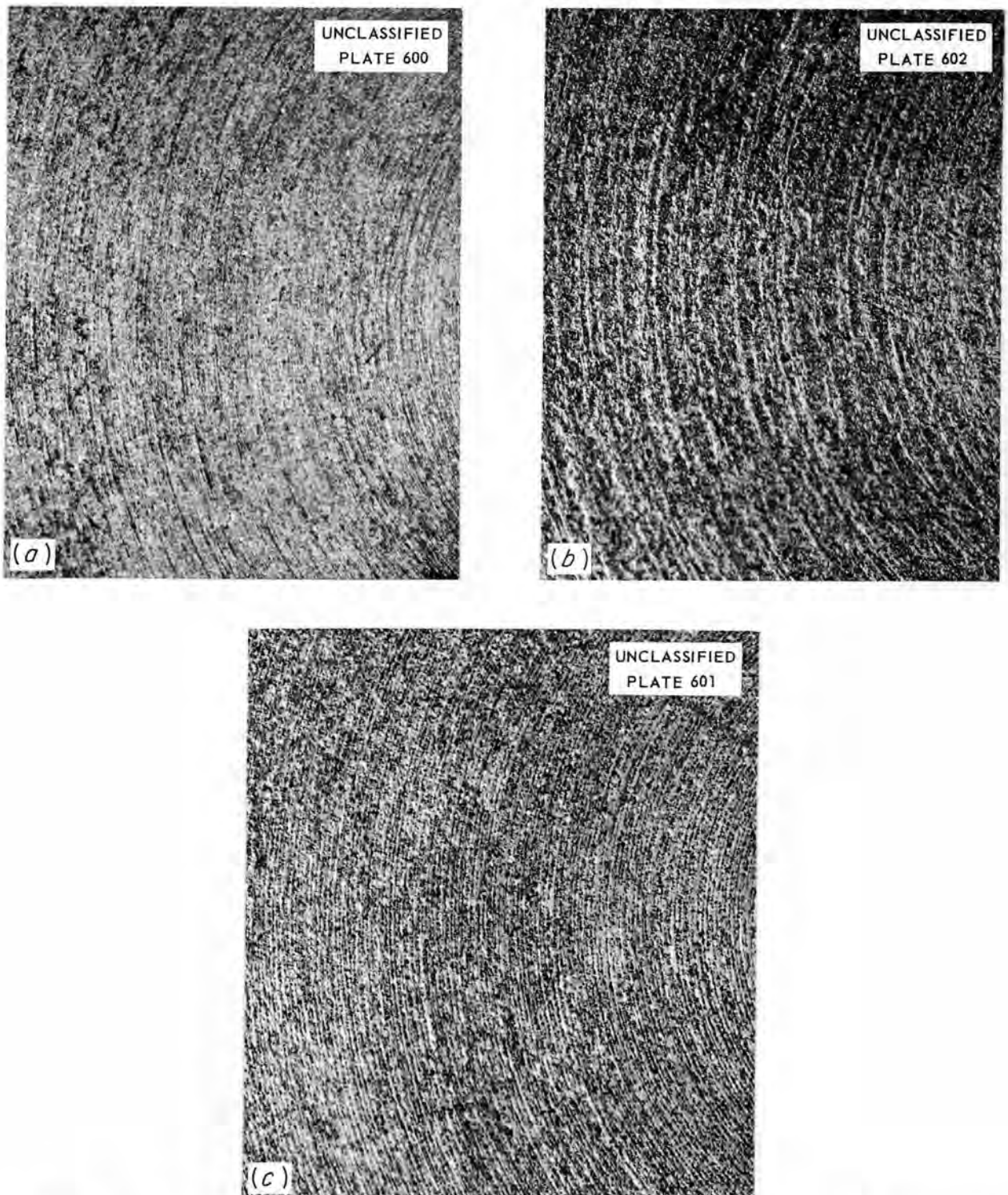


**Fig. 38. Surface Conditions of Defilmed Type 347 Stainless Steel Corrosion Test Specimens After 5232 hr in  $UO_2SO_4$  Solutions Containing 300 g of Uranium per Liter and Pressurized with Various Oxygen Partial Pressures at  $250^\circ C$ . (a) 150 psia of  $O_2$ . (b) 275 psia of  $O_2$ . (c) 650 psia of  $O_2$ . 10X.**

## HRP QUARTERLY PROGRESS REPORT

increased dissolved oxygen content. Localized corrosion attack on specimens in solutions containing 200 g of uranium per liter was not observed after similar exposure times.

### CORROSION OF TITANIUM IN URANYL SULFATE SOLUTIONS

Static corrosion studies to determine the effect of long-term exposure on the tensile properties of titanium metal in oxygenated  $UO_2SO_4$  solutions containing 40 and 300 g of uranium per liter at 250°C were completed during the past quarter. Preliminary data from these tests were described in a previous report.<sup>(12)</sup>

The titanium tensile specimens were machined from 1.270-cm-dia bar obtained from the Allegheny-Ludlum Steel Company. The bar was hot-rolled and annealed in the as-received condition. The over-all length of the specimens was approximately 7.0 cm; the reduced section of the tensile bars was 0.508 cm in diameter and 3.175 cm in length. The titanium metal was designated as commercial grade, with the following nominal chemical composition in weight per cent: C, 0.04 max; Fe, 0.10; N, 0.02; W, 0.08; O, trace; and balance, titanium. The physical properties of the metal in the annealed condition are given in Table 37.<sup>(13)</sup>

The chemical and physical properties of the two uranyl sulfate solutions used in the tests are given in Table 38.

(12) E. G. Bohlmann, J. L. English, and S. H. Wheeler, *HRP Quar. Prog. Rep.* July 1, 1952, ORNL-1318, p. 149.

(13) *Handbook on Titanium Metal*, Titanium Metals Corp., 4th Ed., 1950.

TABLE 37. PHYSICAL PROPERTIES OF COMMERCIAL-GRADE TITANIUM

Ultimate strength	70,000 to 80,000 psi
Yield strength	45,000 to 55,000 psi
Elongation	20 to 30%
Area reduction	45 to 70%

TABLE 38. CHEMICAL AND PHYSICAL PROPERTIES OF  $UO_2SO_4$  CORROSION TEST SOLUTIONS

	BATCH 74	BATCH 52
Total U (g/l)	39.50	300.50
SO <sub>4</sub> (g/l)	15.77	120.60
SO <sub>4</sub> :U ratio	0.990	0.993
U(IV) (g/l)	0.10	0.10
NO <sub>3</sub> (g/l)	0.12	0.10
NH <sub>4</sub> (g/l)	0.10	0.02
Ni (μg/ml)	0.40	2.0
Density at 25°C (g/cm <sup>3</sup> )	1.055	1.405
pH (0.1 M solution)	2.65	2.49
pH (solution as used)	2.38	1.10

The tests were operated with an approximate oxygen partial pressure of 150 psia at 250°C. The oxygen pressure was obtained from the thermal reduction of 30%  $H_2O_2$  added to the test solutions at room temperature. The estimated dissolved oxygen content in the solutions containing 40 and 300 g of uranium per liter at 250°C were 815 and 640 ppm, respectively.

Type 347 stainless steel autoclaves of 225-ml total capacity were used for the tests. The autoclaves were pickled, initially, for 20 to 30 min at 60°C in 10%  $HNO_3$ -4% HF solution. The starting test volume consisted of 148 ml of the respective  $UO_2SO_4$  solution and 2.2 ml of 30%  $H_2O_2$  to produce the desired oxygen pressure at 250°C. The test solutions were replaced with new solutions at the start of each exposure period.

The titanium tensile specimens were placed, unsupported, in a position 30 deg from vertical in the autoclaves containing the corrosion solution; no attempt was made to insulate the specimens from the stainless steel. Close observations

were made during the testing sequence for signs of galvanic corrosion effects on the titanium. Duplicate tensile specimens were placed in each autoclave; two control specimens were retained for comparison of tensile strengths with the corrosion specimens.

The tests were run for two-week periods of continuous exposure at 250°C in electrically heated and controlled ovens. The total test time was 4872 hr (29 weeks). The specimens were examined, scrubbed in distilled water, and weighed at the end of each two-week period; solution samples were withdrawn for uranium, nickel, and pH determinations.

Based on average as-removed weight compared with the weight of the duplicate sets of specimens, corrosion attack on the titanium was three times as great in the solution containing 300 g of uranium per liter as in the solution containing 40 g of uranium per liter. However, the intensity of corrosion attack was very mild in both cases; the cumulative average weight loss of the specimens exposed to the solution containing 40 g of uranium per liter was 0.5 mg/cm<sup>2</sup>, whereas that of the specimens exposed to the solutions containing 300 g of uranium per liter was 1.8 mg/cm<sup>2</sup>. The most interesting observations made on the specimens during the course of the tests were

the color changes in the surface oxide films. The initial color stage of the specimens in the solution containing 40 g of uranium per liter was deep violet, which persisted for eight weeks; after this period the color changed to a deep blue, which faded noticeably during the balance of the test. The specimens exposed in the solution containing 300 g of uranium per liter were initially a deep blue, which changed gradually to light green after eight weeks; this was followed by a pale violet stage, which eventually degenerated to a pink-green color during the last three weeks of test. In all cases, these varicolored films were extremely lustrous in appearance. During the tests, frequent microscopic examinations of the specimens were made for positive signs of corrosion damage, such as pitting, but none were found. There were no indications of accelerated corrosion attack on the areas in direct metallic contact with the stainless steel autoclaves. It was not possible to remove corrosion films electrolytically at the completion of the tests since the specimens were immediately tested for tensile strength values.

The results of the tensile tests are reported in Table 39.<sup>(14)</sup> The

<sup>(14)</sup> Private communication from A. R. Olsen.

TABLE 39. TENSILE TEST DETERMINATIONS ON CONTROL AND CORROSION SPECIMENS OF COMMERCIAL-GRADE TITANIUM

URANIUM CONCENTRATION (g/l)	EXPOSURE TIME (hr)	TENSILE STRENGTH (psi)	ELONGATION (%)
None		60,950	21
		62,380	23
40	4872	61,370	22
	4872	62,380	24
300	4872	62,220	21
	4872	62,090	25

## HRP QUARTERLY PROGRESS REPORT

tests were run on a Baldwin-Southwark tensile machine using a medium-low scale (0 to 6000 lb) at a strain rate of 0.02 inch per minute. It was observed that the rate of drop in load during the "necking" period was much slower for the corrosion specimens than for the control specimens.

There was no effect of long-term exposure in oxygenated  $\text{UO}_2\text{SO}_4$  solutions at 250°C on the physical properties of the titanium specimens. The tensile strength and elongation values for the corrosion specimens were the same as for the unexposed control specimens.

The dissolved nickel content in the test solutions supplied information on the corrosion behavior of the type 347 stainless steel autoclaves during the exposure. The cumulative nickel concentrations in the solutions containing 40 and 300 g of uranium per liter are shown in Fig. 39 as a function of the exposure time. The corrosiveness of the frequently replaced  $\text{UO}_2\text{SO}_4$  solution containing 300 g of uranium per liter was three to five times greater than that of the solution containing 40 g uranium per liter on pickled type 347 stainless steel surfaces. Corrosion rates determined from the dissolved

nickel content after 336 hr were 0.1 and 0.3 mpy for solutions containing 40 and 300 g of uranium per liter, respectively; the final corrosion rates after 4872 hr were 0.03 and 0.15 mpy, respectively. The final cumulative dissolved nickel contents of these solutions, respectively, were 46 and 241  $\mu\text{g}/\text{ml}$ .

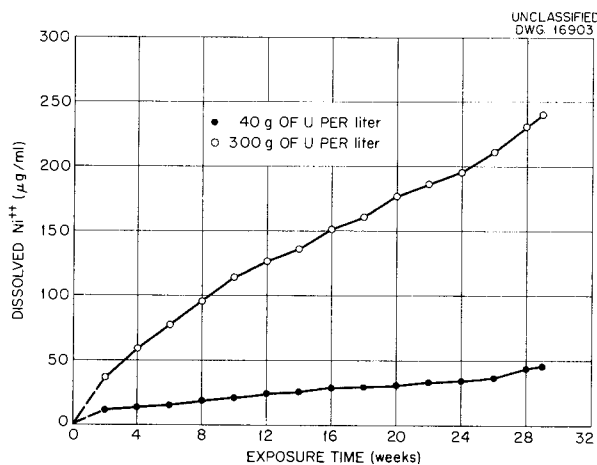


Fig. 39. Increase in Dissolved-Nickel Content Caused by Corrosion Attack on Pickled Type 347 Stainless Steel Surfaces by  $\text{UO}_2\text{SO}_4$  Solutions Containing 40 and 300 g of Uranium per Liter, Pressurized with 150 psia of Oxygen at 250°C.

## RADIATION CHEMISTRY

C. H. Secoy, Group Leader

### LONG-TERM IRRADIATIONS AT HIGH TEMPERATURE AND HIGH FLUX

F. H. Sweeton      W. E. Hill  
W. C. Yee          H. F. McDuffie

A 14-week irradiation of uranyl sulfate in a type 347 stainless steel bomb has been completed and has furnished data concerning the corrosion of the container and the stability of the solution. A stainless steel bomb with a total volume of 5 ml was pre-

treated with 2% chromic acid solution at 275°C for over 4 hours. The bomb contained 2.5 ml (at room temperature) of a uranyl sulfate solution and was connected to a pressure cell by a capillary stainless steel tube. The solution contained 40 g of uranium per liter; it also contained 0.01 M cupric sulfate for facilitating recombination of hydrogen and oxygen. Before the bomb was sealed, enough hydrogen peroxide was added to the solution to

give a partial pressure of 900 psi of oxygen at the operating temperature of the experiment. The neutron flux was approximately  $3.5 \times 10^{12}$ , which is equivalent to a power density of approximately 6 kw per liter. The total burnup of  $U^{235}$  during the test was calculated to be about 1.3%. Several times a week the temperature was lowered to 210°C for a few hours so that the rate of pressure increase could be observed. During shut-downs of the reactor, any hydrogen and oxygen present in the bomb as a result of decomposition of the solution by fission fragments were recombined because of the presence of the cupric ion. The final pressure was considered to be due to steam and the remainder of the excess oxygen that had originally been added as hydrogen peroxide. At the end of the irradiation, the solution was removed and submitted to the Analytical Chemistry Division for analysis.

**Corrosion Results.** The partial pressure of excess oxygen, as determined on consecutive shut-downs, showed a steady decrease, reaching a value of approximately 300 psi after the 14-week period. Since the only oxidizing agent present in such a bomb is the excess oxygen (the free oxygen inactivates the uranyl ion as an oxidizing agent), the pressure of excess oxygen should decrease as the stainless steel is oxidized in the corrosion process. This relationship was calculated for this particular bomb and the results are given in Fig. 40. Uniform corrosion over all the surface wetted by the solution was assumed. The calculated corrosion appears to be linear with the square root of the time for most of the run. The increased corrosion rate during the last two weeks of the run may be related to breaking of the oxide film or to increased radiation damage to the film as a result of the precipitation of uranium, which will be discussed in a following section.

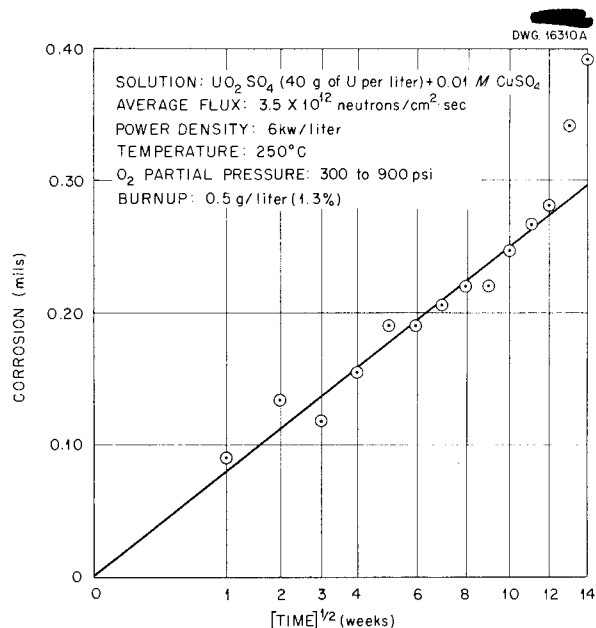


Fig. 40. Corrosion of Type 347 Stainless Steel by Static  $UO_2 SO_4$  Solution Under Neutron Irradiation. Experiment H2.

The analysis of the solution after termination of the experiment indicated that 12.5 mg of nickel had come into solution. This is equivalent to 0.35 mil of stainless steel, a figure that is in good agreement with the corrosion estimated from the loss of oxygen, as is shown in Fig. 40. The calculation assumes that a corresponding amount of iron and chromium was oxidized at the same time.

Two similar bombs were treated in the same way except that they were not irradiated. The result after nine weeks showed an average corrosion of 0.025 mil or less, as calculated from the nickel pickup by the solution. It therefore appears that irradiation increases significantly the static corrosion of type 347 stainless steel by uranyl sulfate solution containing 40 g of uranium per liter at 250°C, since the average rate over a 14-week period at a power density of about 6 kw per liter is approximately 1.4 mpy.

## HRP QUARTERLY PROGRESS REPORT

**Stability of Solution.** As the run progressed, the temperature was occasionally lowered for a few hours to 210°C so that the rate of pressure change could be observed as the pressure began to approach a higher equilibrium value. By plotting the rate of change as a function of pressure and extrapolating back to a pressure corresponding to complete recombination of electrolytic gas present from the decomposition of water, it was possible to estimate the rate of decomposition of water by the fission fragments. This rate should be proportional to the concentration of uranium, since the fission fragment has a very short range and could not emerge from a uranium crystal of any appreciable size. By assuming all the uranium to be in solution throughout the experiment, it was possible to convert the rate to an apparent  $G$  value for the solution. It was found that although this apparent  $G$  value was not very consistent over short intervals of time, it fell off at a steady rate during the course of the experiment. Figure 41 shows these data expressed as the ratio of the apparent  $G$  value to the true  $G$  value. The ratio at the beginning is reasonably close to 1.0 if consideration is given to both the uncertainty in converting pressure in the bomb to the equivalent moles of electrolytic gas and the possibility of error in assuming that diffusion does not affect the result. At the end of the experiment, the ratio had decreased to about 30% of its original value.

The analysis of the solution at the end of the experiment showed that  $30 \pm 2\%$  of the uranium was still in solution and that the pH had increased to 4.3. Since an excess of oxygen was present at all times, it is thought that the precipitation was not due to a reduction in valence but probably to an interaction with the nickel brought into solution by the corrosion process. This hypothesis has been confirmed by

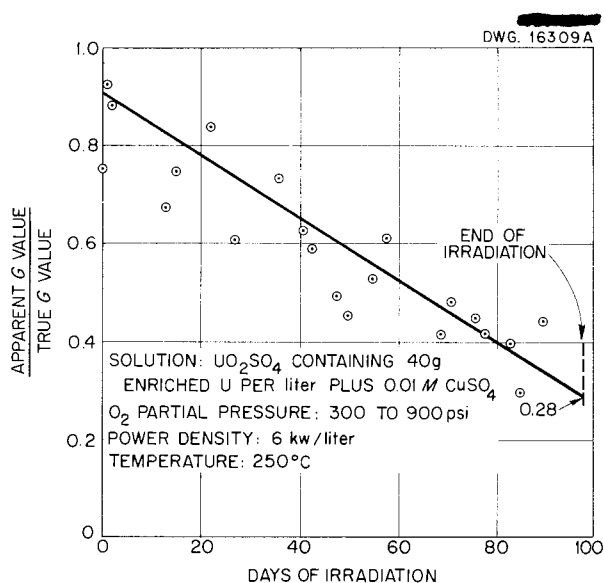


Fig. 41. Effect of Continued Irradiation on Apparent  $G$  Value. Experiment H2.

heating silica ampoules containing a mixture of uranyl sulfate solution and hydrous nickel oxide. A yellow precipitate was formed, which analyses showed to be largely a uranium compound. It was found that the pH was raised to about 4.0. As a result of these ampoule tests, it was concluded that the partial precipitation of uranium in the irradiated bomb was a secondary result of the corrosion process and not a direct effect of the radiation.

Another experiment repeating the above test with uranyl fluoride solutions has been in progress for six weeks and appears to indicate a somewhat greater corrosion rate than that experienced with uranyl sulfate and a similar gradual precipitation of uranium.

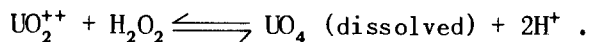
### CATALYSIS IN THE DECOMPOSITION OF HYDROGEN PEROXIDE

M. D. Silverman      G. M. Watson  
H. F. McDuffie

The power level of an aqueous uranium homogeneous reactor appears to

be limited at low temperatures by the concentration of peroxide (not to exceed the solubility of uranyl peroxide) produced by the fission fragments acting on the solution. A study of the kinetics of peroxide decomposition in uranyl sulfate solutions was therefore undertaken. The following report is brief; a more complete description of this work will be given in a forthcoming report.<sup>(1)</sup>

The following reaction occurs when hydrogen peroxide is added to a uranyl sulfate solution:



Earlier work, described in the previous quarterly reports, on the kinetics of peroxide decomposition as a function of temperature was performed by using a chemical or titration method for determining the peroxide concentration. However, the precision of this method is limited at higher temperatures, mainly because of experimental difficulties. Since the chemical method of analysis is precise only at low temperatures and because such a method actually consumes part of the reaction mixture, it was deemed advisable to develop a method for measuring *in situ*.

A conductometric method has been developed to follow this decomposition. The method is reproducible and consistent with that of chemical titration; correlation was established over a tenfold change of rate. The method is adaptable to remote control and automatic recording, and thus appears capable of following fast reactions. It has been tried on a semimicro basis, and microscale runs appear feasible. Finally, since the method is an instrumental one *in situ*, it does not consume or contaminate solutions. A more detailed discussion of this method will be given in a quarterly report of the Chemistry Division.<sup>(2)</sup>

(1) M. D. Silverman, *Peroxide Decomposition in Aqueous Reactor Solution*, ORNL-1400, to be published.

By employing the conductometric method, catalytic studies have been made on the ion species listed in Table 40; some of these are expected corrosion products from type 347 stainless steel, and others are expected fission products. The species listed in the first column are those "as added" and not necessarily the final ones. The second column gives the maximum concentration used for each species, and in most cases it is the plateau value; larger amounts have no effect on the decomposition rate. The third column lists the calculated values of  $\Delta k = k - k_0$ , where  $k_0$  is the specific reaction rate constant for the decomposition of peroxide in uranyl sulfate solution in the absence of any added catalyst, and  $k$  is the value obtained for each addition of catalyst. The last column gives the half lives obtained for the concentration of catalyst noted in the second column.

It is apparent that of the catalysts tried, iron and ruthenium are by far the most effective for peroxide decomposition.

In several instances, a second catalyst was run in the same solution if the first catalyst had only a little effect on the peroxide decomposition rate. In this manner, promoter action was detected for several different combinations. These promoter combinations are also listed in Table 40; it is obvious that the iron-copper combination is extremely effective. It should be noted that the amounts used are probably far from the optimum; further work would be required to determine these quantities.

From the data given in Table 40 for all the catalysts employed in these experiments (except Cu and Ti, which would not be present in the reactor), it is possible to calculate a

$$\Delta k \text{ (total)} = 0.266 \text{ sec}^{-1}$$

(2) *Chem. Quar. Prog. Rep. Sept. 30, 1952*, ORNL-1432, to be published.

# HRP QUARTERLY PROGRESS REPORT

**TABLE 40. CATALYSTS FOR PEROXIDE DECOMPOSITION IN URANYL SULFATE SOLUTIONS**

SPECIES ADDED	CONCENTRATION (ppm)	$\Delta k$ (sec <sup>-1</sup> )	$t_{1/2}$ (sec)
<b>Corrosion products</b>			
Fe <sup>++</sup>	11	0.081	8
Ni <sup>++</sup>	16	0.003	96
Cr <sup>+++</sup>	24	0.005	84
<b>Fission products</b>			
Ru <sup>++++</sup>	29	0.15	4.5
Ag <sup>+</sup>	3	0.0017	108
Ce <sup>++++</sup>	7	0.0012	108
I <sup>-</sup> (I <sub>2</sub> )	154	0.011	38
Rh <sup>+++2</sup>	113	0.0065	64
Pd (black)	293	0.0064	68
Rh (black)	133	0.0025	108
<b>Others</b>			
Cu <sup>++</sup>	850	0.018	31
Ti <sup>++++</sup>	3	0.0010	123
<b>Promoter combinations</b>			
Fe <sup>++</sup>	6	0.34	1.9
Cu <sup>++</sup>	793		
Pd (black)	240	0.061	10
Cr <sup>+++</sup>	24		
Cu <sup>++</sup>	850	0.027	17
I <sup>-</sup> (I <sub>2</sub> )	trace?		

for the concentrations of catalyst used. By using this value as an absolute  $k$  (neglecting  $k_0$ ), a reactor power level of about 400 kw or 8 kw per liter would be indicated as feasible in the HRE at 100°C without fear of uranyl peroxide precipitation. It is expected that even this  $k$  is conservative, because it fails to take into account any promoter action of other species present.

### TITANIUM BOMB EXPERIMENTS

J. W. Boyle                    D. M. Richardson  
 H. F. McDuffie            A. W. Smith  
    L. F. Woo

The aqueous uranyl sulfate-titanium system is being investigated in both

the ORNL graphite reactor and the LITR. To date, four experiments have been inserted in the reactors, the first three in hole 12 (vertical) of the graphite reactor and the fourth in hole C-44 (vertical) of the LITR.

The experiments were carried out in the same manner as the stainless steel-uranyl sulfate experiments described in previous HRP quarterly reports. Except for being made of titanium (Ti-75A), the bombs were duplicates of the type 347 stainless steel bombs. The fittings and connecting tubing were of type 347 stainless steel so that the vapor phase and water (filling the capillary tubing) were in contact with stainless steel and titanium but the solution came in

contact with titanium only. The bombs were sealed at atmospheric pressure, with no attempt being made to deaerate the solutions.

The first experiment was in the graphite reactor for six and one-half days at a power density of about 1 kw per liter ( $nv \sim 7 \times 10^{11}$ ). The uranyl sulfate contained 40.7 g of uranium per liter, 93.2% enriched, with 0.0005 M  $\text{Cu}^{++}$  added to keep the pressure at a convenient level. The maximum pressure reached was approximately 1900 psi at 250°C. At the end of the run, apparently only electrolytic gas was present, indicating that no excess hydrogen was present from corrosion.

The solution was removed from the bomb after one week of cooling and was clear and free of precipitate. This absence of solid matter has seldom been observed with a stainless steel bomb. Table 41 gives a comparison of the solution composition before and after irradiation. The final volume of the sample was greater than the initial volume because some of the water in the capillary tubing was forced back into the bomb before it was opened. This water probably contained the nickel that was found in the analysis.

If it is assumed that the corrosion of titanium was the maximum value permitted by the limit of detection and that the corrosion took place uniformly over the entire surface exposed to the solution, then the corrosion rate would correspond to about 0.05 mpy.

In the second experiment, the solution contained 10 g of uranium per liter, 93.2% enriched, with no  $\text{Cu}^{++}$  present, and was terminated after two days because of instrument failure. There was nothing to indicate that the titanium and the solution were not holding up satisfactorily.

The other experiment in the ORNL graphite reactor is now in its third week of operation and contains a solution with 20 g of uranium per liter, 93.2% enriched, with no  $\text{Cu}^{++}$  present. The maximum pressure that has been reached is 2600 psi, which is much lower than a corresponding run in stainless steel. Thus far, the data indicate the titanium and the solution are holding up well.

The fourth titanium run was put into hole C-44 of the LITR on September 23. The power density in this solution is about 21 kw per liter and the uranyl sulfate solution contains 300 g of

TABLE 41. COMPOSITION OF  $\text{UO}_2\text{SO}_4$  SOLUTION BEFORE AND AFTER IRRADIATION IN TITANIUM BOMB EXPERIMENT

	SOLUTION COMPOSITION	
	Before Irradiation	After Irradiation
Volume (ml)	5.0	5.5
pH	2.42	2.15
Uranium (total, mg)	202.7	200.6 ± 2%
Copper (total, mg)	0.16	0.16
Nickel (total, mg)		0.022
Titanium (total, mg)		None*

\* Limit of detection for volume of sample used was 0.0165 mg.

## HRP QUARTERLY PROGRESS REPORT

uranium per liter, enriched 13% in  $U^{235}$ , and 0.02 M  $Cu^{++}$ . The pressure, temperature, and time data indicate that the titanium and solution are holding up well.

To summarize the radiation results with titanium, titanium appears to be far superior to type 347 stainless steel on the basis of the one completed experiment.

### IN-REACTOR LOOPS

G. H. Jenks

A knowledge of the stability of possible homogeneous reactor fuel systems and containing materials under combined dynamic, chemical, and radiation conditions comparable to those anticipated for reactors, is, of course, highly desirable. There is a good possibility that significant information of this type can be obtained through the use of forced-circulation systems irradiated within existing experimental reactors.<sup>(3)</sup> A program is now under way to develop a circulation system that may be used for this purpose.

This program is still in the initial stages, but an outline description has been given<sup>(3)</sup> of a system that may prove satisfactory. More detailed consideration of this design has not revealed any insurmountable difficulties; however, no experimental tests of the design have yet been made.

<sup>(3)</sup>G. H. Jenks, *Consideration of the Feasibility of Corrosion Studies With In-Pile Forced Circulation Systems*, ORNL CF-52-6-105 (June 18, 1952).

TABLE 42. VALUES OF SOLUTION FIRST-ORDER RATE CONSTANT FOR TWO SOLUTIONS AT FOUR TEMPERATURES

CONCENTRATION OF COPPER (M)	VALUES OF $k_{\pi}^*$ (hr <sup>-1</sup> )			
	At 125°C	At 150°C	At 175°C	At 200°C
0.5	0.272	0.393	0.785	1.36
1.00	0.152	0.254	0.921	1.23

$$*k_{\pi} = \frac{\Delta P}{P(\text{avg}) - P(\text{steam})} \times \frac{1}{\Delta T}$$

Responsibility for the engineering design and for the construction and testing of the in-reactor loop has been assumed by the Engineering Development group under C. B. Graham.

### CATALYTIC RECOMBINATION OF HYDROGEN AND OXYGEN

H. F. McDuffie      E. L. Compere  
H. H. Stone

**Dissolved Catalysts.** A few experiments were carried out with copper sulfate in distilled water to test the hypothesis that the reaction rate would fall off at high concentrations of the dissolved catalyst as a result of the change in the activity of the copper ion. Table 42 presents values of  $k_{\pi}$  (hr<sup>-1</sup>) for two solutions at four temperatures.

The values given in Table 42 were obtained with charges of 5.5 to 6.0 g of solution in 10-ml bombs. Without going into the detailed calculations of the geometry factors and ultimate specific rate constants for the copper, it was obvious that the hypothesis was confirmed and that the reaction rate, although first order in copper concentration at low concentrations, is not first order in copper concentration at high concentrations. It is more likely to be first order in copper ion activity.

The catalytic activity of 0.01 M cupric fluoride in 0.17 M uranyl fluoride solutions was tested at 250°C in one experiment. A rough estimate.

of  $k_{Cu}$ , the specific rate constant for copper, was obtained as 2590, which is considerably lower than the value of 5365 reported previously<sup>(4)</sup> for copper sulfate in uranyl sulfate. The difference is considered to be due to the difference in complexing power between sulfate and fluoride.

#### Suspended Heterogeneous Catalysts.

Interest in the possible operation of reactors at temperatures in the range of 100 to 125°C (where homogeneous recombination of hydrogen and oxygen in the presence of dissolved copper is not rapid) has led to additional consideration of heterogeneous catalysts of the platinum metals group. Preliminary studies on the use of rhodium, ruthenium, palladium, osmium, and platinum have been reported.<sup>(5)</sup>

During the past quarter improved methods for preparing catalysts have been developed; deposition of catalyst on the walls of the containers has been eliminated; improved techniques for obtaining adequate shaking have been devised; and, as a result, more reproducible data have been obtained. Of the single catalysts tested, palladium appears to be the most interesting from the point of high activity combined with resistance to poisoning. Apparatus for in-reactor studies of recombination is being prepared for use in hole 60 of the ORNL graphite reactor.

*Catalyst Preparation.* Catalysts listed in the above-referenced report were prepared by placing the sulfate or chloride salt in solution and reducing with hydrogen at temperatures up to 250°C. This procedure gave good activity but the walls of the vessels became active, presumably because of the plating out of deposits of reduced metal. In attempts that followed, the salts of palladium, platinum, rhodium,

and ruthenium were first reduced chemically to obtain catalysts of colloidal-sized particles. Various reagents, including stannous chloride, titanous chloride, hydrazine sulfate, and hydrazine hydrate, were used. Good dispersions were obtained, but it was very difficult to prevent agglomeration when these reagents were tested in the presence of uranyl sulfate. It was also discovered that the rhodium catalysts conferred activity on the walls of the test vessels. Ultimately, it was discovered that this "plating out" could be avoided only if extreme care was used to remove all metallic ions of unreduced catalyst from the solution or suspension before placing the catalyst in the stainless steel bomb. This was accomplished by several washings with distilled water followed by refluxing for 3 to 5 days with uranyl sulfate (40 g of uranium per liter) in a vessel containing a fresh type 347 stainless steel surface. Efforts were also made to stabilize the catalysts by use of such protective inorganic colloids as SnO, SnO<sub>2</sub>, ZnO, TiO<sub>2</sub>, and SiO<sub>2</sub>. Such stabilizing methods did not prove to be too promising because of catalyst poisoning, instability of particle size, and the difficulty of reproducing batches. Finally, the most successful series of catalysts was prepared by the general method of Mond, Ramsay, and Shields<sup>(6)</sup> as outlined in *Handbuch der Katalyse*.<sup>(7)</sup> A solution of the metal chloride in distilled water was heated to boiling, and sodium carbonate was added to bring the pH to between 6.5 and 7.5. A cold solution of sodium formate in distilled water was then added slowly. An immediate precipitation of the metal was noted along with vigorous decomposition of the formic acid. The

(4) C. H. Secoy, *HRP Quar. Prog. Rep. March 15, 1952*, ORNL-1280, p. 168-169.

(5) H. F. McDuffie et al., *HRP Quar. Prog. Rep. July 1, 1952*, ORNL-1318, p. 129.

(6) L. Mond, W. Ramsey, and J. Shields, *Philos. Trans. Roy. Soc. London, Sec. A 186, Part II*, 661 (1895).

(7) F. M. Schwab, *Handbuch der Katalyse*, p. 659-660, Vol. 7, Part I.

## HRP QUARTERLY PROGRESS REPORT

metal was washed with cool distilled water several times by stirring and decanting, refluxed with uranyl sulfate for five days in the presence of type 347 stainless steel surface, and then washed twice with distilled water by stirring and decanting. The final solid was dried on a hot plate at low temperature, after which it was ground with a mortar and pestle and placed in a weighing bottle.

*Experimental Technique.* The test reactions were carried out in 10-ml bombs made of type 347 stainless steel and connected through capillary tubing to valves and a pressure cell in the manner described in previous reports. The bombs were mounted in a brass cup attached to a brass rod chucked in an Air-Speed pneumatic saw and file. With the pistol-grip handle of the saw gun clamped in a vise so that the bomb was pointing almost straight up (about 10 deg away from vertical), this apparatus gave excellent shaking when attached to the 15-psi laboratory air supply (900 cycles per minute with a 1.25-in. stroke). The brass cup holding the bomb was wrapped with flexible heating tape overlaid with asbestos tape for strength and insulation. The tape was supplied with an alternating current of 75 volts from a 10-amp Variac through a Brown Pyrovane temperature controller actuated by an iron-constantan thermocouple whose hot junction was silver-soldered to the brass cup underneath the heater windings. An additional thermocouple inserted between the brass cup and bomb wall provided a better measurement of the temperature of the bomb and contents. Continuous temperature and pressure measurements were made in the manner described in previous reports with the chart speed set at 12 in. per hour because of the rapidity of the reactions under study.

Stock suspensions were prepared by suspending the ground dry catalyst in uranyl sulfate containing 40 g of

uranium per liter at a level of 1000 ppm based on the weight of the catalyst. A check on the suspension can be made by taking a sample of freshly agitated material, centrifuging, washing with distilled water, and evaporating the centrifugate to dryness for weighing. In conducting experiments, appropriate quantities of the stock suspension and uranyl sulfate solution were mixed in the test bomb or made up in small volumetric flasks. The usual solution volume for a test was 5.0 ml.

When the apparatus was completely assembled, the bomb was charged with oxygen and the shaker was started at slow speed; then the bomb was charged with hydrogen to the desired pressure level, the charging valve was closed, and the shaker was turned to full speed. Thereafter the temperature and pressure records indicated the progress of the reaction. The shaker was operated during the hydrogen charging so as to eliminate an explosion that might occur from the formation of hot spots above the wetted surface. No explosions occurred in tests with catalysts prepared by the method described above when bombs that had not previously been contaminated with plated catalysts were used.

*Results.* Values of  $k_{\pi}$ , the solution first-order rate constant, were determined from the pressure data during the first 1.66 min of the run:  $k_{\pi} = (\Delta P/P) \times (60/1.66)$ ,  $\text{hr}^{-1}$ . Although the order with respect to the gases has not yet been determined, the results expressed in this way are comparable since the starting pressures were the same in each case. Figures 42 and 43 present the variation of  $k_{\pi}$  with changes in catalyst concentration up to 1000 ppm for palladium and rhodium at 90°C.

Considerably larger variations in recombination rate were observed in parallel experiments with platinum. Successive runs in the same system might be alternately fast or slow

under supposedly identical conditions. Catalyst poisoning seemed inadequate as a specific explanation. Reference to the literature had previously shown the reduction of uranyl sulfate solutions by hydrogen in the presence of

platinum black.<sup>(8)</sup> It was thought that uranyl ion might be competing with oxygen as an oxidizing agent in some of the tests at this laboratory at relatively low temperatures. Accordingly, a test solution was withdrawn after a "poisoned" run and was found to contain considerable excess of black precipitate (reduced uranium). When this solution was returned to the bomb and subsequently withdrawn after a "good" run, the excess precipitate was gone, leaving only the relatively small amount of suspended catalyst. The implications of this, both with respect to heterogeneous catalysts other than platinum and with respect to successful reactor operation at low temperatures, are being explored.

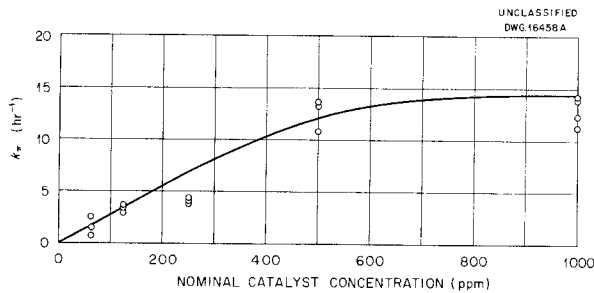


Fig. 42. Effect of Palladium Catalyst Concentration on Hydrogen-Oxygen Recombination at 90°C.

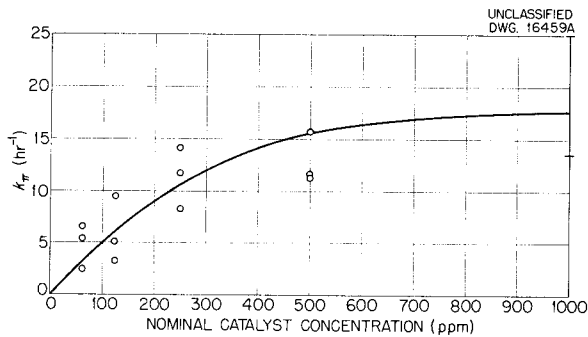


Fig. 43. Effect of Rhodium Catalyst Concentration on Hydrogen-Oxygen Recombination at 90°C.

The temperature of 90°C was chosen for preliminary survey tests for two reasons: First, it was close enough to proposed reactor operating temperatures to permit reasonable confidence to be placed in the results of the survey tests; and, second, it was below the boiling point of water at atmospheric pressure, thus allowing rapid discharging of residual gas from a run without cooling the assembly and without loss of liquid. Firm evaluation of catalysts will ultimately be based on runs at higher temperatures when these are defined by corrosion limitations.

(8) H. Gell and W. Manchot, *Ber.* 58, 482 (1925).

# HRP QUARTERLY PROGRESS REPORT

## SOLUTION CHEMISTRY

C. H. Secoy, Group Leader

### CONDUCTIVITY MEASUREMENTS OF AQUEOUS SOLUTIONS OF URANYL SULFATE AND URANYL FLUORIDE

R. D. Brown      W. B. Bungler  
W. L. Marshall

Investigations of the electrical conductivity of uranyl sulfate and uranyl fluoride in aqueous solution as a function of temperature and concentration have been terminated this quarter. This work will be presented in detail in the forthcoming Chemistry Division quarterly progress report.<sup>(1)</sup> An abstract of the complete report follows.

The conductance of uranyl sulfate in aqueous solution has been studied at 0, 25, 50, 90, 125, and 200°C in concentrations ranging from  $10^{-4}$  to 7.25 N; uranyl fluoride has been studied at 0, 25, 50, and 90°C over a similar concentration range. Both substances proved to be weak electrolytes.

The equivalent conductances at infinite dilution of uranyl sulfate at several temperatures have been calculated assuming incomplete dissociation even in dilute solution. A value of  $\Lambda_0$  (25°C) = 210 ohms<sup>-1</sup> cm<sup>2</sup> has been obtained when no correction is made for the conductivity of H<sup>+</sup> ion present from hydrolysis. Correction for H<sup>+</sup> ion leads to a value of 132 ohms<sup>-1</sup> cm<sup>2</sup>, which appears to give a reasonable value for the limiting equivalent conductance of the uranyl ion. The degree of dissociation of uranyl sulfate into simple ions has been calculated from conductivity data, and a tentative value for  $f^{\pm}$ , the mean activity coefficient, has been calculated. These values have been used to determine  $K$ , the dis-

sociation constant. Finally, the heat, the free energy, and the entropy of dissociation have been calculated.

No fruitful evaluation of the data on uranyl fluoride has been made other than to show that the increase in equivalent conductance with temperature is due to the decrease in viscosity of the solvent.

### VAPOR PRESSURES OF AQUEOUS URANYL SULFATE SOLUTIONS

H. O. Day, Jr.,      W. L. Marshall

Vapor pressure data for some solutions of uranyl sulfate were reported previously.<sup>(2)</sup> The experimental values were obtained by using a differential manometer with di-butylphthalate as the manometer fluid. During this quarter data have been obtained by using *m*-diphenylbenzene as a manometer fluid and the same experimental technique as described previously. However, considerable difficulty was encountered in attaining equilibrium. The data are reported in Table 43.

The uncertainty in concentration units is  $\pm 0.0004_5$  in molality and  $\pm 0.000008$  in mole fraction. The values are reported to the above number of decimal places because it is desired to show concentration changes owing to increased quantities of water in the vapor phase.

Examination of the data reported here and previously<sup>(2)</sup> reveals all too clearly the presence of experimental errors. Before activity coefficients can be calculated, not only must more data be obtained, but experimental errors must be further reduced.

<sup>(1)</sup> *Chem. Quar. Prog. Rep. Sept. 30, 1952, ORNL-1432, to be published.*

<sup>(2)</sup> H. O. Day, Jr., *HRP Quar. Prog. Rep. July 1, 1952, ORNL-1313, p. 138.*

TABLE 43. VAPOR PRESSURE OF AQUEOUS URANYL SULFATE SOLUTIONS

TEMPERATURE (°C)	MOLALITY OF UO <sub>2</sub> SO <sub>4</sub>	MOLE FRACTION OF UO <sub>2</sub> SO <sub>4</sub>	ΔP (mm Hg)
25	1.14482	0.0202083	0.464
30	1.14485	0.0202088	0.615
35	1.14488	0.0202093	0.804
40	1.14492	0.0202100	1.047
45	1.14496	0.0202107	1.342
50	1.14502	0.0202117	1.703
60	1.14516	0.0202142	2.659(?)
70	1.14536	0.0202176	3.844
80	1.14565	0.0202226	5.620
90	1.14607	0.0202299	7.859(?)

SOLUBILITY OF UO<sub>3</sub> IN AQUEOUS  
UO<sub>2</sub>SO<sub>4</sub> AND UO<sub>2</sub>F<sub>2</sub> AT  
175 AND 250°C

E. V. Jones      J. S. Gill  
W. L. Marshall

Investigations of UO<sub>3</sub> solubility in UO<sub>2</sub>SO<sub>4</sub> solutions at 250°C, which have been reported in part for UO<sub>2</sub>SO<sub>4</sub>,<sup>(3)</sup> have been continued and expanded to include solubilities in aqueous UO<sub>2</sub>F<sub>2</sub>. The technique of filtering a solution from excess solid phase at temperatures above 100°C was described previously.<sup>(3)</sup>

**UO<sub>3</sub>-UO<sub>2</sub>SO<sub>4</sub>-H<sub>2</sub>O System.** Data for the solubility of UO<sub>3</sub> in UO<sub>2</sub>SO<sub>4</sub> at 175°C and the acidities of such solutions are given in Table 44. The solubility of UO<sub>3</sub>, the solubility ratio, and the acidity have been plotted individually against uranium concentration and are shown in Figs. 44, 45, and 46, respectively. Curves representing data at 250°C, which were presented in the last quarterly report, are included. This investigation still has not clarified the

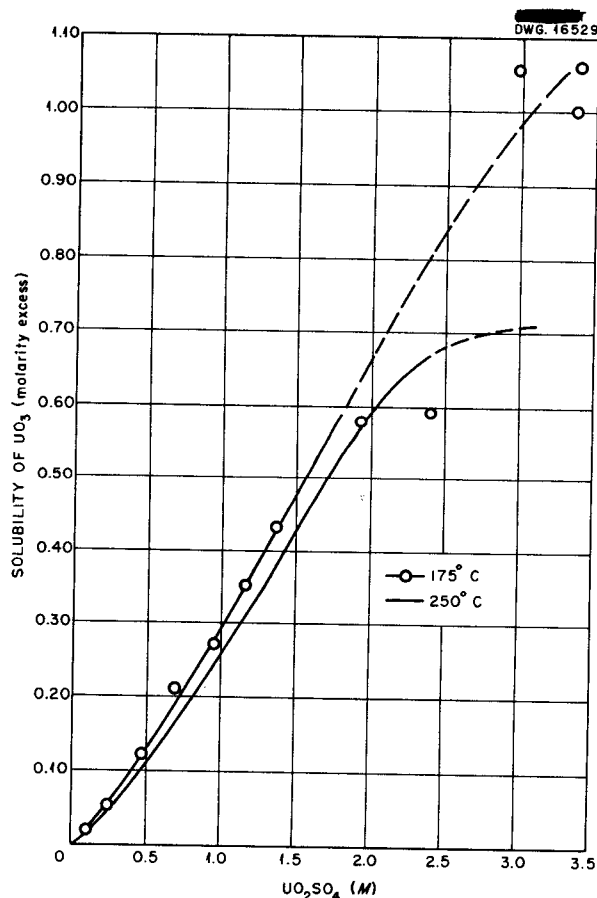


Fig. 44. Solubility of UO<sub>3</sub> in UO<sub>2</sub>SO<sub>4</sub>-H<sub>2</sub>O Solutions at 175°C.

(3) J. S. Gill, E. V. Jones, and W. L. Marshall, HRP Quar. Prog. Rep. July 1, 1952, ORNL-1318, p. 144.

# HRP QUARTERLY PROGRESS REPORT

behavior in the low-concentration region, that is, below 0.1 M. The question is whether the equilibrium ratio, U to  $SO_4$ , drops below 1.00 as concentration is lowered. If the ratio does fall below 1.00, then

the data would best be represented by the system  $UO_3-H_2SO_4-H_2O$ . On this basis, there is no valid reason why the ratio of U to  $SO_4$  must remain

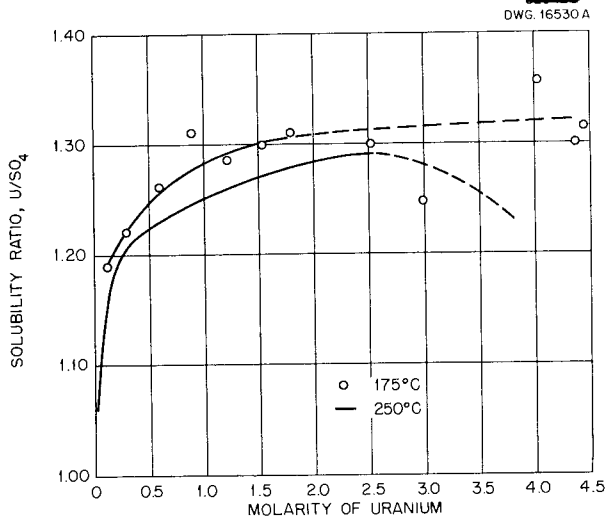


Fig. 45. Solubility Ratio of U to  $SO_4$  in  $UO_2SO_4-H_2O$  Solutions at  $175^\circ C$ .

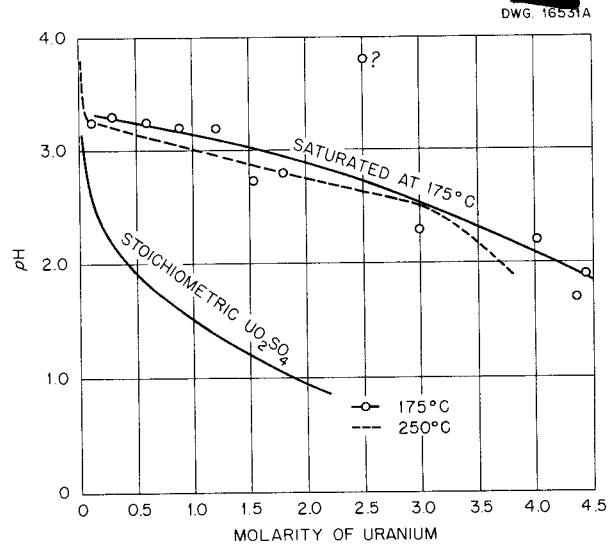


Fig. 46. Acidity Curves for Saturated Solutions of  $UO_3$  in  $UO_2SO_4$  Solutions. Acidities measured at room temperature.

TABLE 44. SOLUBILITY OF  $UO_3$  IN  $UO_2SO_4-H_2O$  SOLUTIONS AT  $175^\circ C$

Molarities based on room-temperature densities

TOTAL MOLARITY URANIUM	MOLARITY $SO_4$	SOLUBILITY EXCESS, MOLARITY $UO_3$	TOTAL MOLE RATIO $UO_3$ to $SO_4$	pH (at $25^\circ C$ )	HOURS OF MIXING AT $175^\circ C$
0.119	0.100	0.019	1.19	3.25	72
0.292	0.239	0.053	1.22	3.30	72
0.594	0.471	0.123	1.26	3.25	72
0.890	0.680	0.210	1.31	3.20	72
1.217	0.948	0.269	1.28	3.20	96
1.528	1.178	0.350	1.30	2.73	72
1.790	1.360	0.430	1.31	2.80	68
2.508	1.934	0.574	1.30	3.80(?)	72
2.986	2.397	0.589	1.25	2.30	72
4.020	2.964	1.056	1.36	2.20	192
4.370	3.370	1.000	1.30	1.70	120
4.440	3.380	1.060	1.31	1.90	192

FOR PERIOD ENDING OCTOBER 1, 1952

equal to or greater than 1.00. Also, for a given sulfate concentration, the ratio should decrease with temperature because of increased hydrolysis of the uranyl ion. During the next quarter an effort will be made to clarify this low concentration region.

The solid phase at 250°C was previously reported<sup>(3)</sup> as  $\text{UO}_3 \cdot \frac{1}{2}\text{H}_2\text{O}$ . This phase has been further identified by x-ray diffraction as  $\text{UO}_3$  hydrate.

$\text{UO}_3\text{-UO}_2\text{F}_2\text{-H}_2\text{O}$  System. Experimental data for the  $\text{UO}_3\text{-UO}_2\text{F}_2\text{-H}_2\text{O}$  system

at 175 and 250°C are given in Table 45 and are shown in Figs. 47, 48, and 49. The data at 250°C are erratic and are included as preliminary data only. In most of the experiments on the fluoride system at 250°C, corrosion of the titanium filter bombs and some reduction of uranium was noted, but this attack was not evident at 175°C.

The ratio, U to 2F, at 250°C appears to decrease below 1.00 at low concentrations; therefore the system probably could be represented best as  $\text{UO}_3\text{-HF-H}_2\text{O}$ .

TABLE 45. THE SOLUBILITY OF  $\text{UO}_3$  IN  $\text{UO}_2\text{F}_2\text{-H}_2\text{O}$  SOLUTIONS AT 175 AND 250°C  
Molarities based on room-temperature densities

TOTAL MOLARITY URANIUM	MOLARITY $\text{UO}_2\text{F}_2$	SOLUBILITY EXCESS, MOLARITY $\text{UO}_3$	TOTAL MOLE RATIO $\text{UO}_3$ TO $\text{UO}_2\text{F}_2$	pH (at 25°C)	HOURS OF MIXING
At 175°C					
0.0483	0.04775	0.00055	1.012	4.65	96
0.1740	0.1685	0.0055	1.033	4.40	96
0.230	0.225	0.0050	1.022	4.30	90
0.954	0.8675	0.0865	1.100	3.90	96
1.964	1.692	0.272	1.161	3.57	96
2.478	2.150	0.328	1.153	3.37	96
3.066	2.409	0.657	1.273	3.20	180
4.121	3.416	0.705	1.206	2.70	180
4.200	3.315	0.885	1.267	2.60	120
At 250°C					
0.169	0.185	-0.016	0.914	2.92	
0.732	0.745	-0.013	0.979	3.50	
1.06	0.993	0.067	1.07	3.90	
1.58	1.40	0.18	1.13	3.60	
1.89	1.71	0.18	1.11	3.49	
3.02	2.69	0.33	1.12	3.90	
3.29	2.82	0.47	1.17	3.25	
3.43	2.95	0.48	1.16	3.10	
2.73*	2.45	0.28	1.11	3.70	
2.42**	2.12	0.30	1.14	3.40	

\*Run made in a Teflon liner.

\*\*Three drops of 30%  $\text{H}_2\text{O}_2$  added.

# HRP QUARTERLY PROGRESS REPORT

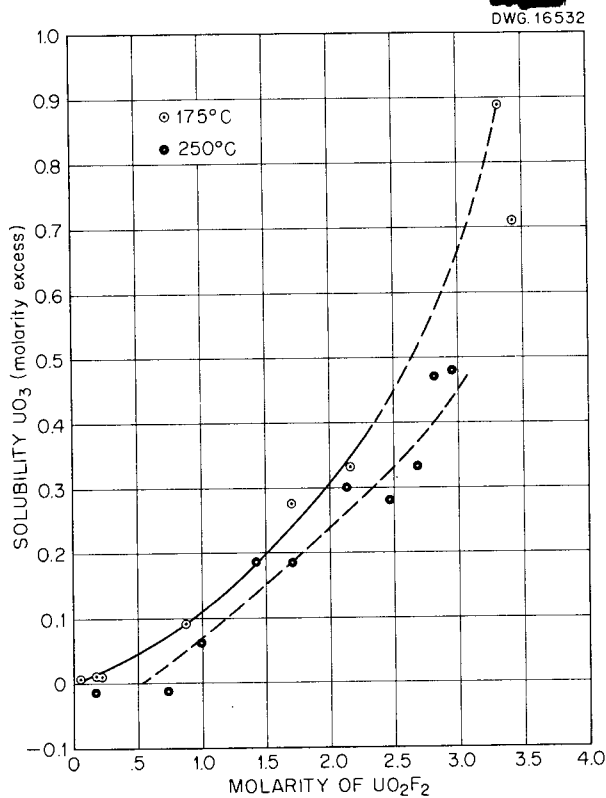


Fig. 47. Solubility of  $UO_3$  in  $UO_2F_2-H_2O$  Solutions at 175 and 250°C.

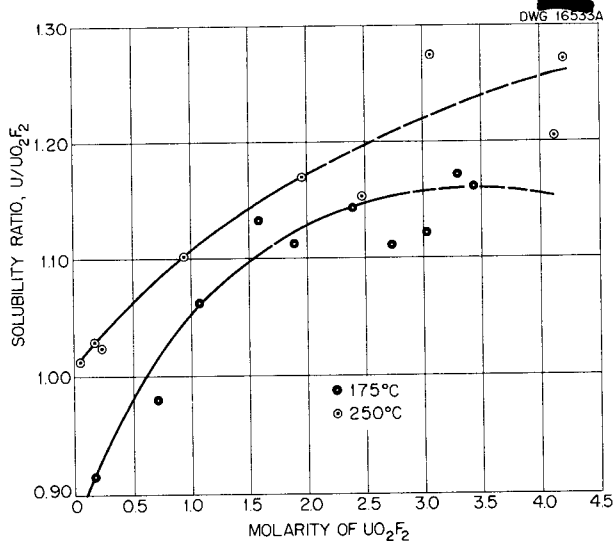


Fig. 48. Solubility Ratio of U to  $UO_2F_2$  in  $UO_3-UO_2F_2-H_2O$  Solutions at 175 and 250°C.

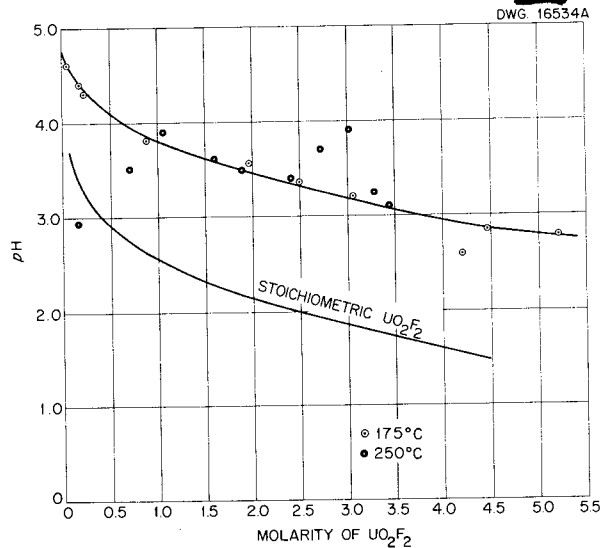


Fig. 49. Acidity Curves for  $UO_2F_2$  Solutions Saturated with  $UO_3$  at 175 and 250°C. Acidities measured at room temperature.

## EXTENSION OF THE STUDY OF THE TWO-LIQUID-PHASE REGION OF THE $UO_2SO_4-H_2SO_4-H_2O$

H. W. Wright      W. L. Marshall

The effect of free sulfuric acid on the coexistence curve of the two-liquid-phase region of the uranyl sulfate-water system at acid concentrations up to about 0.63 M was described previously.<sup>(4,5,6,7)</sup> The acid was found to decrease the scope of the region (increase miscibility) and to shift the minimum critical solution point to higher temperatures. The addition of sulfuric acid elevates the critical temperature not only because of the acid present but also

(4) C. H. Secoy, *Chem. Quar. Rep.* June, July, August 1948, ORNL-176, p. 58-63.

(5) C. H. Secoy, *Chem. Quar. Prog. Rep.* Dec. 31, 1949, ORNL-607, p. 33.

(6) W. L. Marshall, J. S. Gill, and C. H. Secoy, *Chem. Quar. Prog. Rep.* June 30, 1950, ORNL-795, p. 22.

(7) R. E. Leed and C. H. Secoy, *Chem. Quar. Prog. Rep.* Sept. 30, 1950, ORNL-870, p. 29-30.

because of the increased solubility of uranyl sulfate in the supercritical fluid.

The experimental techniques of earlier investigators had two major failings. One was the laborious and time-consuming job of tube preparation, coupled with the long cooling time required before the heating element could be reloaded for subsequent runs. Another limitation was the inability (or perhaps the impossibility) to prepare silica tubes with sufficient strength to withstand the high pressures developed; out of 66 prepared tubes, 46 blew up before data could be obtained.<sup>(7)</sup>

Both the tube failures and the tube preparation time factor were

solved by resorting to commercially available capillary silica tubing, 1-mm base, 1-mm wall thickness. When half filled with water, these tubes withstood temperatures in excess of 750°C and could be prepared in several minutes. The other limitations were overcome by the use of a redesigned heating element (Fig. 50).

The redesigned element consists of a cylindrical, heat-conducting block C (Al and graphite have been used) 30 cm in length and 5 cm in diameter. A hole 8 mm in diameter was drilled through the longitudinal axis. The glass (or silica) sleeve D fits into this hole which acts as a housing for the sample tube and the iron-constantan thermocouple; the

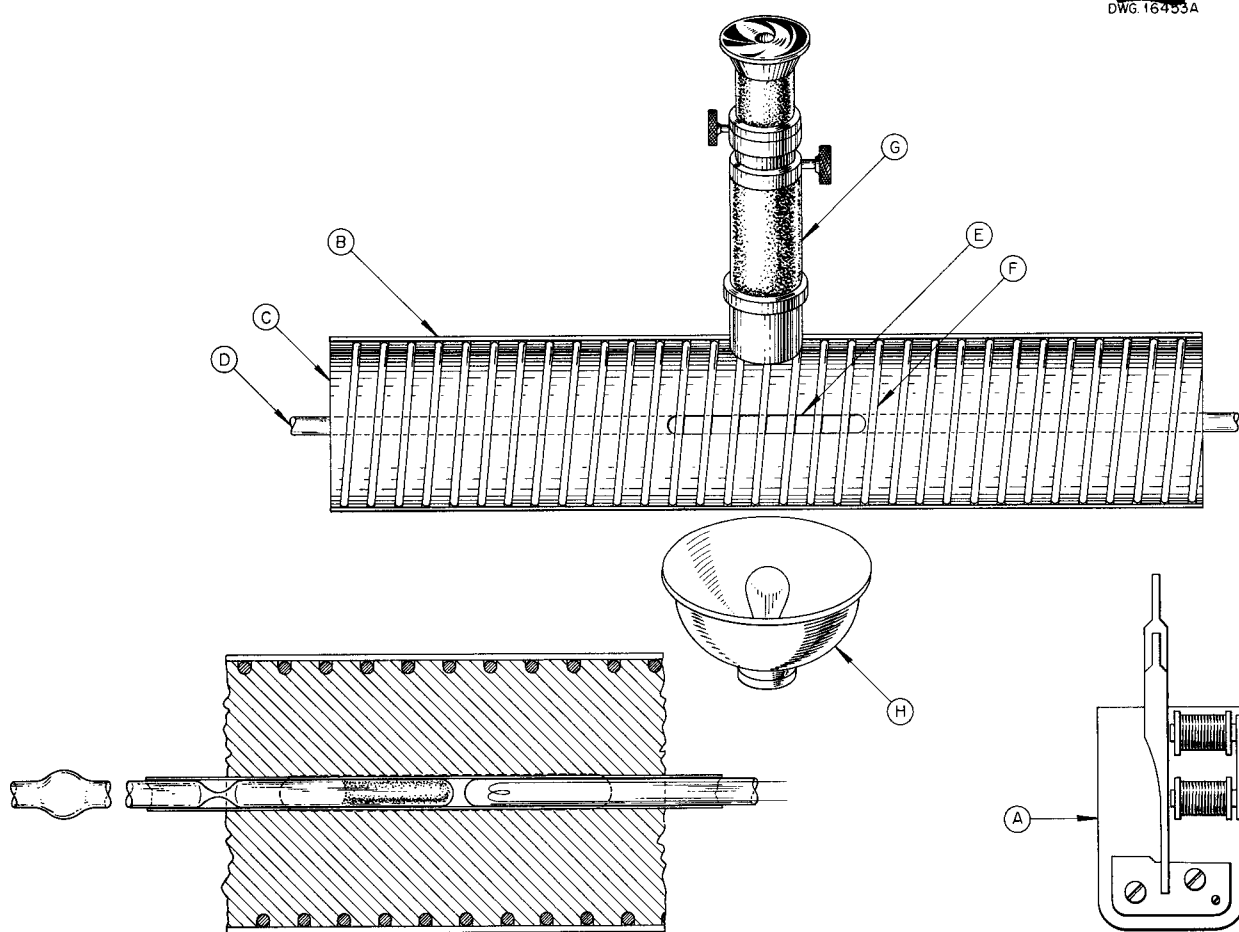


Fig. 50. Apparatus for Phase Transition Studies on Semimicro Scale.

## HRP QUARTERLY PROGRESS REPORT

sample enters from one end and the thermocouple from the other. A window E, 50 by 8 mm, cut normal to the sample hole, allows visual observation of the sample. Evenly spaced grooves F were machined over the block to hold the heating wire. Sleeve B covers the entire block. Sleeves B and D act as insulators and reduce air movement through the slotted areas. The entire heating element rests in a cradle (not shown in the diagram).

The buzzer A is a simple bell buzzer adapted with an alligator clamp in place of a striker. It is mounted on the adjustable arm that holds the sample in position and effects mixing of the sample by automatic, alternate on-off buzzing.

A shield mounted between the observer and the heating element affords complete protection to the observer from explosions. The telescope G along with the light source H located on the opposite side of the window allows one to observe minute changes within the sample before they are discernible to the naked eye.

Temperature control is maintained with the use of a conventional variac and is measured with an iron-constantan thermocouple and conventional instruments.

The use of this new apparatus offers the following advantages:

1. a smaller sample than previously used,
2. greatly increased temperature range,
3. time economy in tube preparation,
4. ease of temperature control,
5. evenness of heating, which reduces temperature gradients throughout the sample,
6. ability to remove and reload samples at high temperatures without the heretofore necessary wait while the heating element cooled,
7. ease of substitution of entire heating unit,
8. reduction of tube explosion hazard,
9. increased visual perception obtainable with the telescope,
10. adaptability of the apparatus to high-temperature visual observations of other systems.

A 10-ml  $\text{UO}_2\text{SO}_4$  solution of approximately 30 wt% uranium with an  $\text{SO}_4$  to U ratio of 1.000 was prepared. A small sample was withdrawn, and the remaining solution was diluted to volume. Again a sample was withdrawn, and the remaining solution was diluted with water. By this procedure, a series of solutions was obtained that varied in uranium concentration but had a constant  $\text{SO}_4$  to U ratio. In similar fashion, five other series were prepared with  $\text{SO}_4$  to U ratios ranging up to 2.955.

Once the  $\text{SO}_4$  to U ratio was established by analysis of the more concentrated solutions, only the uranium concentration of the more dilute samples was measured, since it is evident that the  $\text{SO}_4$  concentration follows that of uranium.

Tubes containing each dilution of each series were prepared in similar fashion with each tube containing approximately the same volume of solution. The samples were heated in the unit described above and the temperature at which the second liquid phase appeared and disappeared was recorded (Table 46) and the data plotted (Fig. 51).

These data can be applied directly to a selection of reactor fuel media. In other words, the two-liquid-phase boundaries can be determined for uranium concentrations up to 30% and for any constant ratio of  $\text{SO}_4$  to U from 0.83<sup>(8)</sup> to 2.9.

The system  $\text{UO}_3\text{-H}_2\text{SO}_4\text{-H}_2\text{O}$  is comparable to  $\text{UO}_3\text{-H}_3\text{PO}_4\text{-H}_2\text{O}$  as a fuel media for homogeneous reactors operating between about 300 and over 500°C. Bidwell, Thamer, and Hammond<sup>(9)</sup> are studying the phosphate system at

<sup>(8)</sup>E. V. Jones, *HRP Quar. Prog. Rep. July 1, 1952*, ORNL-1318, p. 147.

<sup>(9)</sup>R. M. Bidwell, B. J. Thamer, and R. P. Hammond, private communication.

TABLE 46. APPEARANCE TEMPERATURE OF TWO LIQUID PHASES IN  $UO_2SO_4-H_2SO_4-H_2O$ 

CONSTANT RATIO SERIES	URANIUM (wt %)	TWO-LIQUID-PHASE APPEARANCE TEMPERATURE (°C)	CONSTANT RATIO SERIES	URANIUM (wt %)	TWO-LIQUID-PHASE APPEARANCE TEMPERATURE (°C)
CR-I: $SO_4/U = 1.121$			CR-IV: $SO_4/U = 2.481$		
1	29.65	312	1	25.92	
2	21.59	303	2	17.40	Above 530
3	16.01	300	3	11.82	387
4	10.98	299.5	4	7.42	370
5	6.65	301	5	4.04	360
6	4.23	308	6	2.40	356
7	2.20	317	7	1.44	355
8	1.03	327	8	0.75	358
9	0.47	338	9	0.33	364
CR-II: $SO_4/U = 1.428$			CR-V: $SO_4/U = 2.955$		
1	27.85	355	1	22.60	
2	20.49	337	2	17.00	Above 530
3	14.35	326	3	9.98	Above 525
4	10.29	322	4	5.11	372
5	7.28	320	5	2.83	363
6	5.22	321	6	1.23	360
7	3.29	324	7	0.43	364
8	2.27	326	8	0.17	370
9	1.40				
10	0.84	340			
CR-III: $SO_4/U = 1.883$			CR-VI: $SO_4/U = 1.000$		
1	27.02	Above 525	1	30.11	287
2	18.15	379	2	20.07	285
3	12.06	353	3	13.75	286
4	7.70		4	7.89	288
5	4.50	339	5	3.60	298
6	2.61	339	6	1.87	308
7	1.51	342	7	0.99	320
8	0.54	351			

Los Alamos, and some work has been done at ORNL.<sup>(10)</sup> However, there are some distinct differences between the two systems with regard to reactor fuels. First, the ratio  $PO_4$  to U required for phase stability from 25 to above 300°C is between 5.0 and 9.0. These ratios are greater than those

(10) J. S. Gill, H. W. Wright, and W. L. Marshall, *HRP Quar. Prog. Rep. Aug. 15, 1952*, ORNL-1121, p. 119.

required for the sulfate system to reach the upper temperatures. Accordingly, the sulfate might exhibit less corrosion on container surfaces than the phosphate system. Second, the cross section of sulfur is 0.49 barn compared with 0.15 for phosphorus. However, this difference is decreased by the lower amount of sulfate necessary to stabilize a solution of the same uranium concentration.

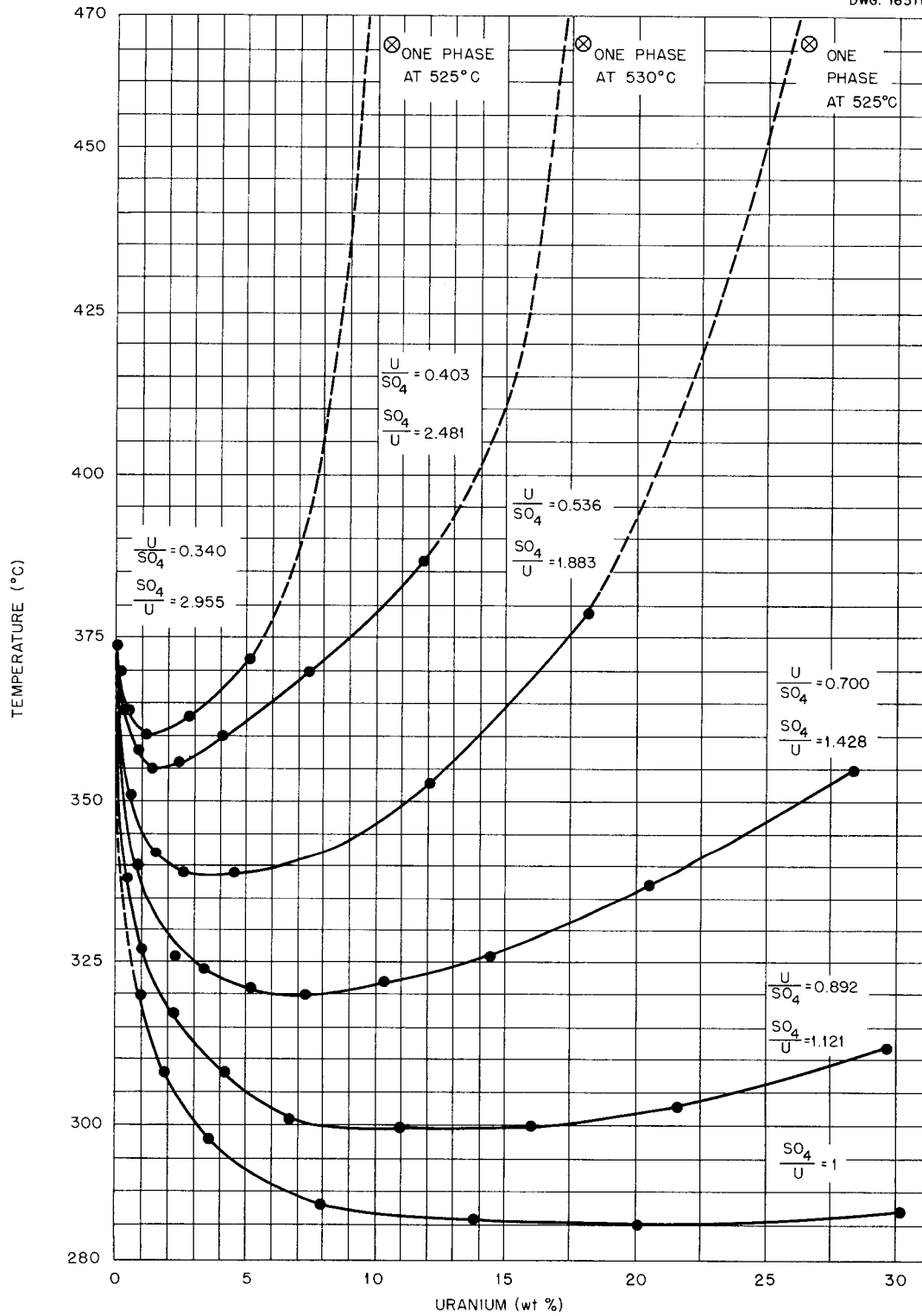


Fig. 51. Coexistence Curves for Two Liquid Phases in the  $UO_2SO_4-H_2SO_4-H_2O$  System. Constant mole ratio of U to  $SO_4$ .

**ALTERNATE FUEL MEDIA AND POSSIBLE  
CORROSION INHIBITORS**

H. O. Day      E. V. Jones  
J. S. Gill     W. L. Marshall  
                 H. W. Wright

It is well known that uranyl fluoride forms double salts easily because uranyl fluoride is, coordinately, unsaturated. J. S. Johnson and K. A. Kraus of the Chemistry Division have also shown that pure  $UO_2F_2$  in aqueous solutions at ordinary temperature forms a dimer,  $(UO_2F_2)_2$ . These facts lead to the supposition that by addition of other compounds to uranyl fluoride solutions the uranyl ion might become so strongly complexed that a very definite inhibition of corrosion of type 347 stainless steel might be obtained upon exposure of the steel to the solution. The work performed so far in this investigation is of an exploratory nature.

Possible additives that might cause complexing, and at least cause an increase in pH, are metallic hydroxides of strongly basic nature and the fluoride salts of such bases. For these additions of  $M(OH)_x$  and  $MF_x$  to be of value the following criteria must be met:

1. Significant quantities of the additive must go into solution with the uranyl fluoride and remain in solution at elevated temperatures (at least 250°C). Although it would not be absolutely necessary that the additive completely dissolve at room temperature, so long as it was completely soluble at 250°C, it would be advantageous if it were soluble over the entire temperature range. A corollary to the quantity of additive that dissolves is the resulting increase of pH. The higher the pH, the better - assuming that phase instability does not occur.

2. The cross section (neutron capture) of the metal hydroxide

or fluoride should be small, and the smaller the better.

3. The added compound causes the corrosion of type 347 stainless steel by the solution to be materially inhibited.

Of these three criteria, the last is obviously the most important, for even if the first two are completely satisfied, the whole object of the addition of the compound is lost if the third criterion is not fulfilled.

The systems being studied experimentally and those for which studies are contemplated can be written in the general form  $M_xO-UO_3-HF-H_2O$ , insofar as the original components are concerned. These systems are tabulated in the following, together with the cross section of the element M as taken from a General Electric Chart of the Nuclides. Lithium has been included because  $Li^7$  might become available.

SYSTEM	CROSS SECTION OF M
$Li_2O-UO_3-HF-H_2O$	67
$Na_2O-UO_3-HF-H_2O$	0.48
$K_2O-UO_3-HF-H_2O$	2.0
$Rb_2O-UO_3-HF-H_2O$	0.7
$MgO-UO_3-HF-H_2O$	0.07
$CaO-UO_3-HF-H_2O$	0.42
$ZrO_2-UO_3-HF-H_2O$	0.40
$Bi_2O_3-UO_3-HF-H_2O$	0.015
$SnO_2-UO_3-HF-H_2O$	0.6
$ZnO-UO_3-HF-H_2O$	1.0

**Static Corrosion Tests.** It can be readily seen that investigation from the viewpoint of phase relationship of so many four-component systems over a large temperature range would be a very formidable undertaking. Since the main consideration is the behavior of these solutions toward

## HRP QUARTERLY PROGRESS REPORT

type 347 stainless steel, some static corrosion tests have been made to serve as a guide. These tests were made in an attempt to decide which of the systems of additives looked promising and thereby warranted more complete investigation of phase behavior. It is realized that if a static corrosion test looks promising, this behavior cannot be extrapolated to dynamic systems. However, if the static test result is poor, the dynamic test would surely be poor also, and thus some  $M_xO-UO_3-HF-H_2O$  systems could be eliminated from further consideration.

Most of the corrosion tests were made at 300°C, but for some the temperature was as high as 310°C. The 300°C temperature was chosen because it was thought that short corrosion tests at 300°C would be equivalent to longer tests at 250°C, thus saving time, and that a system that looked promising corrosion-wise at 300°C would probably be even more promising at 250°C.

The tests were all made in a platinum-lined bomb of about 40-ml capacity. A cleaned and weighed type 347 stainless steel sample was

placed in the bomb and 10 to 15 ml of solution added. The bomb was then sealed and placed in a eutectic mixture of  $LiNO_3$ ,  $KNO_3$ , and  $NaNO_3$ , which was at 300°C. The amount of oxygen present was just the amount contained in 25 to 30 ml of air plus that dissolved in the solution.

The solutions used had more or less random concentrations of various hydroxides and fluorides in  $UO_2F_2$  solutions of various concentrations. Usually, but not always, these solutions had been tested for phase stability before being placed in the bomb. Data obtained from the tests are given in Table 47.

The corrosion tests may be summarized as follows:

1. It has been well established that pure aqueous  $UO_2F_2$  solution with a small amount of oxygen attacks type 347 stainless steel.

2.  $UO_2F_2$  solution with LiOH and practically no oxygen attacks type 347 stainless steel but not so violently or so rapidly as pure  $UO_2F_2$  with a small amount of oxygen.  $UO_2F_2$  with other additives would probably behave similarly.

**TABLE 47. CORROSION RESULTS OF VARIOUS  $M_xO-UO_3-HF$  MIXTURES ON TYPE 347 STAINLESS STEEL**

SOLUTION	LENGTH OF TEST AND PREVAILING TEMPERATURE	APPEARANCE OF SOLUTION AND CORROSION SPECIMEN
Control run: 206 g of uranium per liter of pure $UO_2F_2$	1 day at 300°C	Much uranium reduced; black oxide coated on inside of bomb; heavy oxide film on specimen; specimen gained 20% in weight
0.853 M U	24 hr at 300°C	Solution perfectly clear except some reddish orange crystals resulting from phase instability; specimen gained 0.16% in weight; microscopic examination showed some small pitting
0.627 M Li	48 hr at 210 to 280°C	
1.26 M $UO_2F_2$ 0.228 M LiOH pH = 3.9	22 hr at 300°C	Solution perfectly clear; specimen gained 0.1% in weight; very smooth film of almost coppery appearance on specimen; microscopic examination showed very little pitting
1.26 M $UO_2F_2$ 1.489 M NaF pH = 4.25	72 hr at 305°C	Solution perfectly clear; specimen lost 0.14% in weight; specimen very shiny; microscopic examination showed very smooth film with no pitting; this was one of the best specimens obtained in the static corrosion tests

FOR PERIOD ENDING OCTOBER 1, 1952

TABLE 47. (continued)

SOLUTION	LENGTH OF TEST AND PREVAILING TEMPERATURE	APPEARANCE OF SOLUTION AND CORROSION SPECIMEN
1.26 M $UO_2F_2$ saturated with LiF pH = 2.78	89 hr at 300°C	Solution partly reduced; black oxide inside bomb; heavy film on specimen; microscopic examination showed attack on metal; specimen gained 2.1% in weight
1.26 M $UO_2F_2$ 0.2 M LiOH pH = 3.8	66 hr at 300 to 308°C	Solution clear; no oxide formed in bomb; glossy film on specimen; specimen lost 0.05% in weight; microscopic examination showed only small pitting
1.26 M $UO_2F_2$ 0.2 M LiOH pH = 3.8	17 hr at 300 to 309°C	Solution clear; no oxide formed in bomb; specimen gained 0.1% in weight; no microscopic examination made
0.718 M $UO_2F_2$ 1.027 M NaF pH = 5.12	66 hr at 290 to 292°C	Solution somewhat cloudy owing to phase instability of solution, i.e., a precipitate formed; specimen lost 0.06% in weight; microscopic examination showed practically no pits on one side and about 14/cm <sup>2</sup> on other side
1.26 M $UO_2F_2$ 0.25 M NaOH 1.89 M NaF pH = 6.6	18 hr at 292°C	Solution precipitated a large amount of yellow-orange crystals owing to phase instability; some of original solution, on standing, also precipitated crystals; no oxide formed in bomb; mass change of steel was not determined since yellow crystals covered it
1.26 M $UO_2F_2$ 0.29 M NaOH pH = 4.11	66 hr at 290 to 292°C	Solution clear except for some silky, yellow needles resulting from phase instability; no oxide formed on bomb; specimen lost 0.02% in weight; very glossy even film on specimen; no microscopic examination made
0.168 M $UO_2F_2$ 0.104 M LiF pH = 3.50	18 hr at 300 to 310°C	Solution clear; no black oxide formed; specimen gained 0.1% in weight; microscopic examination showed some rather bad pits, ~10 μ deep
0.168 M $UO_2F_2$ 0.202 M KF pH = 4.37	20 hr at 300°C	Solution clear except for some yellow crystals precipitated because of phase instability; no weight change of specimen; very even shiny film on specimen; some small pits about 1 μ deep observed
Synthetic solution: prepared by heating 22.7 wt % $UO_2F_2$ solution with excess LiOH and filtering at 250°C. Composition: 0.17 M U 0.56 <sub>3</sub> M F 0.252 M Li pH = 6.5	20 hr at 300°C	Solution clear yellow; no black oxide formed on bomb; specimen gained 0.04% in weight; very smooth glossy film on specimen; no microscopic examination made
1.26 M $UO_2F_2$ 0.2 M LiOH pH = 3.8 In addition practically all O <sub>2</sub> had been flushed out of the bomb and solution by use of N <sub>2</sub> gas in an improvised dry box	23 hr at 300°C	Solution partly reduced; black oxide formed on bomb; heavy film on specimen; specimen gained about 2% in weight; pH of solution now 3.6

## HRP QUARTERLY PROGRESS REPORT

3. With small amounts of oxygen and additives such as LiOH, NaOH, NaF, etc., corrosion under static conditions is definitely inhibited. It is not known whether this inhibition is of sufficient strength to be of value so far as dynamic behavior is concerned.

4. The optimum system or optimum concentration of any particular system for inhibiting corrosion is not known. Also, the optimum oxygen concentration for the particular system and concentration is not known.

**Dynamic Corrosion Tests.** Solutions of additives have been tested and are under further tests in the dynamic test loops in operation at the Y-12 site. The results are, as yet, fragmentary and will be reported by the corrosion study groups under the direction of E. G. Bohlmann.

**Conductometric and Acidimetric Titrations.** In an attempt to determine possible molecular species existing in the solutions, conductometric and acidimetric titrations were run. The theory would be that if a strongly

stable species existed and such species showed a composition attainable by titration, a significant break should occur in the titration curve at that point. Nine conductometric and four acidimetric titration experiments have been made. Table 48 gives the molarities of the initial and titrating solution and ratios to which the initial solution was titrated.

In all titration curves, except the pH curves, there were some questionable breaks in the continuity. The pH curves did not show breaks up to the limits of titration. The only sharp break was that shown by the two  $UO_2F_2$ -NaF titrations; the break occurred at a ratio of Na to F of 1:3.

Comparative runs are shown in Figs. 52 and 53. The conductometric data are normalized to start from the same point. A few drops of an equivalent LiOH solution added to  $H_2O$  or to a salt solution not interacting with hydroxyl ions increased the pH to about 11.5 and the cell conductivity to above 30. This evidence indicates the complexing or hydrolysis nature of  $UO_2F_2$  in these systems.

TABLE 48. RESULTS OF TITRATION EXPERIMENTS

NUMBER	TYPE OF TITRATION	INITIAL SOLUTION	TITRATING SOLUTION	METAL-TO-URANIUM RATIO AFTER TITRATION
1	Conductometric	0.126 M $UO_2F_2$	0.10 M LiOH	0.16
2	Conductometric	0.126 M $UO_2F_2$	0.10 M LiOH	0.52
3	Conductometric	1.26 M $UO_2F_2$	4.84 M LiOH	0.54
4	Acidimetric	1.26 M $UO_2F_2$	0.0484 M LiOH	0.42
5	Acidimetric	2.26 M $UO_2F_2$	0.484 M LiOH	0.38
6	Acidimetric	2.26 M $UO_2F_2$	4.84 M LiOH	0.50
7	Acidimetric	3.25 M $UO_2F_2$	0.484 M LiOH	0.47
8	Conductometric	0.05 M $UO_2SO_4$	0.10 M LiOH	0.64
9	Conductometric	0.168 M $UO_2SO_4$	0.10 M LiOH	0.39
10	Conductometric	1.26 M $UO_2F_2$	0.40 M NaF	2.0
11	Conductometric	1.26 M $UO_2F_2$	0.80 M NaF	2.5
12	Conductometric	1.26 M $UO_2F_2$	0.40 M KF	1.9
13	Conductometric	1.26 M $UO_2F_2$	0.80 M KF	2.5

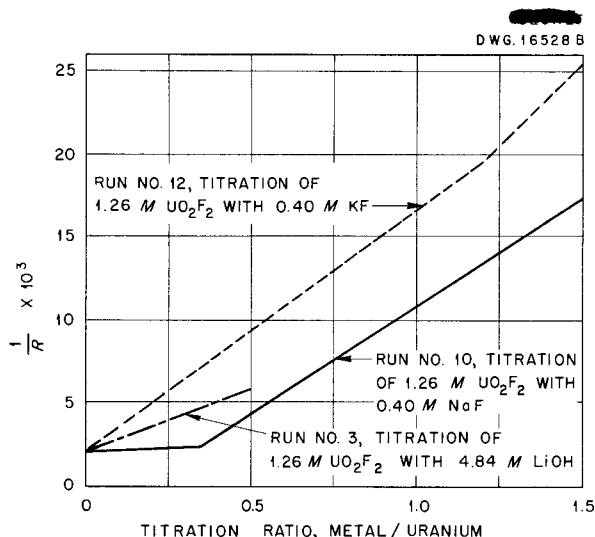


Fig. 52. Conductometric Titration of  $UO_2F_2$  Solution with LiOH, KF, and NaF.

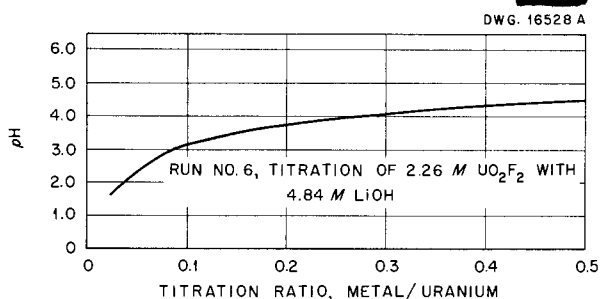


Fig. 53. Acidimetric Titration of  $UO_2F_2$  Solution with LiOH.

The conclusion from this work is that if complexes of composition within the above ratios are present, they do not show up as sharp breaks in conductometric and pH titration curves, with the possible exception of  $UO_2F_2$ -NaF.

**Solubility and Phase Behavior in the  $M_xO-UO_3-HF-H_2O$  System.** Before much work was done on the  $UO_2F_2$  systems, exploratory additions of various metallic hydroxides to 1.26 M  $UO_2SO_4$  solutions were performed. These explorations did not look promising, because either very little of the hydroxide went into solution

or crystals appeared upon heating the solution to 250°C. Thereafter work was confined to the  $UO_2F_2$  systems. No complete phase study has been made of any of the various systems mentioned previously. Since data are as yet incomplete, none of the systems can be completely rejected from a phase stability standpoint, although some systems seem more promising than others.

**$Li_2O-UO_3-HF-H_2O$  System.** A fairly large amount of experimental work has been performed at 250°C on the solubility behavior of the  $Li_2O-UO_3-HF-H_2O$  system. However, since the work is still incomplete and many of the experiments have not yet been repeated to ensure accuracy and since it is not positively known that true equilibrium existed in some of the experimental runs, the results will not be reported at this time.

At 25°C the solubility limit of LiOH in 1.26 M  $UO_2F_2$  is somewhere between 0.305 and 0.381 M. This corresponds to a Li-to-U ratio of greater than 0.242 but less than 0.302. The 0.2 M LiOH is soluble in 1.26 M  $UO_2F_2$  up to 322°C.

The various solid crystals that appear at the upper temperatures in many of the solutions have not been identified.

At 25°C, LiF dissolves in 0.168 M  $UO_2F_2$  to the extent of about 0.11 M. Results so far do not indicate that the LiF- $UO_2F_2-H_2O$  system is of promise as a corrosion inhibitor.

**$Na_2O-UO_3-HF-H_2O$  System.** The limit of solubility of NaOH in 1.26 M  $UO_2F_2$  is between 0.264 and 0.315 M. This corresponds to a Na-to-U ratio of greater than 0.21 and less than 0.25. A solution of the ratio Na to U of 0.23 is very close to the limit of solubility. A solution of this composition on being heated to 320°C and then cooled yields silky, fibrous, yellow crystals that have not been identified. These crystals are unlike the precipitate formed at

## HRP QUARTERLY PROGRESS REPORT

room temperature when the solubility limit is exceeded, since the latter precipitate is made up of fine, yellow crystals of some sort of uranate.

The upper-temperature phase behavior of the NaOH- $\text{UO}_2\text{F}_2$ - $\text{H}_2\text{O}$  system has not been investigated.

Sodium fluoride will dissolve in 1.26 M  $\text{UO}_2\text{F}_2$  to a marked extent at room temperature. The solubility limits are between 1.21 and 1.93 when solubility is expressed as the NaF-to- $\text{UO}_2\text{F}_2$  ratio. Solutions of the former concentration are phase stable up to 300°C. Solutions of lower uranium concentrations have NaF solubilities up to at least 1.43. The values given in Table 49 have been obtained.

**TABLE 49. BEHAVIOR AT ELEVATED TEMPERATURES OF SODIUM FLUORIDE IN URANYL FLUORIDE**

Mole ratio Na to U of 1.43

URANIUM CONCENTRATION (g/l)	pH	BEHAVIOR AT ELEVATED TEMPERATURES
171	5.12	Crystals at 275°C
85.5	5.35	Possibly crystals at 250°C
42.2	5.51	Possibly crystals at 230°C

If NaF is added to a solution of 0.264 M NaOH in 1.26 M  $\text{UO}_2\text{F}_2$  so that the ratio of NaF to  $\text{UO}_2\text{F}_2$  is 1.0, precipitation occurs. The identity of the precipitate is unknown, but the solubility of either NaOH in  $\text{UO}_2\text{F}_2$  or NaF in  $\text{UO}_2\text{F}_2$  or some complex compound in  $\text{UO}_2\text{F}_2$  is reduced if NaOH and NaF are present in the same solution. At least, this is true for this particular concentration range. As can be seen, only fragments of the over-all phase relation of the  $\text{Na}_2\text{O-UO}_3\text{-HF-H}_2\text{O}$  system are known at present.

*$\text{K}_2\text{O-UO}_3\text{-HF-H}_2\text{O}$  System.* The solubility limits of KOH in  $\text{UO}_2\text{F}_2$  are not known at any temperature. It is known that at room temperature and at a K-to-U ratio of 0.5, KOH is insoluble in 1.26 M  $\text{UO}_2\text{F}_2$ .

The system  $\text{KF-UO}_2\text{F}_2\text{-H}_2\text{O}$  is of interest because of the number of different double salts that can be prepared. However, this very properly makes it appear that the system will be impractical as a possible corrosion inhibitor because of lack of phase stability.

When KF is added to 0.168 M  $\text{UO}_2\text{F}_2$  so that the K-to-U ratio is 1.2, the solution is perfectly clear and has a pH of 4.37. On heating to elevated temperatures, crystals of unknown composition appear at 216°C.

When KF is added to 1.26 M  $\text{UO}_2\text{F}_2$  so that the K-to-U ratio is 0.706, the KF at first dissolves, but on shaking, a large quantity of fine, yellow precipitate forms. This precipitate, after washing with cold water, was dissolved in water to the extent of about 62 g/liter. Analysis of a water solution of this precipitate indicated that it had a formula of  $2\text{KF}\cdot 3\text{UO}_2\text{F}_2\cdot \text{XH}_2\text{O}$ . This double salt is not listed in Gmelin, *Handbuch der anorganische Chemie*. Before it can be definitely stated that this compound was the one formed, more work must be done, particularly since the literature<sup>(11)</sup> indicates that  $3\text{KF}\cdot \text{UO}_2\text{F}_2$  should precipitate on addition of KF to  $\text{UO}_2\text{F}_2$  solutions. This salt is supposed to form  $5\text{KF}\cdot 2\text{UO}_2\text{F}_2$  on recrystallizing from pure water or  $3\text{KF}\cdot 2\text{UO}_2\text{F}_2$  on recrystallizing from uranyl nitrate solutions.

A water solution of the possible  $2\text{KF}\cdot 3\text{UO}_2\text{F}_2$  composition forms a yellow precipitate on being heated to 242°C. This precipitate is unidentified at present.

*$\text{Rb}_2\text{O-UO}_3\text{-HF-H}_2\text{O}$  System.* Rubidium hydroxide is an extremely strong base and this system might well be one of the best. However, since RbOH has not been available for investigation, no work has yet been done on this system.

(11) J. J. Katz and E. Rabinowitch, *The Chemistry of Uranium*, NNES Div. VIII, Vol. 5, p. 573-575, McGraw-Hill, New York, 1951.

*MgO- $UO_3$ -HF- $H_2O$  System.* Upon adding MgO to 1.26 M  $UO_2F_2$  so that the Mg-to-U ratio was 0.237, the oxide dissolved. On continued shaking at room temperature, a bulky, yellow precipitate was formed. This solid has not been identified but is probably a uranate. The pH of the supernatant liquid was 3.6, and this solution apparently formed solid crystals on heating to 100°C.

In the  $MgF_2$  system very little of the  $MgF_2$  dissolved at room temperature.

Since Mg has such a low cross section, further investigation will be carried out, although at present the system does not look promising.

*CaO- $UO_3$ -HF- $H_2O$  System.* Addition of  $Ca(OH)_2$  to 1.26 M  $UO_2F_2$  in the Ca-to-U ratio of 0.5 gave a dense, fine, yellow precipitate. A slurry of the crystals formed more crystals on being heated at 270 to 300°C.  $CaF_2$  has not yet been investigated.

*ZrO<sub>2</sub>- $UO_3$ -HF- $H_2O$  System.* Zirconium hydroxide, in excess, was heated with  $UO_2F_2$  solutions of various concentrations in titanium bombs at 250°C, and the mixture was filtered at 250°C. The solutions were then analyzed for U, F, and Zr. The results so far obtained are not so consistent as they should be, and the results will not be reported at this time.

A preliminary static corrosion test was made by placing a type 347 stainless steel wire in a  $Zr(OH)_4$ - $UO_2F_2$  solution and heating to 250°C. The results did not appear promising. No work has yet been done on the solubility of  $ZrF_4$ .

*Bi<sub>2</sub>O<sub>3</sub>- $UO_3$ -HF- $H_2O$  System.* Very little  $Bi(OH)_3$  dissolves in 1.26 M  $UO_2F_2$  solution at room temperature or on heating to 250°C, and the pH is only slightly increased. No work has been done with  $BiF_3$ .

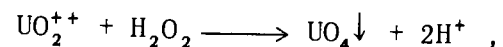
*SnO<sub>2</sub>- $UO_3$ -HF- $H_2O$  and ZnO- $UO_3$ -HF- $H_2O$  Systems.* On adding excess stannic hydroxide to 1.26 M  $UO_2F_2$  solution and excess zinc hydroxide to 1.26 M  $UO_2F_2$  solution, the pH of the solutions

increased, particularly for the  $Zn(OH)_2$  system.

On heating a slurry of the solution and hydroxide to the double-layer temperature, the solid hydroxide dissolved in the heavy uranium layer. This might mean that corrosion of the heavy layer could be reduced by such hydroxide, thereby helping the corrosion situation in a reactor operating in the two-liquid-phase region. No further research has been performed on this possibility, nor has any work been done on the  $SnF_4$  or  $ZnF_2$  systems.

As a general statement, it should be pointed out that should corrosion inhibition prove of practical significance, not only should the complete phase data of the best system be known, but other phase data as well. These data would be the phase behavior of the fission products and plutonium produced in  $UO_2F_2$  solutions containing additives. If  $Cu^{++}$  is used as a homogeneous gas-recombination catalyst, the phase behavior of  $Cu^{++}$  in the  $M_xO$ - $UO_3$ -HF- $H_2O$  system should be investigated to be sure that  $Cu^{++}$  is not precipitated from the solution under operating conditions.

**Kinetic Behavior of  $UO_4$  Formation on Addition of  $H_2O_2$ .** Information concerning the kinetic behavior of  $UO_4$  precipitation from  $UO_2F_2$  solutions containing various additives is only of a qualitative nature. However, it seems worth while to mention it since the behavior is somewhat unusual as compared with  $UO_4$  formation in pure  $UO_2F_2$  solution. When  $H_2O_2$  (3%) is added to solutions of pure  $UO_2F_2$ , varying from 0.168 to 1.26 M, an immediate precipitation of  $UO_4$  occurs. Since the reaction is



a higher pH would tend to aid the formation of  $UO_4$ . However, on adding  $H_2O_2$  to  $UO_2F_2$  solutions containing additives in various concentrations, a considerable period of time elapses before precipitation occurs. This

## HRP QUARTERLY PROGRESS REPORT

induction period varies, but it is usually about 15 seconds. For NaF solutions of high Na-to-U ratio, the induction period is much greater. This behavior could possibly be cited as evidence that the  $\text{UO}_2^{++}$  ion is complexed by the various additives. In the case of the NaF solution, the precipitate may not be  $\text{UO}_4$ , but substances such as  $\text{NaUO}_4\text{F}\cdot 5\text{H}_2\text{O}$ .<sup>(11)</sup>

### NEUTRON CAPTURE CROSS SECTION OF PROTACTINIUM-233

J. Halperin      R. W. Stoughton

Work on the determination of an effective capture cross section of  $\text{Pa}^{233}$  for reactor neutrons has continued.<sup>(12)</sup>

The program of neutron irradiation and processing of thorium slugs for

<sup>(12)</sup>J. Halperin and R. W. Stoughton, *Chem. Quar. Prog. Rep. March 31, 1952*, ORNL-1285, p. 30.

the protactinium cross-section determination is now essentially complete. An evaluation of the data awaits only the mass spectrographic analyses that are being performed by the Y-12 Assay Laboratory. A preliminary value for an effective cross section of  $\text{Pa}^{233}$  for reactor neutrons is  $130 \pm 30$  barns.

A total of 17 thorium slugs (about 1650 g/slug) have been irradiated in both the ORNL LITR and at Hanford. Twelve of the slugs were irradiated in a beryllium element of the lattice of the LITR. This beryllium assembly holds as many as four slugs at one time. The irradiations were carried out over periods of time equivalent to  $ft$  values of  $5 \times 10^{18}$  to  $1.5 \times 10^{20}$   $\text{cm}^{-2}$ . Average cooling periods of four to five months have been utilized to permit the  $\text{Pa}^{233}$  activity to fall to a level that can be handled by Chemical Technology Division Semi-Works equipment.

## METALLURGY

E. C. Miller, Group Leader  
W. J. Leonard, Metallurgy, A. R. Olsen, REED  
W. J. Fretague, Metallurgy, F. J. Lambert, Y-12  
R. G. Berggren, SSD

A substantial part of the effort of the Metallurgy group is of a service nature, involving metallurgical assistance to the Corrosion group, advisory services to the Design and Engineering groups, and nondestructive test work, including radiographic examinations. Such direct service work is not described here, since it appears in other sections of this report where it is pertinent to the work of the groups receiving the services.

Some experimental welding is being carried out in cooperation with the Y-12 shops to establish optimum combinations of design, process

techniques, and electrode compositions for inclusion in procedural specifications directly applicable to HRP requirements and facilities. The results of this work will be reported when the specifications are established.

### TITANIUM PUMP IMPELLER FABRICATION

A. R. Olsen

In continuation of the work reported last quarter, small tensile samples of titanium were welded by the Research Welding group of the Metallurgy Division by using type RC-70 base material and type Ti-75A filler rod. These samples were

## TITANIUM FOR VALVE TRIM

A. R. Olsen

designed to approximate the fastening configuration of proposed joints in a titanium impeller for a Westinghouse model 100A pump. Tests on similar specimens, modified to accommodate rivets, were also made.

Tensile tests on the welded assemblies gave maximum loads ranging from 3500 to 8300 lb, whereas the maximum for any riveted assembly was 2700 pounds. Because of the variations in penetration and consequent loaded area, these figures cannot be converted to a significant load-per-unit-area basis. These results warranted the use of welding as an alternate technique in assembling the titanium impeller; but since the tensile test does not duplicate the service dynamic stressing of the impeller and since the stock from which the impeller was to be machined had a higher carbon content than the test material, dependence was not placed on welding alone, and the fastenings in the actual impeller were made with both welds and rivets.

The information obtained from the earlier welding tests was used by the Y-12 shop in making the welds on the titanium impeller in a dry box. At the same time a test pipe-to-pipe weld and a section containing two pipe-to-pipe welds and two pipe-to-flange welds were made. All welds passed dye-check and x-ray examination. The test section was split into quarters and each piece guide-bent through 150 deg around a 1/2-in. die. These sections were further free-bent to 180 deg, and the two face-bends and one root-bend showed no sign of fracture. The second root-bend fractured during this second stage of testing. Since this section represented the start of the welding and since the current setting was too high, causing severe burn-through, the failure was not unexpected. The titanium impeller has now been operated for a time by the Dynamic Corrosion group; observations on the service behavior of the impeller are reported by that group in another section.

At the request of the Design group, a titanium poppet was hardened in an effort to reduce galling in an experimental plug valve. The entire valve was made at the X-10 Experimental Shop. The titanium disk seat was shrunk into the type 347 stainless steel body, and the titanium poppet was lap-seated to make the valve vacuum tight and then removed for hardening.

Specific information on hardening titanium is limited, but a procedure was developed based on the conclusions in Armour Research Foundation's *Interim Technical Report No. 1, Surface Hardening of Titanium with Metalloid Elements*. Since only a nominal difference in hardness was desired between the poppet and the seat as an antigalling measure, it was decided to follow the Armour recommendations for surface hardening in a nitrogen atmosphere but to limit the time of exposure to reduce the possibility of subsurface embrittlement.

The titanium poppet was placed in the cold end of a tube furnace through which purified nitrogen was passing. The poppet was moved to the hot center of the tube only when the furnace had leveled off at 1800°F. The temperature was maintained for 4 hr and the power turned off to allow for slow cooling of the titanium, which required approximately 2 hr to reach 300°F.

The nitrogen gas that was passing through the tube during the entire cycle was purified through a bed of clean copper turnings at 1200°F and then through Drierite. Hardness measurements before and after this treatment showed a change from Rockwell A 59.5 to 65, or from slightly less than Rockwell C 20 to 30. The surface was a uniform, light-gray color, except for one section where shadowing apparently reduced the free access of gas and interference colors resulted.

## HRP QUARTERLY PROGRESS REPORT

The valve was resealed easily to hold 1000-psi hydraulic pressure and placed in a by-pass line on J loop operating with  $\text{UO}_2\text{SO}_4$  solution containing 40 g of uranium per liter at 250°C. After 110 hr of operation, the valve was removed from the loop and retested at 1500 psi. The leak rate was approximately 6  $\text{cm}^3/\text{hr}$ . On dismantling the valve, the interior was found to be coated with a thin, brown scale typical of that found throughout the entire loop. This scale could be flaked off easily. Rechecking the hardness on the poppet showed no change, and microscopic inspection showed no visible galling or erosion of either the poppet or seat. The valve will be returned to the loop for further testing.

The encouraging results of this test have led to an investigation of the use of titanium valve trim in other types of valves. These tests are reported in detail in another section.

### PROPERTIES OF TITANIUM

W. J. Fretague

**Commercial Titanium Specimen Preparation and Treatment.** Modified Izod impact specimens were prepared from commercial titanium, starting with a 1-in.-dia bar of Ti-75A from heat L782. A 2-ft length of this bar was swaged to 0.238-in. in diameter, sand blasted, pickled in 2% HF-8%  $\text{HNO}_3$ -90%  $\text{H}_2\text{O}$  solution for 15 min, rinsed in water and then in alcohol, and dried in a warm air blast. From the swaged titanium, 36 rods (each approximately 11 in. long) were prepared, vacuum annealed at 500°C for 1 hr, and furnace cooled. Following the annealing treatment, the rods were machined to 0.204-in.-dia by 10 3/4-in.-long, multiple V-notched, impact specimens. After machining and polishing, the individual notches

on each specimen were examined with a binocular microscope for surface finish, and the root diameter of each notch was checked by means of a Shadowgraph. Specimen numbers and the root diameter of each notch were recorded for future reference. Of the 36 specimens machined, 4 were scrapped in machining and the remaining 36 were accepted.

An order for 50 ft of 1/4-in.-dia Ti-75A rod, scheduled for delivery August 1, 1952, was held up because of the steel strike, and it was necessary to swage an additional 6 1/2 ft of 1-in.-dia Ti-75A bar (Item 24, Heat L782) to about 100 ft of 0.249-in.-dia rod. Ten 9 3/4-in.-long pieces (for static corrosion testing in  $\text{UO}_2\text{SO}_4$ ), ten 11 5/16-in.-long pieces (for dynamic corrosion testing) and thirty 10 3/4-in.-long pieces (for miscellaneous treatment) were cut from the swaged rod and treated as above. Approximately one half of the swaged titanium is being held in reserve.

Specimens were subjected to the following treatments subsequent to machining and prior to testing:

1. Four of the eight specimens were exposed in loop A to  $\text{UO}_2\text{SO}_4$  solution containing 250 g of uranium per liter at 250°C in the presence of  $\text{H}_2$  and  $\text{O}_2$ . Detail of the corrosion testing will be reported when results of impact tests are available.

2. Four specimens were loaded in a type 347 stainless steel bomb and exposed to  $\text{UO}_2\text{SO}_4$  solution containing 40 g of uranium per liter with hydrogen and oxygen present in a 2:1 ratio at a pressure of 750 psi at room temperature. The bomb was heated to 250°C for ten days. It was necessary to recharge with hydrogen and oxygen (to maintain pressure) every two days.

3. Four specimens were connected in series and cathodically treated in approximately 1 M  $\text{H}_2\text{SO}_4$  solution at a total current of 0.1 amp for 8 hr at room temperature (70°F).

4. Four specimens were given the same electrolytic treatment as above, but they were exposed for 168 hours.

5. Four specimens were delivered to the Radiation Chemistry group for the same type of static exposure in  $\text{UO}_2\text{SO}_4$  as the specimens in the second group above, but for a longer period. These specimens may be subjected to radiation while in the  $\text{UO}_2\text{SO}_4$  solution.

6. Eight specimens received no treatment (other than 1 hr vacuum annealing at  $500^\circ\text{C}$  prior to machining) before they were impact tested.

7. Ten specimens prepared from the second lot of swaged titanium will be reserved for static corrosion tests by the Radiation Chemistry group.

8. Ten specimens prepared from the second lot of titanium that was swaged were delivered to the Dynamic Corrosion group for testing.

9. Thirty specimens were retained for miscellaneous metallurgical treatments prior to impact testing.

*Impact Testing.* Impact tests to determine the transition temperature of the available Ti-75A material have been performed on eight specimens that were vacuum annealed prior to machining. These represent a total of 80 individual impact tests in the temperature range from  $-170$  to  $200^\circ\text{C}$ . The data obtained are plotted in Fig. 54.

Impact tests were performed on four Ti-75A specimens cathodically treated in  $1\ M\ \text{H}_2\text{SO}_4$  for 8 hr and on four Ti-75A specimens exposed in  $\text{UO}_2\text{SO}_4$  solution at  $250^\circ\text{C}$  for ten days. The data from the cathodically treated specimens represent 40 individual impact tests in the temperature range from  $-120$  to  $200^\circ\text{C}$  and the data from the  $\text{UO}_2\text{SO}_4$  treated specimens represent 36 individual impact tests in the temperature range from  $20$  to  $190^\circ\text{C}$ .

All data collected to date (except for some fragmentary data collected on cathodically treated specimens exposed for 168 hr) appear in Fig. 54.

**Iodide Titanium Specimen Preparation and Treatment.** Eight melts of iodide titanium have been prepared by inert atmosphere (argon), d-c arc melting. Individual melts were swaged to approximately 0.210-in.-dia rods (two melts were swaged to 0.243 in. in diameter), vacuum annealed to  $500^\circ\text{C}$  for 1 hr, and machined to 0.204-in.-dia by 10  $\frac{3}{4}$ -in.-long (actually the lengths of individual specimens vary from 5  $\frac{3}{4}$  to 10  $\frac{3}{4}$  in.) impact specimens.

*Impact Testing.* After machining, two specimens, I-8-1 and I-7-1 (prepared from iodide Ti melts 8 and 7, respectively), were tested in the temperature range from  $-195.8$  to  $-200^\circ\text{C}$ . Seventeen individual impact tests were performed. The data obtained appear in Fig. 54.

**Discussion of Results.** In considering the results obtained from commercial titanium, it appears that the various treatments to which the specimens were subjected in an attempt to load them with hydrogen in aqueous media at temperatures up to  $250^\circ\text{C}$  had little or no effect on the transition temperature, as compared with untreated titanium tested at the same temperatures. This observation is based on limited data and should be considered as tentative until results are available from specimens exposed for much longer periods.

Iodide titanium behaved in a very ductile manner, even at temperatures slightly above the temperature of liquid nitrogen. No transition temperature was found for iodide titanium vacuum annealed at  $500^\circ\text{C}$ . In fact, the impact energies recorded for specimens from two separate melts of iodide titanium, when tested at  $-195.8^\circ\text{C}$  (liquid nitrogen boiling point), were of the same order as those obtained above the transition temperature on commercial titanium Ti-75A. Concerning the shape of the impact curves for iodide titanium, quite a bit of the impact energy

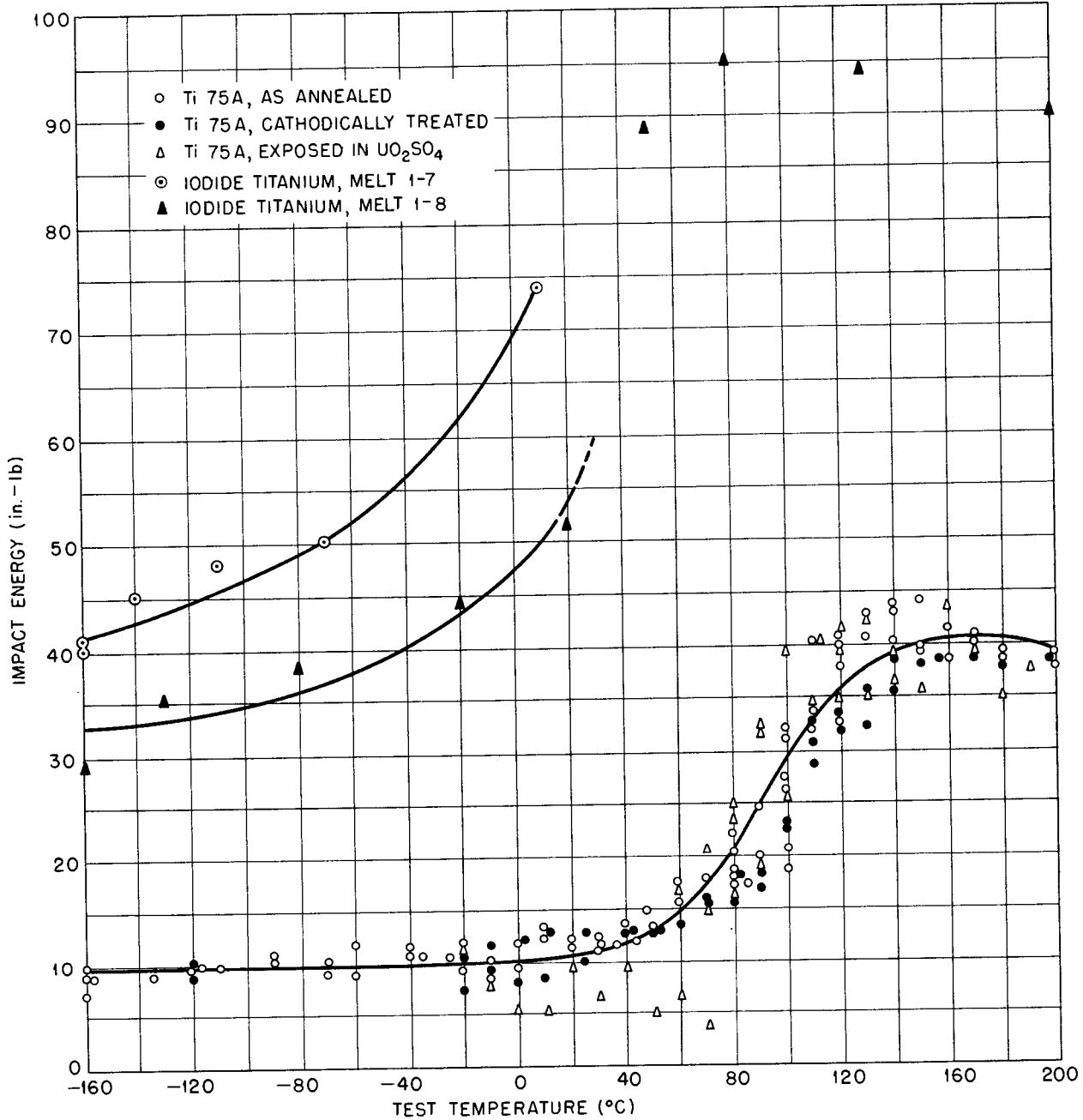


Fig. 54. Impact Resistance of Titanium as a Function of Testing Temperature and Treatment.

recorded by the testing machine was absorbed in bending the specimen. As the testing temperature was raised slightly above room temperature (50°C), the iodide titanium specimens

were so ductile that they bent down (without breaking completely) far enough to permit the striking hammer of the impact pendulum to slide over the specimen. For this reason, all

points above 20°C on the curve for iodide titanium should be disregarded as quantitative values.

A 3-ft length of 1-in.-dia, Ti-75A (Item 24, Heat L782) bar was swaged to 0.507-in.-dia rod for pump impeller rivets. The swaged rod was cut to 12-in. lengths, sand blasted, pickled in 2% HF-8% HNO<sub>3</sub>-90% H<sub>2</sub>O solution for 15 min, vacuum annealed at 500°C for 1 hr, and furnace cooled.

**Future Work.** Impact tests will be performed on four 10 3/4-in.-long Ti-75A impact specimens, cathodically treated in 1 M H<sub>2</sub>SO<sub>4</sub> for 168 hr at 80°F, and on four similar specimens exposed in loop A with varying concentrations of UO<sub>2</sub>SO<sub>4</sub> and varying gases and pressures in the loop.

An attempt will be made to determine, by slow-bend testing, the energy absorbed in bending the iodide titanium impact specimens prior to fracture. This will permit determination of the energy needed to break the specimens and thus give a more realistic idea of the form of the impact curve for iodide titanium.

If this line of approach is successful, the impact curves for all melts of iodide titanium will be determined, and any remaining specimens of iodide titanium will be exposed to H<sub>2</sub>SO<sub>4</sub> by cathodic treatment and to UO<sub>2</sub>SO<sub>4</sub> solutions in static and dynamic systems. In addition, work is progressing on a modified Sieverts apparatus to prepare titanium-hydrogen alloy specimens by heating the specimens in a purified hydrogen atmosphere. This equipment will be employed to prepare alloys of both commercial and iodide titanium with hydrogen.

Experience gained during the course of the impact testing completed to date shows the necessity for minor revisions of some of the auxiliary equipment on the remotely controlled impact tester. These modifications are being made before the equipment is permanently installed in a hot cell. These changes have delayed the testing of some samples that are treated and ready to test, but the proposed changes are necessary to facilitate the testing of irradiated samples.

## CHEMICAL PROCESSING

F. R. Bruce,	Section Chief
D. E. Ferguson	R. G. Mansfield
G. I. Cathers	W. E. Tomlin

### COMPARISON OF CHEMICAL PROCESSING METHODS

An economic comparison of three proposed methods of chemical processing for a 2000-megawatt plutonium-producing reactor using a uranyl sulfate solution fuel is presented in Table 50. The methods considered were (1) batch operation of the reactor and processing of the entire charge by Purex, (2) continuous removal of plutonium from the reactor, together with the optimum amount of uranium (500 kg/day) for

decontamination and re-enrichment, and (3) continuous plutonium and fission-product removal with no uranium recycled to the enrichment plant. The batch method of reactor operation results in processing 1600 kg of uranium per day and requires a fuel enrichment of 1.06%. The continuous plutonium removal, along with 500 kg of uranium, requires an enrichment of 1.40%. If no uranium is removed, an enrichment of 54.5% is required and provisions must be made for removing fission-product poisons.

# HRP QUARTERLY PROGRESS REPORT

**TABLE 50. ECONOMIC COMPARISON OF THREE METHODS OF CHEMICAL PROCESSING**

Basis: 15-ft-dia spherical reactor using uranyl sulfate solution as fuel and operating at 2000 megawatts

	METHOD I BATCH PUREX	METHOD II CONTINUOUS Pu REMOVAL AND PROCESSING OF 500 kg of U PER DAY	METHOD III CONTINUOUS Pu REMOVAL AND NO U PROCESSING
Chemical Processing Cost (dollars per gram of Pu)			
Amount of U processed (kg/day)	1600	500	0
U decontamination and chemical conversions at \$10/kg	\$ 8.00	\$ 2.50	\$ 0.00
Pu removal at \$2.00/g	0.00	2.00	2.00
Pu decontamination	5.00	5.00	5.00
Fission product removal	0.00	0.00	1.00
<b>Total</b>	<b>\$13.00</b>	<b>\$ 9.50</b>	<b>\$ 8.00</b>
Inventory Charges (at 16% per year)			
Pu at \$300/g	\$ 8.50	\$ 7.00	\$ 7.00
D <sub>2</sub> O at \$80/kg	13.20	9.50	8.10
U in reactor at \$94.60/kg	0.82	0.82	0.82
U in process at \$94.60/kg (100 days holdup)	4.05	1.25	0.00
Fuel (60 days holdup)	3.40	1.75	1.35
<b>Total</b>	<b>\$30.00</b>	<b>\$20.30</b>	<b>\$17.30</b>
Fuel Cost*			
Feed to enrichment plant and enrichment cost based on U at \$52/kg	\$26.00	\$29.00	\$42.00
Reactor Cost**			
Plant costs	\$24.00	\$24.00	\$24.00
Operational costs	4.40	4.40	4.40
<b>Total</b>	<b>\$28.40</b>	<b>\$28.40</b>	<b>\$28.40</b>
<b>Total cost (dollars per gram of Pu) no power credit taken</b>	<b>\$97.40</b>	<b>\$87.20</b>	<b>\$95.70</b>

\*Fuel costs were based on a cost of \$52 per kilogram of natural uranium and \$110 per kilogram ideal separative work expended during enrichment.

\*\*Reactor plant costs were obtained by extrapolation of cost data given in ORNL CF-52-8-7. Operational costs were taken from ORNL CF-52-7-59.

The results of the comparison indicate that the method of operation involving both continuous plutonium removal and recycling 500 kg of uranium back to the diffusion plant has a decided economic advantage.

Another advantage to the continuous removal of plutonium is that if no oxygen pressure is added to the reactor other than the stoichiometric amount from  $D_2O$  decomposition, the solubility of plutonium will be about 0.010 mg/ml. This would result in a  $Pu^{240}$  concentration of only 0.2% in the product, if the insoluble plutonium is removed as it is formed. Therefore continuous removal of plutonium is not only more economical but also produces a more desirable product.

A schematic flowsheet for a reactor system based on continuous plutonium removal is given in Fig. 55.

#### PLUTONIUM CHEMISTRY

In order to establish the optimum method of continuously removing plu-

tonium from an aqueous solution homogeneous reactor, it is necessary to understand the chemical behavior of plutonium in the reactor fuel solution. Present data indicate that plutonium will precipitate as  $PuO_2$  from a uranyl sulfate solution reactor at either 250 or 100°C. The equilibrium solubility of plutonium will depend on the temperature and oxygen pressure of such a reactor. If the reactor operates at 250°C with no added oxygen, present data indicate an equilibrium solubility of 0.010 mg/ml. If the insoluble plutonium is removed as it precipitates, such a system will produce plutonium containing only 0.2%  $Pu^{240}$ .

**Effect of Plutonium Concentration on the Behavior of Plutonium in 1 M  $UO_2SO_4$  Solution.** The results of experiments conducted at various plutonium concentrations indicate that an equilibrium exists between hexavalent plutonium and tetravalent plutonium in solution. When a 1 M  $UO_2SO_4$  solution containing more than

DWG. 16450A

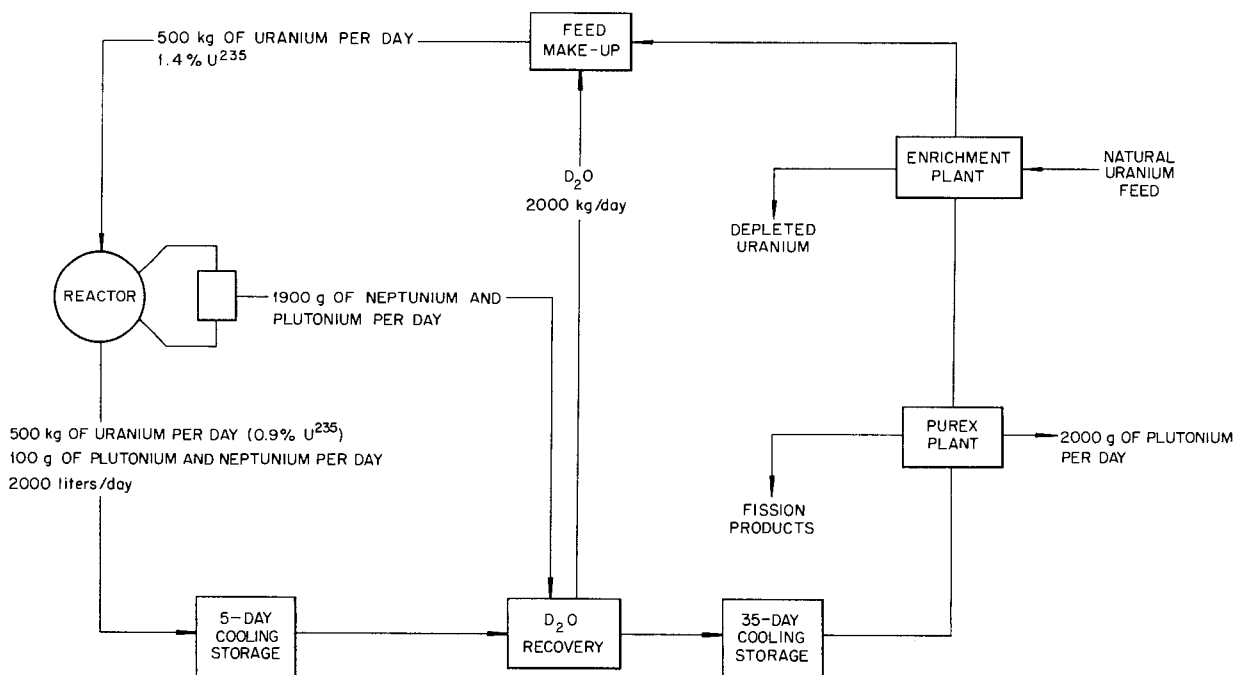


Fig. 55. Schematic, Continuous Plutonium Removal Flowsheet for 15-ft-dia, Homogeneous, Plutonium-Producing Reactor Operating at 2000 Megawatts.

## HRP QUARTERLY PROGRESS REPORT

0.1 mg of Pu(VI) per milliliter was heated to 250°C for 150 hr under 200 psi of oxygen, the hexavalent plutonium was observed to be partly reduced. Under the same conditions, but with an initial Pu(VI) concentration of 0.05 mg/ml, significant oxidation of Pu(IV) to Pu(VI) was observed. In all cases, the final ratio of hexavalent to tetravalent plutonium (see Table 51) was about 42:1.

**TABLE 51. EFFECT OF PLUTONIUM CONCENTRATION ON PLUTONIUM BEHAVIOR IN 1 M UO<sub>2</sub>SO<sub>4</sub> SOLUTION**

Temperature: 250°C  
 Heating time: 150 hr  
 Oxygen pressure: 200 psi  
 Initial ratio of Pu(VI) to Pu(IV): 1:1

INITIAL Pu(VI) CONCENTRATION (mg/ml)	FINAL Pu(VI) CONCENTRATION (mg/ml)	FINAL RATIO OF Pu(VI) TO Pu(IV)
0.445	0.436	44:1
0.274	0.228	41:1
0.213	0.088	15:1
0.097	0.091	41:1
0.056	0.084	42:1

**Solubility of Tetravalent Plutonium at 100°C.** The solubility of tetravalent plutonium in 1 M UO<sub>2</sub>SO<sub>4</sub> at 100°C was found to be 0.010 mg/ml compared with 0.003 mg/ml at 250°C. The rate of hydrolysis and precipitation is much slower at 100°C than at 250°C. The reaction is only about 90% complete in 48 hr at 100°C, whereas the precipitation is essentially complete in 12 hr at 250°C. The hydrolysis rate of tetravalent plutonium (see Table 52) at 100°C in 1 M UO<sub>2</sub>SO<sub>4</sub> solution is extremely sensitive to free acid concentration. The addition of 0.07 N H<sub>2</sub>SO<sub>4</sub>, which lowers the pH of a neutral solution from 1.63 to 1.16, lowered the rate constant of the reaction from 1.5 days<sup>-1</sup> to 0.17

days<sup>-1</sup>, and at an acid concentration of 0.13 N no precipitation of plutonium was observed in five days at 100°C from a solution containing 0.25 mg/ml of plutonium.

**TABLE 52. EFFECT OF ACID CONCENTRATION ON THE SOLUBILITY OF TETRAVALENT PLUTONIUM AT 100°C**

Solution concentration: 1 M UO<sub>2</sub>SO<sub>4</sub>  
 Initial Pu concentration: 0.25 mg/ml as Pu(IV)  
 Temperature: 100°C

ACID (N)	HEATING TIME (hr)	Pu(IV) IN SOLUTION (mg/ml)
Neutral	48	0.023
	150	0.010
0.03	48	0.03
	150	0.01
0.07	48	0.18
	150	0.10
0.13	48	0.200*
	150	0.238*

\* No precipitation occurred.

**Effect of Oxygen Pressure on the Rate of Oxidation of Pu(IV) at 100°C.** The results of a series of experiments, given in Table 53, show that the rate of oxidation of tetravalent plutonium in 1 M UO<sub>2</sub>SO<sub>4</sub> at 100°C is slow compared with the hydrolysis and precipitation rate. Of the 0.25 mg/ml of tetravalent plutonium in the original solution, about 90% precipitated, on the average; and of the 10% remaining in solution, only about one-half was oxidized to Pu(VI) in 48 hours. Furthermore, increasing the oxygen pressure from 20 to 200 psi only doubled the amount of plutonium oxidized in 48 hours. These results are essentially the same as those obtained at 250°C.

**Effect of Oxygen Pressure on the Reduction of Pu(VI) at 100°C.** As stated before, hexavalent plutonium is

not completely stable at concentrations exceeding 0.1 mg/ml, even under an oxygen pressure of 200 psi. A series of experiments was run to test the effect of oxygen pressure on the reduction of Pu(VI) at 100°C in 1 M UO<sub>2</sub>SO<sub>4</sub> solution. The results, given in Table 54, indicate that about 5% of the hexavalent plutonium in the original solution was reduced in 48 hr at 200 psi, whereas at 20 and 40 psi 13 to 16% of the Pu(VI) was reduced in 48 hours.

**Effect of a Stoichiometric Hydrogen-Oxygen Mixture on the Behavior of Plutonium in 1 M UO<sub>2</sub>SO<sub>4</sub> Solution.** When a 1 M UO<sub>2</sub>SO<sub>4</sub> solution containing

a mixture of Pu(IV) and Pu(VI) was heated for 24 hr at 100°C under partial pressures of 38 psi of oxygen and 76 psi of hydrogen, there was partial reduction of hexavalent plutonium but no precipitation occurred (see Table 55). When another portion of the same solution was heated at 250°C for 24 hr under partial pressures of 53 psi of oxygen and 106 psi of hydrogen, 95% of the plutonium precipitated, and of the plutonium remaining in solution 97% was Pu(IV). This amounts to essentially complete reduction of hexavalent plutonium in 24 hr at 250°C in the presence of the stoichiometric mixture of hydrogen and oxygen.

**TABLE 53. EFFECT OF VARIOUS OXYGEN PRESSURES ON THE OXIDATION OF Pu(IV) IN 1 M UO<sub>2</sub>SO<sub>4</sub> SOLUTION**

Temperature: 100°C

Heating time: 48 hr

Initial solution: 1 M UO<sub>2</sub>SO<sub>4</sub> solution containing 0.002 mg of Pu(VI) per milliliter and 0.24 mg of Pu(IV) per milliliter

OXYGEN PRESSURE (psi)	FINAL CONCENTRATION Pu(VI) (mg/ml)	FINAL CONCENTRATION Pu(IV) (mg/ml)	Pu(VI) (%)	Pu(IV) (%)
200	0.016	0.013	55	45
100	0.009	0.013	40	60
40	0.007	0.011	39	61
20	0.007	0.010	41	59

**TABLE 54. EFFECT OF VARIOUS OXYGEN PRESSURES ON THE BEHAVIOR OF PLUTONIUM IN 1 M UO<sub>2</sub>SO<sub>4</sub> SOLUTION AT 100°C**

Heating time: 48 hr

OXYGEN PRESSURE (psi)	INITIAL Pu(VI) CONCENTRATION (mg/ml)	FINAL Pu(VI) CONCENTRATION (mg/ml)	REDUCTION (%)
200	0.199	0.188	5.5
100	0.195	0.178	8.7
40	0.184	0.154	16.3
20	0.168	0.147	12.5

## HRP QUARTERLY PROGRESS REPORT

**TABLE 55. EFFECT OF A STOICHIOMETRIC HYDROGEN-OXYGEN MIXTURE ON THE BEHAVIOR OF PLUTONIUM IN 1 M UO<sub>2</sub>SO<sub>4</sub> SOLUTION**

Heating time: 24 hr

CONDITIONS	CONCENTRATION OF Pu(VI) (mg/ml)	CONCENTRATION OF Pu(IV) (mg/ml)	TOTAL Pu IN SOLUTION (mg/ml)
Initial solution	0.180	0.059	0.239
Initial solution with 38 psi of oxygen and 76 psi of hydrogen at 100°C	0.162	0.078	0.240
Initial solution with 53 psi of oxygen and 106 psi of hydrogen at 250°C	0.0004	0.0124	0.0128

### DECONTAMINATION OF PLUTONIUM BY TTA EXTRACTION

An investigation of TTA chelation as a method of decontaminating plutonium from a homogeneous, plutonium-producing reactor is being conducted. This method will later be evaluated by comparison with the tributyl phosphate extraction process on the basis of economy.

A homogeneous plutonium-TTA chelation process has been devised and appears to offer promise of economy of contact time in processing. Satisfactory recoveries of plutonium have been obtained by forming the plutonium-TTA chelate in the aqueous feed solution and extracting the chelate with a solvent. In this process, optimum recovery of plutonium is obtained from 0.05 N acid solutions. Large amounts of iron do not interfere with the plutonium extraction; however, the presence of appreciable concentrations of sulfate ion prevents adequate plutonium recovery. The experimental work to date has largely been exploratory in nature, and the following results are qualitative in nature.

**Homogeneous TTA Chelation.** An objection to the use of TTA is the long equilibration time needed to get efficient transfer of plutonium from an aqueous to an immiscible organic

medium. If the plutonium-TTA chelate could be formed in the aqueous phase and then extracted into an organic solvent, a contact time attainable in conventional contactors could be achieved. To that end, work has been carried out, at tracer levels, to determine the efficiency of plutonium recovery in such a process.

It was found that one volume of 0.22 M TTA in either acetone or ethyl alcohol could be added, with agitation, to five volumes of aqueous solution without precipitation of TTA. Such proportions were used throughout these experiments. The concentration of plutonium was set at  $8.8 \times 10^{-3}$  mg/ml.

After addition of TTA to the plutonium-bearing solution, stirring was continued for about 10 minutes. At the end of that time, a one-half volume portion of benzene was contacted with the aqueous solution. A single extraction was sufficient to remove essentially all the extractable plutonium from the aqueous phase. For example, in one run the first benzene extract showed a counting rate of  $3.8 \times 10^5$  c/m/ml, whereas a second benzene extract gave only 35 c/m/ml. Stirring time after addition of TTA and before addition of benzene was limited to 10 min, since a series of runs showed decreased extraction with longer stirring. For example, after

a 10-min contact, a distribution coefficient of 5.4 was obtained. This dropped to 3.1 after 30 min of stirring and to 2.7 after 1 hour.

The effect of the acidity of the aqueous phase on plutonium extraction is shown in Table 56. From these data an acid concentration of 0.05 appears to be the optimum for plutonium recovery.

**TABLE 56. EFFECT OF ACIDITY ON RECOVERY OF PLUTONIUM**

Conditions: One volume of aqueous plutonium solution reacted with 1/5 volume of 0.22 M TTA-acetone solution for 10 min, followed by extraction with one 1/2 volume of benzene.

ACIDITY ([H <sup>+</sup> ] per liter)	PLUTONIUM RECOVERED (%)
4.90	0.1
2.05	2.3
1.02	76.4
0.52	96.7
0.13	81.6
0.09	87.2
0.08	91.0
0.045	96.2
0.006	47.5

**Effect of Iron and Sulfate on Plutonium Extraction.** The effects of iron and sulfate on plutonium extraction have been examined. It was found that iron present to the extent of 1000 times the concentration of plutonium did not adversely affect plutonium recovery. At higher concentrations of both plutonium and iron, the only adverse effect anticipated will be increased consumption of reagent.

The effect of sulfate on extraction of plutonium by TTA chelation was found to be pronounced. From a 0.2 M sulfate solution, the distribution coefficient of plutonium between the organic and aqueous phase was found to be 0.05, whereas for a nonsulfate sample treated in the same way, a distribution coefficient of 3.8 was

obtained. On the average, the effect of sulfate was to decrease the distribution coefficient by about a factor of 100. This effect may be magnified because of the high level of sulfate as compared with plutonium, but the results indicate that sulfate should be avoided, if possible, in any processing scheme using TTA.

**Dissolution of PuO<sub>2</sub> by TTA Chelation.** When the hydrogen-ion concentration of a plutonium solution was reduced to less than about 0.01 mole per liter, the iron present in solution precipitated as hydrous oxide, carrying with it the plutonium as a hydrous oxide. Presumably this precipitate is the same as that expected from precipitation of plutonium and iron in the reactor fuel solution. Addition of TTA-acetone, in the proportions previously mentioned, to a suspension of this precipitate in water gave a deep-red precipitate. After centrifugation, treatment of the precipitate with acetone resulted in dissolution of the plutonium in the organic phase. Although varying amounts of the plutonium initially present were recovered, the general results were encouraging. Some variations in technique have given as high as 95% recovery of plutonium in a single treatment. This general method may provide a desirable means of getting the precipitated plutonium from the reactor back into solution and at the same time give some degree of decontamination. The possible decontamination value of such a treatment will be investigated.

#### SOLVENT EXTRACTION

A tributyl phosphate extraction process for the isolation and decontamination of plutonium and uranium from spent uranyl sulfate solution fuel has been worked out and reported.<sup>(1)</sup> The developmental work on the solvent

<sup>(1)</sup> HRP Quar. Prog. Rep. March 15, 1952, ORNL-1280.

## HRP QUARTERLY PROGRESS REPORT

extraction process has since been limited to studying neptunium behavior and determining the susceptibility of the solvent to radiation damage. The study of neptunium behavior is now complete and has been discontinued.

**Neptunium Behavior in Tributyl Phosphate Extraction Process.** For chemical processing of a 2000-megawatt, homogeneous, plutonium-producing reactor after 45 days of cooling, a neptunium decontamination factor of  $10^4$  for adequate decontamination of plutonium and a decontamination factor of 100 for uranium are required. It was found that these required neptunium decontamination factors could be obtained in one cycle of the standard Purex process by adjusting the valence of neptunium to the inextractable Np(V). This is not the case, however, for processing uranyl sulfate fuel. Apparently the presence of  $1.2 M UO_2SO_4$  in the Purex feed promotes the reduction of Np(V) to Np(IV) under process conditions and results in a large fraction of the neptunium being extracted by tributyl phosphate. Fortunately, the neptunium that is extracted follows the uranium through the plutonium strip column and a neptunium decontamination factor of greater than  $10^4$  is obtained for plutonium in the first cycle. An additional factor of 10 is gained in the second plutonium cycle, yielding an over-all separation of plutonium from neptunium by a factor of  $10^5$ . It was further shown that the second uranium cycle gave the required separation of uranium from neptunium; however, the carry-over of neptunium from the first cycle will increase the level of radiation encountered in the second uranium cycle.

From a two-cycle, countercurrent, batch test of neptunium behavior in the processing of uranyl sulfate solution, the following results were obtained: neptunium decontamination factor for the first cycle extraction column, 1.1; decontamination factor

for plutonium in strip (IB) column, greater than  $10^4$ ; decontamination factor for second uranium cycle,  $1.7 \times 10^3$ .

**Radiation Damage.** Chemical processing of short-cooled homogeneous reactor solutions or slurries by solvent extraction may be affected by the radiation the solvent receives in the operation. Work has been done in examination of this problem as it applies to processes employing tributyl phosphate as the solvent.

The radiation effect present in the Purex extraction column using short-cooled homogeneous solution feed may be duplicated by exposing 30% tributyl phosphate solvent to gamma emission from a  $Co^{60}$  source. The results of such experiments indicate that significant effects on process performance are realized only for radiation dosages of at least 10- to 100-fold greater than that expected for the 15-day cooled material. The products of radiation damage appear to be due mostly to hydrolysis of tributyl phosphate to mono- and dibutyl phosphate.

*Effect of Radiation Obtained by Chemical Extraction Test.* A simulated Purex 1A column feed was made up by spiking a  $1.2 M UNH-2 M HNO_3$  solution with plutonium to an activity of  $1.1 \times 10^7$  c/m/ml and with 120-day cooled dissolver solution to a gross beta count of  $8.4 \times 10^7$ . In preliminary work, 4 ml of this solution was equilibrated with 10 ml of 30% TBP in Amsco solvent, followed by two 3-ml  $2 M$  nitric acid scrubs, and three equal-volume water strips. The initial test portion of Table 57 shows the results for nonirradiated solvent, together with those for solvent irradiated in a  $Co^{60}$  source. Irradiation markedly increased the beta retention in the scrubbed organic, but did not have much effect on the plutonium concentration. However, after stripping, the irradiated solvent

TABLE 57. EFFECT OF GAMMA RADIATION ON PLUTONIUM AND GROSS BETA RETENTION TEST

DESCRIPTION OF SOLVENT	ENERGY DOSAGE (watt-hr/liter)	PLUTONIUM (c/m/ml)			GROSS BETA (c/m/ml)		
		Scrubbed Organic	First Aqueous Strip	Stripped Organic	Scrubbed Organic	First Aqueous Strip	Stripped Organic
Initial Test							
Nonirradiated control	0	$2.0 \times 10^6$	$1.5 \times 10^6$	$1.5 \times 10^3$	$4.3 \times 10^3$		$1.6 \times 10^3$
Co <sup>60</sup> irradiation	130	$1.8 \times 10^6$	$1.3 \times 10^6$	$1.2 \times 10^5$	$1.4 \times 10^5$	$4.9 \times 10^4$	$3.1 \times 10^5$
X-ray irradiation, 100% TBP		$1.0 \times 10^6$	$5.4 \times 10^5$	$8.6 \times 10^5$	$3.5 \times 10^5$	$9.1 \times 10^3$	$5.6 \times 10^5$
X-ray irradiation, 100% Amsco		$1.4 \times 10^6$	$9.2 \times 10^5$	$1.3 \times 10^3$	$1.7 \times 10^3$	700	800
Revised Test							
Nonirradiated control	0	$8.4 \times 10^5$	$1.4 \times 10^5$	520	870	74	72
Co <sup>60</sup> irradiation	48	$8.0 \times 10^5$	$1.3 \times 10^5$	$2.4 \times 10^4$	$2.0 \times 10^5$	$8.3 \times 10^3$	$5.6 \times 10^4$
	242	$8.1 \times 10^5$	$7.8 \times 10^4$	$3.3 \times 10^5$	$7.7 \times 10^5$	$1.1 \times 10^3$	$6.4 \times 10^5$
	333	$9.7 \times 10^5$	$7.2 \times 10^4$	$5.2 \times 10^5$	$1.0 \times 10^6$	$2.4 \times 10^3$	$7.5 \times 10^5$

showed much higher retention of both plutonium and gross beta material than the unirradiated control.

An experiment which indicated that the higher retentions were due to the effect of radiation on TBP rather than Amsco was carried out by exposing pure samples of each to the radiation from a 50-kv, high-intensity, x-ray machine at Vanderbilt University. After exposure, the samples were made up into a standard 30% solution and given the extraction test. The results in Table 57 show that the retentions in the case of the TBP were very high, whereas those of the Amsco are comparable to the data for unirradiated 30% TBP mixture.

The chemical extraction test was revised in later work to improve material balances and data consistency. The scrub was changed to two equal volume equilibrations with 3 N nitric acid, and two fivefold volumes of water were used for stripping. Centrifugation was employed to improve phase separation. The data in the revised test portion of Table 57 for irradiations with different Co<sup>60</sup> sources confirmed the results of the previous work.

The two Co<sup>60</sup> sources used in this work were calibrated by the ceric sulfate-spectrophotometer method as being 6,330 and 32,100 r/min, respectively. The energy dose received in any experiment was calculated on the basis that a roentgen is equivalent to 93 ergs per milliliter of energy dissipation in the solvent.

*Behavior Shown by Extraction Test on Dilution of Irradiated Solvent.* A sample irradiated in a Co<sup>60</sup> source for 14 days (333 watt-hr/liter dosage) was used to make up a series of dilutions with unirradiated solvent. The plutonium and gross beta retentions obtained on these samples by the chemical extraction test are plotted in Figs. 56 and 57 as logarithm of retention (c/m/ml) vs. logarithm of concentration. The retentions were corrected for the retention observed for unirradiated solvent. The plutonium plot in Fig. 56 is nearly linear, indicating that an equation of the form  $C_{Pu} = AC_R^{1.8}$  would be a close approximation where  $C_{Pu}$  is the retention of plutonium in counts per minute per milliliter,  $C_R$  is the concentration of the irradiated material, and  $A$  is a constant. The plutonium

# HRP QUARTERLY PROGRESS REPORT

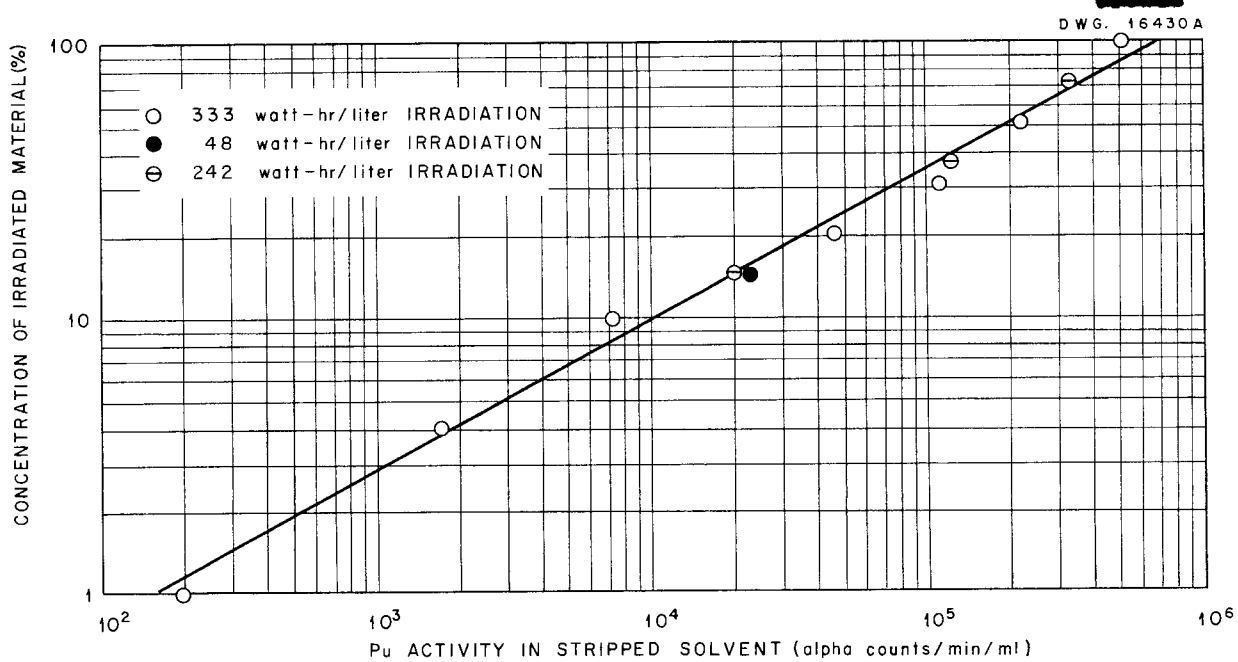


Fig. 56. Effect of Dilution on Plutonium Retention in 30% TBP-Amsco After Irradiation.

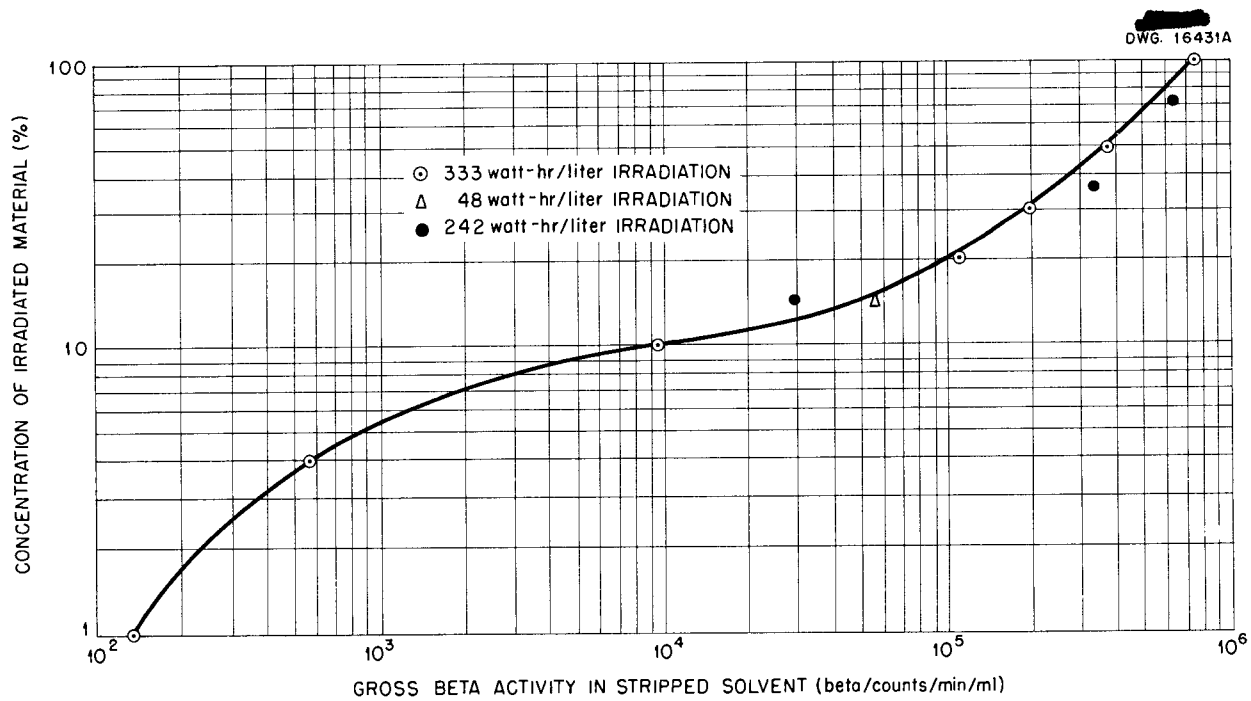


Fig. 57. Effect of Dilution on Gross Beta Retention in 30% TBP-Amsco After Irradiation.

retention was therefore very nearly second-order with respect to the impurities formed by radiation in the solvent.

The corresponding plot of the gross beta retentions in Fig. 57 is not linear, showing additional complexity owing either to more than one impurity or to more than one fission product being extracted.

*Equivalence Between Dilution and Irradiation.* The data in Table 57 for material with 48 and 242 watt-hr/liter irradiations were also plotted in Figs. 56 and 57 after correction for background. It was assumed that 100% on the abscissa was equivalent to a dosage of 333 watt-hr/liter with the 48 and 242 watt-hr data plotted proportionately. The dose agreement with the 333 watt-hr/liter data indicates that the radiation effect is linear with respect to time, and decreasing the amount of irradiation is closely equivalent to dilution of the impurities formed by radiation.

*Uranium Retention in Irradiated Solvent.* Some data were collected on the retention of uranium after stripping with two fivefold volumes of water in the revised extraction test. In non-irradiated solvent, the retention is of the order of  $10^{-3}$  mg/ml. The 242 watt-hr/liter irradiated sample gave a retention of 2.9 mg/ml. Dilutions to 50 and 20% showed retentions of 2.1 and 0.45 mg/ml, respectively.

*Products Possibly Formed by Irradiation.* Since it was known that mono- and dibutyl phosphate affect TBP solvent extraction and since they were likely products of radiation-induced hydrolysis, an effort was made to prepare pure samples of each for runs with the extraction test.

Crude butyl phosphoric acid was refluxed with 3 N  $\text{HNO}_3$  for 2.5 hr to break down pyrophosphates, then mono- and dibutyl phosphate were separated by countercurrent extraction with 20% carbon tetrachloride. This yielded

97.8% monobutyl phosphate and 95.5% dibutyl phosphate.

These MBP and DBP samples were used to contaminate a pure 30% TBP-Amsco mixture to simulate the effects of radiation. The results are shown in Fig. 58 in terms of plutonium, gross beta, and uranium retention from the standard chemical extraction test. It is shown that MBP has a very large effect on both plutonium and gross beta retention in comparison with DBP. Part of the retentions shown by DBP may well be due to the MBP impurity present. In the case of uranium, however, the DBP gave larger retentions than MBP.

*Comparison of Radiation Effect with MBP-DBP Results.* The plutonium, gross beta, and uranium retentions in irradiated 30% TBP-Amsco mixture can be attributed, at least in part, to formation of MBP and DBP. The uranium retention for the 20% dilution of the 242 watt-hr/liter sample was 0.45 mg/ml, corresponding to 0.1% DBP, from Fig. 58. The plutonium retention for this sample of  $2.1 \times 10^4$  c/m/ml corresponds to about 0.02% MBP. This is a DBP/MBP ratio of 5:1. Although the value is not critical, the ratio 5:1 can be used to predict the results shown in Figs. 56 and 57 from Fig. 58 by assuming that 0.02% MBP is equivalent to about 48 watt-hr/liter irradiation or 14.5% on the scale of Figs. 56 and 57. Calculation of the energy efficiency from the above figures indicates that the G value is extremely low, about 0.03 (molecules affected per 100 ev).

*Estimation of Probable Radiation Exposure in Chemical Processing.* The activity of spent homogeneous reactor fuel from a 2000-megawatt reactor will be about 5 watts/liter after 30 days of irradiation and 15 days of cooling. Gamma absorption by the solvent during processing is negligible in comparison with the beta adsorption. Assuming a column feed-to-scrub ratio of 1.5:1,

# HRP QUARTERLY PROGRESS REPORT

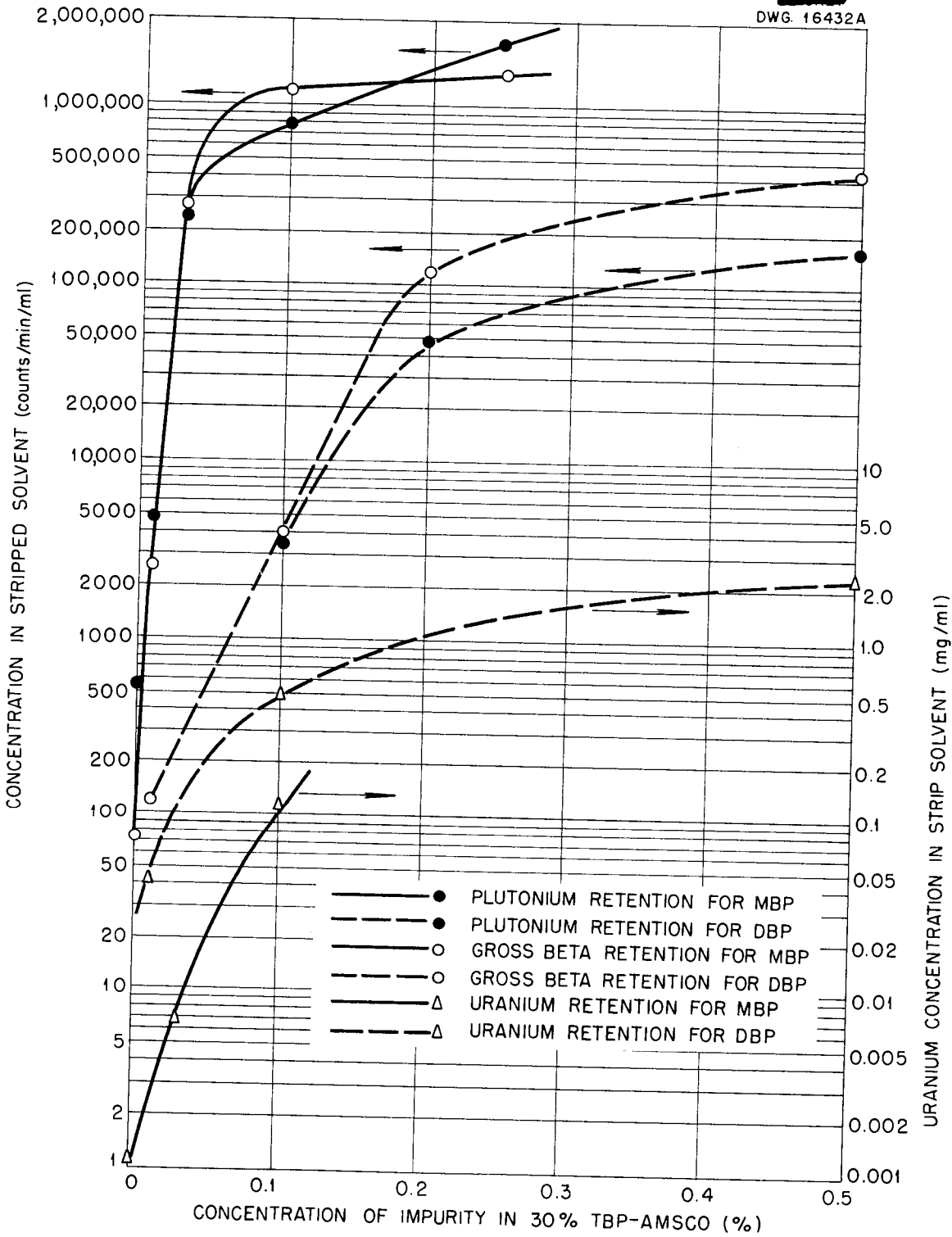


Fig. 58. Effect of Monobutyl and Dibutyl Phosphate on Plutonium, Uranium, and Fission-Product Beta Retention in TBP.

as in the Purex 1A column, an average value of 3 watts/liter is obtained for the power density in the part of the process where 30% TBP-Amsco mixture is exposed. The length of time that solvent would be exposed to this radiation field is about 5 min in a pulse column. Therefore the energy adsorbed in the solvent would be approximately 0.25 watt-hr/liter. This is far below the energy dosages used in this experimental work and indicates that radiation decomposition would not be a serious factor in the process.

There is some evidence of materials other than hydrolysis products of TBP being formed by radiation. Washing irradiated solvent with dilute sodium hydroxide and then with water results in considerable interfacial crud and precipitate. There is no evidence to what this can be attributed. MBP or DBP do not give rise to anything of this nature. Furthermore, caustic treatment of irradiated solvent does not reduce the retentions in the extraction test to the values obtained with unirradiated material.

#### HOMOGENEOUS REACTOR CHEMICAL PROCESSING DEVELOPMENT AT VITRO CORPORATION<sup>(2)</sup>

The Homogeneous Reactor Chemical Processing group at the Vitro Corporation is developing an evaporation method for recovering heavy water from

<sup>(2)</sup>Prog. Rep. June, 1952 Homogeneous Reactor Processing, KLX-1602 and Prog. Rep. July, 1952 Homogeneous Reactor Processing, KLX-1603.

uranyl sulfate-heavy water fuel. The method consists of recovering the bulk of the heavy water by evaporating to a 60% uranyl sulfate solution, drying the concentrated solution to a cake batchwise, and finally drying at 400 to 500°C. Tests of this method, on a laboratory scale, using cakes 0.25 to 1 in. thick have indicated heavy water losses of 0.1 to 0.3%, based on the weight of uranyl sulfate.

Preliminary tests on the removal of fission products from uranyl sulfate solution by adsorption and ion exchange have been encouraging. A batch equilibration of 10 ml of IR-120 with 100 ml of 1 M  $\text{UO}_2\text{SO}_4$  containing promethium resulted in a removal of 71% of this rare earth from the solution. In similar tests, several inorganic materials such as activated alumina,  $\text{MnO}_2$ , and preformed  $\text{LaF}_3$  were found to remove large percentages of activity from uranyl sulfate solutions containing mixed fission products. This phase of Vitro's work applies directly to removing the fission-product poisons from the highly enriched core of a two-core homogeneous reactor.

Several methods of converting  $\text{UF}_6$  (from a diffusion plant) to a heavy water solution of uranyl sulfate have been considered by the Vitro group. The most attractive method appears to be the reaction of  $\text{UF}_6$  with 70%  $\text{H}_2\text{SO}_4$ . This produces a crude  $\text{UO}_2\text{SO}_4$  precipitate that can be adequately purified by washing and roasting. The outstanding problem in this work is to find materials that are corrosion resistant.